

Stabilisation of loess clay surfaces at the example of the Terracotta army in Lintong

Thesis for Doctorate from the faculty for Geosciences

at the Ludwig-Maximilian-University, Munich

**STABILISATION OF LOESS CLAY SURFACES IN THE
ARCHAEOLOGICAL EXCAVATIONS WITH THE EXAMPLE
OF THE TERRACOTTA ARMY OF QIN SHIHUANGDI**



from
Rupert Utz
from
Wasserburg a. Inn

2004

Stabilisation of loess clay surfaces at the example of the Terracotta army in Lintong

Thesis submitted at the 8. March 2004

1. Assessor: Prof. Dr. R. Snethlage
2. Assessor: Prof. Dr. D. D. Klemm

Day of the oral examination: 18. June 2004

Translation:

Nick Beckett
Barbara Beckett
02/2006

Index of content

Summary		6
1	Introduction	10
1.1	Ancient soil structures in the excavations of the Terracotta army	10
1.2	Damages and their causes of the historic soil structures	14
1.3	Aim of the thesis	23
2	Material analyses of the ancient stamped soil of Lintong	23
2.1	The raw material loess (Chapter deleted!)	23
2.1.1	Loess, clastic sediment of a special kind (Chapter deleted)	23
2.1.2	History of the formation of the Chinese loess- plateaus (Chapter deleted)	23
2.2	Soil mechanical properties	23
2.2.1	Mesh analyse/ sedimentation analyse	23
2.2.2	Limits of consistency after Atterberg, grain density and carbonate content	26
2.2.3	Shrinkage	30
2.3	Mineral composition and structure properties	31
2.3.1	SEM-Analyses at undisturbed samples and texture samples	31
2.3.2	Thin section microscopy at undisturbed soil samples	34
2.3.3	Kryo-SEM images at undisturbed samples	37
2.3.4	Determination of CEC and the exchanged cations	42
3	Interaction between the solid phase, air and water in the soil	44
3.1	Types of bonded water in mineral soil	44
3.2	Swelling of the clayey structures	46
3.3	The structural – preservation effect of the water in the binding soil	47
3.4	The function of the clay minerals in the soil structure of the stamped soil of Lintong	48
4	Impact of chemical swelling reducers and SE stone consolidant on the stamped soil in the excavation of Lintong	52
4.1	Swelling reducers	52
4.1.1	Preliminary examinations of the impact of the off the shelf swelling reducer at the stamped soil of Lintong (chapter deleted)	53
	Conclusions from the Preliminary examinations	53
4.1.2	Modification of the chemical swelling reducers	54
	Concentration	55
	Anion	55
	Length of the molecules	56
4.1.3	Preliminary tests with modified, chemical swelling reducers (Chapter deleted!)	58
	Results of the preliminary tests with modified swelling reducers (Chapter deleted!)	58

Stabilisation of loess clay surfaces at the example of the Terracotta army in Lintong

4.2	Silica ester (SE) stone consolidant	59
	Mode of operation of the SE consolidation	62
4.2.1	Preliminary tests for the choice of the SE stone consolidant for the stamped soil of Lintong (Chapter deleted!)	62
	Results and conclusions	62
4.3	Laboratory tests to the effect of modified chemical swelling reducers and SE Stone consolidant (F300E) on the original stamped soil of Lintong	67
4.3.1	Treatment medium, objectives, sampling	67
4.3.2	Treatment of the test pieces	69
	Treatment with modified swelling reducers (DE and DEBH)	69
	Treatment with SE stone consolidant (F300E)	70
4.3.3	Analyses and results to the porosity	71
	Analysing methods (Chapter deleted!)	73
	Summary of the results to the porosity	81
4.3.4	Examinations and results to the water transport	83
	Analysing methods (Chapter deleted)	84
	Results of the examinations	84
4.3.5	Examinations and results of the swelling effect of the water at the treated samples	90
	Examination methods (Chapter deleted!)	91
	Examinations results	91
4.3.6	Examinations and results of the mechanical stability	98
	Analysing methods (Chapter deleted!)	99
	Analysing results	99
	Summary of the results of the mechanical stability	117
4.4	Modelling of the heat and moisture transport for building elements made out of stamped soil, with and without surface treatment.	118
4.4.1	Input parameters for the modelling, with Wufi-2D- building element layout, material data and climate data	119
4.4.2	Modelling results in the behaviour of the untreated soil in atmospheric humidity change	121
4.4.3	Effect of the treatment methods on the moisture transport in the surface treated soil	127
5	Summary and fundamental evaluation of the results on treatment methods – referring to the situation in the pits of the Terracotta army	131
5.1	Treatment with swelling reducers	131
5.2	Consolidation treatment	133
5.3	Combination treatment	135
6	Literature	138
7	Appendix	150

Stabilisation of loess clay surfaces at the example of the Terracotta army in Lintong

7.1	Plans	150
7.2	History of the excavation	154
7.3	Soil-moisture profiles	156
7.4	Climate data	160
7.5	Dust analyses	162
7.6	Selected measuring data for the laboratory tests	165
7.7	Input parameter for Wufi-2D modelling (deleted!)	167
7.8	Technical data sheets	168

Summary

For many decades now, the image of the Archaeologist has changed from a simple treasure hunter to a discoverer and surveyor of complex cultural relics. The necessity of the long-term conservation and museum presentation for archaeological relics from less precious materials such as earth, wood, textiles etc is now a central topic in soil archaeology for the protection of the environment.

The Protection of historic monuments, as an idea to conserve the cultural heritage of humankind, has since been spread across the whole world. In many parts of America, Africa and in Asia a significant part of the Architectural sites are built out of soil, therefore, the conservation of soil as a building material is becoming more and more important. The science of conservation has only made a few small steps to the systematic analyse to this preservation problem.

With the Analyse of the deterioration of the soil structures in the terracotta museum of Lintong and the development and systematic examination of specific treatments, this work should contribute to solve this problem.

Aims of this work:

1. The analysis of the stamped soil in the museum of the Terracotta army. Material properties, their change in the hygroscopic and the super hygroscopic humid range.
2. The examination and development of specific conservation treatments for the stabilisation of the surface of soil structures, in the halls of Lintong museum. The augmentation of resistance against mechanical and climatic stress in the hygroscopic humid environment is at the forefront.
3. The examination of the influence of the conservation methods on the material properties of the original stamped soil of Lintong. Thereby an attempt is made to transfer the methods of stone conservation onto the building material soil.
4. The validation of the possible stress requirements with a computer supported modelling of the moisture transport in the soil.
5. The evaluation of the methods used, for their protection qualities against mechanical and climatic surface stress. Their compatibility to the untreated substrate, especially in consideration of the condition in the pit of the Terracotta army.

To 1 The soil of the stamped clay walls in the Terracotta army museum is, due to the grain fraction of the carbonate component, classified as “Loess” or clay loess. Sedimentary evidence shows a clear connection to local standing, in early and middle Pleistocene loesses of the Wuheng and lower Lishi formations.

The analysed material shows, that at the erection of the clay walls, these loesses from the museum surroundings had been used without any organic or inorganic additions at water content under the material specific plastic limit.

From the mechanical characteristics, the ground of the stamped earth has to be classified as normal active, little plasticized clay. The clay fraction is dominated mainly by layer silicates off the Illite-Muskovite-row and chlorite.

Despite the soil not having a considerable amount of swellable clay minerals, the hygroscopic swelling reaches up to 2mm/m. With the submergence of the material under water, it dissolves immediately. In the hygroscopic moisture environment, the swelling of the soil structure results from inter crystalline swelling mechanism between the clay minerals that sit between the grain contacts of the grain supported silt structure. The tests showed, that the structural conditions are additional to the mineral components an important criterion to the hydroscopic contraction of the soil. Therefore, it could be problematic to rely on material analysis of soil from recreated samples.

To 2 The damage assessment in the pits of the terracotta army suggests that the conservation treatments on the surface of the soil in the excavations aim to reduce the hydroscopic swelling and to improve the resistance against mechanical abrasion. For the reduction of the hydroscopic swelling in connection with this work, for the first time bi-functional cationic tensides have been used on the material, soil. The formulas of these tensides, as they are used for comparable purposes in stone conservation, could be improved in their concentration, molecular size, and reaction residues and adapted to the requirements of soil. Additionally the use of consolidates on the base of monomer ethyl silicate ester could be tested. Both methods as well as their combination did not show any negative effects on the visual appearance of the surfaces.

To 3 The test series for the analyse of the effect of the described treatments on the soil, was carried out on untouched original material. For the first time in the conservation science of clay building materials, the low destructive analytic for small samples of the stone conservation, was transferred to the material soil. The complete

Stabilisation of loess clay surfaces at the example of the Terracotta army in Lintong

recording of all relevant hydrous and physical parameters on the original material and the treated original material is unprecedented in the conservation of soil. This was, until now, mostly restricted to the methods on large sample material soil mechanical methods.

The gathered data from the ultrasonic measuring, bending strength test, measurement of the vapour diffusion resistance etc, allow the evaluation of the material due to its susceptibility for long-term deterioration processes.

To 4 Based on the rich data material from the test series, it was possible to evaluate the damaging potential of the climatic changes of the soil surfaces in the pits of the terracotta army with and without conservation treatment. With the help of a *Wufi-2D* Modelling of the hygroscopic water transport in the surface near zones of treated and untreated soil the depth effect of the climatic fluctuations during a daily, monthly and yearly cycle could be adjusted. Therefore, the tested treatment methods does not interfere the humidity content of the soil. With the simulated depth effect of the climatic fluctuations the tension potential of the hygric expansion in the critical transition zone between the untreated and the treated material can be evaluated. The result for the treated types was that a minimum penetration of two to three centimetres is necessary.

To 5 The test of the treatment possibilities showed that treating with the swelling reducers have a slight, but positive influence on the mechanical properties and on the abrasion resistance of the soil. The treatment achieves a reduction of a hygroscopic swelling of more than 50% and therefore it can reduce, to a high extent, the damaging potential of the fluctuations in the hygroscopic climate. The tensides have an input only on the micropores of the soil. They prevent the elutriation of the soil when water is infiltrated and therefore can be used for the protection of the surface with direct contact with water. This treatment, however, reduces the drying process of the soil, consequently the application outside has to be proven. For the requirements in the pits of the terracotta army, the treatment seems to be appropriate.

The consolidation reduces parts of the capillary porosity; therefore, it changes the vapour diffusion resistance and the capillary water adsorption of the soil. The hygroscopic conditions in the pits of the terracotta army (without fluid water access) results in no corrosion relevant disadvantages.

Concerning the effect of the consolidation, the treatment is very successful. The structural stabilisation of the pore space is strong enough to ensure form stability of

Stabilisation of loess clay surfaces at the example of the Terracotta army in Lintong

small format column samples submerged in water for several days. The stabilisation and the abrasion resistance should be more than enough for the mechanical surface stress in the museum halls of Lintong. From the conservation view, the consolidation has one effect that questions the long-term effect of this treatment. As an effect of the consolidation, the swelling inside the humidity range increases to 30 to 80%. This means that for the application in the museum halls, the higher stability of the consolidated surfaces reacts contrary to an extra inner tension potential that can cause in long-term damages.

When treated with this combination, the effects of the swelling reduction and the consolidation overlap. Consequently, the treated samples are mechanically consolidated, but the hygroscopic tension potential is on the same level as the untreated soil. If an irreversible consolidation on the surface of the excavations in the museum of the terracotta army is required, the method of the combined treatment seems to be encouraging due to the effect and long-term stability.

1 Introduction

In March 1974, the first fragments of the over 2200-year-old terracotta army of the first emperor of China; Qin Shishuangdi (259-210 B.C.) were discovered at the digging of a well near the small city of Lintong. The army was probably set up to protect the nearby grave of the emperor (see imag.2). Their discovery was an archaeological sensation, because the Chinese history writer Siam Qian in his detailed report on the emperors grave (Nienhauser, 1994) does not mention it. Before their accidental discovery, neither archaeologists nor historians had contemplated their existence. Even today, the excavations at the subterranean



erected clay army are still ongoing. The archaeologist prognosis is that there are over 7000 terracotta soldiers. At present approximately 1000 figures have been excavated, restored and displayed in situ (see imag.1). Since 1979 the pits of the terracotta army have been open for the general public.

Image 1 In situ erected Terracotta soldiers in pit 1
(Image: museum of the terracotta army)

The Terracotta army is, together with the Great wall and the Emperor's palace in Beijing, one of the most important and well-known cultural heritage sites in China. Every year 1.5 million people visit the Terracotta museum. The burial site of Qin shihuang was listed in 1987 as a world heritage site by UNESCO. All findings of this area are of the artistic and historic highest value.

1.1 Antique soil structures in the excavation of the Terracotta army

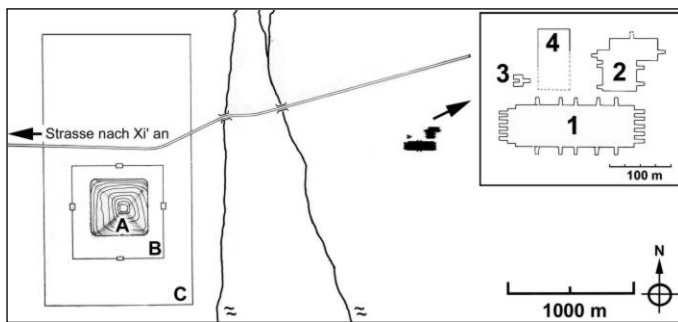
The architecture of the Terracotta army:

The Terracotta army is one of many similar built subterranean sites belonging to the Emperors mausoleum (called "Qin Ling") (see appendix 7.1). The clay figures were erected, divided into three separate pits, in subterranean corridors, that have brick tile floors. Thick walls of stamped clay (Chinese "hangtu") divide the corridors. This carried a roof construction with a solid beam layer, then covered with straw mats and

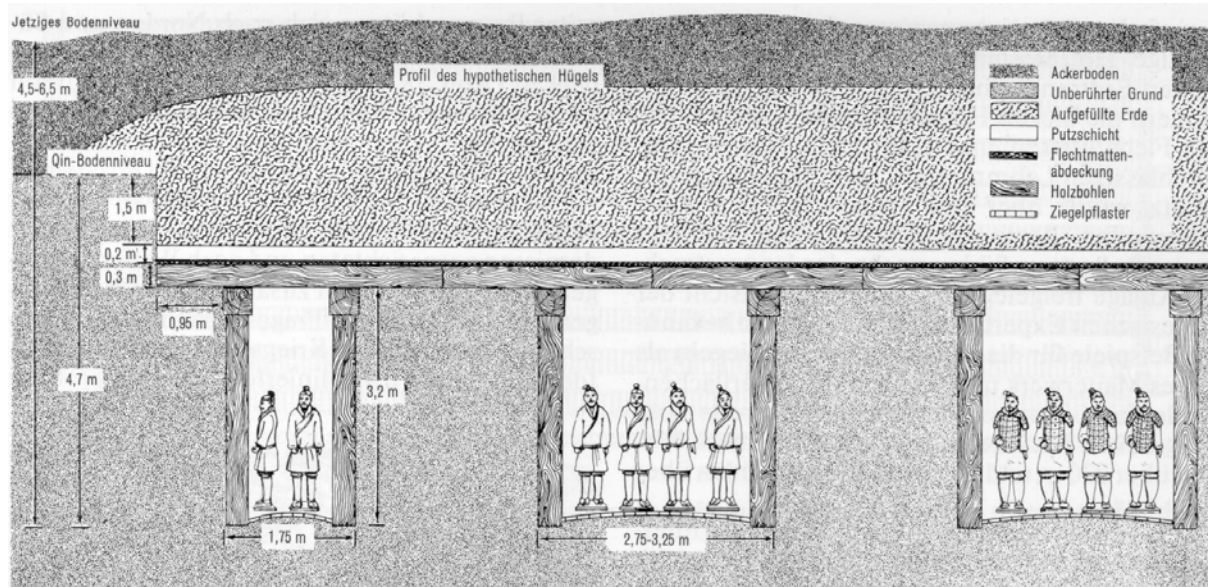
Stabilisation of loess clay surfaces at the example of the Terracotta army in Lintong

lastly covered with a layer of soil. To reduce the weight of the roof on the walls of the corridors further carrying beams were built in (see Imag.3).

The technique of stamped clay walls is still widely used in China. For the erecting of these walls, moist clay is compressed into wooden shuttering. This shuttering is gradually made higher, so that the wall grows every step one clay layer higher (see Imag.4). Occasional the prints of the shuttering boards can still be seen. The height of one of these layers was as a result about 8-10cm. In between, the layers there had no built in supporting materials. Mainly in Europe weaved mats, twigs, lime and other stabilising additions were often used between the layers of the stamped clay walls (Houben, 1994). The clay also does not contain any added extras such as straw or hemp to improve the structure.



Imag.2 The army in the pits one to four (pit 4 containing no soldiers) is situated outside the main burial area. The earth pyramid (A) over the grave of the Emperor and parts of the walls of the burial (B and C) are today decidedly visible (image out of Roger, 2000). A detailed plan of the burial area is shown in the appendix 7.1.



Imag.3 Reconstruction of pit building, using pit 1 as an example (image taken from (Brinker, 1980)). Before the erection of the stamped clay walls, the pits were dug down to the floor level of the figures. Further cross sections see appendix 7.1.

Stabilisation of loess clay surfaces at the example of the Terracotta army in Lintong

Imag.4 Technique of the stamped clay walls in old China. The wooden shuttering is held together with round timbers and wickerwork. At the bottom, it is stabilised to prevent slipping.



History of the decay:

Only few years after finishing, a rebel army plundered the Terracotta figures. Parts of the pits were burnt out, roof beams collapsed and corridors fell down. Charcoaled wood, red-burnt soil and terracotta show now the devastation. In the subsequent years, the moist beam layer bends from 50 to 100cm over the brick floor that is under the pressure from the overlaying soil. The Terracotta figures underneath fell down and fractured into pieces. The remaining hollow spaces in the corridors filled with sand and slime because of several floods. Now, in the area of the mausoleum, up to seven sedimentations of flooding can be detected in the excavations. (Work report, 2000).

History of the excavation and present condition:

First test excavations started on the east side of **pit 1** in the year of the discovery 1974, at that time in open air. After a couple of test diggings, in 1979, a closed hall construction was made out of steel and metal plate to cover pit 1. From then on, the hall is open daily for the general public. To this present time, it protects the excavation against rain, but does not give sufficient protection against climatic changes, entry of dust or other environmental influences. These are the stated requirements for archaeological protection buildings in TEUTONICO (2001). Within this period since 1979 large parts of the pit 1 had been excavated up to the roof beams, but had been refilled. The easterly part has been fully excavated. The roof beams have been completely removed and the restored figures are re erected in their old positions (image 1). At the Western ends of the pit, vast excavations until recently were in progress (see appendix 7.1). Now the excavations of the pit 1 are inactive.

In **pit 2** extensive excavations were started 1994 after the museums building protection was finished over the area of the dig. With this massive construction, the protection of pit 2 is able to guard the excavation against rain, sunlight, climatic changes and dust. However, for years the advantages of this building (due to dust and climatic change) are more or less annulled with the daily use of an unfiltered ventilation system (Utz, 2001b).



Image 5 Uncovering of the roof beams in pit 2
(Image: museum of the terracotta army, 1997)

Between 1994 and 1997 the whole of pit 2 had been excavated up to the level of the roof beams (see image 5). Excavations down to the floor level of the corridors are concentrated up until now to the sectors T15 up to T21 (see appendix 7.1). After a two year excavation break around the year 2000, in 2001 excavations started again in sector T21 (G18-G20).

A detailed list of the history of the excavation; please find in appendix 7.2. The excavation activity in the pits 1 and 2 was limited in the last 15years, because the conservation methods for the findings, especially for the polychromy of the terracotta figure were still in development.

The soil bridges became smaller and wider in the 2000 years under the pressure of the overlying soil. On their rounded surfaces, prints of the roof beams had been preserved (see Image 6. appendix 7.1). The standing height at the excavation of the Inner walls is 1.2 – 1.5m. The high amount of water during the floods, while the corridors had been partially flooded, probably enabled a plasticized deforming of the walls. Surprisingly the steep flanks of the walls were preserved. Collapsed inner walls were only rarely found.

The climatic situation in the building shelters of the pit 1 and 2 are discussed in UTZ (2001B). It can be summarized as follows:

Stabilisation of loess clay surfaces at the example of the Terracotta army in Lintong

The outside temperature can reach, in Lintong, values from +45° C to –10°C. The summers are hot, so that in the July month the average measurement is around 25°C. The winter months are cold and with low precipitation and often very dry (see appendix 7.7).

In the building shelter 2, the walls can buffer the changes of outside temperature, therefore only few frosts occur (but only when the ventilation system is not switched on). In the building shelter 1 however, the inside temperature follows approximately the outside temperature.

At new excavations, a lot of water is evaporating from the moist soil surfaces. Near the ground, there is a relative humidity of between 70% and 95%. This caused at the large excavation in pit 2 (1994-1997) immense problems with mould. However, the mould growth disappears after a year, because of the quick drying out of the soil, after the excavations are finished (Warscheid, 2001).

With the drying out during the last years also in pit 2 the measurements of the relative humidity are gradually approaching the monthly average values of the outside temperature. The fluctuations of the relative humidity during the day are buffered near to the ground, because of the high adsorptive reactivity of the dried out soil.

1.2 Damages and their causes of the historic soil structures.

The soil bridges with the print of the roof beams have, as evidence for the pit architecture, high conservation value. On the surface of the soil there are preserved prints of organic material (such as reed mats, straw mats, wooden chariots and wooden crossbows etc.) the material evidence itself has decayed away centuries ago (see image 8). In addition, the roof beams do not exist any more in wood, but the soil that has replaced the wood recreates their structure. As these surface structures of the soil are mostly the only evidence of the above-mentioned materials and things, they should also be preserved.

Due to the soil structures in the pits of the Terracotta army, there are two damages, these differ in scale as in the cause of the damage:

A: Tearing apart of large correlated soil structure during drying out

B: Loss of material on the surface of the earth structures

To A: Drying out and shrinkage cracks

The drying out of the soil structures in the pits starts with the building of the shelters. In correlation to the sorption isotherms, the surface of the soil is not able to keep

more than 6 weight percentages without direct water input, even at constant relative humidity of over 90% (see Chapter. 4.3.3; appendix 7.6). If they dig, just to the roof beams, as they have done in pit 2, then within the first two years after the end of the excavation, a distinctive **crack system**, with parallel cracks along the parting and the edges of the soil bridges, appears. The distance between the parallel cracks is 1 and 1.5 meters. In addition, cracks arise that cross this dominant system at an acute and right angles. The first cracks always occur there, where the soil dries out the fastest. The parting areas are predestined, because they are furthest away from the ground water. This means they contain less water at their excavation and are better ventilated by the atmospheric air, than the valleys between the soil bridges (see: Image 5).

When the soil bridges are revealed completely, then the partings, which are ventilated on both sides, dry out fastest. Consequently, **dangerous flank parallel cracks** develop (image 6), these cracks with the help of the gravitational traction on other parts of the soil bridges can also slip off (image 6).

Large cracks with a width of more than 1cm have largely damaged the uncovered soil bridges in pit 1. Additional to this there is the danger that the flanks falling down and damage the re-erected terracotta figures (see image 6). In general, it is not possible to prevent the drying of the soil and the therefore developing shrinking cracks. For securing the soil bridges in the pits, a suitable anchor system was introduced in recent years with inlaid sand anchors (Miculitsch, 1996), (Utz, 2003b).

The drying out of the soil is dangerous for the polychromy of the terracotta figures that remain in the soil. The undercoat lacquer of the figure paint is detaching from the terracotta at relative humidity under 94% (Thieme, 1993). If the shrinking cracks reach the terracotta fragments and dries out the soil, where they are imbedded, under water content under 6%, the paint could be already damaged before the excavation. Therefore, it was important to find out how quick and up to which depth in the excavation the soil dries out and if the obvious damages of pit 1, will be repeated in the later opened, moister pit 2.

The important factor for the moisture content of the soil at the excavation and for the speed and depth effect of the following drying out is the distance of the excavation horizon to the surface of the ground water. In the first month after the excavation, additionally the relative humidity influences the development of the damages. Uncovered surfaces dry out in the dry winter month much quicker than in summer. The long-term drying progresses are influenced from the yearly average value of the relative humidity, which is in the surrounding of Xián around 75% (appendix 7.7).

Stabilisation of loess clay surfaces at the example of the Terracotta army in Lintong

Under the floor tiles in the corridors of the pits there is down to the groundwater homogenize non-layered loess. Inside the area of the museum buildings, the difference of the height of the surface of the groundwater is even less than the normal yearly fluctuations of 20-25%. The average distance from the floor tiles to the groundwater is 10m. Pit 2 lies a little lower. The level of the floor tiles rises in pit 2 from Northwest to Southwest, therefore the distances of the floor tiles to the groundwater varies in pit 2 between four meters in Northeast corner and six meters in the Southwest corner (Utz, 2001c).

In spring, 1999 and autumn 2000 the distribution of the moisture in the ground was measured with drilling soundings at two soil bridges and in the well drain of pit 2 (see appendix 7.3). The development of the drying out was modelled for these three positions, for the next 25years after the excavation, with the computer programme "Wufi-2D" (see image7 and appendix moisture distribution). For the outside climate, the average monthly values of Xi'an were used. Details to the "Wufi 2D modelling program please find in chapter 4.4, and the input data for the drying out model in appendix 7.7.

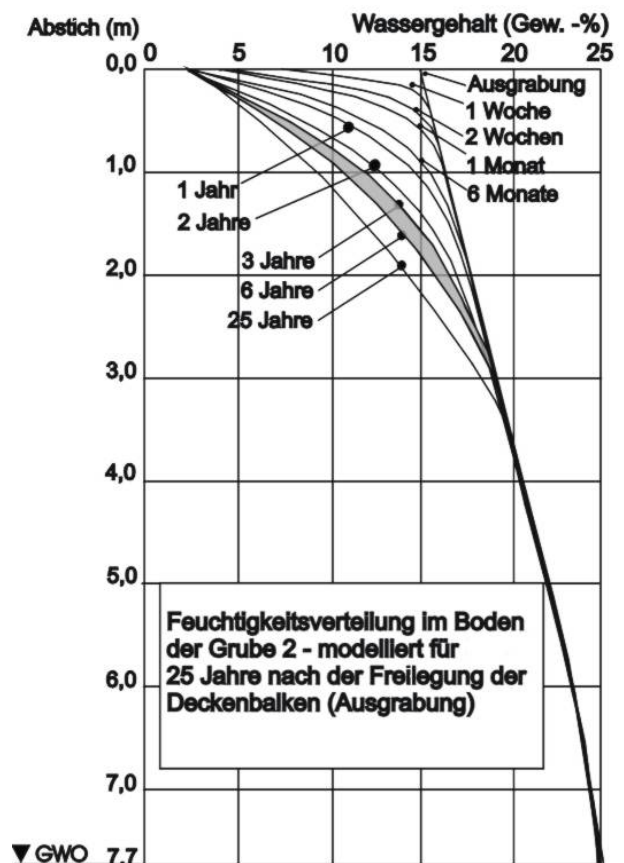
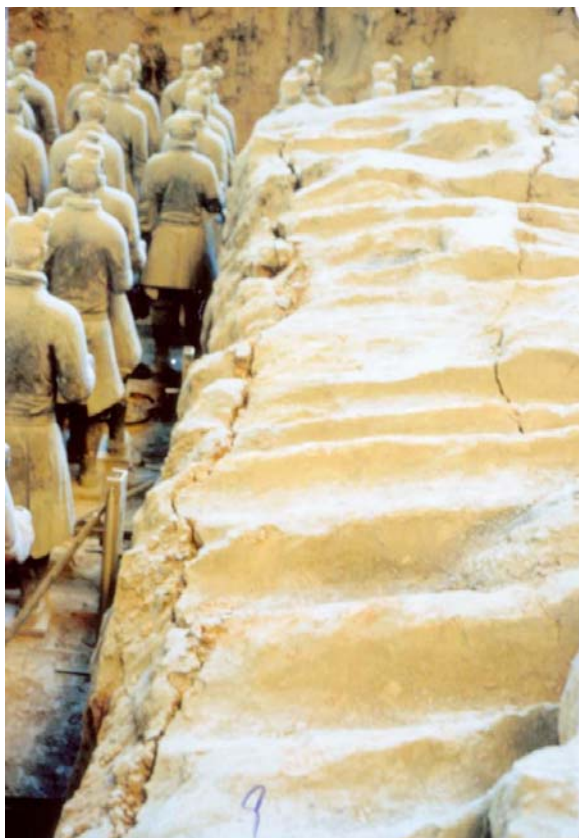


Image 6 left: Dried out soil bridge in pit 1. At the shrinking cracks near the edges, the flanks of the soil bridge seem to slip down. In addition, the soil bridges, together with the shoulders and heads of the Terracotta soldiers are covered with a grey dust layer.

Stabilisation of loess clay surfaces at the example of the Terracotta army in Lintong

Image 7 right: “Wufi-2D modelling of the drying out of the soil in pit 2 at the position of the well drain. The modelling was created with the average monthly climate values of Xi’an (see appendix 7.7). The curves of the moisture between 3 and 6 years match to the results of the sounding results of the well drain from the years 1999 and 2000 (see appendix 7.3).

The first results of the models match in the dry range excellently with the condition measurements of the soundings of the ground in 1999 and 2000. At the digging depth over 4m and in the area of the capillary water seam there are deviations between the model and the measurements. This is caused by the transformed porosity through the pressure of the overlap and the rising water saturation (see image 7 and appendix 7.3).

Starting from the condition, in 2000, the soundings of the ground and models give the following drying out prognosis for the drying out of pit 1 and 2:

- Due to the level of the excavation in 2000, the development of the drying out cracks have finished
- In pit 1 the polychromy of the terracotta fragments, with less than 90cm complete soil coverage, are in danger.
- The drying out of pit 2 will continue in the next years at a lesser rate.
- In the NE-corner of pit 2, the drying out cracks will spread out up to 1m under the layer of beams, in the southwest part, up to 1.4meters.
- For a secure storage of the polychrome terracotta in pit 2, a complete cover with soil of up to 0.5m is necessary.
- At further excavations the drying out development has to be recalculated
- The dangerous crack formation at the sides of the uncovered soil bridges will develop in pit 2 similar to pit 1, because the drying out of the flanks is not slowed down sufficiently by the higher moisture in the core of the profile of the bridges.
- The uncovering of the moist soil bridges in pit 2, one example is the soil bridge in sector T21 where samples have been taken, gives expectations of stronger damages by cracks as in pit1. Due to the high moisture content in the core of the bridges, at the drying out of the flanks, very steep moisture gradients are formed. The tensions between the dried out surface and the moist core, due to the shrinking, will be stronger than at the excavation in pit1. This effect could be reduced if you wait as long as possible with the uncovering of the soil bridges. Then the drying out border is able to spread deeper downwards and subsequently the shrinking gradients at the flanks of the soil bridges will be less after their uncovering.

To B: Loss of material at the surface of the soil structures

The surface of the inner walls with the prints of the laid on beams are well preserved at the excavation. Straight after the uncovering, additionally, the imprints of the straw mats and wooden chariots and relicts of pigment from the figures can be clearly seen, (see image 8).

Small dimension shrinking cracks:

The development of small-dimensioned shrinking cracks in the upper centimetres of the soil take place shortly in the first weeks after the uncovering (see: drying out modelling in appendix 7.3). The surfaces were dissected by the shrinking cracks in decimetre areas. Between the cracks, there remain dried out fields, where no new shrinking cracks develop, unless the archaeologists water them again. Then the shrinking process is repeated and new crack structures arise (sometimes the soil imprints were moistened to close the shrinking cracks and improve the colour impression, for taking images).

It is possible to delay the shrinking process and the division of the surfaces with a temporary covering of plastic foil. With this method a larger scale crack pattern occurs, because the drying out gradients to the soil below is getting smaller. The faster the surface dries out, the smaller dimensioned surface cracks arise and therefore the damage due to the shrinking is much higher at the preserved imprints in the soil.

How as already mentioned at the soil bridges, the shrinking cannot be prevented, even under optimised climatic conditions (Miculitsch, 1996). Normally the shrinking during the drying out of the surface structures is a singular damage phenomenon. It is finished after the drying out to about 4-5 Vol.-% water content and then does not cause any area loss of material.

Loss of the surface:

Surface pulverisation

In Image 8 it clearly shown that years after the uncovering at the surface of the soil, there is serious, area loss of material. The upper grain layers are loosened from the support and disperse like dust. Through this process, in the last decades, most of the preserved prints in the soil in pit 1 are forever lost. This damage is described as "pulverising surfaces".

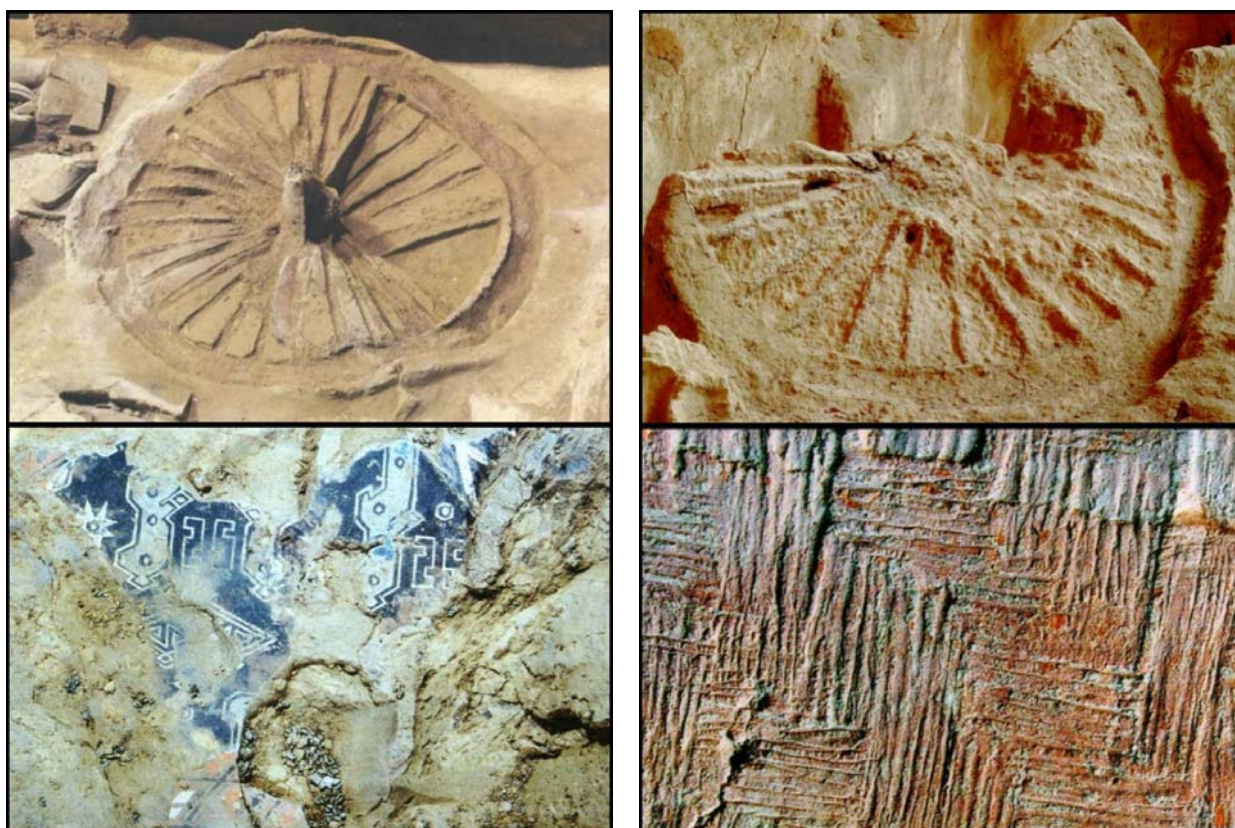


Image 8

At the surface of the soil, many important archaeological findings are preserved (image: museum of the Terracotta army).

Above: Prints of the wheels of the wooden chariots (left: shortly after the excavation, right: after several years exposure), bottom line of the image is approximately 1.8m.

Below left: At the excavation of the Terracotta figures, the paintlayer is detached from the terracotta remains in the soil. Bottom line of the image is approximately 0.4m.

Below right: Imprint of a reed mat at the surface of a soil bridge. Bottom line of the image is approximately 0.1m.

Scaling:

Of Secondary importance, you can also see the problem of scaling of the surface. This can be seen clearly in image 8 (below left) small scales with a width of 0.2-1cm are detached from the subsoil.

Theories for the cause of these losses of surface:

The causes for the pulverisation and scaling of the Terracotta army have been discussed in the past. Today some of them could be disqualified due to more detailed observations, test trials and a wide knowledge of the used material:

- Frost as a reason for the loss of surface by scaling

The stamped clay of Linton is not at all safe against frost (see chapter 2.2). However, frost is only able to rupture the pore space structure of the soil when it is

Stabilisation of loess clay surfaces at the example of the Terracotta army in Lintong

near the water saturation point. After the erection of the museum buildings, the soil in the pits was too dry to be damaged by frost, which is perfectly possible in winter. Some of the damages of the surface in the Eastern part of pit 1, which had been excavated in the 70's under open air, are probably caused by frost. The watering of the surface on a large scale, as it was done during the excavations to reduce the generation of dust, theoretically could also cause frost damage. However, there are no excavations in winter; therefore, this theory can be eliminated.

- Scaling through watering and compressing of the surface

The before mentioned watering of the surfaces during the excavation, causes additional strong swelling movements and encourages the development of cracks. At the same time, the excavation workers had used the soil bridges as walkways. Together with the water input, the inner structure of the upper soil layer can be irreversible compressed through the pressure of the feet. If the change of the surface near the inner structure is so big, that their physical properties differentiate clearly from the support, the compressed surfaces can detach in a climate change. With the growing diligence of the excavation team, this damage should now never occur. It is also possible that through the frequent watering and drying out, the water-soluble compounds concentrate at the surface compress and become brittle, so as to peel off in scales.

- Change of climate as a reason for the pulverisation of the surfaces.

The change of climate in the museums halls has similar values and frequency to the outside climate. They are not at all near the so called "museum climate" that demands constant values of 20° C with 55%relative humidity. The hygroscopic humidity expansion of the stamped soil in Lintong surpasses with 2mm/m of the hygroscopic expansion of sandstones by storage in water (Hilbert, 1995). For some sandstone, it is stated, that cycle of watering weakens the bindings (Wendler, 1996b). It seems obvious, that expansion movements caused by climate, leads to the detachment of upper grain layers of the soil. The possible mechanism for the damaging influence of humidity changes on objects made of soil and clay are discussed in Müller (2002). With dust traps, which had been fixed at the vertical soil walls in pit1 and pit 2, to measure the quantity of the dust on the surface, could not so far verify the theory of damage through climate change. On 14 test fields in 3 years, non-grain has been detached from the surface. But nevertheless hygroscopic expansion cannot be excluded as a reason of the loosening of the surface.

- Mechanical stress

Beautiful imprints in the surface are more often dusted than other soil structures. With the use of brushes and vacuums, material losses at the upper grain layers cannot be avoided (see image 9, right image). It is interesting, that the overhanging flanks of old soil bridges in pit1 , that are sheltered against dust, with already strong “weathered” surfaces, look as though they are freshly uncovered. At these flanks there cannot be seen any material losses. These observations in the pits of the Terracotta army lead to the conclusion, that the main cause for the loss of the surface of the soil structures is mechanical stress (brushing, walking, etc...). Probably also crawling and drilling insects have an “input” to this form of the damage (see image 9, left image).

- Dust

The dust deposits in the pits of the Terracotta army are enormous (see image 6). The theory, that the dust arrives from the pulverised surfaces of the excavations could be disproved with the analyse of the dust on the Terracotta figures. The dust in the pits contains great amounts of soot particles and gypsum, that not of origin from the pit (see appendix 7.5). Just the comparison of the colour of the dust and the grounded stamped soil proves, that at least 80% of the dust in the pits is of meteoric origin (see image 9, middle picture). The dust burden is not an immediate problem for the soil surfaces. However, because the dust has to be removed continuously from sensitive surfaces, for the visitors, these surfaces suffer from mechanical stress. Therefore, dust is one of the main causes for the loss of the soil structures in the museum of the Terracotta army.

Stabilisation of loess clay surfaces at the example of the Terracotta army in Lintong

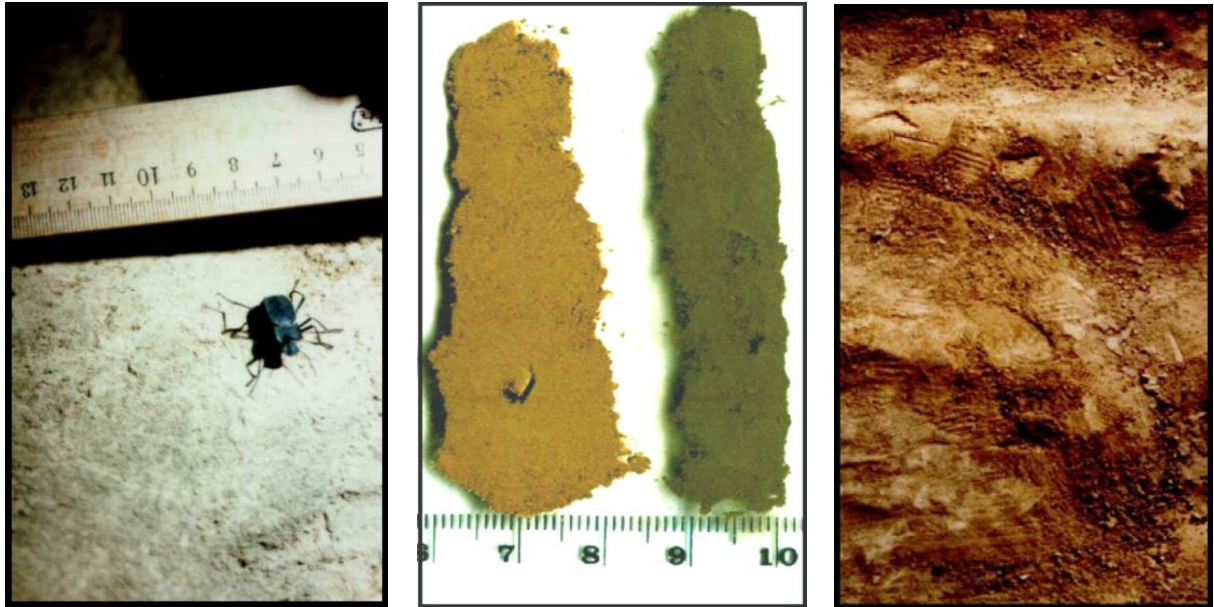


Image 9: causes of damages additional to the climatic stress:

Left: digging and drilling insects have an impact of the damage of the surfaces

Middle: Comparison of the colour of the dust of the stamped soil (left) with the “meteoric dust”, that had been deposit in pit one on the surface of the soil and the figures (sample is taken from the shoulder of an Terracotta soldier)

Right: foot prints and brush strokes on an uncovered soil bridge.

Conclusion:

The reasons for the loss of the surface of the soil structures in the museum of the Terracotta army are various. Improving the building of the museums halls could advance the climatic stress and the dust deposit in the pits. The main cause for the loss of the surfaces is based in the extreme mechanical and climatic sensitivity of the material, soil. It cannot withstand the stress caused by a museum use. Therefore refilling of excavated sites to shelter the soil structures is often carried out with success (Chiari, 2000b), (Goodman, 2002). This possibility is ruled out at the pits of the Terracotta army.

The following work will analyse and find possibilities to improve the resistance of the soil surfaces against mechanical and climatic stress. The main interest is thereby not the use on a large scale, but the conservation treatment of small, especially important structures.

1.3. Aim of this thesis

The examinations shown in this work have the following points as an aim.

1. Analyse of the stamped soil in the museum of the Terracotta army due to their material properties and their changes in the hygroscopic and hyper hygroscopic range.
2. Analyse and development of specific conservation treatments for the stabilisation of the surface of the soil structures in the museum halls of Lintong. The improvement of the resistance against mechanical and climatic stress in the hygroscopic humidify are of main interest.
3. Analyse of the influence of the conservation methods on the material properties of the original stamped soil of Lintong. Thereby the test is made to transfer methods of the stone conservation onto the building material soil.
4. Evaluation of possible stress requirements with computer based modelling of the moisture transport in the soil.
5. Evaluation of the methods, in relation to their protective properties against mechanical and climatic surface stress and their compatibility with the untreated substrate - with special care to the situation in the pits of the Terracotta army.

2 Material analyses of the ancient stamped soil of Lintong

2.1 The raw material loess (Chapter deleted!)

2.1.1 Loess, clastic sediment of special kind (Chapter deleted!)

2.1.2 History of the formation of the Chinese loess- plateaus (Chapter deleted)

2.2 Soil mechanical properties

The basic physical data of the stamped soil of Lintong has been measured at the Institute for soil mechanics and rock mechanics at the University of Karlsruhe. Four samples (M1-M4) from different inner walls of pit 2 have been sent to the institute. The measurement data are documented in MICULITSCH (1996). Further important material data please find in chapter 4.3

2.2.1 Mesh analyse/ sedimentation analyse

The process and devices for the measurement of the distribution of the grain sizes of granular soil are fixed in DIN 18123 (1983). Binding soil with clay and silt are elutriated after the drying, weighing and washed through a sieve with the width of the

Stabilisation of loess clay surfaces at the example of the Terracotta army in Lintong

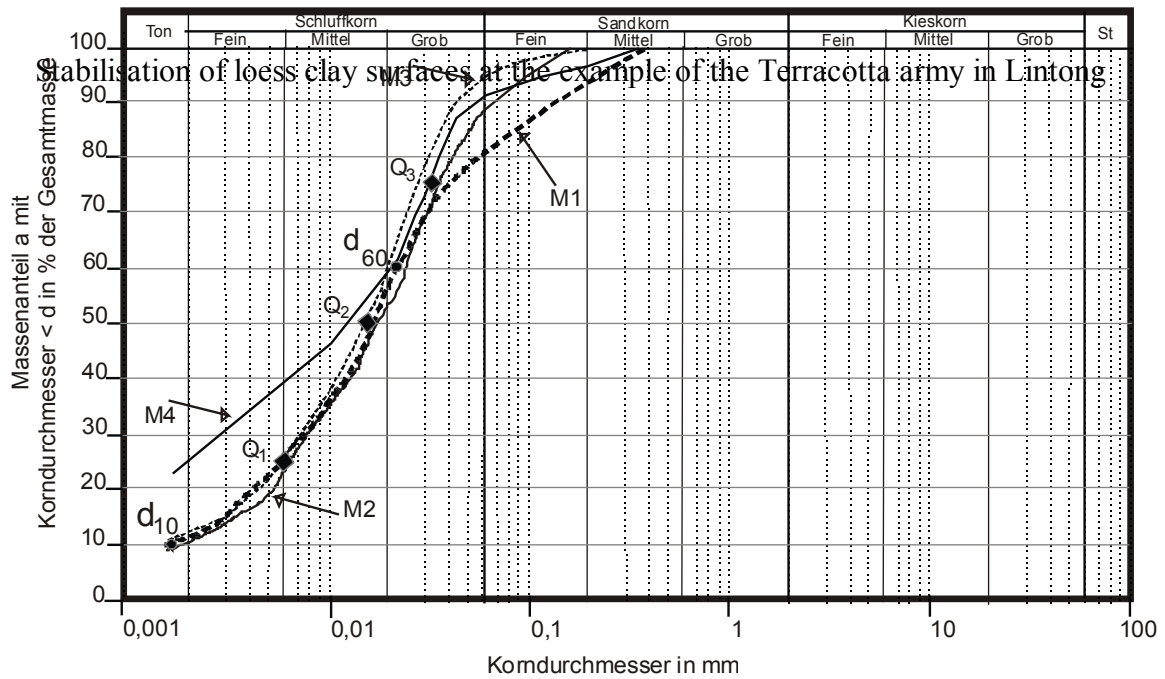
mesh being 0.063mm. The remaining contents of the sieve is dried again and sieved. The distribution of the grain sizes from this sieving is measured by sedimentation analyse with the Aerometer method after CASAGRANDE (1934). The method is based on the principal, that different size of grains sink down in the elutriation at different speeds. The “Stokesche” law describes this correlation from grain size, density and sinking speed for spherical volumes in a fluid. Therefore, this method does not give a division in grain sizes, but of “equivalent grain diameter” in spherical form (Prinz, 1991). To avoid coagulation (flaking) the dispersion material Sodium pyro phosphate ($\text{Na}_4\text{P}_2\text{O}_7 \cdot 10 \text{H}_2\text{O}$) is added to the suspension. The distribution of the stamped soil of Lintong was measured with the sieve analyse and sedimentation analyse. The results are shown in a sum curve diagram in image 10.

The most important, soil physical and sedimentary data, deriving from the grain curve, are listed in table 1:

The grain curves of the samples M1-M3 run very similar. With about 80% silt, about 10% clay and 10% fine sand; this grain size distribution corresponds with the standards for loess. With over 50% weight percentage and a loess typical grain size of a maximum between 10 and 60 μm , is characteristic. Small deviations inside the silt fraction are reflected in the grain characteristics, which show the percentage of parts of the single fractions, rounded to ten percent (see table 1). The soil of this sample has to be called after DIN 4022, T1 as “silt light clay, light fine sandy”.

The sample M4 differs by a higher percentage in the clay fraction. In contrary to the other samples that can be described as loess M4 is better described as loess clay.

The bending of the grain curves shows the regularity and irregularity of the soils that is important for different soil properties, e.g. the compressibility of soil (Prinz, 1991). In numbers it is expressed in the distortion number U ($U = d_{60}/d_{10}$). Thereby d_{60} and d_{10} are the grain sizes in mm; at the point, the sum curve cuts the 60% or 10% line. After DIN 18196 (1988) the soil with the distortion number larger than 6 is classified as “irregular”.



Grain curve - DIN 18123
Grain diameter in mm

Image 10: Grain curves of four soil samples of the stamped clay walls. The grain size distribution of this soil is characteristic for less (M1-3) and/or loess clay (M4). The part of the silt fraction is 65%-95%. The characteristic grain size maximum between 10µm and 50µm is characteristic for loess sediments

	Soil mechanical characteristics after DIN4022T1 (1987)			Sedimentary petrographic characteristics (Visher, 1969)	
	Grain characteristic number	Kind of soil	U= d_{60}/d_{10}	median (mm) (Q_2)	$S_o = (Q_3/Q_1)^{0.5}$
M1	1.142.110	Silt, light clayey, light sandy (U, t', s')	13	0,015	2,6
M2	1.134.100	Silt, light clayey, light sandy (U, t', s')	13	0,015	2,4
M3	1.143.100	Silt, light clayey, light sandy (U, t', s')	13	0,015	2,3
M4	2.223.100	Silt, light clayey, light sandy (U, t', s')	~ 20	0,012	4

Table 1: Mechanical properties from the mesh and sedimentation analyse of the samples M1-M4. U: Distortion number: So: Sorting coefficient

Due to DIN 1896, the loesses of the excavation of Lintong belong in the group of the binding soils that divide themselves by a high water binding ability from the more coarse-grained, non-binding soils. The transition from the non-binding to the binding soil is in the middle silt area. In this grain fraction there arises a strong force of attraction between the grains, although this whole silt fraction is still quartz and rock fragments and not reloaded layer silicates (Prinz, 1991).

The binding soil belongs to the kind of soils that are difficult to compress. The ability to compress depends a lot on the water content. Thereby the irregular types are

better than the regular ones (Prinz, 1991). Soils, such as the soil from Lintong with $U > 12$ are classified as irregular, compressible and difficult to dissolve.

Different parameters out of the grain distribution (form of the sum curve, position and amount of the maxima in the frequency of the distribution curve etc.) are used as indicators for the sedimentation conditions of clastic slack sediments (Reineck, 1980). For a simple correlation of the samples of Lintong with the loess- stratigraphy after Liu (1966) (see: **Fehler! Verweisquelle konnte nicht gefunden werden.**), as well the median of the sum curves (Q_2), that was used by Liu, as the sorting coefficient "So" for the samples M1-M4 have been calculated and filled in the stratigraphy in **Fehler! Verweisquelle konnte nicht gefunden werden.** $So = (Q_3/Q_1)^{0.5}$; Q_1 (mm) is read thereby at the 25%-marking and Q_3 at the 75% marking of the sum curve (see image 10). The clay and fine silt components are diminish in the younger loesses of the Lishih- and Malan- series. Through this the average median of the grain curve from under 0,015mm in the Wucheng – loesses raises to 0.03mm in the loesses of the upper Lishih. At the same time raises the sorting grade of the loesses. The sum curves of the middle and late Pleistocene loess is steeper, the sorting coefficient diminishes from 4 to 2. According to the Median and the sorting coefficient, the samples M1-M3 are the most similar to the samples of the lower Lishih. The sample M4 better corresponds in the grain size distribution to the Wucheng loess out of the early Pleistocene (see: **Fehler! Verweisquelle konnte nicht gefunden werden.**)

It is uncertain that, if at the erection of the Terracotta army the inferior sorted older loess sediments had been used by accident or in particular, because of their better properties for the clay building.

2.2.2 limits of consistency after Atterberg, grain density and carbonate content

For binding soils, the state of condition is changing with the water content. At higher water content, they are liquid. If water is extracted from the soil, they transform gradually in ductile (mushy, soft, stiff), half-solid and finally solid state of condition (see image 11). The water contents of the consistency transition are in direct connection with the grain size distribution and the mineral components of the soil. Especially the proportion of fine silt, clay and the quality and quantity of the clay minerals have a great impact on the position of the consistency transitions. Their classifications are fixed from ATTERBERG (1911). The consistency transitions **shrinking limit (w_s)**, **coasting limit (w_p)** and **fluid limit (w_L)** are defined as Atterberg consistency boundaries (see image 26). Their specifications are in mass

Stabilisation of loess clay surfaces at the example of the Terracotta army in Lintong

percentage water content. The plastic limit and fluid limit are the most important basic data for the classification of the plastic malleable conduct of binding soil. The difference between the fluid boundary and plasticized boundary is the plasticity number I_P ($I_P = w_L - w_P$). The plasticity number is measurement for the moisture expansion and the plasticity of a binding soil.

The soil mechanical definition, if it is silt of clay results after DIN 1896 (1988) and the plasticity diagram from Casagrande (see Image 12).

The **activity number** I_A gives the relation between the plasticity and the content of clay ($I_A = I_P / \text{mass.-%} < 0.002\text{mm}$). It is a measurement for the activity and the loading potential of the clay minerals. Soil with an I_A under 1.25 are classified as normal active. While soils with activity numbers over 1.25 are swell able clay minerals has to be anticipated (see image 13) (Soos, 1980).

The limits of the consistency for the soil of Lintong (fluid boundary, plasticity boundary and shrinking boundary) are determined according to the guidelines in (DIN1812T1, 1976) and (DIN 18122T2, 1987).

Grain density ρ_s – Also called specific weight or absolute density- is defined as the correlation between the anhydrous mass (mass of the single components m_s) of soil sample to the volume of the compact mass (volume of the single components V_s : $\rho_s = m_s/V_s$). The grain density depends mainly on the mineralogical compounds of the soil. The mass of the single components m_s t was gathered by weighing the dried sample. The volume of the single components V_s was determined with the capillary pycnometer after (DIN18124, 1989).

The **lime content** is the part of Ca carbonate and magnesium carbonate in weight percentage, relating to the dry mass of the soil. The lime content of the soil samples M1-M4 was determined by gas volumetric after (DIN18129, 1990).

The results of the examinations to the consistency boundaries, grain density and to the lime content of the samples M1-M4 are listed in table2. The mechanical classifications of the soil in Lintong please find in image 11 to image 13.

Stabilisation of loess clay surfaces at the example of the Terracotta army in Lintong

Characteristic number:	Sample number			
	M1	M2	M3	M4
Grain density (g/cm ³)	2,74	2,63	2,7	2,7
Lime content (Gew. -%)	9,7	7,5	11,6	9,2
Clay content (Gew. -%)	12	11	13	25
Shrinking limit w_s (Gew. -%)	5	5	-	-
Plasticity limit w_p (Gew. -%)	19,4	19,0	20,8	18,9
Fluid limit w_L (Gew. -%)	31,8	31,7	31,8	31,7
Plasticity number I_p (%)	12,4	12,7	11	12,8
Activity number I_A	1,03	1,15	0,85	0,5

Table 2: Soil mechanical characteristics of the four samples from the stamped soil of Lintong (measuring data out of MICULITSCH (1996)).

The lime content of the samples is at the lower limit of the usual data in the loess plateau that are numbered from DERBYSHIRE (1982_A) with 8-28%. Addition of lime for stabilisation, that is common at the erecting of stamped soil walls, can therefore be eliminated. The middle grain density between 2.63 and 2.74/cm³ and the component clay also correspond to the specifications in DERBYSHIRE (1982_A).

Stabilisation of loess clay surfaces at the example of the Terracotta army in Lintong

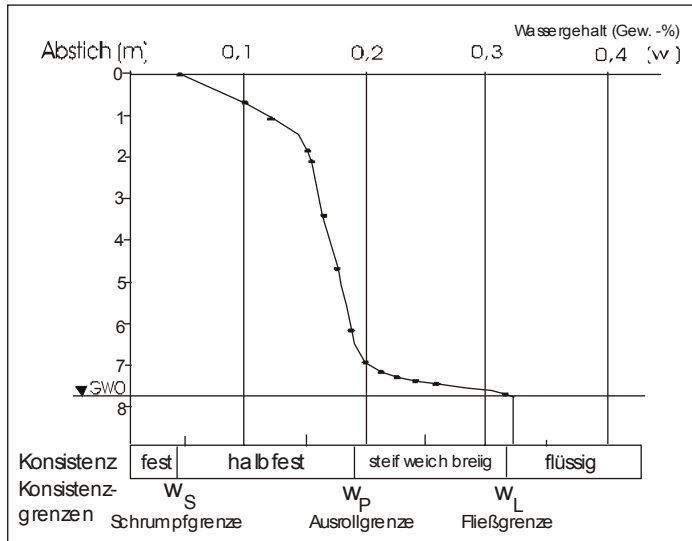


Image 11: Diagram of the averaged consistency boundaries of the stamped soil of Lintong, at the so-called consistency bar of ATTERBERG. Assuming constant consistency boundaries in the soil profile over the humidity distribution, it is possible to read the condition of the soil in the unsaturated zone between the ground water surface and the excavation level (measuring data from the sounding in the well in pit 2, in October 2000).

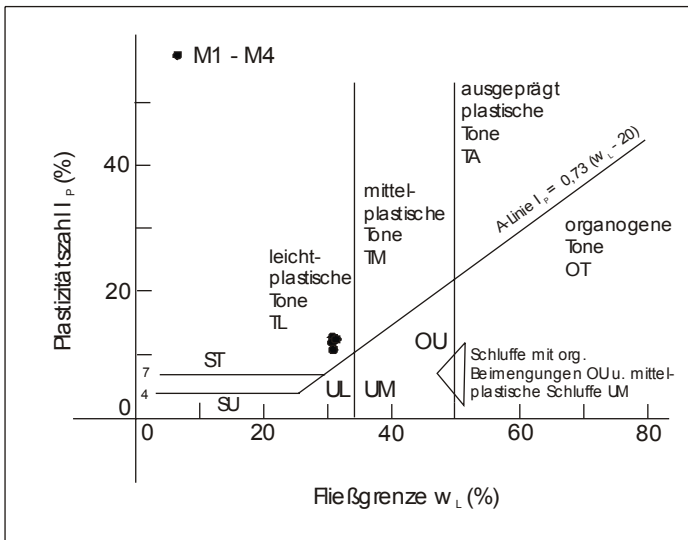


Image 12: Position of the stamped soil of Lintong in the plasticity diagram after CASAGRANDE. After soil mechanical definition, all soils over the A-line are defined as clay. The distinguishing in light, middle or very ductile is orientated at the liquid limit. Therefore, the samples of the stamped soil are classified as light ductile clay (TL).

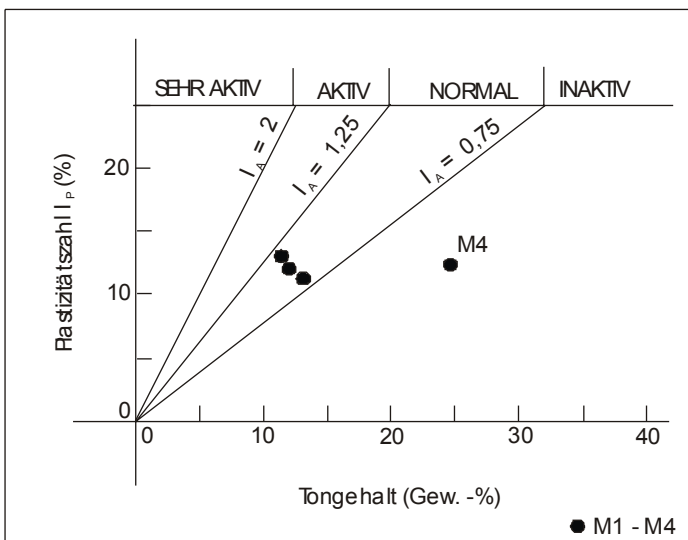


Image 13: The activity number I_A of the stamped soil samples, visualized as the relation between the plasticity number I_P and the clay content from the sedimentation analyse. The content of clay in the soil is classified as normal active or inactive. Swellable clay minerals are not to be expected.

From the comparison of the parameter in table 1: and table 2: together with the bibliographical references over the loesses of the region of Xi'an, it is obvious that at the erection of the stamped clay wall in the pits of the Terracotta army, they made use of loess from the surroundings without the addition of any aggregates.

After DIN 18196 the stamped soil of Lintong, is soil mechanically classified, as light ductile clay (TL) (Image 12). The activity of the clay fraction is "normal active" or "inactive" (image 13) it seems to contain no swellable clay minerals. But the material has to be catalogued due to the classification as TL in the German technical regulations for street construction, as frost sensitive (ZTVE-StB76, 1976)

2.2.3 Shrinkage

The shrinkage, by the drying out of water saturated binding soil, is carried out mainly in the following two steps. As long as the soil is in a two-phase system of mineral particles and water, the volume of the soil diminishes at the same amount as the water. Thereby, the water particles are moving towards each other, and increasingly overlap the enclosed water layers and/or grain contact points develop. This linear shrinking process is called "**Normal shrinkage**". After TARIQ (1993_B) the Normal shrinkage ends after it falls below the plasticity limit of the so-called "swelling limit" (MS) (see image 14). At further water reduction the resistance of the particles rises. The particles are still enclosed by water ("diffuse layer") (see Chapter 3.1). Air penetrates in the large pores and the soil seems lighter. Beneath the swelling limit one talks of "**Rest shrinkage**". The volume of the water in the soil is now further reduced than further compacting of the primary particles (Scheffer, 1998) can alter it. The further water reduction after the so called. "Air entry point" is already in the range of the adsorption isotherm (see Chapter 4.3.3). The water menisci are secluding themselves in more and smaller capillaries; the diffuse layers dwindle. The negative pressure in the remaining water and its contracting strength on the mineral particles thereby the more, the specific surface of the soil particles rises is higher (Scheffer, 1998). The characteristics and the limits of the two shrinking steps are influenced by the mineral composition and by the history of the load of the soil (Tariq, 1993a).

Therefore, they have to be found out for every soil independently. Since drying out soil reacts in the range of normal shrinkage, yet ductile and the particles can still orientate themselves, the soil reacts on the loss of volume with one-dimensional pressure orientated shrinking- "soil setting". Not until the rest shrinking, shrinking cracks are developed.

The critical points during the drying out of the stamped soil derives from the shrinking curve in image 14. These critical water contents from the shrinking curve are important hints for the evaluation of the situation in the pits (see Chapter 1.2).

For example from the diminishing of the water content in the soil of pit 2 (0-2m racking (see image 11) between the bending of the curve (about 16 mass % water content in 2m depth) and the dried out surface due to the linear normal shrinkage results in an average subsidence of 6 to 8cm. The vertical drying out cracks should not be expanding further in the soil than the swelling limit of 11 mass % water content (see image 14). This means in October 2000 a maximum expansion of the drying out cracks up to one meter below the surface (see image 11).

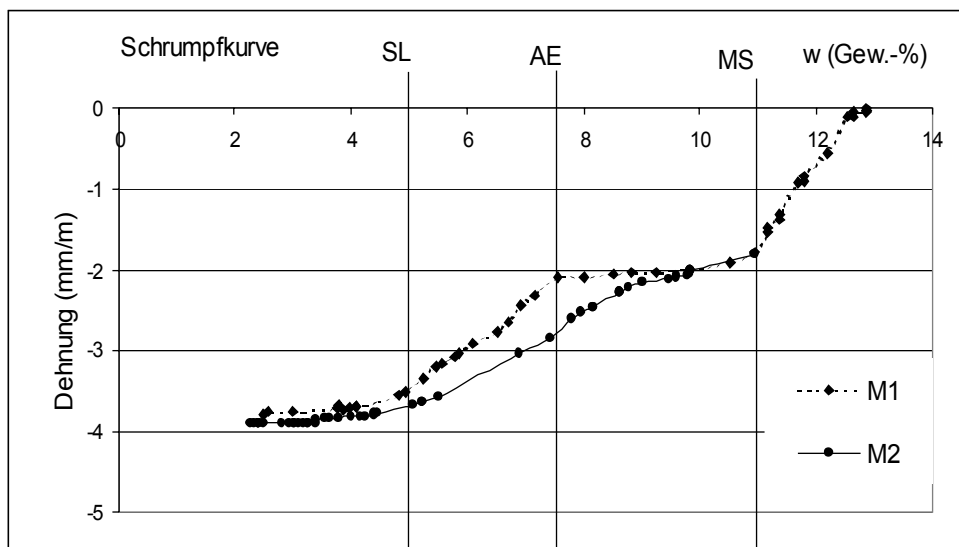


Image 14: Shrinking curves of two stamped soil samples after the measurement results of Miculitsch (1996). Marked are the critical points after the drying out model of TARIQ, AND DURNFORD (1993_{A,B}) SL: shrinkage limit (w_{s}), AE: air entry point, MS: swelling limit (Tariq, 1993a), (Tariq, 1993b). The tests had been carried out at the cuboids of 4x4x5cm. At every moisture step, the regular water distribution was waited for.

2.3 Mineralogical composition and structure properties

2.3.1 XRD Analyses at the bedding preparations and texture preparations.

The sand grains of the stamped soil of Lintong had been analysed under the incident light microscope. There is predominately quartz. Additional acid, alkaline intrusive and carbonate concretions are obvious. Gradually larger light mica, hornblende and pyroxene can be identified.

The mineral phases of the complete clay fraction (< 2 μ m) and of the clay fraction under 0.63 μ m grain size have been analysed separately with a diffractor meter from the Company Siemens Type PW 1800, with CuK α X-ray at an detecting rate of 1.5° 2 θ /min. The clay fraction under 0.63 μ m is measured separately, because of the largely missing quartz, feldspar, etc in the middle clay area and fine clay field. This

Stabilisation of loess clay surfaces at the example of the Terracotta army in Lintong

eases the evidence of small amounts of swellable clay minerals (e.g. smectite and vermiculite (Tributh, 1979), (Heim, 1990). The often coexistence of chlorite and Kaolinite in loess sediments makes it necessary for additional heating of the preparation at the use of the diffractometer analyses, because of the overlapping of the 002-reflex of chlorite with the 001 reflex of Kaolinite (Ruhe, 1982), (Bailey, 1988). That is why at the middle and fine clay fraction ($< 0.63\mu\text{m}$) a sample has to be heated up to 450°C for 15 minutes, a secondly for two hours at 600°C .

Swellable clay mineral components shall be identified with the glycerine- swelling samples. The settings up of the swelling samples have been done from the guidelines of HEIM (1990).

In the diffractometer diagram of the complete clay fraction, the stratum silicates of the muscovite –illite row and chlorite are dominant over quartz, feldspar and calcite (see image 15).

The analyses of the different samples in the middle and fine clay fraction are compared in image 16. The contingent of quartz and feldspar are in the clay fraction just barely there. Crystalline calcite does not show up any more. In comparison to the complete clay fraction (image 15), the relation between the chlorite to the muscovite illite row diminish. Swellable three stratum silicates (smectite, montmorillonite and vermiculite) and Kaolinite are detectable.

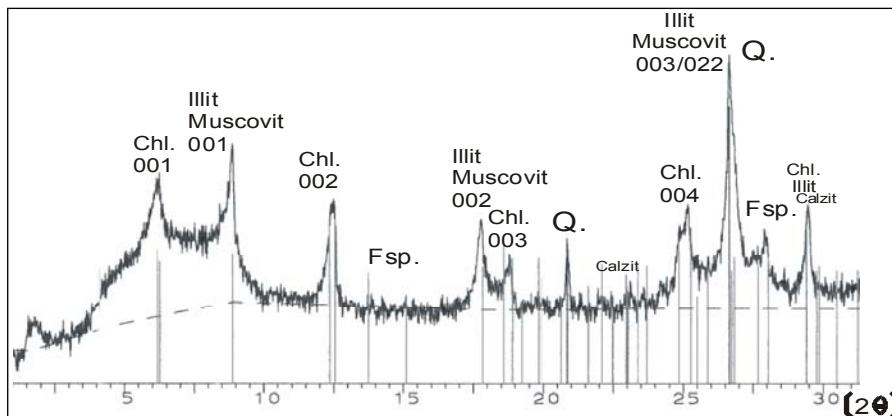
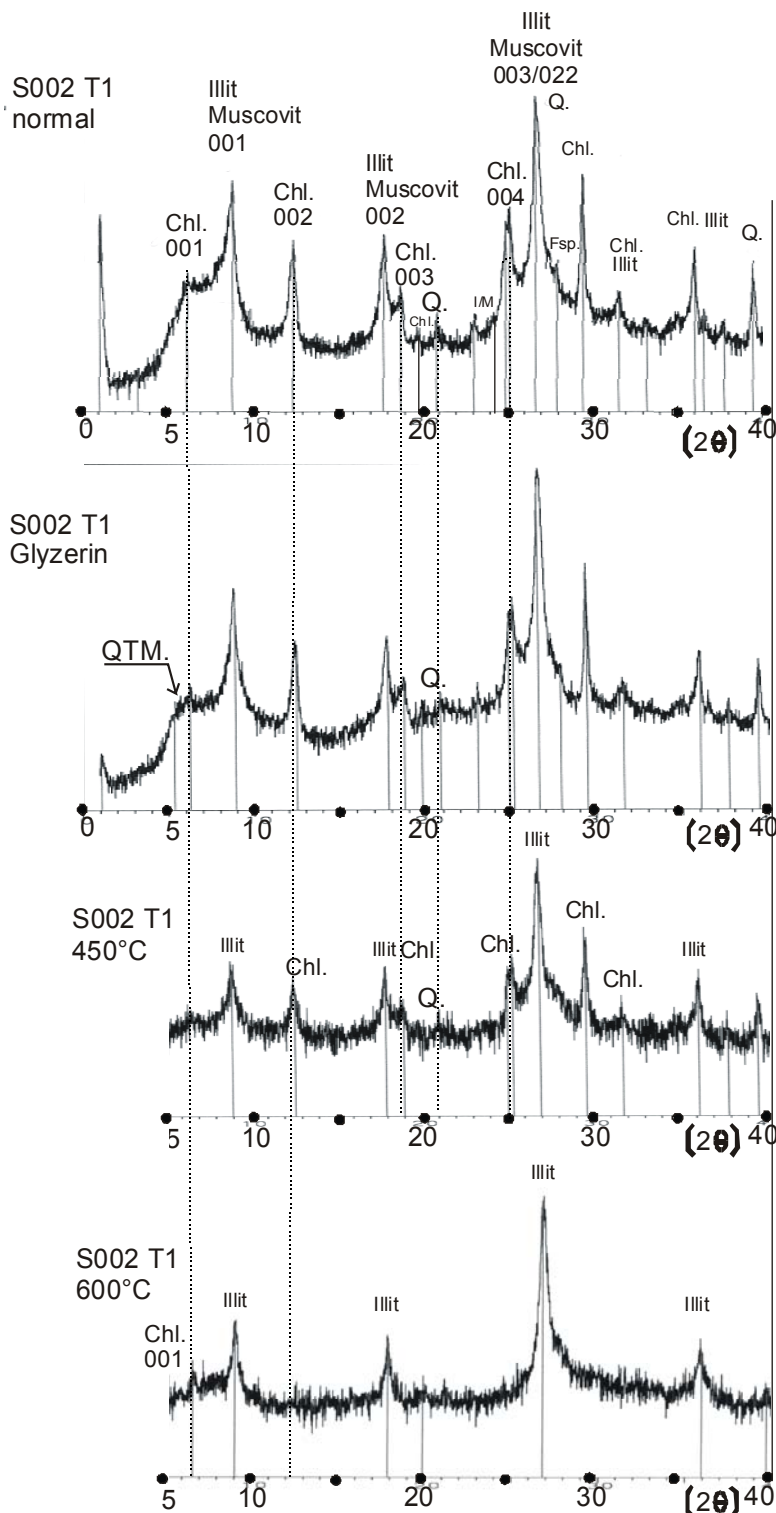


Image15: Diffractogram of the structure samples of the complete clay fraction ($< 2\mu\text{m}$) of the sample S002 quartz (Q) and feldspar (Fsp.) out of the rough clay fraction are clearly detectable. The 001 reflexion of the chlorite emerges noticeably. Illite-muscovite- row (I/M); chlorite (Chl).

This set of minerals in the silt fraction and clay fraction of the stamped soil is often in the loess plateau- but there also exists many kinds of analyses, in which smectite, montmorillonites and Kaolinite as important components of the clay fraction could be detect (Derbyshire, 1982b), (Derbyshire, 1982a). Chlorite can be often found in loesses. Especially the larger aggregates has to be seen mostly as pedogene new

Stabilisation of loess clay surfaces at the example of the Terracotta army in Lintong

sprouts out of amphibole, biotite, or similar (ground chlorites) (Heim, 1990), (Scheffer, 1998).



In contrary to the complete clay fraction (see image 15) the reflexion bands of Q.; Fsp. and calcite are widely gone. The 001- reflex of swella- ble three stratum minerals (~ 12-20 Å) is missing. The structure density d0 14.1-14.5 Å (001 reflex of the chlorite) is weaker, but still clearly seen.

In the swelling sample, there is no clear reflex of widened structure units with $d > 15\text{Å}$ in evidence. At veritable contents of smectite, montmorillonite or vermiculite many reflex ions between 2° and $5^\circ 2\theta$ are to be expected (Heim, 1990)

The starting of the dehydrating of the independent octahedron layers in the chlorite leads to the distribution of the 002 reflex. At mixtures with the Kaolinite that is stable up to over 500°C , two maxima would be visible at the tempering (Bailey, 1954), (Biscaye, 1964).

At temperatures, over 600°C from the chlorites only remains the 14Å -Reflex (Bailey, 1988). In addition, the 10Å - structure units of the K^+ -fixed three-stratum minerals are remaining.

Image 16 Diffractograms of different texture samples of the middle and fine fraction ($< 0, 63\mu\text{m}$) of a soil sample. It dominates the non-swella- ble three stratum minerals of the illite- muscovite – row (I/M) and the non-swella- ble chlorites (Chl.), quartz (Q.) and feldspars are in the range of the detection limit. Swella- ble clay minerals (QTM) are not visible.

2.3.2. Thin section microscopy at undisturbed soil samples.

To produce thin sections with 30µm layer thickness out of undisturbed clay samples a previous consolidation with synthetic resin is essential. For the examination at the sections colourless and stained consolidates have been used. The staining should help the visualisation of the porosity. However, due to the low viscosity of the consolidation material, this effect was only at large capillary pores successful. Additionally the staining disturbs the natural colours in transmitted light and the pleochronism of the clay mineral phases.

The thin section pictures in image 17 and image 19 are giving information about the main structure characteristics of the stamped soil of Lintong. The structure is none layered and none textured. In the microscopic and in the macroscopic view it has to be seen as coherent structure (Scheffer, 1998). It consists out of a brown yellow silt matrix, in which- uniformly distributed- angular fine sand grains swims (image 17 and image 18). Matrix supported clay structures, especially with a high clay content are by far more ductile, but less stable under pressure as grain supported. They achieve, due to the supporting effect of the grain contact in the fine sand area, higher compressive resistances (Müller, 2002). In the fine sand component, quartz dominates over stone fragments, calcite and feldspar. Additionally in the middle and rough silt of the matrix (0.0063-0.063 mm), none rounded quartz and rounded at the edges quartzes, that are typical for loess stand out. Significantly, there are often etched (solved) carbonate clasts. The rate of the layer silicates (muscovite, chlorite and weathered biotite) dominates the picture, due to the high interference colours of these minerals. At a closer look, it is possible to estimate the proportion of quartz in the middle and rough silt area at a minimum of 60%. Red and black hydroxides and oxides (Goethite, hematite) are filling the pores gussets or attached at larger layer minerals (see image 18). Higher proportions of iron hydroxides also lead to a macroscopic darkening of the colour impression. In contrast to that, zones with microcrystalline carbonate separations; that are often found in the surrounding of larger pore structures, change the colour impression into a light yellow beige (see image 19).

The real inter crystalline matrix porosity between the mineral phases is difficult to resolve in the microscope and cannot be seen in the images. Clearly visible are the spherical large pores (10-200µm) that had been created by water inclusion during the compacting of the stamped soil at the erection of the clay walls. These pores are often lenticular squeezed; due to the pressure during the packing d clay, walls (see Image 18). Round sections of the pores give the conclusion of root channels. The microbiological decomposition of the organic filling and precipitations out of the soil

Stabilisation of loess clay surfaces at the example of the Terracotta army in Lintong

solution could be the reason for the often seen carbonating at the walls of the pores.
(See image 19).

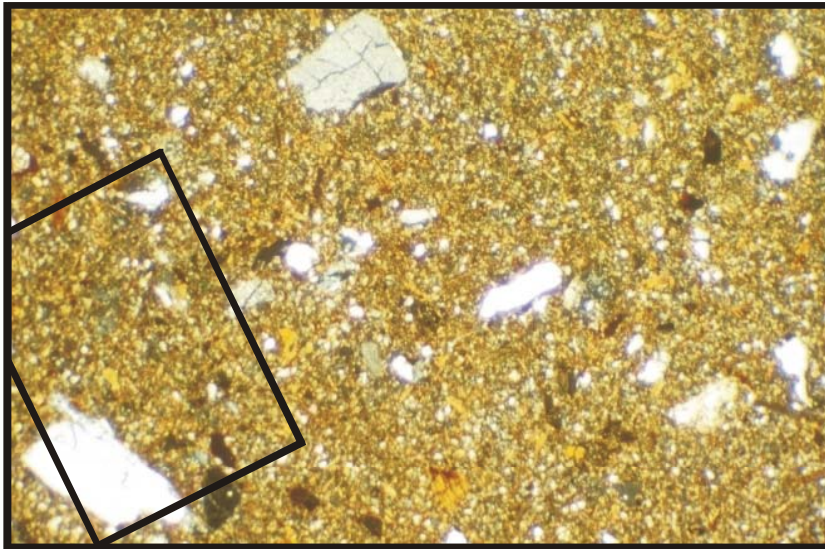


Image 17

Thin section image; X-pole filter; the image base line is approximately 2.7mm. The structure is matrix supported. Edge rounded, square and components out of quartz, feldspar, carbonate and stone fragments of the fine sand fraction are swimming together with larger mica in a yellow red silt matrix. A rectangular section of the matrix is shown in detail in image

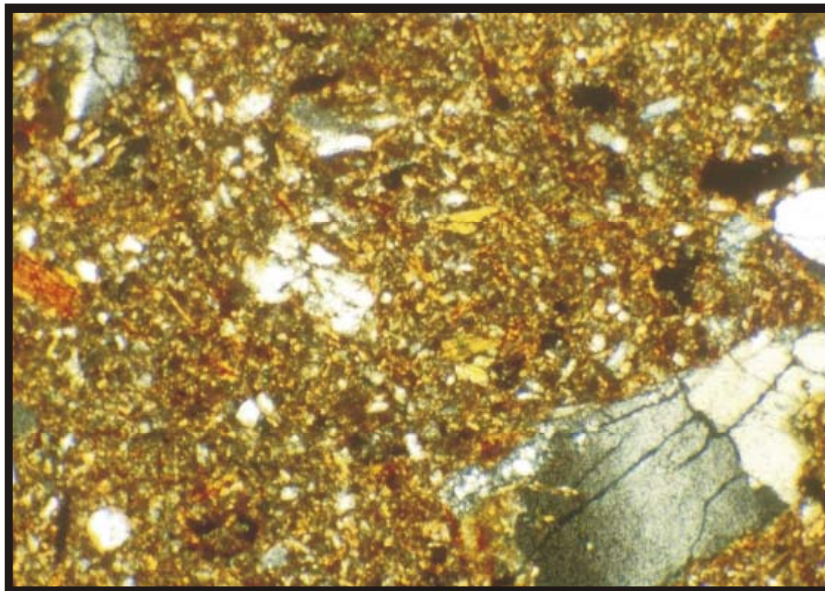


Image 18

Thin section image; detail out of image 17, X-pole filter, the image base line is approximately 1 mm. The matrix has no poled texture. Spherical rough pores (10-200µm), that are deriving from water inclusions, during the compacting of the stamped soil, appear black in the image. The red staining is due to the needle and foliaceous iron oxides and iron hydroxides.

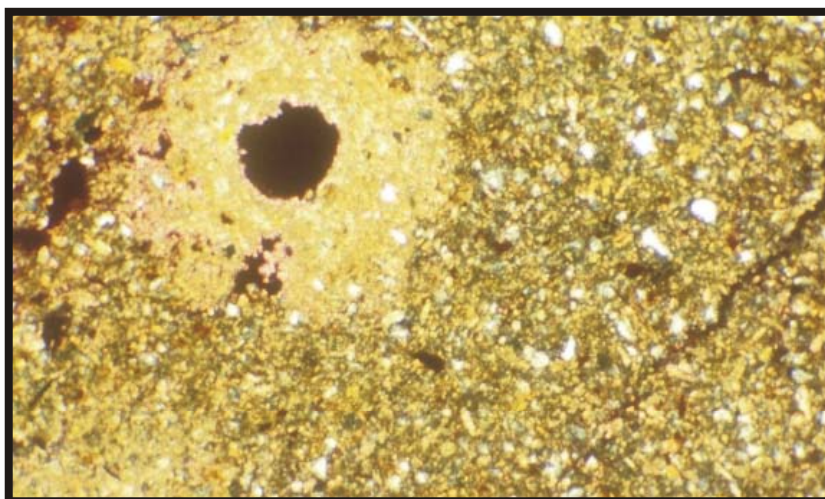


Image 19

Thin section image; X-pole filter, the image base line is approximately 1.3 mm. Areas with a high content of carbonate (mostly calcite) appear due to the high refraction yellow beige. The section shows the carbonated edge zone of a root channel.

2.3.3 Kryo-SEM images at undisturbed samples

Raster scanning microscopic analyses can be used effectively for the qualitative evaluation of the corn structure in the silt and rough clay area. Further, the use of a Kryo table enables one to visualize the reaction of the structure with moisture. The results of the structural changes due to swellings in wetted samples are explained in chapter 3.4. The examinations have been carried out at the material testing institute in Bremen on a Hitachi S4000 Kryo table. They are focussed on fresh fraction surfaces at undisturbed stamped soil samples at three different moisture levels.

- Dried samples: 48h drying at 60°C, cooling in the exsiccator over a drying agent, Kryo-preparation in melting nitrogen, freeze fracture.
- Normal climate: conditioning of small samples (approx. 2cm³) over 48h at 65% relative humidity.
- Plasticity limit: (images of this step in chapter 3.4). Moistening of a sample with 18 mass % water deionised, 24h storage- rapped in PE plastic film (for the even distribution of the moisture in the sample). Kryo-preparation in melting nitrogen, freeze fracture.

The observations from the thin section microscopy to the composition of the soil are confirmed by the SEM-examination. Larger fine sand grains are floating in a compact matrix out of spherical and platy silt components (see image 20). The matrix consists mostly out of angled and at the edges rounded quartz, feldspar and mica that build up a grain-supported structure with a high porosity between the grains (image 21 and image 22). This inter granulated matrix pores consist of spherical pores with good cross-linking. The pores diameter is up to 15µm.

Singularly, there are also accretion (coagulates) out of clay, fine silt in silt grain size (image 22). The pore sizes inside these accretions are in the scope of 0.1-1µm. Clay and fine silt create, in addition, storage pads between the grain contacts of the silts or garland like connection structures (Image 21). At the grain contacts of the silt matrix dominate “edge to face“ and “edge to edge“-contacts.

The texture and the matrix can be called as non-directional and spherical porous.

Due to the relatively small content of clay, the structure is all together very “clean“ and open. However, all the silt components are covered with a fine clay layer (image 23). The clay minerals are lying mostly in “face to face“ contact to each other and give, due to the surface of the components, a laminated scaly texture. The thickness of the layer of the coatings varies, it is mostly under one Micrometer (see image 23

Stabilisation of loess clay surfaces at the example of the Terracotta army in Lintong

and image 24). In this surface layer, that continues also between the contact points (mostly thickened), the main part of the clay minerals of the micro porosity seems to be concentrated. (see chapter 4.3.3).

The coatings of the silt grains are typical for Aeolian sedimentary loesses (Smalley I.J., 1973). At fluvial coatings, it is often washed off. The accretion out of clay and fine silt are also an indication against a fluvial sedimentation of the raw material (Derbyshire, 1982b).

The Matrix structure of the stamped soil of Lintong matches the description of DERBYSHIRE (1982B) of the microstructure of Aeolian Malan- and Wucheng loesses out of the east of von Xi'an positioned Meng Xiang.

An open, non-textured matrix structure with existing accretion (coagulates) and missing clay minerals, (how they deposit themselves in the recent water menisci during the drying out of the pore gussets of the dispersion) indicates a low water content of the raw material during the building of the stamped earth wall (Houben, 1994). The water content during the compacting at the building of the stamped soil wall has a strong influence on the building structure of the dry clay. The structure of the stamped soil of Lintong indicates for a low water content during the building, was in the range of the w_{PL} or lower (w_{Pr} = optimal

Water content out of the proctor curve ~ 14 mass-% for the stamped soil of Lintong), but in any case beneath the coasting limit (about 18 mass-%)

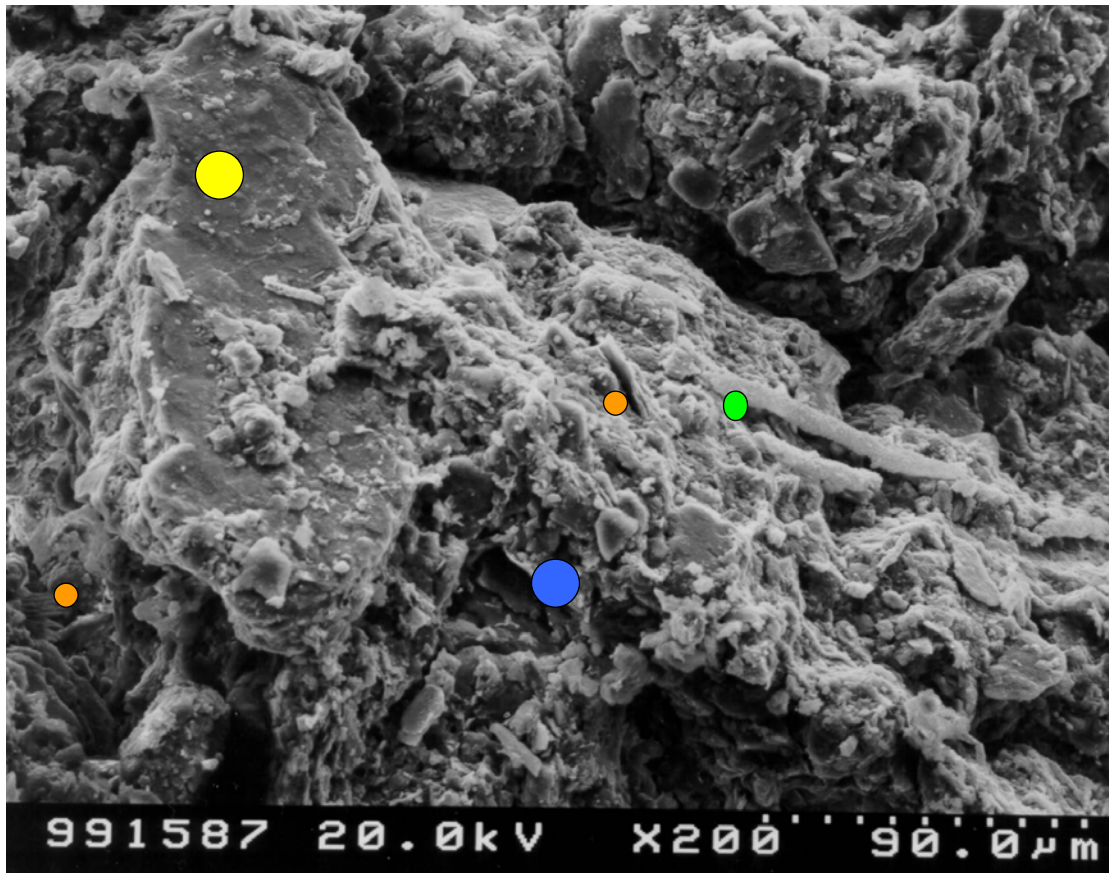
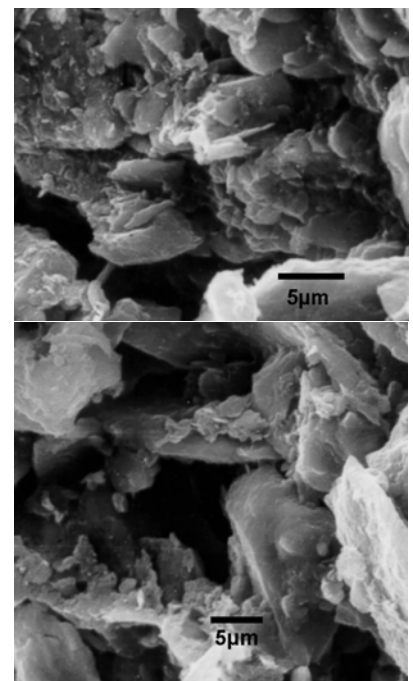
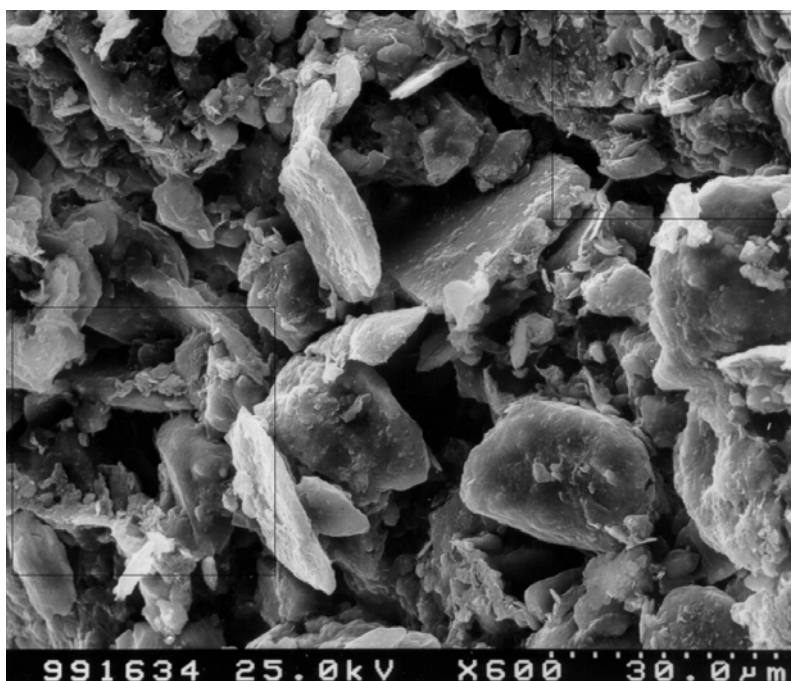


Image 20:
Kryo-SEM image (secondary electronic image) of a stamped soil sample with “norm climate”. Conditioning: Overview image over the structure of the stamped soil. One fine grain content (yellow) floats in a undirected silt matrix (Blue). Singular larger stratum silicates can be seen in a typical chart house structure and larger Oxalate – tubes (green).



Stabilisation of loess clay surfaces at the example of the Terracotta army in Lintong

Image 21:

Kryo-SEM image (secondary electronic image) of the matrix of a dried stamped soil sample. The structure building silt grains have a diameter of 5 – 25 μm . Spherical quartz and platy shaped stratum silicates are square-edged or slightly rounded at the edges. The texture of the components stands out due to its missing orientation and space creating “edge to face“ and “edge to edge“ contacts. The grains are mostly only over clay bridges adnated. These loose structures creates a lot of space for the inter particle matrix porosity with a pore diameters of up to 15 μm (see.: chapter **Fehler! Verweisquelle konnte nicht gefunden werden.**). In the detailed enlargements, you can see that the fine silt- and clay fraction accumulates its own aggregates (coagulate) (above) or attaches to the surfaces of the larger grains (below).

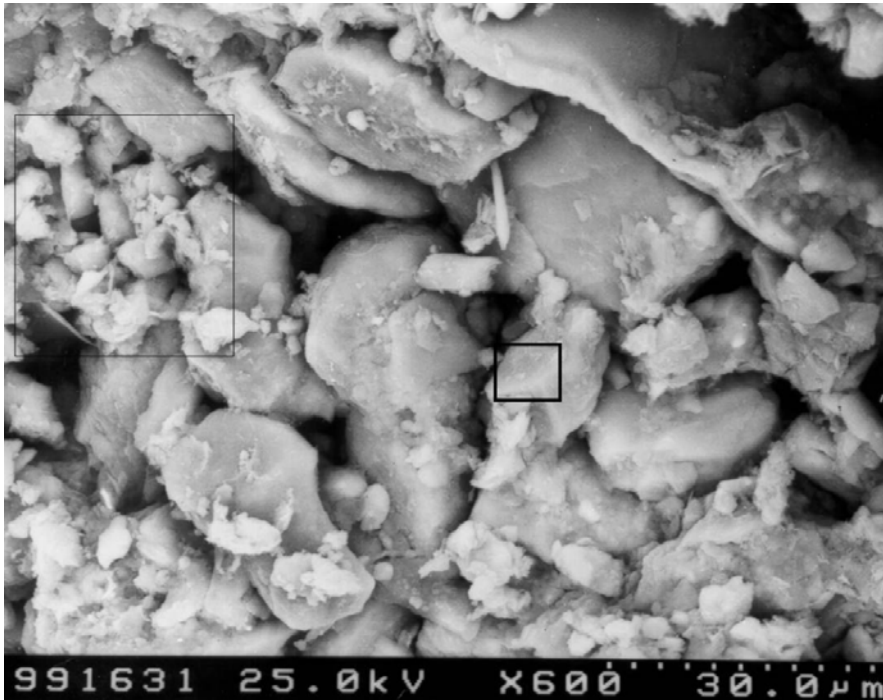


Image 22:

Kryo-SEM image (reflective electronic image) from the matrix of a dried out stamped soil sample. The structure is denser packed as in image 21. Large pores are often filled with coagulates of spherical fine silt and rough clay particles (e.g. quartz) (small frame). The inter crystalline porosity between these particles are in the area of 0.1 to 1 μm pore diameter (see. chapter 4.3.3)

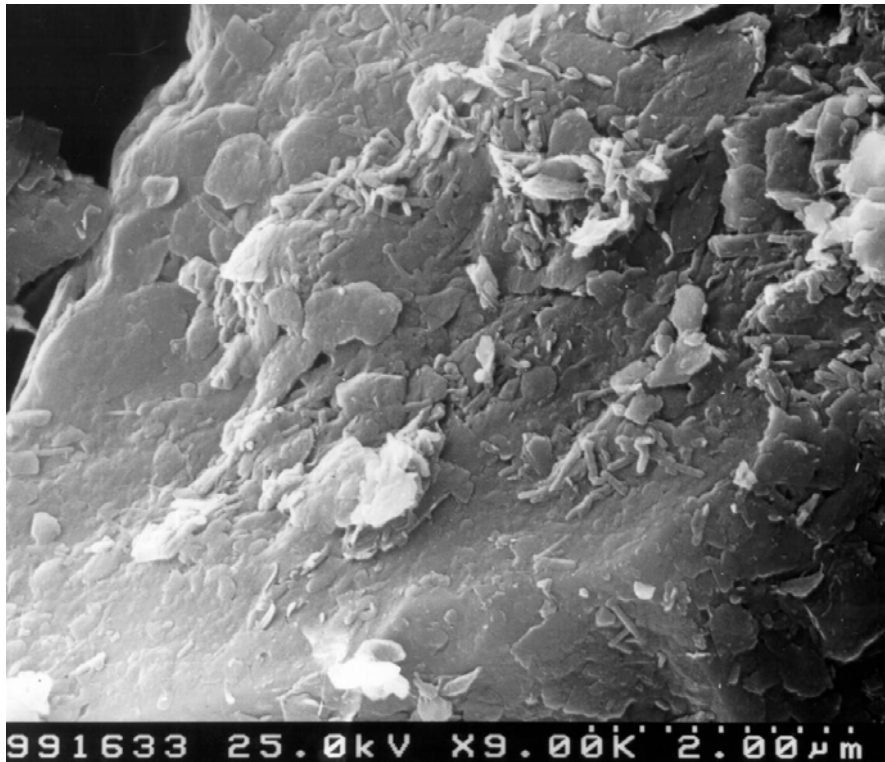


Image 23:
Surface of a quartz grain in the secondary electronic image- Detail out of image 22 (darker edge frame). The surfaces of the silt grains are coated with several stratum clay minerals. Inside these “coatings” lie intercrystalline porosity with pore diameters of max. 0.01µm.

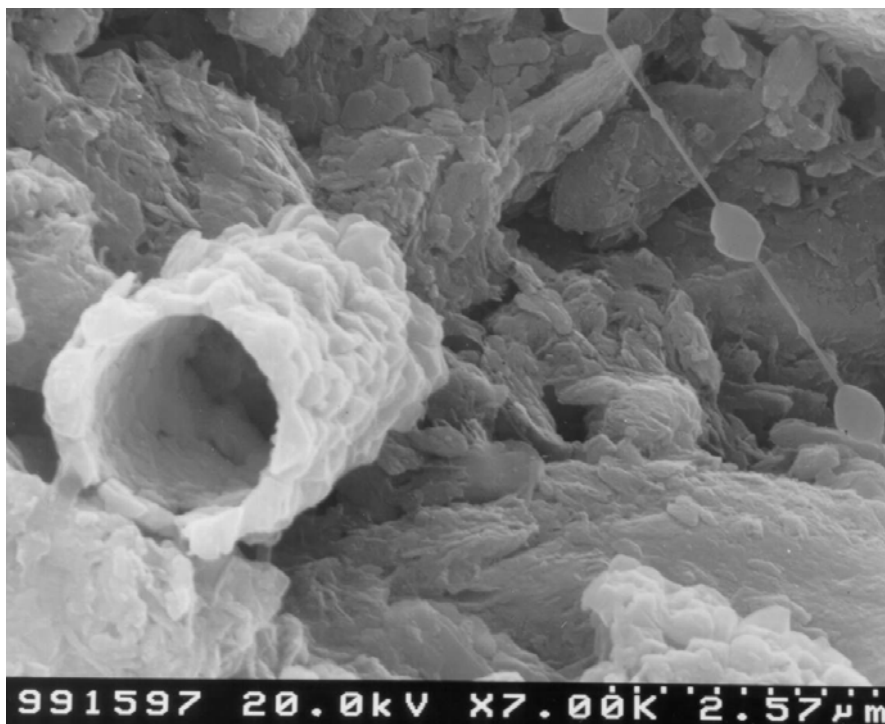
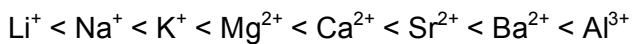


Image 24:
Kryo-SEM image at normal climate (secondary electronic image). The oxalate tube in the front and the pearl necklet shaped structure in the background of the picture are selected examples of a lot of evidences from former and recent microbiological growth in the pore space of the stamped soil. The tube is lying on “felt” out of clay minerals.

2.3.4 Determination of the CEC and the exchangeable cations

At the negative loaded layer surfaces of the clay minerals, cations attach. This applies also to the outside surfaces as for the inner layers. At the surfaces and at the expandable interlayer they can be exchanged easily with other ions with equivalent loadings (Heim, 1990). The respective concentrations of the different cations at the loaded elementary layers of the clay minerals are subject to the concentration in the surrounding Electrolyte. More important is their specific bond strength (assembly strength), because the cations are differing in their built-in strength, due to their relation between the valence and atomic size, this attaching is selective.

Inside the periodical system, the assembly strength increases with the increasing valence from left to right and inside the same group from top to bottom with the increasing radius of the "bare", non hydrated atoms. Out of these the lyotropic series results, in this the cations are sorted due to their assembly strength. Lyotropic series after HEIM (1990), the assembly strength increases from left to right:



The cationic- exchange capacity (CEC) of a soil is the sum of the exchangeable cations, specified in mval/100g.

For the cationic exchange capacity, not only the swellable three stratum minerals with their expandable Z layers contribute but also the surfaces of the clay minerals with their permanent charge.

The CEC is a value for the activity and quality of the clay minerals in the soil. It is an important parameter for the biological-chemical reactivity of the soil (nutrient adsorption capacity, heavy metal binding, etc.) and for the soil mechanical attitude (swelling ability, thixotropy, plasticity, strength, etc). It depends on the pH value and is refers to the mineral soil to a neutral milieu (pH 7 or 8.2).

The maximal possible CEC is at carbonate containing soils with a pH 7-8 the actual is the same as the effective CEC. In acid milieu, the actual CEC measured in the real pH value of the soil, stays behind the potential CEC at pH7 (Schwertmann, 1984).

The determination of the CEC was carried out with the barium chloride method after Mehlich, as recommended in (DIN19684, 1977) for mineral soil. Five grams of an air dried soil sample are extracted four times with a pH 8.1 buffered loading solution out of Triäthanolamin and barium chloride. Thereby exchangeable soil cations are exchanged with Ba^{2+} -Ions. The exchanged soil cations in the solution are measured quantitatively with the atomic adsorption spectrometer (AAS).

Afterwards the exchanged Ba^{2+} -Ions in the soil material are exchanged back with Ca^{2+} -ions with potassium chromate solution and precipitated with barium chromate.

Stabilisation of loess clay surfaces at the example of the Terracotta army in Lintong

The precipitated amount on changed and re changed barium is measured in the solution colorimetric.

From the amount of the bariums per 100g soil and the equivalent weight of barium, the cations exchange capacity of the soil is calculated.

Following the guidelines in KRETZSCHMAR (1984), this method was carried out at three samples on the stamped soil of Lintong. The results are summarized in image 25. In AAS, the content of sodium, potassium, magnesium, calcium, iron and aluminium was measured.

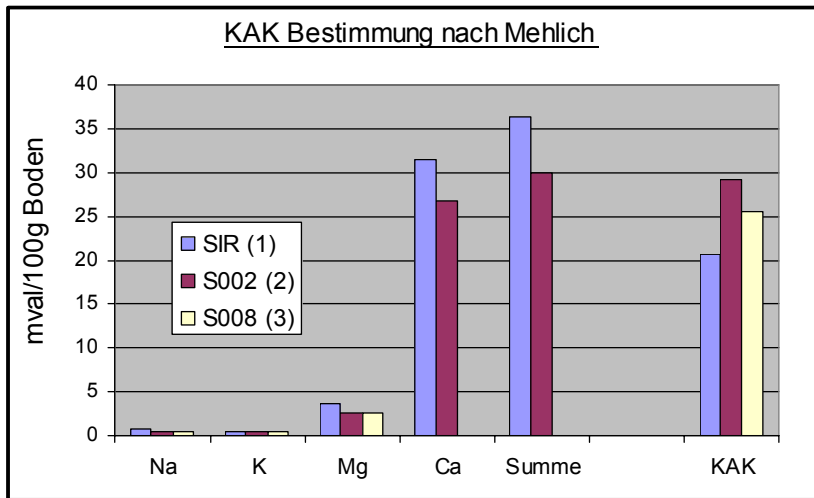


Image 25:

The exchangeable cations with the total values and the potential cation exchange capacity in the three soil samples of the stamped soil in Lintong. At sample S008, the exchanged Ca^{2+} -Ions were not measured. Iron and aluminium, at all samples, were under the detection limit.

At the clay minerals in 100g stamped soil are 7 - 12mg Na^+ -, 12-15mg Ca^{2+} -, 30 - 45mg Mg^{2+} - and 500-600mg Ca^{2+} -Ions attached and exchangeable. At lime containing soils, it is possible that- in the case of sample SIR (1) - the sum of the exchanged cations is over the loading equivalent of the CEC because at the loading procedure, lime is dissolved and enlarges the Ca^{2+} part. Aside from this, the vast accordance of the loading equivalent in the CEC with the sum of the exchanged cations, shows that the most important cations had been detected and that these are really derive from the agglomeration places of the clay minerals and not from soluble salts.

According to SCHEFFER (1998) this cation layer of the soil minerals is typical for soils from farmland in a humid moderate climate. According to this Ca^{2+} predominates, as long as the pH is more than 5 (the pH from the stamped soil is between 6.7 and 7.0). Then follows Mg^{2+} . The amount of K^+ - is mostly under 10%, the amount of Na^+ - mostly under 1%, because Na^+ is weakly bonded.

In addition, the cation exchange capacity of the stamped soil goes with 20-30mval/100g soil according to the normal values of mineral soil. These vary

Stabilisation of loess clay surfaces at the example of the Terracotta army in Lintong

depending on the amount and quality of the clay minerals between 15 and 50mval/100g in the soil (Kretzschmar, 1984). Rich in humus upper soils can achieve higher exchange capacities. In table 3: there are listed the CEC values of the most important clay mineral groups

Kaolinite	Chlorite	Allophane	Illite	Smectite	Vermiculite	original soil components
3-15	10-40	10-50	20-50	70-130	150-200	200-300

Tab. 1: Table 3: cation exchange capacity at pH7 in mval/100g after HEIM (1990) and KRETZSCHMAR (1984)

3. Interaction between the solid phase, air and water in the soil

Soil is a material, which is composed from different components and different phase conditions. It consists of a gas phase (air), liquid phase (water) and solid (mineral and organic components). The phase and the most important material technical properties of the soil are dominated, especially at binding soils with a high content of silt and clay, from the interaction between water and the solid phase. Thereby the clay minerals with the clay and fine silt fraction are of special importance.

3.1 Types of bonded water in mineral soil

Water that infiltrates into the soil or that is bonded by the soil can be divided into different "kinds of water", owing to the type of binding at the solid. The forms of the binding with their properties are explained in image 26 and table 4. Which of the kind of bindings dominates, and therefore determines the consistency phase, depends on the complete water content of the soil and is also primarily on the proportion and quality of its clay minerals.

Stabilisation of loess clay surfaces at the example of the Terracotta army in Lintong

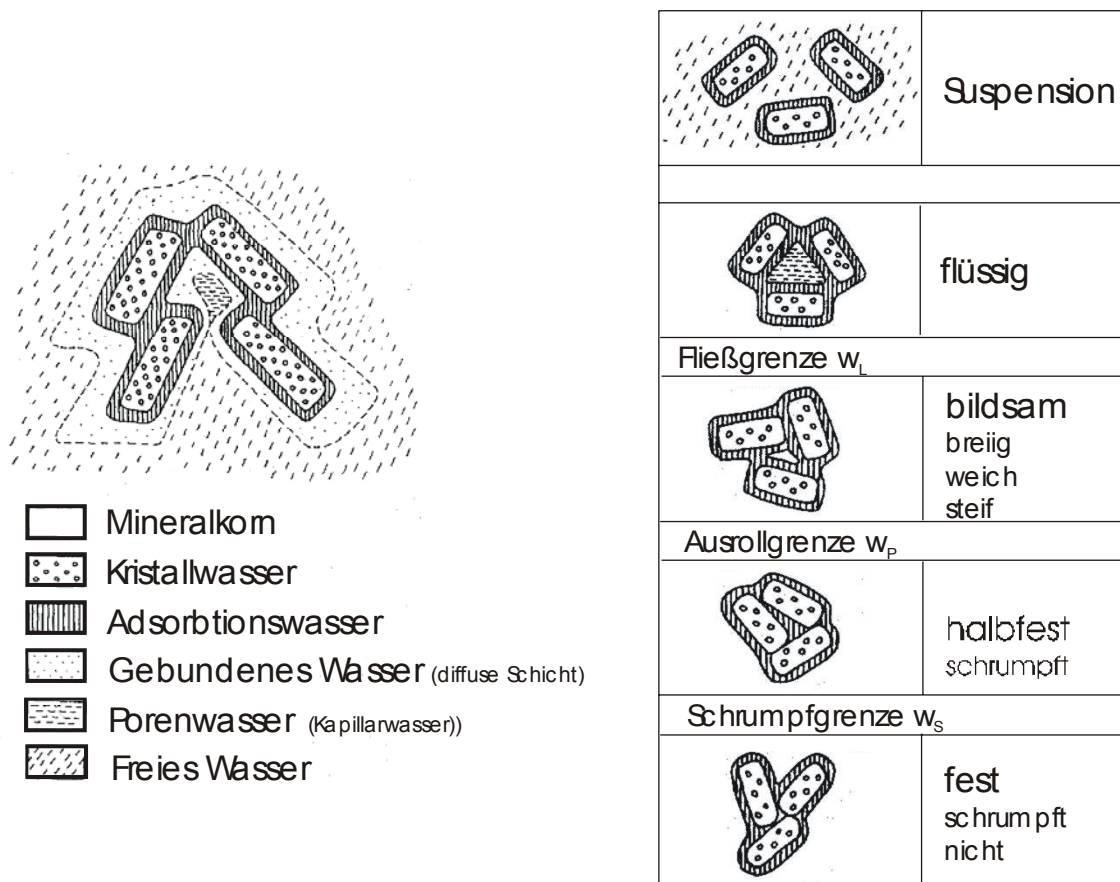


Image 26 left: Binding forms of the water at mineral soil components.

Right: Simplified picture of the phases of the soil and their transmissions, after HOUBEN (1994). The bonded water and the adsorbed water are summarised in the hatched areas.

Differing water terms:	Description and properties
Free water	Free water, is pore water in large pores (> 1mm) that moves freely in the pore space, following the laws of the hydro static pressure. In nature, it appears at free water saturation in the area of the ground water or at open rain. It leads to the dispersion of the clay mineral structure without any pressure from the surrounding. When this sample is taken out of the water, the free water is seeping due to gravitation out of the sample.
Pore water/ Capillary water	The pore water accumulates between (but not at) the clay particles. In the capillary pores, (0.1-1000µm pore diameter), due to the tension at the borders between air, water and solid wetting angles are created that lead to the formation of menisci between the mineral particles. The water menisci of the pore water have under pore pressure a cohesive impact onto the pore structure. The pore water is isotropic. It does not differ in density and concentration of electrolytes from the free water. Its movements are not controlled by the isostatic pressure, but from the capillary strength. Especially small pore radiuses are being filled with water already in the hygroscopic range are over 50% relative humidity due to the capillary condensation (see Chapter 4.3.3). Pore water can be removed by long drying at room climate or at oven drying at 50°C.

Bonded water/ Diffuse layer	The diffuse layer is a coating water film around the clay minerals, in that the loading potential between the loaded adsorbed water and the surrounding, non-loaded electrolyte is slowly degraded. The smaller the distance of the water molecules and the cations of the diffuse layer to the intra crystalline water, the more oriented, compact and denser they are supported and the higher are the cation concentration. The thickness of the diffuse layer depends of the loading of the clay minerals and from the electrolyte concentration in the pore solutions. The ductile property of clay containing sediments is often explained on the strong formation of this diffuse layer. The bonded water is able to evaporate at room temperature.
Adsorbed water/ intra crystalline water	In moveable water dipole and cations, that are accumulating at the negative loaded tetrahedron layers (between the inner layers and at the surfaces). In the interlayer up to four layers of water can be accumulated (~10Å , depending of the cationic assignment .This loading bonded water has to be seen as an undirected, compact hardly immoveable layer (Star layer), that acts more like a solid (Pimentel, 1996). The intra crystalline water is being adsorbed in the hygroscopic humidity. Evaporation at temperatures between 100 and 200 °C. is reversible
Crystal water/ structural water	Not water in the main sense, but hydroxyl groups, which are tightly built-in in the crystal grid of the minerals. In clay minerals, the crystal water is situated in the simple octahedron layers and in the additional octahedron layers of the four stratum chlorites. Only at temperatures more than 550°C (additional O-layer at the chlorides), the crystal water can be removed. The grid structure of the clay minerals is irreversibly changed.

Table 4: Different kind of water at clay minerals (after (Heim, 1990), (Houben, 1994), (Scheffer, 1998) and (Pimentel, 1996).

3.2 Swelling in clayey structures

The properties of the above-mentioned types of waters implicate three different working swelling mechanisms. The swelling mechanisms are called intra crystalline swelling, osmotic swelling and mechanical swelling and deploy their effect with increasing water supply, in this order (ISRM, 1994), (Einstein, 1993).

Inter crystalline swelling:

The inter crystalline swelling relies on the hydration of exchangeable cations in the intermediate layer of swellable three stratum minerals and on the outside surface of the clay minerals. The impact of the hydration energy is spatially limited to the thickness of one elementary layer (~10 Å). Thereby maximal four water layers can be attached, depending on the cationic loading (**adsorbed water/ inter crystalline water**). This is at the hydration of an intermediate layer equal to the doubling of the mineral volume (Heim, 1990). The agglomeration is adsorptive in the hygroscopic humid area (table 5). Depending on the cationic loading of the elementary layers at the inter crystalline swelling pressure between 200 to 400N/mm² can arise (Van Olpen, 1963).

cation	32% rel.humidity.	52% rel. humidity	79% rel. humidity	water
K ⁺	11,9	11,9	12,1	non determined
Na ⁺	12,5	12,5	14,8	non determined
Ca ²⁺	15,2	15,1	15,5	19,0
Mg ²⁺	15,1	15,1	15,2	19,5

Table: 5: widening of an montmorillonite in Å, at different intermediate cations and relative humidity (Mac Ewan, 1984)

Osmotic Swelling:

During the further filling of the pore spaces, the diffuse double layer agglomerates around the clay minerals, there, the electrical potential between the surfaces of the hydrate coating of the adsorbed water and the pore solution diminish. With the help of diffusion actions, the added pore water attaches into the **diffuse layer**. This agglomeration procedure tries to adjust the ion concentration of the diffuse layers to the concentration of the pore water (osmotic equilibrium). At diffuse double layers between two clay mineral surfaces or in the widened intermediate layer of sodium – montmorillonites the osmotic swelling leads to the swelling of the mineral surfaces. The degree of the osmotic swelling depends on the specific surface loading and the cations in the diffuse layers, mostly on the ion concentration in the pore water (Heim, 1990). In contrary to demineralised water the osmotic swelling of water with high Electrolyte concentrations is reduced up to a tenth (Pimentel, 1996). The swelling pressure at the osmotic swelling is much smaller, than the one caused by inter crystalline swelling. They are in the range of 3N/mm² (Madsen, 1988).

Mechanical swelling:

The reason for the change of the content of **free water** is mainly of mechanical nature. The water agglomeration with increasing volume is favoured by the isostatic pressure from outside and it is called therefore mechanical swelling. It becomes e.g. operative at the storage of a soil sample under water. After Pimentel (1996) the swelling pressure of this swelling is ten cubing lower than at the osmotic swelling.

3.3. The structural preservation effect of the water in binding soil

Binding soil has in dry or dried condition a solid structure. This divides them clearly from the other rough grain kinds of soil such as sand or flint. The cohesive interaction in dry silt or clay is explained with the attractive force between the loaded (clay) mineral surfaces that become operative at proximity less than 1.5mm (Scheffer, 1998). To this count: the Van-der Waalsche-forces between atoms and molecules,

Stabilisation of loess clay surfaces at the example of the Terracotta army in Lintong

Coulombsche forces between the positive and negative surface loadings and bridge bindings over chain molecules.

Water access leads primarily to the softening and dissolving of the soil structure. Considering overall, the impact of water on the structure of binding soils is ambivalent, because, depending on the kind of water on one hand, it pushes the mineral structure apart (intra crystalline swelling, Osmotic swelling, mechanical swelling and dispersion) on the other hand keeps it also together (cohesive binding of the pore water in negative pressure). Therefore, the structure of clayey silt resists due to its large inner surface with the accordant capillary water content, much higher water contents than silty sand. In principle the cohesive and loosening mode of action due to the water content, replace each other successively. In different size pores, they also can exist in parallel.

Important transitions in the cohesive mode of action of water:

The first transition is in the hygroscopic humidity over 50% relative humidity, when over capillary condensation more and more pore water is available. The pore water eliminate the strong electrical bindings between the minerals, consisting of intersections of inter crystalline water, or diffuse double layers and replaces it by less strong mechanical bindings of the surface tension. The gradually change of the binding quality, that starts here, can be seen as a first transition from a brittle to a ductile behaviour. It happens together with an erratic reduction of the cohesiveness (see image 70 and image 72) and increases with the rising water content to the plasticity limit, at that the material, after the definition, reacts ductile. The second transition is between the plasticity limit and the fluid limit. The negative pressure of the capillary water gradually diminishes with further water supply.

At the same time, the amount of free water increases. With the elimination of the cohesive water menisci, the mineral particles float apart and finally disperse in the surrounding free water.

3.4. The function of the clay minerals in the soil structure of the stamped clay of Lintong

In the structure of the stamped soil of Lintong, the clay minerals lay as thin coatings on the surfaces of the silt grains (see chapter 2.3.3).

Only closely fitted on one side of the structure supporting silt grains, the main part of the clay minerals has no influence on the stability and the swelling property of the

complete structure. In the case of the swelling of the clay coating, the clay minerals can spread themselves unhindered in the open pore space and doesn't put any pressure on the structure of the silt matrix. However, the same clay coatings can get swelling active, when they are covered with a rigid silica gel film from a silica gel consolidation (see. problematic of the swelling at a silica gel treatment in chapter 4.3.5). Clay minerals and fine silt also lie, as a coating or in form of larger coagulates, between the structure building silt grains. In dry condition, they act as a binding media that binds the silt grains tightly together. Due to the strong electrical bonding forces at their mineral surfaces, the clays contribute at the grain contacts of the silts to the mechanical strength of the complete structure.

The same clay structures in the grain that make contact between the silt grains are also responsible for the swelling of the soil in the hygroscopic humidity. Although the clay content of the soil is not especially high and there are no nameable parts of swellable clay minerals with voluminous, inter crystalline swelling (see Chapter 2.2.2, 2.3.1 and 2.3.4), the stamped soil of Lintong reaches a hygroscopic expansion in the hygroscopic humidity of 2mm/m (see chapter 4.3.5). The water storage in the hygroscopic range is limited to the pore radius under $0.01\mu\text{m}$, as it occurs in the stamped soil only in the clays and fine silts (see Chapter 4.3.3 and 2.3.3). The hygroscopic swelling of the earth can be traced back only on the intercrystalline and osmotic swelling processes on the surfaces of the overlying clay minerals. Up to 50% relative humidity hydrations processes at the cations of the clay mineral surfaces are dominant (intercrystalline swelling). At rising humidity (50%-98% relative humidity), when the capillary condensation in the micro porosity between the clay mineral surfaces supplies more water, diffuse layers are built-in between the clay minerals. They enlarge due to the osmotic pressure and make the single minerals disks swell out. As this swelling mechanism of the stamped soil of Lintong takes place between all grain contacts of the silt matrix, the resulting swelling and the loss of strength of the whole structure is relatively high. The positioning of the clay mineral packages in the structure plays an important role.

Therefore, the swelling in the hygroscopic range is, at compressed samples with the same composition that had been produced in the range of the liquid limit, 50% reduced (see chapter 4.1.3). A changed structure could be the reason for the reduced expansion of these samples. In water overspill, the clay packages wash off the silt grains. At the compacting with high water content, less coagulates are formed, as in general acknowledged (Houben, 1994). Probably at this form of production, the clay minerals attach more in the pore space and less in the grain gussets of the matrix structure. The reaction of soil structures to the fluctuations of

Stabilisation of loess clay surfaces at the example of the Terracotta army in Lintong

the humidity, especially in the hygroscopic humidity, is therefore not only limited to the amount and quality of the clay minerals. The positioning of the clay mineral packages in the structure of the soil is also an important influential factor for the material behaviour of the soil. It is for every soil material different and therefore should be considered in connection with conservation analyses of soil structures.

The water reposition in the hygroscopic humidity could not be visualized with the Kryo-SEM images (chapter 2.3.3). Only at a further state of capillary filling with water contents in the range of the plasticity limit, it was possible to visualize the structural destroying effect of the water in the pore structure of the stamped soil (see Image 27 to image 30).

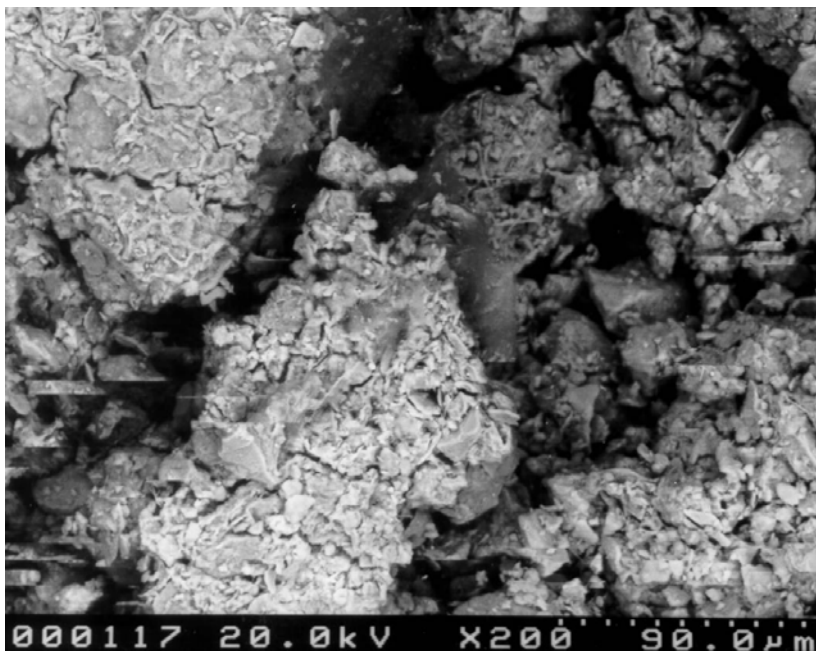


Image 27 Kryo-SEM image (secondary electronic image) of a stamped soil sample with about 18 mass % water content. Small swelling cracks grow to a new capillary pore system together. Compact matrix areas (higher fine silt or clay parts?) can still sustain their structural conditions (left above), while others have already lost completely their structure and have dissolved in the free pore water (right above).

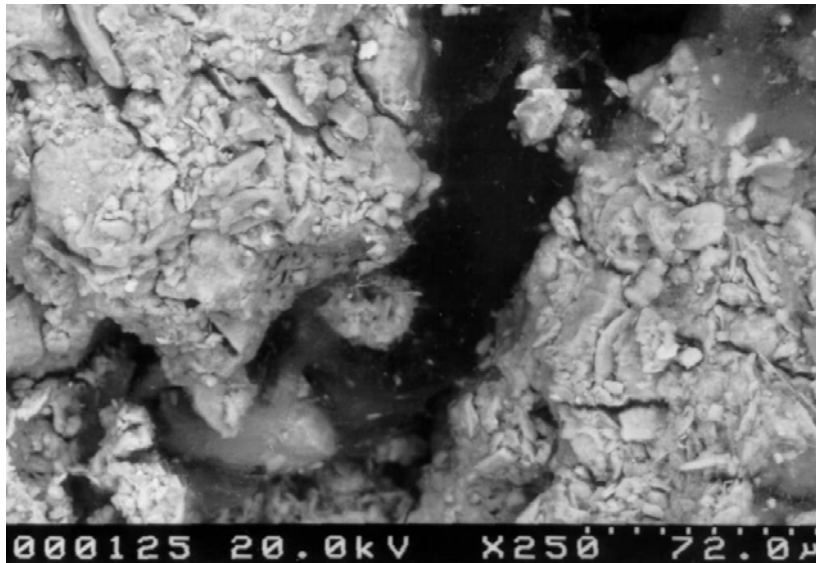


Image. 28 Kryo-SEM image (secondary electronic image) of a stamped soil sample with approx 18 mass % water content. The fine pore system is bonded together from surface potency and capillary potency (right above) and coagulates (middle) are floating in the free water of new swelling pores.

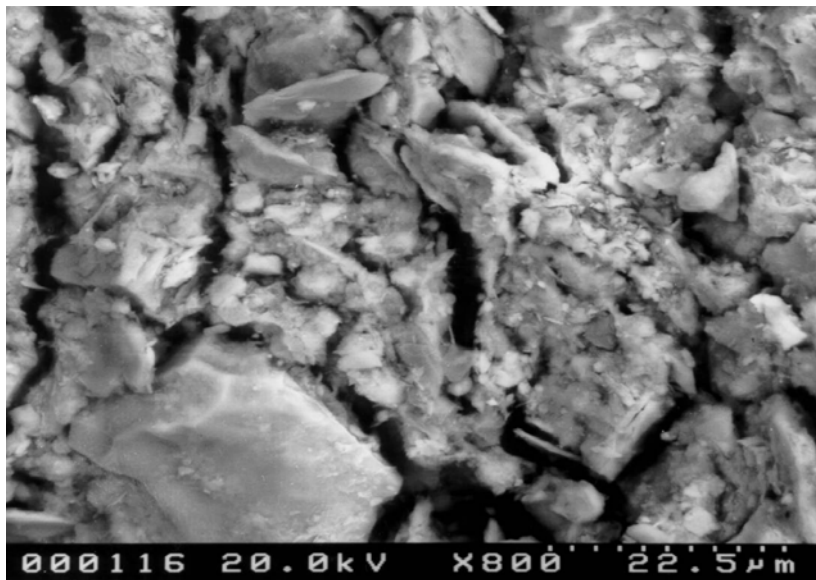


Image. 29 Kryo-SEM image (secondary electronic image) of a stamped soil sample with about 18 mass % water content. The swelling opens the structure and creates new pore systems. The clay fraction is loosening from the silt aggregates and disperses into the widened pore spaces.

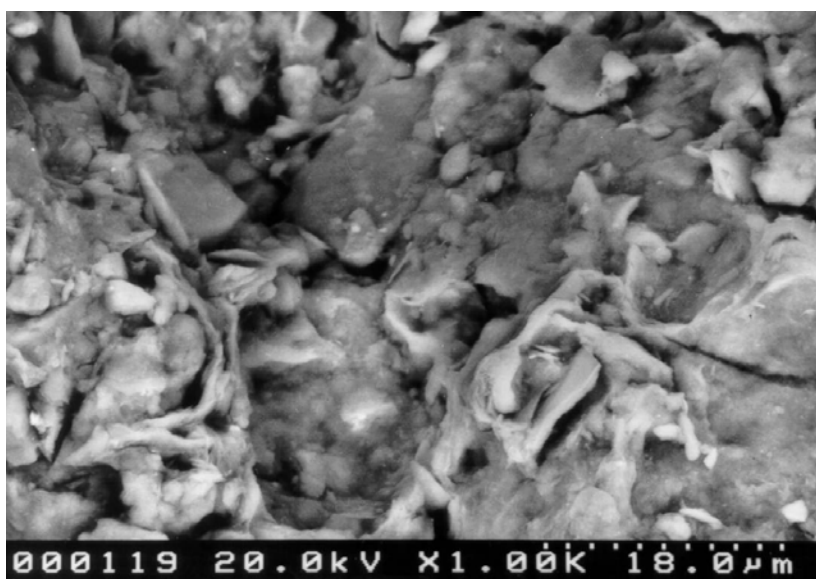


Image 30 Kryo-SEM image (secondary electronic image) of a stamped soil sample with about 18 mass % water content. The clay grain coatings are obviously swollen. They often are separate by a complete layer from the silt components

4 Impact of chemical swelling reducers and SE stone consolidant on the stamped soil in the excavation of Lintong

4.1 Swelling reducers

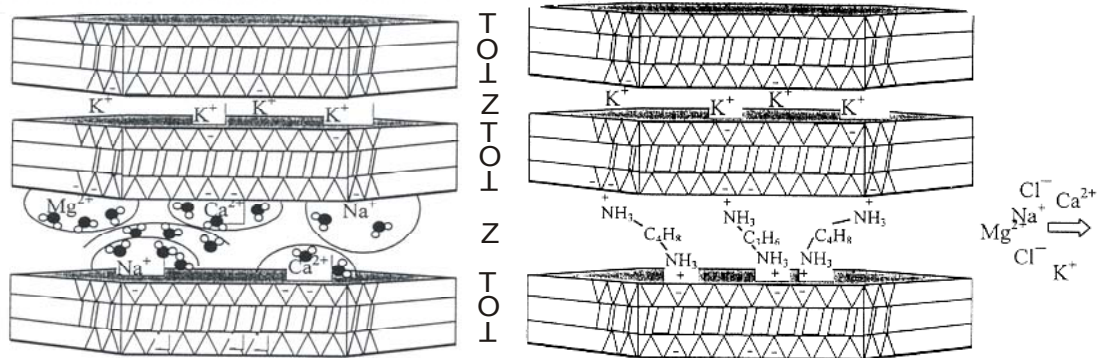
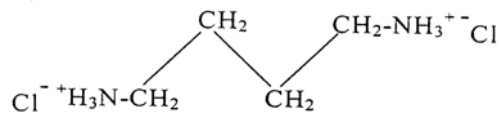
Since the beginning of the 90^s of the last century the impact of swelling reducing substances for the reduction of the hygric swelling of clay containing natural stone was analysed (Snethlage, 1991b), (Hilbert,1995). In the centre of these works had been cationic, bifunctional tensides, also carbon chains, that attach with their positive loaded ammonium double ends ($R-NH_3^+$) to the negative loaded intercrystalline basic areas of the swellable clay minerals (Snethlage, 1991b). Ammonium ions are especially suitable for the substitution of exchangeable cations, because out of steric reasons similar strong bindings can be built up similar to the potassium ion to the tetrahedron layers of the clay minerals (see K^+ -fixation und lyotropen row) (Lagaly, 1969), (Snethlage, 1991b), (Heim, 1990), (Corti, 1999). The use of the exchangeable cations at the Z-layers of clay minerals with the help of n-alkyl ammonium ($C_nH_{2n+1}NH_3^+$) is used, also, at the production of swelling preparations (Heim, 1990).

In the application on clayey natural stone the swelling reducing impact of the bifunctional tensides results from the displacement of the exchangeable cations through an ammonium group at the end of the tensides. Consequently, less hydrate able cations as the elicitor of the osmotic swelling in the intermediate layers are available (Heim, 1990). Also two opposite layers loading centre, that stick with the help of ionic binding at the coupling ends of the Tensides, were held together with an aligning alkyl group.

The tenside 1.4– Butyl diammonium chloride (short BDAC) (0.2 Mol/l H_2O) dissolved in water turned out as a suitable material for stone conservation in the context with the work of Snethlage and Wendler. Since then it is distributed by the company “Remmers” under the name “Antihydro” and is used in many cases in the field of natural stone conservation (Wendler, 1996b). Its mode of action is demonstrated as a schematic in image 31. To date, there are no examinations to the impact of these Tensides on clayey soil or adobe.

Stabilisation of loess clay surfaces at the example of the Terracotta army in Lintong

Structural fomula of Butyldiammoniumchloride



Three-layer clay mineral with K⁺ fixed
Intermediate layer and swellable intermediate
layers (assignment with hydrated,
exchangeable Mg²⁺, Ca²⁺, Na⁺ -Ions

Coupling of the negative loaded tetrahedron
layers over cationic, bifunctional Tensides.
Migration of the exchanged cations and the
chloride ions in the pore solution

Image 31: Mode of operation of the cationic, bi functional tenside, Butyl diammonium Chloride (active agent in “Antihydro”) in a watery solution (illustration after (Keßler, 2000)).

4.1.1 Preliminary examinations of the impact of the off the shelf swelling reducer at the stamped soil of Lintong (chapter deleted)

Conclusion of the preliminary examinations

The treatment of the soil with the cationic bifunctional tenside 1.4 Butyl diammonium chlorides, used in the stone conservation, leads to an explicit reduction of the swelling rates in the hygroscopic field.

As shown by SNETHLAGE and WENDLER (1991), the swelling reduction can be improved with an increasing dose, until a material specific quantitative threshold value. Thereby, due to the effect of darkening, several treatments with a lower tenside concentration has to be preferred, rather than a singular treatment with a high concentration. The quantitative threshold value has been determined empirical by these tests at Sander sandstone. Without doubt, with this quantitative threshold value, the loading equivalent of the amount of tenside, has reached the CEC of the sandstone. The maximal effect of the bifunctional Tensides is reached when all the possible loading positions, the one of the exchangeable cations, are clogged.

Stabilisation of loess clay surfaces at the example of the Terracotta army in Lintong

The inner surface and therefore the CEC of the stamped soil of Lintong is a lot higher than the one of the Sander sandstone. In contrary to the measured 20 – 30 mval/100g in the soil is the cation exchange capacity (CEC) of the Sander sand stone between 4 and 12 mval/100g (Wendler, 1988).

Out of this reasoning, in the soil, a higher amount of tenside is necessary to reach the maximal swelling reduction. A higher treatment dose and in combination with the aversion of the material against too high water contents (fluid limit), requires for the application, a higher concentration of tenside in the treatment agent then it is reset at the “Antihygro”.

This high concentration of the Butyl diammonium causes a significant darkening of the material. In addition, the treated samples have an unpleasant smell. Both effects are, from conservation view, not suitable.

A further negative effect of the described tenside treatment is the strong adsorption of the treated sample that leads with several days' storage under 100% humidity to a transgression of the ductile limit. This can be probably ascribed to the chlorite entry during the treatment and the associated creation of hygroscopic salts such as CaCl_2 and MgCl_2 .

4.1.2 Modification of the chemical swelling reducers

The preliminary trials have shown that the treatments with bifunctional cationic tensides, as used in stone conservation, are capable of reducing the hygric swelling considerably.

Starting from the formula from the stone conservation – 0.2 mol/l 1.4 Butyl diammonium chlorides- for the application at the soil from Lintong. The following modifications are necessary.

Concentration

Augmenting the active agent concentration for the reduction of the amount of solution in the application.

Anion

Exchange of the chloride-ions by anions that does not form hygroscopic salts in the pore solution.

Length of molecules

Adaptation of the alkyl group length at the inner and inter crystalline intermediate layer in the pore structure of the soil, for optimising the bridging of the loading centres.

Concentration

For the modified alkyl, diammonium solution 0.66 molar solution concentration was chosen. For the complete loading of the loading centres of the original soil of Lintong at this concentration, you need a 0.19ml watery tenside solution per gram soil, around 20 mass-%. This value corresponds with the plasticity limit of the material (see Chapter 2.2.2). With the 0.66 molar solution it is possible to bring in the necessary complete amount of tenside solution into the soil, without exceeding the stability limit of the material.

Anion

As a substitute for the chloride-ions Oxalate-ions and sulphate, ions were chosen. For the production of the tenside solution, the alkyl diamines are dissolved in water. These basic solutions were mixed, for so long, with the oxalic acid ($C_2H_2O_4$), or sulphuric acid (H_2SO_4), to reach a pH of 7. By separation of the protons from the acid, the alky diamin ions were protonised to double positive alky diammonium ions. The acid power of the sulphuric acid (pK_{s1} : -3; pK_{s2} : 1.92) and oxalic acid (pK_{s1} : -1,4; pK_{s2} : 4,4) are less than the dissociations constant of the hydrogen chloride (pK_s : -7), that is used at the "Antihygro" for the protonising of the alkyl amine. However, both acids are stronger than the alkyl ammonium with pK_s 9. 2. Therefore, at the chosen acids a complete protonising of the Tensides is warranted.

In contrary to the "Antihygro" with the use of these cationic Tensides in the clay minerals in the soil, no chloride ions are released, but oxalate ions or sulphate ions. These anions precipitate out of the pore solution, together with the exchangeable cations as oxalates or sulphates. The tests for protonising with sulphuric acid were before long interrupted, because at the test application in pit II, after a few days, sulphuric effloresces appeared on the treated soil surfaces. The advantage of the protonising with oxalate acid is the stability of the oxalate salts that develop during the application. The calcium oxalates Whewellite ($Ca(C_2O_4) \cdot H_2O$) and Weddellite ($Ca(C_2O_4) \cdot 2H_2O$), that can be expected, are in water practically insoluble (Neumüller, 1979). In very small amounts, the development of $(Mg(C_2O_4) \cdot 2H_2O)$ or soluble alkaline oxalates are likely. No negative influence on the mineral structure or the hygric properties of the soil is to be expected from these salts.

Furthermore, there already exists biogenic calcium oxalates in the pore space of the soil (see Chapter 2.3.3).

Length of the molecules

The material examinations have shown that the stamped soil of Lintong contains only few swellable clay minerals. The swelling of the material can therefore be less traced back on the inter crystalline swelling of the three stratum clay minerals with swellable intermediate layers, than more on the inter crystalline, osmotic swelling at the diffuse double layers of the loaded clay particle surfaces. At the muscovite illite row and at the swellable smectite and montmorillonites, the distances of the Z-layers ranging from 3 Å (potassium fixation) up to 8 Å at maximal intra crystalline swelling (Heim, 1990), (Klockmann, 1978). The intra crystalline distances of the loaded clay mineral surfaces can be extremely variable, especially because the tenside exchange takes place in a humid, therefore swollen pore space (see Image 32).

With the different lengths of molecules of the alkyl diammonium ions, the test should be made to bridge optimally the distances between these loading centres. Starting from Diamines butane, that is best for the fixation of clayey sandstones, then continuing for the next preliminary trials the two next situated, alkyl chain were chosen (table 4). Over the protonising, with the oxalic acid out of these diamines, three bifunctional cationic Tensides with different length of molecules should be produced. Their chain lengths are chosen so they can fit into the distances of closed, swollen Z-layers.

Raw product with molecule length (Å)	Protonising	cationic Tenside structural form
1,2-Diaminoethan C ₂ H ₈ N ₂ 3,75 Å	C ₂ H ₂ O ₄	Ethyl diammonium oxalate C ₂ H ₁₀ N ₂ ²⁺ (C ₂ O ₄ ²⁻) $\left[\text{H}_3\text{N}-\text{CH}_2-\text{CH}_2-\text{NH}_3 \right]^{2+} \quad \text{C}_2\text{O}_4^{2-}$
1,4-Diaminobutan C ₄ H ₁₂ N ₂	C ₂ H ₂ O ₄	Butyldiammoniumoxalate C ₄ H ₁₄ N ₂ ²⁺ (C ₂ O ₄ ²⁻)

Stabilisation of loess clay surfaces at the example of the Terracotta army in Lintong

6,23 Å		$\left[\text{H}_3\text{N}-\text{CH}_2-\text{CH}_2-\text{CH}_2-\text{NH}_3 \right]^{2+} \text{C}_2\text{O}_4^{2-}$
1,6 Diaminohexan		Hexyldiammoniumoxalate $\text{C}_6\text{H}_{18}\text{N}_2^{2+} (\text{C}_2\text{O}_4^{2-})$
$\text{C}_6\text{H}_{16}\text{N}_2$	$\text{C}_2\text{H}_2\text{O}_4$	$\left[\text{H}_3\text{N}-\text{CH}_2-\text{CH}_2-\text{CH}_2-\text{CH}_2-\text{CH}_2-\text{CH}_2-\text{NH}_3 \right]^{2+} \text{C}_2\text{O}_4^{2-}$
8,72 Å		

Table 6: Chain length of the bi functional Tensides due to the minimal, middle and maximal swelling of the inter crystalline intermediate layers of clay mineral

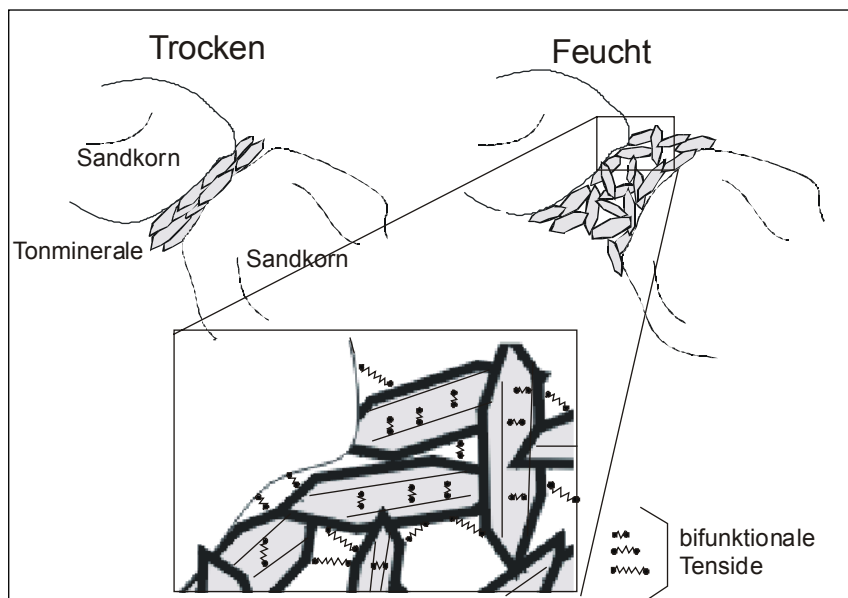


Image 32: Bridging of the intra crystalline and inter crystalline loading centres of the clay minerals with bi functional Tensides of different molecule length. The structure is swollen during the treatment (Müller, 2002)).

4.1.3. Preliminary tests with modified, chemical swelling reducers
(chapter deleted!)

Results of the preliminary tests with modified, chemical swelling reducers
(chapter deleted!)

Summary and conclusion:

The tests have shown that all used tensides, exchange cations from loaded stratum silicate surfaces. Obviously, they succeed in the coupling at the loading centres, because with all the Tenside treatments the swelling rate of the soil samples is reduced. The treatment with ethyl diammonium achieves the best results. Because of the treatment with some tensides, the hygroscopicity of the samples rises and an obvious darkening is to be seen. Thereby the influence of the alkyl chain length is apparent. The longer the alkyl chain, the more the water absorption rises. This effect can be partly connected with an overdose of the Tensides during this treatment. It can be assumed, that positive loaded ammonium ends of the tensides, that could not find a coupling space, due to the overdose, hydrate and so raise the hygroscopicity of the soil. The amplification of this effect with rising alkyl chains shows, that short molecules are better capable as swelling reducers, as it is easier for them to reach the loaded surfaces of the clay minerals. In table 7: are summarized results of the preliminary tests. In the overall evaluation, SE and SEBH have the best results.

Additional, this examination has shown that pellets out of elutriated soil are so different on their pore space of the undisturbed sample material, that they cannot replace the original undisturbed soil in the further test series.

Treatment type	Colour impression	swelling -90% rel. humidity	swelling -100% rel. humidity	Swelling rate	Adsorption	Ion exchange
SE	0	++	++	++	-	+++
SB	-	++	0	++	--	++
SH	--	-	---	+	---	++
SEBH	-	+++	0	+++	---	+++
SH2O	0	0		0	0	0

0 like untreated pellet

+ good

++ very good

+++ exceptionally good

- bad

-- very bad

--- exceptionally bad

Table 7: Compilation of the assessment criterion for the treatment types with the different alkyl chain length. The evaluation refer always direct to the untreated pellet

4.2 SE (silicate ester) stone consolidant

There are various possibilities to consolidate building materials out of soil and improve their resistance against environmental influences. The various methods from the addition of animal protein, strengthening with fibres, to the impregnation with the juice of banana leaves are described in detail in Houben and Guillaud (1994) and due the existing state of information evaluated.

Thereby the aim is mostly to produce new building material similar to adobe or stamped soil, their product properties can be directly manipulated by the addition of cement, bitumen, straw, puzzolana and similar.

However, for the consolidation of already existing earth structures the choice of methods is greatly reduced. Especially when the surface should not be damaged and their optical appearance should not be changed.

The research in this matter is concentrating, similar to stone conservation, on the application of synthetic organic polymers like acrylates (Koob, 1990), (Zhou, 2000), Polyurethane und Polyisocyanates (Coffman, 1990) or silicate binders similar to sodium- und potassium-silicate (Li, 1990), fluoric silicates (Huang, 1990) and silicate ester (Chiari, 1990), (Chiari, 2000a), (Coffman, 1990).

Often the aim of this consolidation was to make the historic clay brick wall "weatherproof", resistant against rain, wind, frost, temperature fluctuations and variations of humidity. Selwitz (1995) published this comprehensive securing

treatments with combinations out of structural consolidation, sealing of the surface, synthetically enhanced protection of the flanks and closing water repellent treatment (Selwitz, 1995).

Overall, the opinion had established that chemical consolidation on existing soil structures are only necessary and make sense only in a few particular cases. Mostly roof constructions and drainage systems are sufficient to eliminate running water, the main damage cause at cultural heritage sites out of soil and adobe (Taylor, 2000).

Furthermore the long-term effects of consolidations, is in the most case, not sufficiently calculable (Taylor, 2000). Even approaching, in stone conservation, every consolidation has to be adapted to the individual problems. CHIARI has summarized the main criteria for a sustainable chemical surface treatment of soil (Chiari, 1990):

1. Water permeability, fluid and vapour
2. The porosity must to stay open.
3. Rising of the mechanical strength and weathering resistance in dry and humid conditions.
4. Deep penetration of the consolidant.
5. No formation of a film or scales.
6. The thermal dilatation of the consolidant must be similar to the material.
7. No change of colour or gloss.
8. Enhancement of the resistance against stress that occurs with salt crystallising, capillary water transport and frost dew change.
9. Stability of the polymerised consolidant against water, oxidation and UV irradiation.
10. Cost effective. Easy to apply also on wet material.
11. Non-toxic
12. Reversible

The author points out, that none of the known products fulfils all of these requirements, and especially the reversibility is at the consolidation of soil, only in very few cases possible. During the previous years of the consolidation of soil, one had come to the opinion that the chemical consolidation of soil is equal to the production of a new material ,“consolidated soil”. To guarantee the long-term success of the consolidant, the complete knowledge of the hygric and physical data of the new building material is essential. The ideal should be, to stay as close as possible to the properties of the original (Taylor, 2000), (Chiari, 2000a). During the examination of the hygric and physical properties of the treated soil, the research for the conservation of soil is still far away from the standard of stone conservation. In many

Stabilisation of loess clay surfaces at the example of the Terracotta army in Lintong

cases, the consolidations had not been conducted by material analyses, as it is standard practise in stone conservation, for many years (Snethlage, 1997a).

For the selection of a suitable consolidant, it is important to define the aims exactly. As explained earlier (see Chapter 1.2) the damaging of the soil surface in the excavation is mainly caused by external mechanical stress. The damaging potential of the fluctuation of the indoor climate is not yet resolved.

In this case, the securing of selected imprints in the excavation of the Terracotta Army in Lintong, the aim of the consolidation, is to improve the resistance against abrasion and compressive strength at the surface. Additionally, the mechanical resistance of the surface shall be slightly raised to a depth of a few centimetres, without creating an over consolidated scaling. All the other material properties similar to vapour permeability, colour impression, water absorption, hygroscopicity, swelling attitude, etc. should stay, as much as possible, unchanged, because the surfaces are still, after the consolidation, grown together with the "alive soil". It has to accede all the interactions of the soil with its surroundings (water adsorption, water desorption, water diffusion and hygric swelling and hygric shrinkage). The consolidation must not give protection against rain and other direct water infiltration.

With regard to this problematic, amongst the known consolidants, the use of silicate ester (SE) or respectively Tetra ethyl-ortho silicates (TEOS) lends itself as a solution. In contrary to most of the other systems, the use of TEOS in soil structures has been analysed several times (Coffman, 1990), (Chiari, 1990). Positive experiences with the long-term impact of the silica gel in the soil are well recognized (Chiari, 2000b).

The advantages of the consolidation of soil with Tetra ethyl-ortho silicates (TEOS) are:

- Moderate consolidation, deep penetration; In contrary to diisocyanides there is only a little risk of over consolidation and the formation of scales, (Coffman, 1990)
- No optical change of the material
- Chemical compatibility of the binding media silica gel with mineral components of the soil
- No inserting of foreign ions, such as potassium silicate or fluoric silica
- No formation of a film on the surface
- Easy application and handling
- Well known material from stone conservation
- Non reversible, but possible to treat again

Mode of operation of the silicate ester (SE)
(Chapter deleted!)

4.2.1 Preliminary examinations to the selection of the SE stone consolidates, at the stamped soil of Lintong (Chapter deleted!)

Results and conclusions

After the drying out of the samples, the soaked area of the cuboid samples cannot be distinguished optical from the untreated soil over the capillary seam of the soaking. The surface is neither darkened nor shiny. The abrasive strength and the stability of the edges are at all treated types, with the exception of F300E1/2 in the consolidates zone, clearly increased. Also for the treatment type, F300E1/2, a slight increase of the abrasive strength is noticeable.

In the pore space of the cylindrical samples, on all types of treatment almost the same amount of silica gel is separated (see Gel separation Table 8).

The highest concentration with eight mass percent was measured at the double treatment with 2xF300E $\frac{1}{2}$. The values of the gel separation of about 30 mass percent of the consolidant adsorption with F-OH and F300E correspond to the information given in the technical data sheet (see appendix 7.8).

The surprisingly high adsorption and gel separation with the diluted treatment with F300E, 1/2 has to be traced back; probably to an excessively long soaking. After the saturation of the cylindrical sample, it remains over 30 min in capillary contact to the treatment solution. In this time, the Monomer concentration in the sample could be augmented by the evaporation of the solvent.

Through the comparison of the ultrasonic-transmission speed, after the consolidation (table 8), it seems, nevertheless, to be for the single treatment with a lower active substance concentration (F300E1 /2), a lesser consolidation effect. But this comparison should not be evaluated too rigorously, because the natural variations, depending on the material, of the ultrasonic speed of the soil- with the equilibrium moisture at 40% and 20C° - is between 1.2 and 1.6 km/s (**Fehler! Verweisquelle konnte nicht gefunden werden.**).

Stabilisation of loess clay surfaces at the example of the Terracotta army in Lintong

Gel separation at the cylindrical samples	F-OH	F300E	F300E 1/2	2 x F300E 1/2
Agent adsorption (kg/m ²)	9,17	9,05	6,06	11,77
Gel separation (kg/m ²)	3,17	2,68	1,83	2,58
Agent adsorption (g/gram soil)	0,17	0,23	0,20	0,39
Gel separation (g/ gram soil)	0,06	0,07	0,06	0,08
Gel separation (M.- % Treatment solution)	34,55	29,65	30,25	21,62
Ultrasonic speed of the cylindrical samples (km/s) (average value per sample)	1,85	1,95	1,5	1,8
Gel separation at samples (kg/m ²)	3,65	5,10	4,32	8,65

Table 8: Results of the mass balances before and after the soakings

Better comparable results for the increase of the resistance are given by the ultrasonic measurements on the profiles of the cuboid sample. The absolute transmission speed is shown in image 33. Since the initial values for the ultrasonic speeds in the untreated material differ strongly (right-hand of the curves in fig33), for the evaluation of the strengthening effect of the different treatments also including the relative rise of the ultrasonic speeds from the non consolidated to the consolidated profile sections, are compared (fig 34)

The visible penetration depths of the treatment (capillary edge during the soaking) are dependant on the treatment 1.5 – 3.5 cm. The effect of consolidation seems to continue even further than the visible soaking horizon in the ultrasonic profile. For F300E the acoustic velocities indicate a consolidation effect up to 4 cm profile depth (image 34).

At all treatment types the ultrasonic-transmission velocities have a maximal value at the soaking range, that diminish with the sample height (see image 33). Speeds of 1.8 to 2 km/s, as previously achieved with the treatment, with F-OH and 2x F300E¹/₂ are 20 to 25% over the average value of the untreated soil (1.5 km/s) and can be clearly traced back to the consolidant effect of the treatment.

Comparing the decline of the ultrasonic velocities (image 34); it is obvious that the most augmentation was reached with F-OH. At this treatment, the ultrasonic velocities are at the base 45% over the initial value. After a penetration depth of 3 cm, they decline quickly to the initial value. In addition, a rising of the curve can be seen direct at the base at this treatment. This course of the curve and the large rise of the transmission speed refers, compared with the flatter curves of the other

Stabilisation of loess clay surfaces at the example of the Terracotta army in Lintong

treatments, to a higher potential for the over strengthening and scale formation. Especially dangerous is to valuate, the obvious “compaction” in the first centimetres of the profile.

The double treatment with diluted F300E ($2 \times F300E_{1/2}$) has, with a 25% increase of the ultrasonic velocity, the second highest effect of consolidation. The course of the curve of the consolidation profile is further balanced as at the F-OH. The depth of penetration is 2.5-3cm less than the one with F-OH (3.5-4cm). In contrast, the consolidation effect of the single treatment with F300E is very small and with 1.5cm not sufficiently deep.

The consolidant effects of the treatment with F300E penetrates furthest and diminish in the main, continuously and at the slowest. The maximal ultrasonic speed is 23% over the initial value. The danger of an “over consolidation” is, therefore, lower as at the F-OH and $2 \times F300E_{1/2}$.

Regarding the comparison of the consolidation profiles in the stamped soil of Lintong, the single treatment with F300E has to be preferred to the other types of treatment.

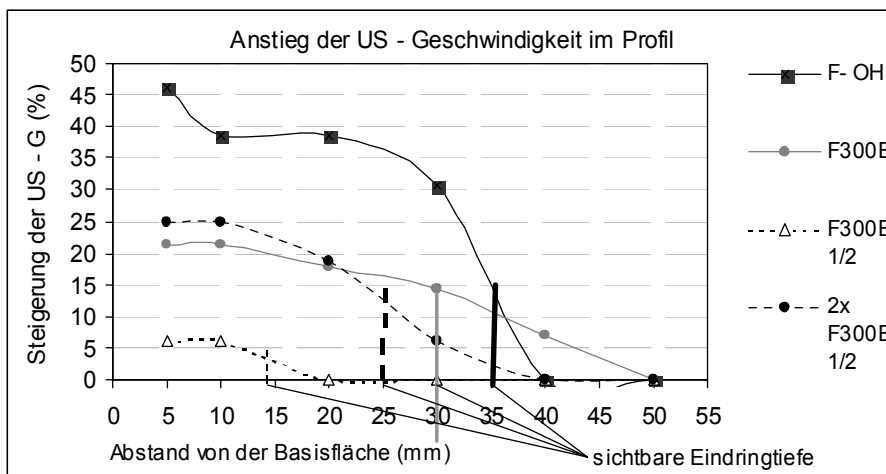


Image 33 Profile of the ultrasonic velocities in the soil cuboids, after the soaking with SE stone consolidant

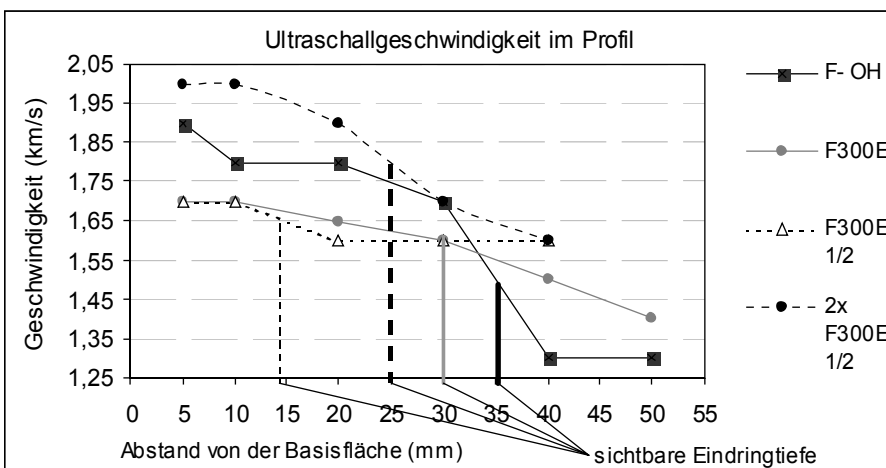


Image 34 Relative decline of the ultrasonic speed in the profiles of the cuboid samples

The investigation of the consolidating silica gel films in the scanning electron microscope (SEM), can show characteristic typologies of the creation of the film and the penetration depth of the consolidation (Alvarez de Buergo, 2000). The images of single, small details, of the pore structure can only give conditional conclusions; if a consolidation was successful or not. Furthermore, it is not possible, to document in single detailed, images the overall picture of longsome microscopic examinations.

Nevertheless, the SEM examinations provide the direct proof for the separation of the silica gel in the pore space of the consolidated material. The main observations are shown in images 35 to image 40. As a conclusion, the SEM investigations have given the following results:

With all the treatment types, it was possible to detect the silica gel films in the pore space. The Gel film at F-Oh seems to be thicker, than at the different treatments with F300E. In the Gel there are nearly everywhere shrinkage cracks. Large pores (10 μ m – area) seem to be partially entirely filled with the Gel. In other finer porous areas, there cannot often be detected, any film. F-OH appears not to penetrate in the finest gussets of the pore structure.

The Gel films of the treatment with F300E and 2x F300E1/2 are, in comparison, finer and covers the whole area. Nearly all the structures are covered with fine films. Their evidence is often not easy to prove, due to the low amount of shrinkage cracks.

By the single treatment with F300E1/2, only on a few areas, it is possible to find an obvious gel film. Either it has not been formed everywhere or it is so thin that it is difficult to detect it in the SEM.

The results of these preliminary examinations only regarding the described form of application on the stamped soil of the intermediate walls of Lintong. They cannot be transferred in anyway directly to other clay samples or adobe samples. Other consolidates could perhaps attain better results. The results of the preliminary examinations show, that for the stamped soil of Lintong, a moderate consolidation is possible with silica acid ester. It is possible to achieve penetration depths to a minimum of 4cm with a balanced consolidation profile. The silica gel is connecting well to the mineral surfaces of the pore structure and can build up mineral coatings, grain-to-grain bridge connections and fillings of the gussets. The resistance against the surface abrasion is augmented. The visual impression is not altered. From the examined selection, the single treatment with F300E has arrived at the best results. It is, therefore, chosen for the following examinations.

reducers on soil has never been analysed. Furthermore, the results of this examination give the necessary database for the problem, which of the introduced treatment is useful and justifiable due to conservation and restoration evaluation criteria; whereas the conservation evaluation of the material change, due to the treatment at soil structures is not yet clear. On the other hand, in stone conservation, because of long experience and systematic examinations it has been largely standardised (Snethlage, 1997a), (Sasse, 1996), (Snethlage, 1997b), (Snethlage, 2002). The material examinations on the original soil and the preliminary test with artificially produced samples have shown, how difficult it is, to reproduce artificially the stamped soil from Lintong with its 2000 years of stratification, so that the new material is comparable in structure, pore space distribution, mechanical and hygric properties with the original.

Therefore, the test row has been carried out, not with reproduced material, but with formatted samples out of undisturbed original material. The thus far analyses for the chemical modification of soil from archaeological excavations, mostly work with artificially produced clay samples (the samples were often made out of the powder of the original clay with the addition of water in standardised sample forms). The examination pieces for the following test series have been drilled and sawed out of the dry soil. It has been worked in the dry drilling and dry sawing method. Thereby unsilted, diamond core drill and diamond saw plates were used. They are normally used for wet drilling and sawing of stone.

The formatting of the samples requires, due to the fragile material, very diligent and careful working. While core drilling, it is very important to vacuum the drilling dust away.

The original material out of China has been analysed in Germany. The source was limited. Therefore, smaller test body masses have been chosen, than they are usually for material analyses after DIN. Furthermore the soil is very often pervaded with shrinkage cracks, so that it was not possible to produce a connected 16cm length formatted sample.

For the test series drilling cores with diameters of 3cm and 4.5cm, have been taken out of undisturbed soil block; from the north end of the stamped clay wall between G18 and G18 in sector T21 of the pit II (see: appendix 7.1). Out of this, discs (Sc), columns (S) and irregular small samples have been formatted. Altogether, the series comprises of 60 samples. The exact amount of samples, their formats and their treatments are listed in table 9.

Identification code of the treatment	A	B	C	D	E	F
treatment	-	F300E	DE und F300E	DEBH und F300E	DE	DEBH
column (S) d:~ 3 cm h: ~5 cm	4	4	4	4	4	4
disc (Sc) d:~ 4,5 cm h: ~0,6 – 0,8 cm	4	4	4	4	4	4
small samples (Sa) m: ~ 80 g	2	2	2	2	2	2

F300E (SE (silicate ester) stone consolidant Funcosil 300E – Fa. Remmers)
 DE (swelling reducer: 0,6 molar, watery solution of Ethyl diammonium oxalate)
 DEBH (swelling reducer: 0,6 molar, watery solution of Ethyl-Butyl- and Hexyl di ammonium oxalate in the mixture 1:1:1)

Table 9: List of the samples of the test series, for analysing the effect of chemical swelling reducers and SE stone consolidant on the original stamped soil of Lintong

4.3.2 Treatment of the test pieces

The double treated series, C and D, have been treated with swelling reducers, before the consolidation (F300E).

Treatment with modified swelling reducers (DE and DEBH)

The treatment of the sample series C, D, E and F, with modified swelling reducers, was carried out for all the samples in parallel. With sprayers, the respective treatment solution was sprayed singularly on the formatted samples, in three identical dosage steps. Between the applications steps, there was always a time delay of five hours.

To enable the tenside solution to distribute evenly in the sample, the samples have been singular packed in sealable PE (polyethylene) bags, in an exsiccator at 100% relative humidity in the waiting time and for further 48h after the last treatment. Therefore, it was possible to control, for every sample, the absorbed amount of treatment medium, independent from the loss of solvent due to the application. Overall, it was attempted to achieve for every samples as close as possible to the ideal metering target value from 0.19ml solution per gram soil (see Chapter 4.1.2).

The gravimetric measured medium absorption of the samples is shown in image 41.

Although the measurement of the wet samples cannot be extremely exact (water films, small loss of material during the handling of the samples, etc.) the application

Stabilisation of loess clay surfaces at the example of the Terracotta army in Lintong

amount could be adjusted relatively accurately to the aimed region of 0.19g/g soil. In addition, the dry weight increase after the tenside treatment (image 41) is in the region of the theoretical mass increase. This is calculated out of the molar mass of the tensides for the soaking with 0.19g solution per gram soil. The theoretical values are 0.019 g/g soil for the DE solution (series C and E) and 0,023g/g soil for the DEBH solution (series D and F).

In contrary to the high dose treatments of the preliminary examinations (see Chapter 4.1.3), the tenside treatment of the series C, D, E and F had no effect of the optical appearance of the sample items.

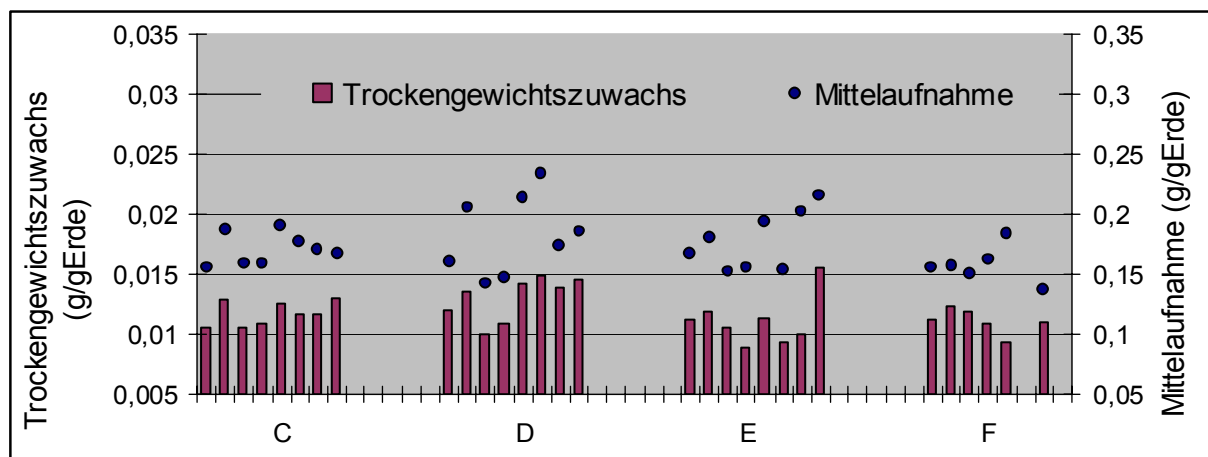


Image 41 Absorption of the medium and increase of the dry weight at the treatment with modified swelling reducers

Series C and E: 0.6 molar watery solution of Ethyl diammonium oxalate (DE)

Series D and F: 0.6 molar, watery solution of Ethyl-Butyl- and Hexyl di ammonium oxalate in the mixture 1:1:1 (DEBH)

Treatment with SE (silicate ester) stone consolidant (F300E)

The samples of the series B, C and D have been capillary soaked, as described in chapter 4.2.1. However, the time of the soaking was not preset (1h in the preliminary test). After the sample was completely capillary soaked, then place up side down on the grid, it was dabbed off, weighed and put into a climatized box. After the treatment, the samples were stored for seven weeks in an acclimatized box of 75% relative humidity and 20°C.

The Gel separation rate (%) and the separated gel (g) were determined by weighing before and after the treatment (image 42). With an average 4.8 to 5.1% by weight polymer content, the values correspond to the values of the mass adsorption of tests with silicate ester on clays and adobes in Fort Seldon, USA (Coffman, 1990), (Selwitz, 1990). The preliminary treatment with swelling reducers (series C and D) does not seem to have any effect on the separation of the silica gel.

Stabilisation of loess clay surfaces at the example of the Terracotta army in Lintong

Accordingly, referring to the results from the preliminary test the treatment with F300E has no influence on the optical appearance of the test items. In addition, the series C and D with the double treatment does not differ optically from the untreated material.

The scratch resistance and the edge stability are increased noticeable at all of the consolidated samples.

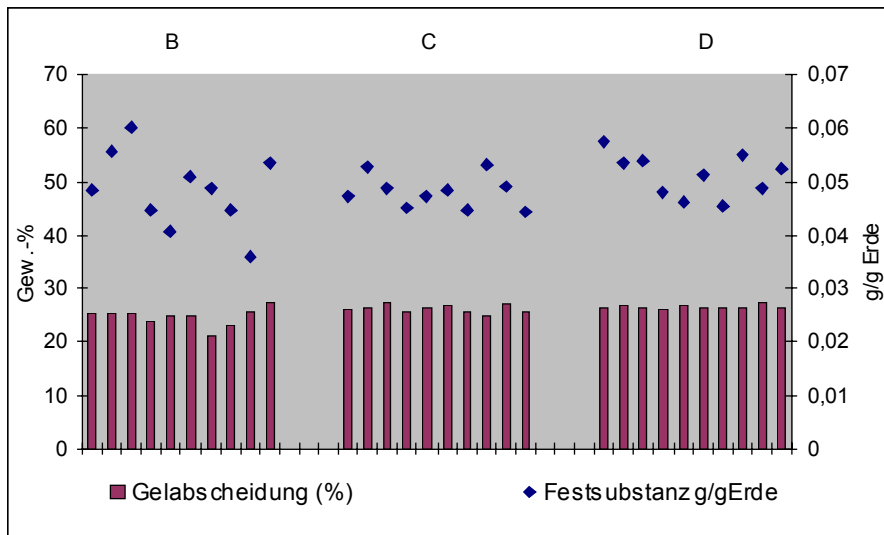


image 42 Gel separation rates in mass-% of the adsorbed treatment medium and the percentage by weight of the incorporated silica gel for the samples of the series B,C and D;

Average value of the series:

	%	g/g S.
B:	25	0,048
C:	26	0,048
D:	27	0,051

4.3.3 Analyses and results to the porosity

The condition of the pore space is one of the basic parameter for the moisture transport and the storage capacity of porous mineral building material (Krus, 1995).

The pore space is the place in the building material, where all the decay relevant chemical and physical processes such as water storage, salt crystallisation, solution processes, separation processes, etc. take place (Fitzner,1994). Also in the building material soil, the processes of the moisture transport and moisture storage are controlled by the porosity. In contrary to the diagenetic hardened natural stone, the porosity of soil has, however, no constant value. Osmotic swelling, suffusion and collimation of clay and silt components can, within two to three water saturations, change the character of the porosity greatly. In the case of the soil mechanics and the classical hydrogeology, the description of the whole pore volume of classical

material is restricted and therefore limited to the determination of the complete pore volume plus the usable porosity (Hölting, 1996). In the soil science, however, one also deals with transport activities of the unsaturated zone. Akin to, building physics these transport mechanism happen in the three-phase system of, mineral phase, water phase and gas phase.

The pedological methods for recording of the porosity in the unsaturated zone are therefore transferable to the system soil as a building material in many areas. For the qualitative and quantitative description of the porosity, here the microscopically analyse of impregnated thin section samples (Cousin, 1999), mercuric porosimetry and gas adsorption measurements is used (Richard, 2001), (Echeverria, 1999).

The literature for the conservation of soil was limited until now, to the microscopic analyse (Shekede, 2000). At COFFMANN (1990) for the first time, the mercuric pressure porosimetry for verifying of an adobe consolidation with Di isocyanides and stone consolidant OH was tested. In this case, the values of the consolidated samples do not differ from the values of the untreated one.

For the roofed pits in Lintong, the soil can be seen as “dry”, porous mineral building material with stable pore space structure. It is not planned in the future to expose the soil to free water entry, because this could certainly destroy (treated and untreated) the structures that have to be conserved. Under the assumption, that the soil structures are also kept in the future in the hygroscopic humidity and at water levels under the plasticity limit (water content < 18 mass. - %), the structure and porosity of the soil stays the same. In this “unsaturated” condition, there are the same principals for the behaviour of water in the pore space, as with clayey sandstone, water vapour adsorption, vapour diffusion, surface diffusion, capillary condensation and capillary transport. They are explained in detail in (Klopfer, 1974), (Kießl, 1980), (Krus, 1995) and (Snethlage, 1984).

Just like natural stone, for the soil structures in Lintong, the effects of the conservation treatments on the porosity of the material, have to be tested (Sasse, 1996).

The tenside treatment with a maximal chain length of 9 angstrom should not have any effect, with the exception of the smallest pore radiuses, on the porosity of the soil. At the consolidation wit silicate ester, it is to be predicted that there is a decrease of the overall porosity. The examinations are related only to the so-called primary porosity of the soil (Scheffer, 1988), that depends on the granulation and the grain shapes of the structure. Secondary pores such as drying cracks, drilling holes, root channels, etc, that are only interesting for the seep flow, were not recorded.

Stabilisation of loess clay surfaces at the example of the Terracotta army in Lintong

Their amount could be minimised by the small format of the samples. For the classification of the pore sizes, different nomenclatures, exist depending upon the question (see. table 10 :). The following analyses evaluate the properties of the water in the complete primary pore spectra of the soil material, from the nanometre to the millimetre range. If there are no special notes, then this text is based on the building physics nomenclature. This classification comprises of the widest pore size spectra and is related to different water transport functions in its classification.

Soil science (Scheffer, 1998) (availability for plants)	Fine pores < 0,2 μm	Middle pores 0,2 – 10 μm	Rough pores
Building physical classification (Klopfer, 1985) (water transport mechanism)	Mikro pores < 0,1 μm	Kapillary pores 0,1 – 1000 μm	Makro pores > 1mm
IUPAC-classification (Sing, 1985), (Gregg, 1982) (adsorption mechanism)	Mikro pores < 0,002 μm	Meso pores 0,002 – 0,05 μm	Makro pores > 0,05 μm

Table 10: Classification of the pore diameter in the soil science, building physics and applied chemistry.

Analyse methods (Chapter deleted!)

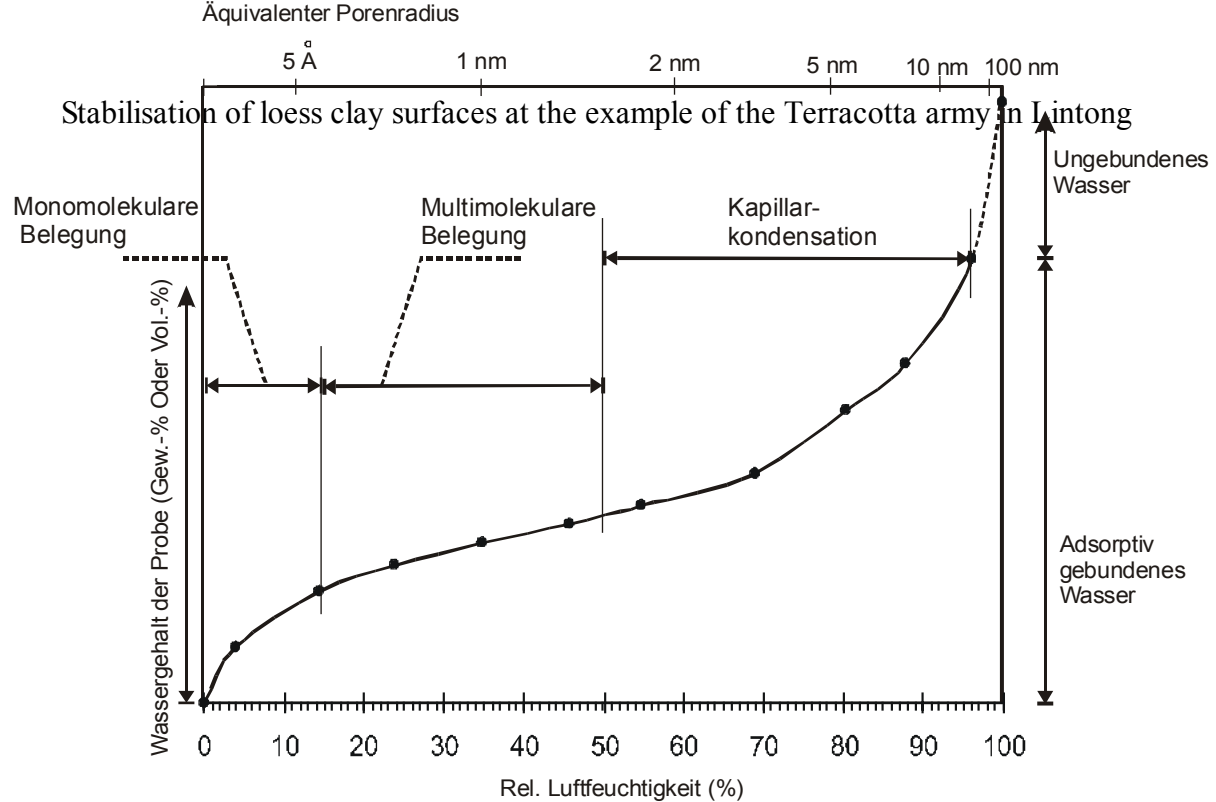


Image 43 Typical water vapour sorption isotherms for clay and other porous building materials. The vapour pressure of the surrounding air is related to the approximate pore radius, which should be filled. Accordant to the cylindrical capillary model. Illustration after (Kießl, 1983).

Analyses results

The graphics in image 44 show the influence of the treatment on the **dry gross density and the complete porosity** of the test pieces. The dry gross density of the untreated soil range between the extreme values 1.55 and 1.6g/cm³. Over 90% of the raw density values in the series E and F are also inside these marks. The values of the series B are at 50%, the series C and D are 100% over the maximum value of the untreated series A. For the treatment with ethyl silicate ester, there can be registered a distinct increase of the raw density and a similar decline of the complete porosity. The single treatment with swelling reducers (series E and F) has in contrary, results in no measurable changes of the raw density and of the complete porosity. Comparing the average values of the porosities, the pore volume of treatment type B is reduced by 5.7%, for D by 7.8% and for C yet more by 10%, while the average porosities of the series E and F do not differ more than 1% from the initial value. For better comparison, for the general classification of these changes in the building material clay, it has to be added, that after the classification of the German clay building rules in the DIN standards for the building material, clay are summarized,

Stabilisation of loess clay surfaces at the example of the Terracotta army in Lintong

and the transition of straw clay to massive clay is at a gross density of 1.7 g/cm^3 . The upper limit of the massive clays that are used as stamped clays is given with 2.2 g/cm^3 . Clay building materials with raw densities of 0.3 und 1.2 g/cm^3 are classified as light clays. The clay bricks (Adobe) that are more often mentioned in the conservation literature, mostly have dry gross densities of $1.3 - 2.0 \text{ g/cm}^3$ (Walker, 2000); (Houben, 1994). The German classification in clay building material, out of light clay, straw clay and massive clay is international not used.

Inside this large bandwidth of the clay building material, the changes of the variables through the treatment can be classified as unimportant. Nevertheless, a reduction of the porosity at $10 \text{Vol} \%$, due to the treatment, as in the case of the series C has to be seen from conservation view as a clear intervention.

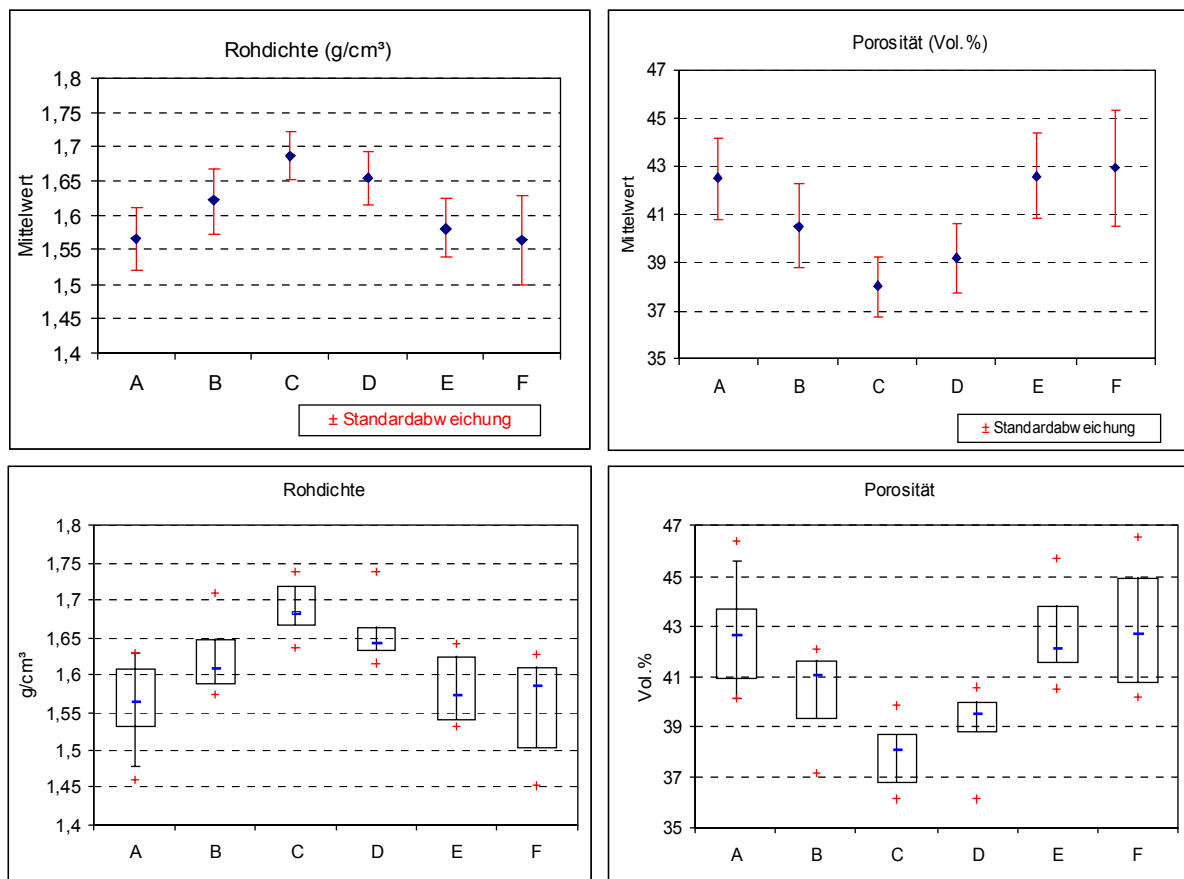


Image 44 Statistical distribution of the raw densities (diagrams left) and the porosity (diagrams right) treated (row B-F) an untreated (row A) samples. Single values in the rows: A-29; B-6; C-7; E-6; F-6.

Amazingly the dry gross density for the double treated series C and D is up by 2-4 % higher than at the single consolidation in series B, even though the separated gel mass is nearly identical at around 5 mass percentage (see image 42). The reason for

these differences in the dry gross density is probably in the relative widened pore structure in series B during the impregnation with F300E.

Even before the impregnation, in equilibrium condition with the ambient air humidity (approx 40% relative humidity, 20°C), the volume of the samples, that are treated with swelling reducers, is calculative to around 0.5% less than at the series B, due to the minor hygric swelling (see chapter 4.3.5). At the capillary impregnation with the consolidant and the subsequent storage at 75% relative humidity, the volume difference of the series would increase, so that in the case of series B, compared with the pre-treated series C and D, a relative widened (swollen) pore space would be consolidated. After the separation of the silica gel, the stabilised pore structure cannot shrink any more in adequate dimension, during the drying. Therefore, the measurements in the series C and D have a higher dry gross density and a lower complete porosity than the single consolidated samples of series B.

The pore radius distribution from the **mercury porosimetry** is shown in image 45.

For the untreated sample (A), the measurement limit has reached at 0.015 μm .

With higher compression phases, the sample collapses, so that smaller pore entrances cannot be dissolved any longer. For the other samples, this measure limit is not reached until 0.007 μm .

The pore radius maximum is in an untreated sample in the capillary pore space is 0.4 μm . After a further two maxima between 1 μm und 10 μm the curve decline is steep. The amount of pores over 100 μm is negligibly small.

The mercurial pore radius distribution of the sample with swelling reducer's mostly follows the curve in the untreated sample. The position of the maxima and the flattening of the curve at the large capillary pores are identical. Apparently, the treatment with the swelling reducers has no influence on the pores with a pore radius more than 0.01 μm . The silica gel consolidation shifts the pore radius maximum from 0.4 μm auf 2.5 μm with the treatment type B and respectively to 4 μm at the treatment type C. According to this, the gel has closed, in particular the pore radius in the lower capillary pore area between 0.1 und 1 μm . This matches the results of the SEM analyses that are verified for F300E gel layers between 0.1 und 1 μm thick (see chapter 4.2.1).

The upper range of the micro porosity between 0.01 and 0.1 μm is not substantially changed. The mercury access to the micro porosity seems not be disturbed by the silica gel film in the capillary pores. So the less the consolidation film can screen the micro porosity against the access of water and water vapour. It seems that, the film gives, due to its own porosity, cracks and losses enough apertures that the micro

Stabilisation of loess clay surfaces at the example of the Terracotta army in Lintong

pores situated behind cannot be protected. The self-porosity of the SiO_2 -gel is approximately 50 volume-%. During the evacuation, before the mercury intrusion, this pore space is emptied and the remaining water in the gel is removed.

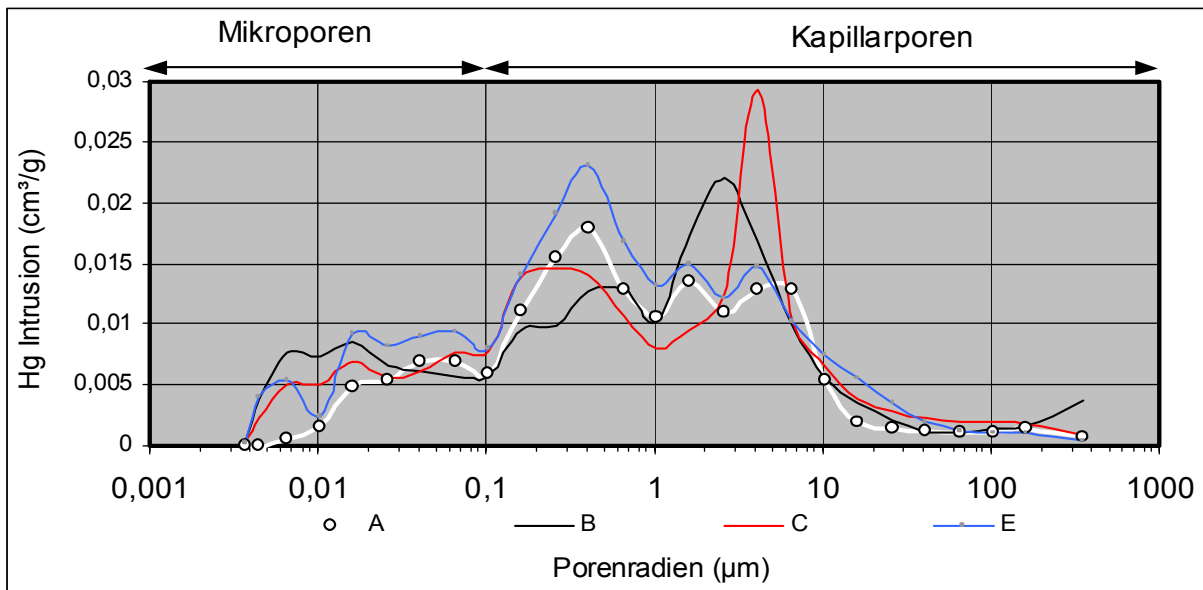


Image 45 Pore radius distribution from the results of the mercury porosimetry

The **water vapour adsorption isotherm** in image 46 shows clearly, that the access of the micro porosity, also under $0.01\mu\text{m}$, is not affected by the silicate ester consolidation alone (series B).

At the comparison of the adsorption of the treated and untreated series, an early separation of the graphics is registered in the humidity area of 0-40% relative humidity. This relates to the areas of the monolayer allocation (15% relative humidity) and the multilayer allocation ($\sim 50\%$ relative humidity) in the micro pore space after IUPAC-classification (see image 43).

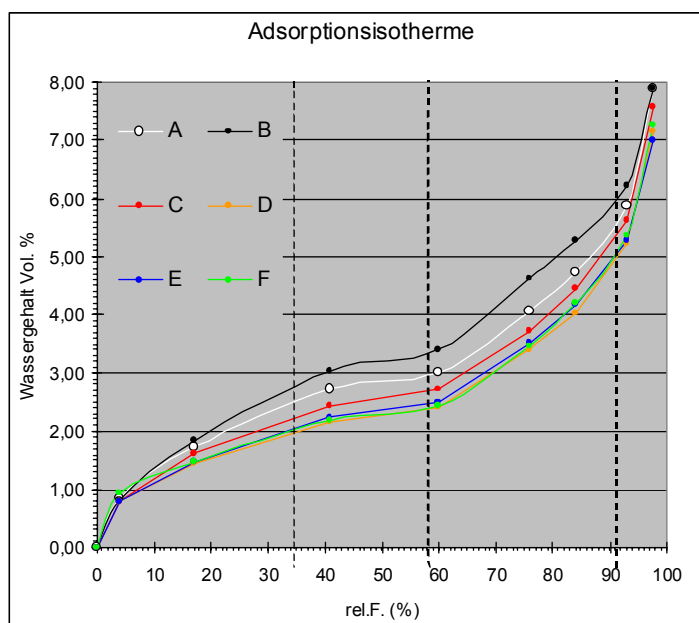


Image 46 Water vapour adsorption isotherm for the untreated (A) and treated soil sample (B-F) The treatment has an influence, especially on the water adsorption in the lower humidity area, of up to 40% relative humidity. The vertical lines divide the abscissa in three hygroscopic areas that have been conducted for the three pore radius classes (see image 47 to image 50)

The single SE treatment, therefore, causes an increased water vapour adsorption in the pore space to 0.002 μm pore radius. The treatment with the swelling reducer reduces the water adsorption in this area. The different tenside mixtures (series E and F) are in their effect identical. In addition, for the extra-consolidated samples of the series C and D the water vapour adsorption in the lower area is reduced. The water vapour adsorption in the lower area of the isotherm reacts mostly proportional to the swelling potential of a porous material (Kocher, 2003). It is an important piece of evidence, for the effect of the treatment, on the swelling reaction of the soil (see Chapter 4.3.5)

The progressive increase of the curves, in the area of the capillary condensation, proceeds in parallel. In the upper hygroscopic part, the curves seem to converge.

In contrary to the results to the preliminary examinations, both variations of the treatment cause a reduction of the adsorption in the hygroscopic area. This adsorption reduction corresponds to the theory of the tenside coupling, to the footprint of the clay minerals. Therewith, the presumption is confirmed, that the increased hygroscopicity of the treated soil, with modified swelling reducers, in the preliminary tests can be traced back on the overdose of the treatment medium (see chapter 4.1.3).

The directives for the evaluation of the compatibility and the durability of consolidations of natural stone in (Sasse, 1996) demand, that the area under the water vapour adsorption isotherm of the treated material, has to be smaller, or the same as the area in the untreated material. In contrary to the single consolidation in series B this default is kept in the treatments of the series C, D, E and F.

The calculation of the proportion for the pore radius under **0.01 μm from the water vapour sorption isotherm** results from the accumulation of the water adsorption (Volume % of the sample volume) inside the hygroscopic area of the isotherm. The adsorbed water, inside defined pore radius categories, is calculated on the accordant part at the whole pore space of the sample (after image 44). The results are compiled in image 47 to image 50. For easier differentiation of the adsorption character of the series, the radii are divided into three pore categories. They are orientated at the adsorption kinetic after (Kießl, 1983):

Category 1: < 0,001 μm	-Monolayer und Multilayer allocation
Category 2: > 0,001 – 0,002 μm	-Multilayer allocation, start of the capillary condensation
Category 3: > 0,002 – 0,01 μm	capillary condensation

Stabilisation of Fe-oxides on clay surfaces as the example of the

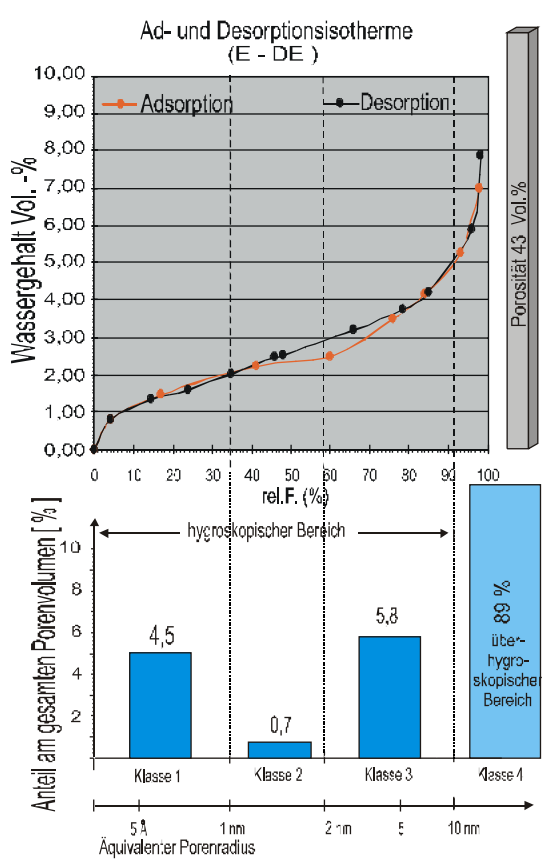
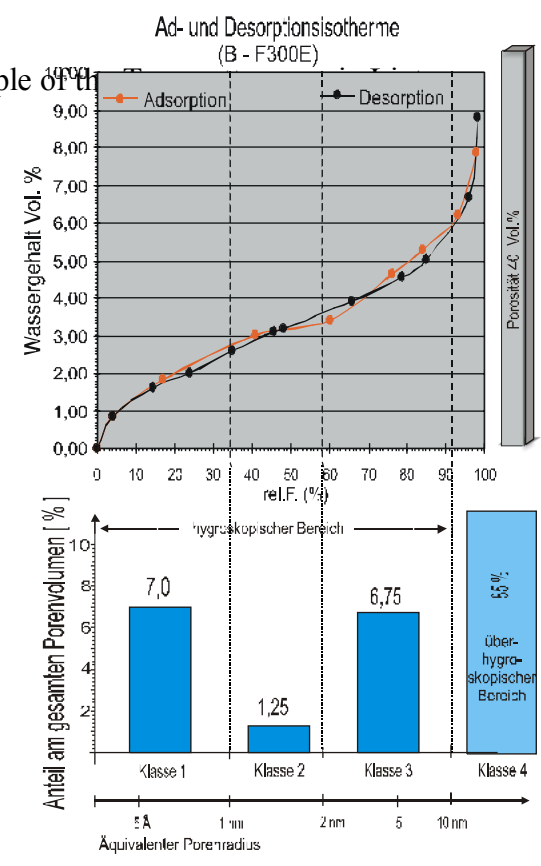
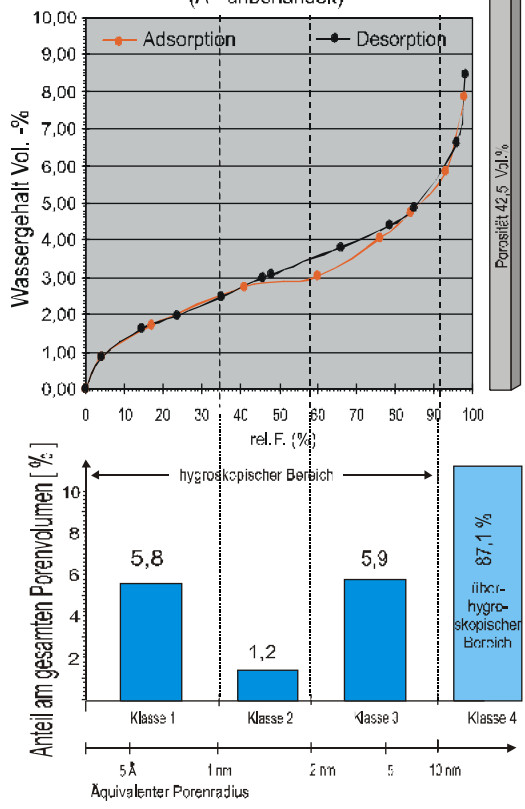
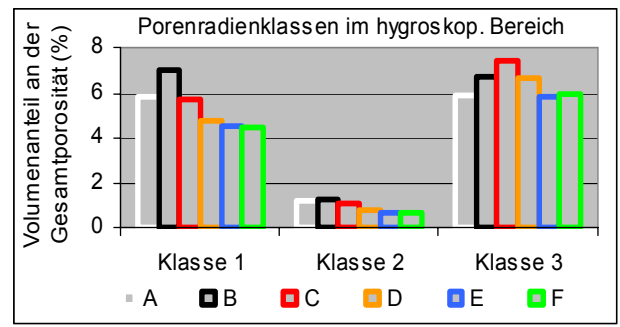


Image 47 left above: ad- and desorption isotherm of the untreated soil (A) with the corresponding pore radii. The amount of hygroscopic filled pores at the complete pore space is divided in three categories (layout after Kocher, 2003).

Image 48 right above: Analogue to image 47, ad- and desorption isotherm of the soil with single F300E treatment (B).

Image 49 left below: Analogue to image 47, ad- and desorption isotherm of the soil after the tenside treatment (DE)

Image 50 right below: Comparison of all series due to their amount of pores in the hygroscopic area. Division of the Categories like in image 47-image 49



In the images 47-49, show simultaneous the ad- and desorption isotherms of the series (A, B, and E). The hystereses between the ad- and desorption isotherms are minor. The calculation of the pore radius distribution in the column diagrams under the isotherms is based on the adsorptions curves. The isotherms of the series C, D and F are because of their similarity to E, not separately shown.

In image 50, are compared the **hygroscopic pore radii categories** off all series. The **amount of pores in the category 1** ($< 0.001\mu\text{m}$) is for the untreated soil 5.8% of the complete pore volume. For the single treatment with swelling reducing tensides (E and F) this amount is reduced, at constant complete porosity (see image 44), to 4.5%. Both tensides mixtures have the same effect. Through a single treatment with F300E, the pore radius proportion increases inside category 1 to 7%. Thereby, it has to be considered, that the increase in series B, to a lesser amount, also benefits calculative by the reduction of the complete pore volume. The additional pores during the consolidation are deriving probably from the own porosity of the silica gel. Possibly, also the shrinkage cracks in the gel as well as the hollow spaces between the gel film and the mineral structure below plays a role. These last phenomena are described in the results of the SEM-examinations (see Chapter 4.2.1). Similar pore space enlargements, in the micro pore area of consolidated sand stones, due to the consolidation, are described in (Sattler, 1992) and (Grasegger, 1992b).

Through the coupling of the tensides at the mineral surfaces as well as the therewith-connected decrease of the concentration of hydrate able cations and the osmosis potential, the water access of the pores in category 1 for the series E and F is reduced to 20%. The changes due to the treatment of the pore volumes in category 1, are for both methods approximately 20% in opposite direction.

For the combination treatment of the series C and D, both effects seem to overlap in the category 1. However, the influence of the tenside treatment seems to be more obvious. The porosity of the treatment C, corresponds to the untreated samples. For the treatment type D, the water accessible pore volume seems to be reduced.

Category 2 shows the same treatment effects as in category 1, but in reduced form.

During category 3, the adsorption reducing effect of the tenside treatment (Series E and F) is lost. The amount of pore radii corresponds to the untreated sample. In the combination treatment, the additional pores of the gel film have still an effect. Through the abolition of the tenside influence in category 3, also C and D show higher porosities than A.

Therewith, the limitation of the activity of the bi functional cationic tensides is proven for pore sizes less than $0.002\mu\text{m}$. This result correlates well with the dimension to the chain length of the tensides (see Chapter 4.1.2).

Stabilisation of loess clay surfaces at the example of the Terracotta army in Lintong

The acquired volume differences in the lower area of the micro porosity are indeed small, but nevertheless has an important relevance for the swelling properties of the soil (see chapter 4.3.5). These micro pores, as contacts between mineral particles are the initial zones of the hygric swelling.

Summary of the results to the porosity

For better comparison of the effects of the treatments on the entire pore space of the soil, the results of the adsorption isotherm and mercury porosimetry have been brought together in an integral graphic of the pore radii distribution in image 51. Out of this, the most important parameters for the evaluation of the moisture transport have been calculated with the pore radii distribution (Fitzner, 1988). The calculated values are compiled in table 11: The results for the specific surface from the nitrogen adsorption measurements are shown in image 52.

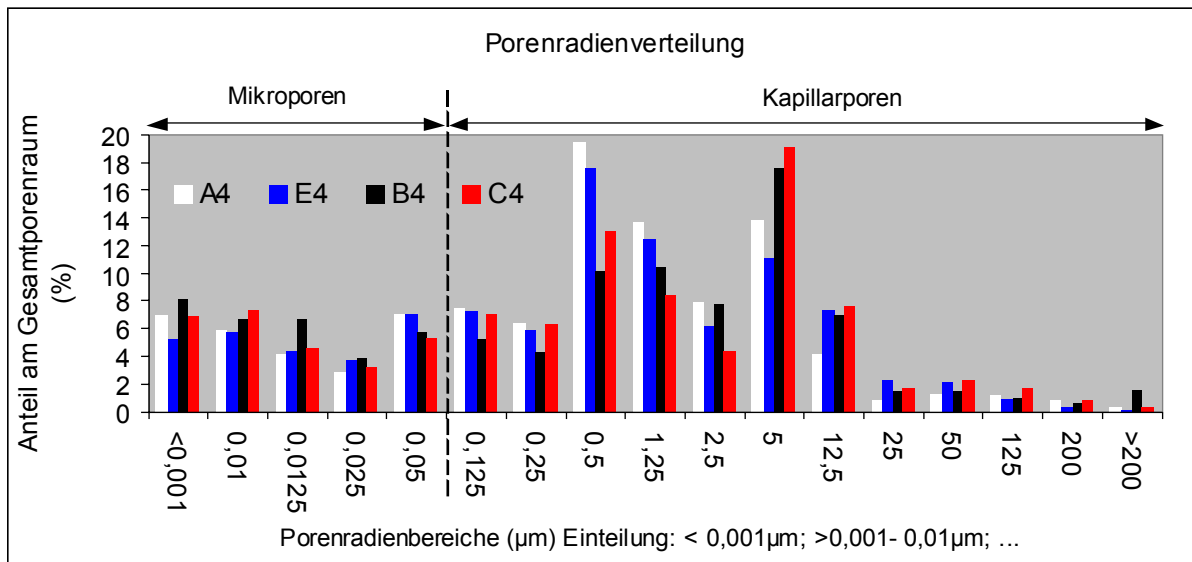


Image 51 Amount of the pore sizes at the entire pore volume of the samples classified in 17 pore radii classifications; combination of the results out of the water vapour sorption isotherm (fraction up to 0,01 μm) ; of the mercury porosimetry (fraction over 0,01μm) and the dry raw density (entire porosity of the samples).

Stabilisation of loess clay surfaces at the example of the Terracotta army in Lintong

Type of treatment	Median of the pore volume (position μm)	Micro pores Proportion at the porosity (%)	Capillary pores Proportion at the porosity	Position of the pore radii maximum (μm)
A (untreated)	0,5-1,25	24	76	0,25-0,5
B (F300E)	0,5-1,25	31	69	2,5-5
C (DE/F300E)	0,5-1,25	27	73	2,5-5
E (DE)	0,5-1,25	26	74	0,25-0,5

Table 11: Characterisation of the pore space in relation to the entire pore radii distribution, shown in image 51.

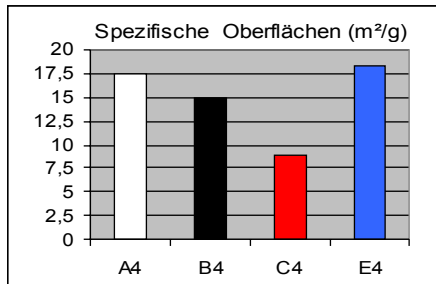


Image 52: Specific surface from the nitrogen adsorption measurement. The reduction of the inner surface of the samples, consolidated with SE (B and C) results from the diminishing of the pore volume in the lower area of the capillary porosity. The treatment with swelling reducers has no important influence of the inner surface of the soil.

The untreated soil has no noteworthy amount of pores with more than $200\mu\text{m}$ pore radius. The volume proportion from micro porosity and capillary porosity is at 24:76; the pore radius maximum is between $0.25\mu\text{m}$ und $0.5\mu\text{m}$. It is not changed by any of the analysed treatments.

By the consolidation with F300E, the silica gel is, built into the pores, larger than approximately $0.1\mu\text{m}$ pore radius. With this, a greater amount of the pores in the lower capillary radii area between $0.1\mu\text{m}$ and $1\mu\text{m}$ are sealed. The pore radius maximum is shifted to the area from $0.25\mu\text{m}$ to $5\mu\text{m}$. The built-in gel reduces the complete porosity up to 10%. This reduction is more distinctive at the combined treatment (series C and D), than at the single treatment with F300E (series B). It also reflects in the reduction of the specific inner surface. The silica acid consolidation does not reach the micro porosity of the soil. Despite the coating of the larger pores, it does not constrict the water access to the micro pores. The porosity of the silica gel even contributes to the micro porosity with pore radii lower than $0.0125\mu\text{m}$. Thereby, the water vapour adsorption is noticeable increased in the hygroscopic range. At a single consolidation treatment, the volume proportion of the micro porosity and capillary porosity, shifts with 31:69 in the direction of the micro porosity, due to the coating of the larger capillary pores; it does not prevent the entry of water into the micro pores. Therewith, the consolidation with silicate ester causes a higher water storage capacity in the sorption humidity area and a reduction of the capillary moisture transport.

The effect of the tenside treatment on the porosity of the soil is extremely small. Inside this small effect, it is not possible to see differences between the formulations of series E and F. Through the treatment with swelling reducers, neither the entire porosity nor the inner surface of the soil has a detectable change. Nevertheless, the Tenside treatment causes a distinct reduction of the water access in pores smaller than 0.002 μm pore radius.

The tenside treatments reduce the water storage capacity in the completely hygroscopic humidity area. This reduction is contrary to the observations of the preliminary examinations. The increased hygroscopicity in the preliminary examinations was, therefore, an effect of the overdose. For the combination treatments in the series C and D, the aforementioned changes due to the silica acid consolidation are dominant in the capillary pore space. However, in the range of the micro porosity, the effects of both treatments (swelling reducer and consolidation) can overlap; so that, especially for the lower sorption humidity area (up to 40% relative humidity) pore space parameters are adjusting, similar to the untreated soil.

4.3.4 Examinations and results to the water transport

The variables of the water transport have been established as important basis information for the evaluation of the durability of surface conservation treatments (Sasse, 1996). Like the outsides of the stone façades, the soil surfaces in the museum halls of the Terracotta army are permanently in contact with the high humidity deviations of the ambient air. On one hand, water is adsorbed from the surface, out of the air and transported into deeper zones; on the other hand, moisture is transported out of the soil to the surface and released into the atmosphere. The experiences in stone conservation have shown that changes of the water transport coefficient, due to treatments, can cause dangerous congestions of moisture near the surface at the boundary layer of the treated zones. Because the soil reacts with swelling and a decreased stability much quicker and stronger on rising humidity than natural stone, breaks in the moisture gradient, of surface near profiles, will probably lead to a much quicker formation of scales or similar damage symptoms to this material. Additional to this is the structure damaging effect, that salt concentrations and frost fractures can evocate in the accumulation zones (Poschlod, 1990), (Wendler, 1991).

The most important parameters for the moisture transport function are, in the sorption humidity area, the water vapour sorption isotherm, the water vapour diffusion coefficient and respectively water vapour diffusion resistance number (μ -value). In the hyper hygroscopic area, the moisture transport is mainly affected by the water

absorption coefficient (w -value) and the free water saturation under atmospheric pressure (w_a) (Kießl, 1983), (Künzel, 1994), (Krus, 1995). Furthermore, these four parameters are the basic values for the calculation of the moisture transport in the WUFI modelling software. The influence of the treatment on the water vapour sorption isotherm has been discussed in the previous chapter. According to the guidelines in (Sasse, 1996), the variables of the treated soil should, as much as possible, not deviate from the values of the untreated soil, that the explained discontinuities between the treated surfaces and the untreated substrate does not occur. In contrary to the mercury porosimetry and the nitrogen adsorption, the water transport coefficients are determined by so-called “direct methods”. The actual reaction of the water in the material is analysed. Therewith it is shown, that the expectations from the results and the interpretations of the pore space analyse corresponds with real interaction between water and treated soil.

Analysing methods (Chapter deleted!)

Results of the examinations

The average values, from the results of the dry-cup and wet-cup trials, for the determination of the **water vapour diffusion resistance** are compiled in image 53.

The untreated samples have, in the humidity range (wet-Cup) μ -values of 6. 4. This responds to the diffusion resistances from the examinations of the FEB (research laboratory for experimental building, Kassel). They measured, for comparable massive clays, diffusion resistances between 6 and 7 (Minke, 1995). The examinations in the ongoing project Terra, also show, that the wet-cup values for adobe-samples are in the same dimensions (Bourges, 2003). In this test series it is also shown, that the diffusion resistance is diminishing in humidity range with increasing amount of clay. This can be traced back to the increased activity of the surface diffusion by the increased micro porosity.

As previously mentioned, the overlaying fluid transport of the surface diffusion drops out in the dry area method (up to 50% relative humidity). The water vapour-diffusion resistance of the untreated sample is three times higher in the dry cup test.

Therefore, the amount of the water vapour diffusion in the gas phase is just a third of the complete liquid transport in the sorption humidity area. The consolidation with SE seals up to 10% of the capillary pores and reduces, therewith, the free passage area for the gas diffusion (series B, C and D). The diffusion resistance in the dry area

Stabilisation of loess clay surfaces at the example of the Terracotta army in Lintong

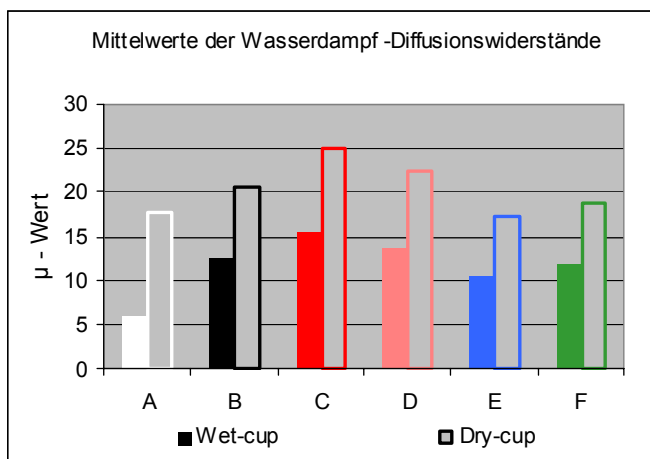
method increases up to 12% for the series B and 40% for series C (compared with the untreated soil).

The single treatment with swelling reducers (series E and F) does not change the diffusion value in the dry area method. The free passage area for the water molecules in the gas phase is not changed by the treatment. This confirms the results of the mercury porosimetry that does not show any changes of the capillary space due to the treatment.

Nevertheless, through the tenside treatment, the diffusion resistance is doubled in the moist area. This refers to an interference of the surface diffusion through the coupling of the bifunctional tensides. If the diminishing of the surface diffusion is caused only by the “blockage” of pore spaces under $0.002 \mu\text{m}$ (see summary of the results of the porosity), or if the tensides also disturb the liquid diffusion at the sorbat layers of the larger micro – and capillary pores, cannot be quantified.

However, the high amount of the diffusion decline leads to the conclusion, that the tenside have coupled also at the pore septum/walls of the large pores and have reduced the thickness of the sorbat layers by the reduction of the hydrate able cations and increased their liquid diffusion resistance.

The combination treatment of the series C and D have the highest diffusion resistances in the humidity range method, because here, the “slow down effects” of the consolidation (gas phase) and of the tenside treatment (liquid phase) are complementing to one another. For the surface consolidation on natural stone facades SASSE UND SNETHLAGE (1996), recommend, that the μ -value from the wet



cup test should increase more than 20%, by the treatment. The treatments of the test series exceed this threshold by far. The wet-cup values of the series E are the lowest. However, their average value outranged the diffusion resistance of the untreated sample up to 64%

Image 53: Average values from the dry-cup and wet-cup diffusion measurements, at the treated and untreated sample discs.

The changes due to the treatment of the **capillarity and the free water saturation** are not relevant for the specific problem in the museum halls of Lintong, because for the uncovered soil structures direct water contact is not foreseen.

For a more complete evaluation of the treatment methods and their transferability to comparable conservation problems, the knowledge of their influence on the specific values of the capillary transport is necessary. Furthermore, an unwanted water entry can never be 100% eliminated even for the sheltered excavations of Lintong.

From the tests of the capillary water adsorption, the water adsorption coefficient and capillary water capacity have been calculated. The average values of the series are shown in image 54. The single results for the water saturation are given in image 55. The water adsorption coefficient of the untreated soil is between 10 and 14 kg/m² h^{0,5}. They are, therefore, much higher than the few comparable values from the literature; this gives for clay bricks an adobe water adsorption coefficient between one and six (Bourges, 2003); (Minke, 1995). In contrary to this, the capillary water capacity is with values between 20 and 30% comparable with the values in (Minke, 1995).

That means, that the capillary pore volume of the soil of Lintong is quite similar to the modern clay building material, analysed by Minke. Nevertheless, the capillary pores of the soil of Lintong are quickly accessible. The position of the pore radii maxima, in the capillary pore area, has a big influence of the soaking speed of the material. Consequently, pores with a larger capillary diameter, soak in the water faster than narrow capillary pores (Krus, 1995). In addition, the amount and quality of the clay minerals have a strong influence on the water adsorption coefficient. Gernot Minke writes "It is interesting, that strong silt containing clays show a much higher w-value than clayey adobes. It derives from the different pore-structure of the clays and that the clay containing adobe is swelling stronger and therefore its pore volume diminishes stronger" (Minke, 1995).

The pore volume does not diminish at the swelling, but the swelling in clayey adobes can diminish the access to the capillary porosity and the capillary porosity itself. This "sealing" of the capillary pores lead to the reduction of the quotient of the water adsorption and the square root of time. This effect could be the reason for the "bending" of the original linear dependence, which can be observed at some samples in the graphical evaluation, of the trials to the capillary water adsorption (see appendix 7.6).

Stabilisation of loess clay surfaces at the example of the Terracotta army in Lintong

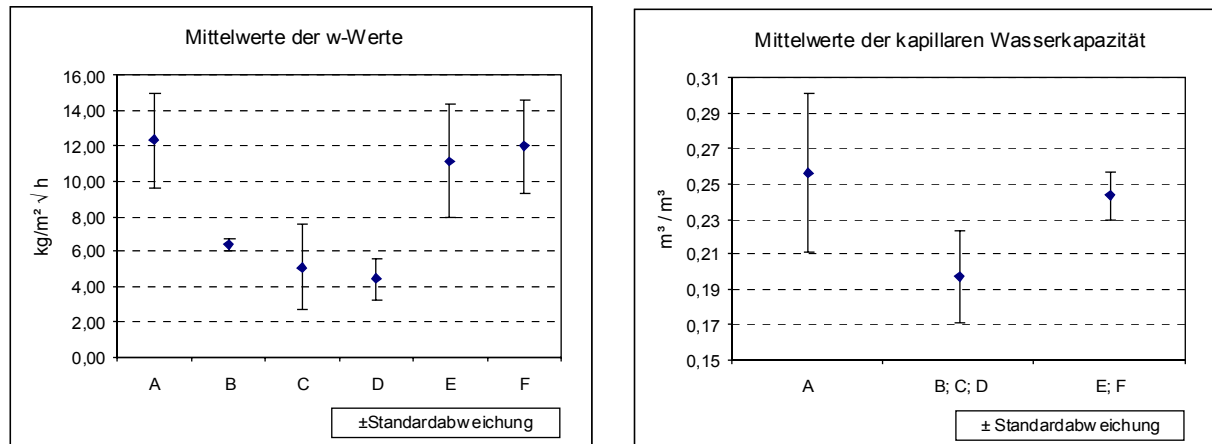


Image 54 Results from the measurements from the capillary water adsorption. Left: Average values and standard deviations of the water adsorbent coefficient. Right: Average values and standard deviations of the capillary water capacity.

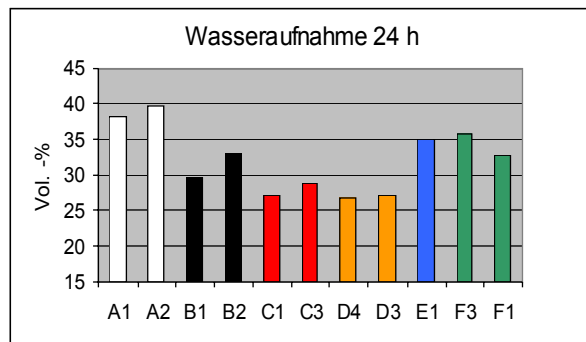


Image 55: Water adsorption at single soil samples in 24 hours under water storage (w_a). The values of the series A, E and F are due to the trial afflicted with grave measurement errors (+/- 15%).

The comparison of the samples in the test series shows, that the consolidation with F300E, nearly cut in half the water adsorbent coefficient (sequence B, C, D), while the swelling reducers have not had a visible effect on the capillary behaviour of the soil (image 54). The reduction of the water capacity from 26 to 19 volume % proves the observation from the mercury porosity, that the consolidation with silica acid silicate ester reduces the capillary pore volume. The reduction of the capillary water adsorption is, from the viewpoint of conservation, in principle critical. The guidelines in (Sasse, 1996) say that the w value should be after the treatment smaller or equal to the original.

The **free water storage** gives in comparison of the treatment methods, for the treated samples, a related picture similar to the complete porosity (see image 44). The consolidated samples have less porosity, accessible for water, than the untreated samples or the samples with tenside treatment. It is interesting, that the water accessible parts of the entire volume at the double treated samples (series C and D) with 68% turn out to be minor, than at the single F300 consolidation (series B) with about 77% water accessible of the entire porosity. It seems, also the treatment

Stabilisation of loess clay surfaces at the example of the Terracotta army in Lintong

with swelling reducers diminish the volume of the free water adsorption. While the untreated samples in the trials fill about 89% of the complete pore volume with water, the soil with the swelling reducers just fill it with approximately 80%.

Without the described “packaging” the untreated soil would be completely filled with water and would elutriate- not so the treated soil (see chapter 4.3.5)

Summary of the results of the water transport

In the sorption range between 50 and 100% humidity, the moisture in the soil of Lintong is transported more or less in equal parts by the surface diffusion and the water vapour diffusion. The examinations have shown that the consolidation treatment slows down the water transport, through the reduction of the open pore diameter in the capillary pore area. The tenside treatment again slows down the water transport through an interference of the surface diffusion at the pore walls. Out of the combination of both effects, results for the combination treatment (series C and D) the largest measured vapour diffusion resistance. Although the diffusion resistance of the soil is increasing through the treatment, the soil still stays very porous. Neither the tenside treatment nor the consolidation with SE reacts as a “vapour break” in the usual meaning. To ease the evaluation of the μ -values and the w values from the series, they are confronted in table 13 with reference values from the literature.

The soil of Lintong has a strong capillary exhaustion rate. The water adsorption coefficient and the capillary water capacity are approximately halved by the consolidation with silicate ester. The treatment with swelling reducers has no effect on the capillary properties of the soil.

The interaction of the capillary water adsorption and the water vapour resistance was compiled by H.Künzel for the example of the sprinkling and drying of façade surfaces, in the so-called “Künzel number” (Künzel, 1969). On the base of the μ -value and the w -value, the drying attitude of a porous building material is described. In stone conservation, this “Künzel number” is used as a guideline for the evaluation of consolidation and hydro repellent treatment due to their effect on the moisture balance in the outside walls (Meinhardt-Degen, 2002). At open façade areas in Western Europe the Künzel number should be smaller than $0.1 \text{ kg/mh}^{0.5}$, to avoid the risk of a constant humidity concentration in the walls. Compared with the guideline value, the data in table 11 shows as expected, that the soil of Lintong is not suitable as a façade material in West Europe. However, the numbers make clear the negative influence of the treatments to the drying behaviour of the soil- in the case of

Stabilisation of loess clay surfaces at the example of the Terracotta army in Lintong

direct water wetting. The simple treatment with swelling reducers results badly here, because it slows down the vapour diffusion that is necessary for the drying out. At the same time, it also does not reduce the high capillary water adsorption of the soil. In the case of an open façade, there is the rule, that the doubling of the diffusion resistance is not dangerous, as long the w-value is small (Snethlage, 2002). Therefore, the treatment of the series B, C and D has the better water transport properties in the case of a direct wetting with water.

In the given example of the museum hall in Lintong, without water wetting from outside, but with the evaporation from lower layered soil depth, that are still moist (ground water, etc), there is the danger that by the vaporous rising water, moisture concentrates at the surface. In the case of the soil structures, in the museum halls, is the w-value irrelevant, but the permeability for water vapour is the main parameter.

The variables for the water transport are describing the direct reaction of the water to the changes of the soil, due to the treatment. Their correlation with the interpretation out of the previous pore space analyse shows, that it is possible for the soil of Lintong to transfer the approach of the cylindrical model from the building material science and the analytical methods used in stone conservation, to the building material soil. For adobes with higher amounts of clay and smectite montmorillonites clay minerals, this transfer will be more difficult.

A	B	C	D	E	F
60	84	75	63	121	144

Table 12: The “Künzel-numbers ($\text{kg/m}^2 \text{h}^{0.5}$)” for the test series. The number is calculated out of the water vapour equivalent to the air film thickness (s_d (m)) and the w-number. Thereby applies: $s_d = \mu * s$, whereas s (m) is the thickness of the sample. The calculation formula is: Künzel number = $s_d * w$ -value.

material:	μ - value (wet-cup)	w- value ($\text{kg/m}^2 \text{h}^{0.5}$)	material:	μ - value (wet-cup)	w- value ($\text{kg/m}^2 \text{h}^{0.5}$)
soil Lintong untreated	5 - 8	10 - 15	limeplaster	7	3
soil Lintong treated	9 - 18	3 - 7 (F300E)	Solid brick	10 - 17	18 - 24
Straw light clay	2 - 3	3 - 4	„Ummendorfer“ sand stone	14	16
Massive clay	6 - 8	1.5 - 4	„Zeitzer“ sand stone	70	0.2
Adobe plaster with lime	8 - 15	-	„Krensheimer“ shell limestone	140	0.5
Adobe plaster with water repellence and consolidation	10 - 18	-	concrete	100 - 200	0.5 - 1

Table 13: Water vapour diffusion resistance values (wet-cup) and water adsorption coefficient of clay (data out of: (Minke, 1995) and from building materials (data out of material bank in (Künzel, 2002)).

4.3.5 Examinations and results of the swelling effect of the water on the treated samples

Humidity changes close to surface has been for a long time seen as the cause for weathering damages on building blocks, because the swellings and shrinkage due to the change of moisture, stress the mineral structure (Riederer, 1973), (Toracca, 1997). In particular, on building blocks containing clay, this process, cannot only be induced by the capillary water adsorption, but also often by atmospheric moisture, can lead to dissolution effects in the structure.

In the clay construction, capillary water adsorption leads to a decline in the stability and often causes an immediate loss of material. Therefore, it is undoubted, that water infiltration enhances the decay of clay building material. The water is the known enemy of the clay architecture and any water infiltration has to be avoided on this material, whatever happens (Houben, 1994), (Minke, 1994).

If regular and strong changes of atmospheric humidity are also a catalyst of surface decay at clay building material, as often suggested, but until now not proven. For example, recently in the “Terra project” no changes in the structure of adobe bricks could be detected after 15 humidity cycles between 30 and 92% relative humidity (Bourges, 2003). In addition, the dust traps in the museum halls of Lintong have shown, that in 3 years no loss of material occurs, due to atmospheric humidity changes. It is possible, that the soil despite their high adsorption – and desorption turn over, and the therewith connected high swelling rates, due to the high porosity and the flexible structure, can resist the atmospheric humidity changes better than some other mineral building material.

In any case, it is very important to record the effects of the treatments on the hygric swelling in the range of the changes of the atmospheric humidity, because of the reduction of the swellings (as expected from the swelling reducers) could certainly reduce the mechanical stress in the mineral structure and therefore prevent against decay. In contrary to this, treatments that lead to an increase of the hygric dilatation in this area can be proven to be damaging for the structure in the long term. The untreated soil of Lintong dissolves immediately in water. Most of the previous conservation approaches tried to void the elutriation of the soil in water. Despite direct water attack with the connected high swelling rates, up to the elutriation, is not crucial for the special problem of the museum halls of Lintong, because for the uncovered soil structures no direct water contact is envisaged. The “elutriation test” is

Stabilisation of loess clay surfaces at the example of the Terracotta army in Lintong

necessary for the complete evaluation of the treatment methods and their general transferability to similar conservation problems.

Examination methods (chapter deleted!)

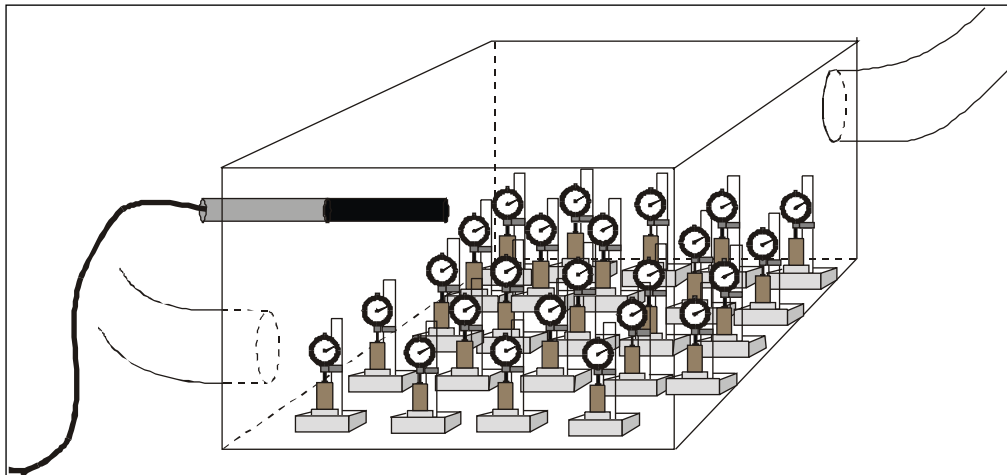
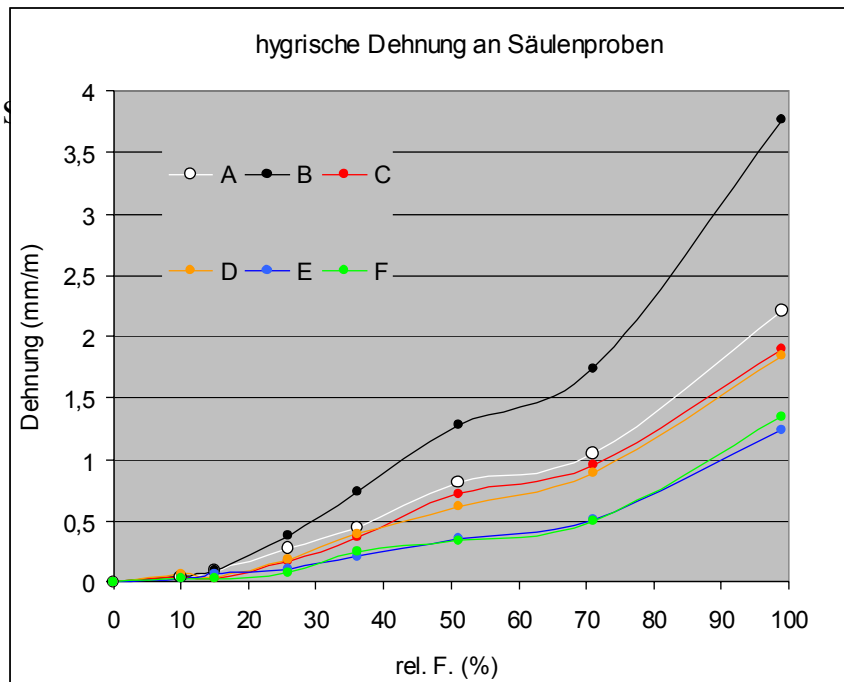


Image 56 Climatised box with measurement racks, moisture sensors and ventilation tubes, for the measurement of the hygric dilatation in the hygroscopic atmospheric humidity.

Examination results

The results of the three basic types of treatment (consolidation, treatment with tensides and the combined treatment) from the **test to the hygric swelling** are confronted in image 58 to the swelling of the untreated series A. In the direct comparison of the average values of all series (see chapter 57) it is obvious, that the used types of tensides (DE and DEBH) do not differ in their effect. The series C and D and the series E and F have identical swelling curves.

The curve for the single consolidated samples of the series B ascends steeper than the untreated series A. The consolidation causes with an end value of 3.75%, an increase to 75% in the maximal atmospheric humidity (see table 14).



army in Lintong

Image 57 The average values of the swelling in every series, measured in seven successive, incremental steps inside the hygroscopic water adsorption.

series:	A	B	C	D	E	F
swelling (mm/m)						
26% to 98% rel. h.: (possible)	1,92	3,38	1,72	1,66	1,14	1,27
30% to 85% rel. h.: (often)	1,2	2,2	1,15	1,05	0,7	0,75
40% to 70% rel. h.: (normal)	0,6	0,8	0,5	0,45	0,25	0,25
45% to 65% rel. h.: (aim)	0,25	0,4	0,25	0,25	0,1	0,1
Swelling in contrary to the untreated sample series (%)						
26% to 98% rel. h.: (possible)	100	176	90	87	59	65
30% to 85% rel. h.: (often)	100	183	96	88	58	63
40% to 70% rel. h.: (normal)	100	133	83	75	41	41
45% to 65% rel. H.: (aim)	100	160	100	100	40	40

Table 14: Hygric swelling (mm/m) of the analysed soil samples in the different atmospheric humidity areas (above) with the related comparison values to the untreated series A, in percent (below). The humidity areas (possible, often,) are orientated at the museums halls in Lintong.

Stabilisation of loess clay surfaces at the example of the Terracotta army in Lintong

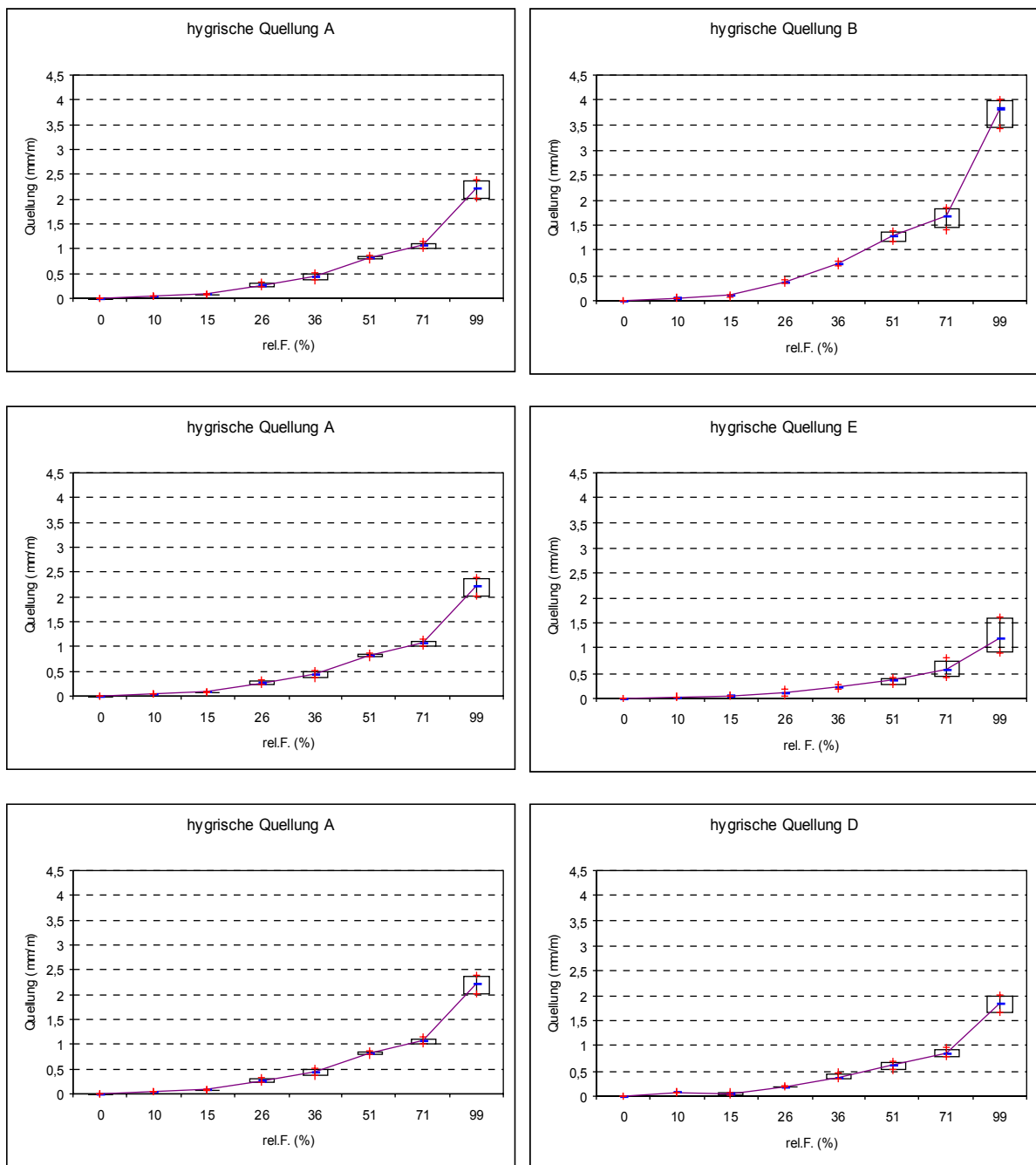


Image 58 Hygric swelling of the single samples of series A, B, E and D compiled in box & whisker diagrams for each wetting step. Examples of the single consolidation (B), the tenside treatment (E) and the combination treatment (D) on the right side are directly confronted with the untreated series (A) on the left side. The small column height of the box & whisker graphic shows, that the measurement values of the single samples inside the series are very close. The summary in image 57 seems therefore justified. The graduation of the x-axis is not linear.

Stabilisation of loess clay surfaces at the example of the Terracotta army in Lintong

The single tenside treatment reduces the swelling depending to the humidity at 35 to 60%. At the combination treatment, the swelling stays in the area of the untreated sample (see table 14, image 57 and image 58).

Looking at the swelling curves (image 57), fundamental agreements are obvious between the comparison of the series and the course of the curve with the results of the water vapour –adsorption isotherm (see image 46). After a steep incline in the dry range, the swelling curves level between 40 and 65% humidity, then once again steeply incline in the humid atmosphere, parallel to the strong water adsorption. Theoretically, the swelling curve should be convex between 0 and 15% relative humidity analogue to the water adsorption isotherm, but this area is difficult to measure at the swelling measurements and should not be incorporated. In general, the swelling of the series reacts in the hygric area analogue to the water adsorption.

With a precise comparison of the water vapour adsorption isotherms with the swelling curves, it becomes clear, that in the treated series not only the volume water adsorption but also the swelling reaction of the material changed. (See image 46 and image 57). Therefore, the adsorptions isotherms are approaching again to the limit of the over hygroscopic range, while the differences in the swelling values are increasing in the same range. Further evidence is the curves of the combination treatment (series C and D). Their adsorbat volume is very similar to the single tenside treatment (series E and F). However, the swelling values are much higher than at the single tenside treatment. The dependence of the swelling from the adsorbed amount of water is shown in image 59. At the same water adsorption, the samples of the consolidated series B are swelling much more than the untreated samples. The tenside treatment once again achieves at the same water adsorption a swelling reaction. In the combination treatment, these effects adjust themselves.

The increased swelling due to the gel adsorption is traced back probably to the effect of the “limited swelling space”, as described at WENDLER (1996) (Wendler, 1996a). Accordingly to the results above, at the consolidated soil (see image 59), Wendler observes that clayey sandstones with a silica gel consolidation increased swelling rates at the same water adsorption.

He explains this effect with additional compression stress between the clayey mineral structure and the gel that lines in the pore spaces. Without a gel film, the clay mineral packages can grow without any resistance at the pore barriers in the free pore space during the hygric swelling.

In this space, blocked by gel film, additional swelling pressure builds up, that discharges itself in additional material swelling (see chapter 3.4)

Stabilisation of loess clay surfaces at the example of the Terracotta army in Lintong

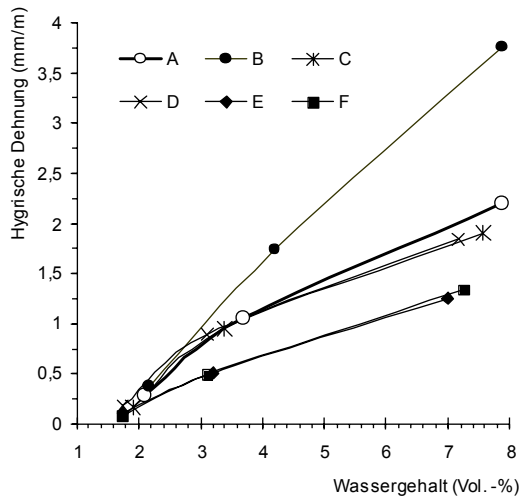


Image 59 water content- swelling- curves from all series for the humidity range between 26% and 98% relative humidity. The changes in the swelling property of the treated samples cannot be explained only with the hygroscopicity.

The tenside treatment, however, can reduce the hygric swelling at the same water adsorption. Obviously the aimed reduction of the osmotic swelling inside the micro porosity reacts in this way, that less water can infiltrate in the pores and therefore the swelling pressure is limited (see chapter 4.3.3). If this effect is based on the reduction of the hydrate able cations or in the bridging of the mineral surface with the alkyl chains of the tenside, then it cannot be differentiated here.

The requirements for the changes of the material properties at consolidated natural stone say that the hygric swelling should not increase due to the treatment in the hygroscopic and super hygroscopic area (Sasse, 1996). The single consolidation with silicate ester (series B) does not comply with this requirement. This type of treatment leads because of the higher swelling rates, to additional mechanical stress in the atmospheric humidity change. If therefore, despite the increased stability, the liability for decay increases in comparison to the untreated soil, it could be clarified by wetting/drying cycles in the hygroscopic humidity changes. A negative influence is also possible at a single consolidation as the positive influence by the treatment types C,D,E, and F, which reduces the hygric swelling in the atmospheric humidity. However, the real effect of the changed swelling values can only be evaluated with the implication of the resistance and the elasticity of the treated material (see chapter 4.3.6).

From the **elutriation tests** gathered observations are demonstrated at selected images in image 60 and image 61. The high osmotic pressure in the micro pore space of the samples, combined with the low structural stability of the soil, leads to water deionised at once to an elutriation of the untreated soil from Lintong (A). The treated soil stays stable. After DIN 18952 side 2 the untreated soil is classified as "easy elutriate able" and therefore non-viable for clay building.

Stabilisation of loess clay surfaces at the example of the Terracotta army in Lintong

In the case of a tenside treatment, the osmotic pressure is reduced so far, that the sample does not elutriate in water. The samples adsorb a lot of water and get soft but keep their shape. Pulling the disc sample E (image 60) out of the water, the samples break due to its high own-weight because it is soaking. Other tests have shown that the cylindrical samples of the series E and F also keep their shape under water. Exposed to the air, the water-saturated cylinders cannot stand their own weight and collapse. Exposed to air, the water-saturated cylinders cannot withstand their own weight and collapse inwards. Due to their stability, there was no obvious difference between the treatment type E and F. The structural strengthening effect of the tensides in water storage is significant evidence, that the clay mineral surfaces are really connected over the alkyl chains of tensides.

The lack of structural stability in the tenside treated samples is achieved in series B, C and D with the consolidation treatment. The samples stay completely stable under water. Knocking at the sample with a pencil, after several days of water storage, the samples can resist at least the same pressure as the untreated dry soil sample (see image 61). If you take this sample out of the water, they keep their form and dry off apparently without any damage. Between the single consolidations (B) and the both combined treatments (C and D), there are no qualitative differences.

At least at single water storage, the stabilising gel film can adsorb the strong inner tensions, which can be expected in the single treated series B, due to the osmotic pressure.

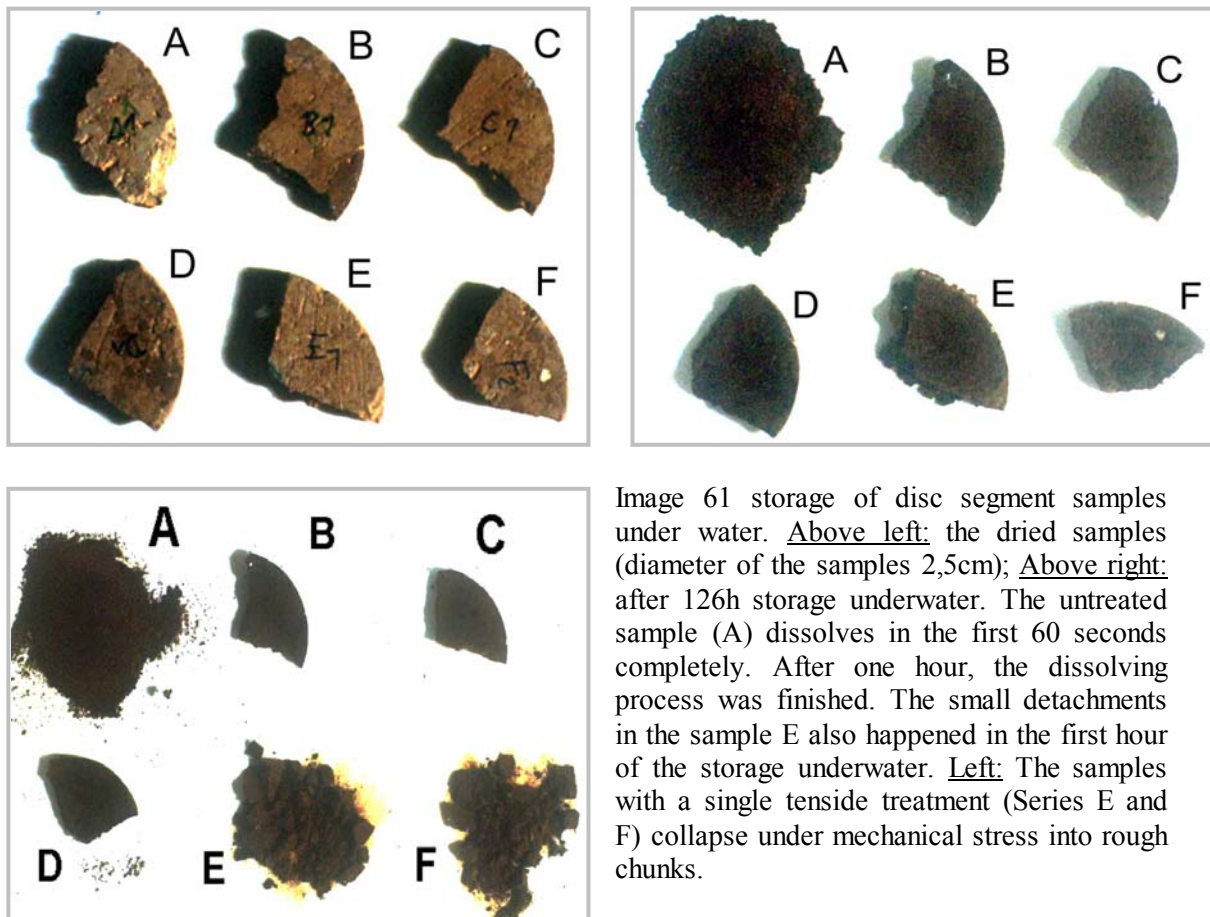
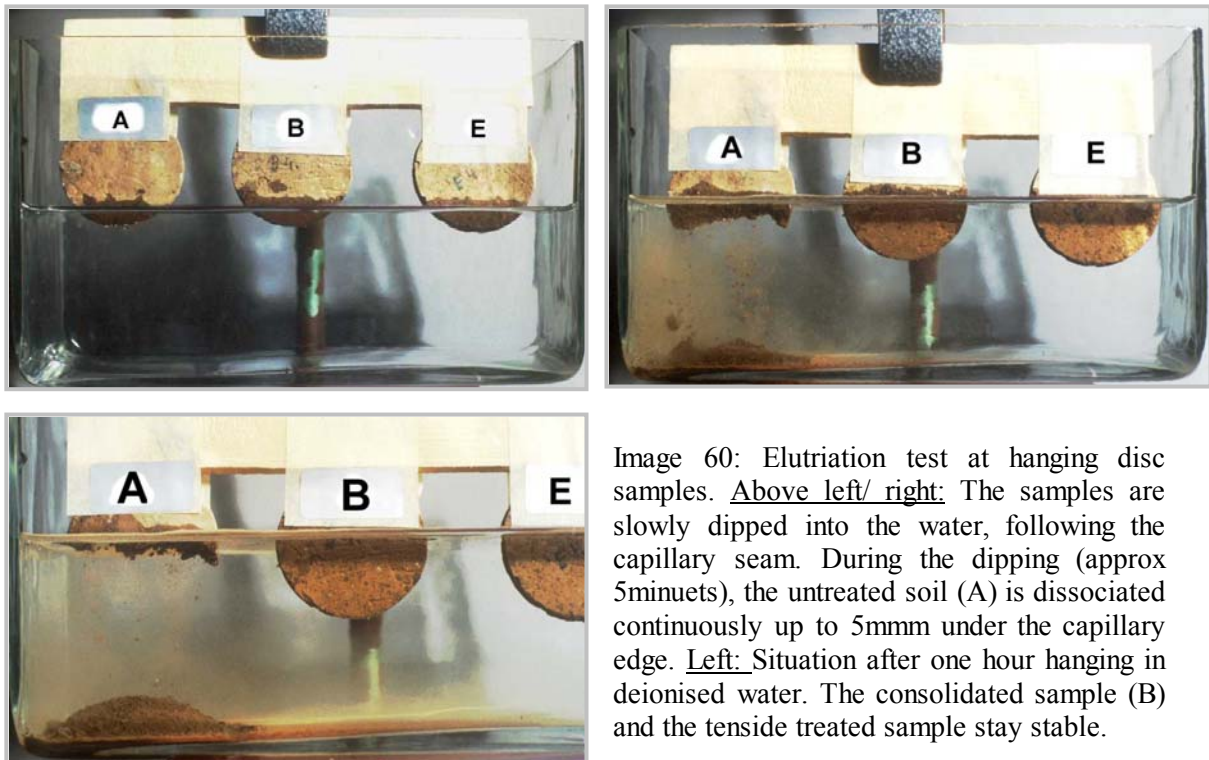
Previous experiences with the consolidation of adobe wall in Fort Selden, New Mexico with Di isocyanides and silicate ester have shown, that the consolidated soil cannot resist the tensions from the hygric dilatation in a larger scale (decimetre) and breaks (Agnew,2002). Even small, consolidated samples cannot resist multiple water storage and break (Chiari, 2003).

For the combination treatment (series C and D) there could not be found any advantage in this elutriation tests in comparison to a single consolidation. But because the osmotic pressure at the treatment with the bi-functional tensides is clearly reduced, corresponding to the single tenside treatment, it is to assume, that inside the consolidated structure of the combination treatment, there is much less tension during the water storage, than in the single consolidation. Therefore, it is possible to prognose a much better stability and durability for the combination treatments in wetting and drying cycles.

With the elutriation tests it was shown, that it is even possible without a consolidant, just with a tenside treatment, to avoid the solution of the soil in water, or at least to increase clearly the resistance against fluid water. The combination treatment seems

Stabilisation of loess clay surfaces at the example of the Terracotta army in Lintong

to be much more promising for a long term stability for soil in the hyper hygroscopic humidity, than single consolidations.



4.3.6 Examinations and results of the mechanical stability

The loss of the sensitive surfaces in the excavations of the terracotta army is mostly traced back on the mechanical stress during the cleaning (brushing, hovering, etc.)(See chapter 1.2). With the examinations to the stability, the success of the resistance is now quantified. This is used for the evaluation, if the changed mechanical properties of the treated surfaces correspond to the stress requirements and if they are still compatible with the untreated substrate.

From the main factors for the mechanical stability in porous mineral materials, as they are described in (Schuh, 1987) ; (Sattler, 1992); (Alfes, 1989), the SE and swelling reduction treatment could influence especially the porosity, the number and stability of the grain contacts and the filling of the empty space with liquid phases.

For the Identification of the stability of mineral building material, serve in general the test of the pressure, bending strength and adhesive tensile strength. At most of the stones the proportion between maximal tear strength and maximal pressure strength is 1/15 and 1/30 (Alfes, 1989). Surface near failure of these materials are based mostly on exceeding the shear stress and tensile stress. Therefore, in the conservation of natural stone the tear strength and the bending strength are used as a criteria for the progress of decay and the resistance against weathering (Schuh, 1987), (Snethlage, 1991a).The relation of tensile strength and pressure strength in the soil of Lintong is in the air-dry condition approx.. 1/3 (see: image.70). Houben (1994) gives, in the connection of investigations on 28 days old, un consolidated stamped soil with a Proctor compression, a relationship of 1/4.Regarding this balanced relationship with unconsolidated soils, it is to be considered however that the results originate from a one-axial compression test at prisms without lateral extension restriction.

With this kind of pressure tests on prisms, in the end even exceed of the tensile strength in the transverse strain can lead to a failure of the test sample.

At the open surface areas of the soil structures, especially at the convex surfaces, edges and angles, there are also few transverse strain resistances. Even at the single axis pressure strength of the soil surface, it exceeds the shear stress and tensile strength transverse to the stress direction, will cause failure of the material. At the open-lying surfaces of the soil structures, particularly at convex surfaces, corners and edges, likewise very small lateral extension restrictions are present. In addition, during one-axial pressure load at the soil surfaces the excess of the shear strength and tensile strength will cause the failure of the material transverse to the load direction.

Stabilisation of loess clay surfaces at the example of the Terracotta army in Lintong

To record the changes, that are relevant for the direct damages, the changes of the tensile strength are the main interest of the examinations.

Since clay has in contrary to most of the natural stone, only few phase contact and the bonding force of the coagulation, contacts are dissolved very quickly underwater, the fluctuations of the material humidity in the sorption humidity has a strong influence on the material strength. These changes of the strength, due to humidity have to be considered also for the evaluation of the consolidation success.

Analyses methods (chapter deleted)

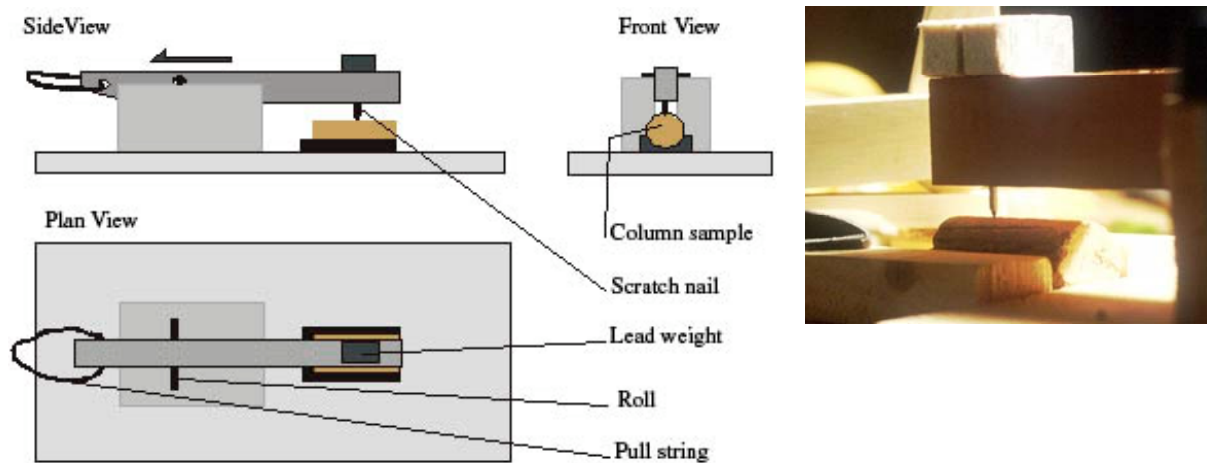


Image 62, sketch and image for the experiment set-up of the scratch test on conditioned column samples. The soil columns are approximately 5cm longer. The scratch nail made out of steel has a 2.5mm diameter and is abraded to a round cone with a 53° degree acute angle. It is upright to the sample flanks and is pressed with $1.7N \pm 0.05N$ weight on the sample. With the pull string, the wooden beam with the scratch nail is moved with constant speed of about 0.025 m/s across the sample.



Analysing results

The bending strength tests have been carried out for each disc, of every series after the conditioning, up to a weight absolute term of 40% relative humidity and 21°C. That correlates, depending on the treatment type on water content of 1.3 and 1.9 weight %. Some samples could not be tested successfully, because they were already cracked before the measurement, or they burst during the mounting into the measuring fixture. In image, 63 the load curve and strain curve of the successfully tested discs are shown. In the lower area of the curve increase, the material is in the miner elasticity area. The expansion is due to the Hookesch elasticity law, directly

Stabilisation of loess clay surfaces at the example of the Terracotta army in Lintong

proportional to the inserted strength. In the lower third of this linear range, the increase, for the calculation of the e-module is read off. If the pressure increased, the soil sample starts to yield back irreversibly with plastic flowing. In the vertex of the curve, the sample breaks. Here the power F_{max} is read off for the calculation of the bending strength σ_{Bz} . Although the height of the vertex cannot be equated with the bending strength of the sample, because the different thicknesses of the samples are not considered, it is obvious from this measurement protocol, that the consolidated samples have higher and steeper load curved and strain curves than the non treated series. Therefore, the consolidation leads to a significant rise of the breaking load and the elasticity of the sample.

Neither between the consolidated series nor between the untreated series a significant difference could be seen in the bending strength properties of the single discs.

Therefore, the six series have been summarized in the groups non consolidated (A/E/F) and consolidated (B/C/D) (see image 64).

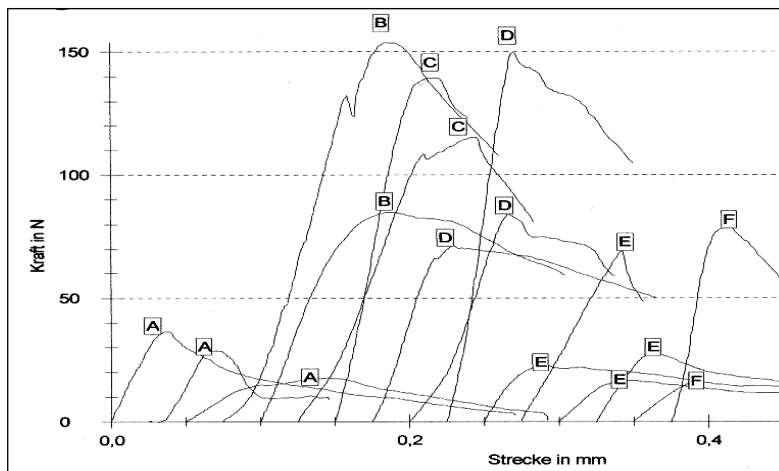
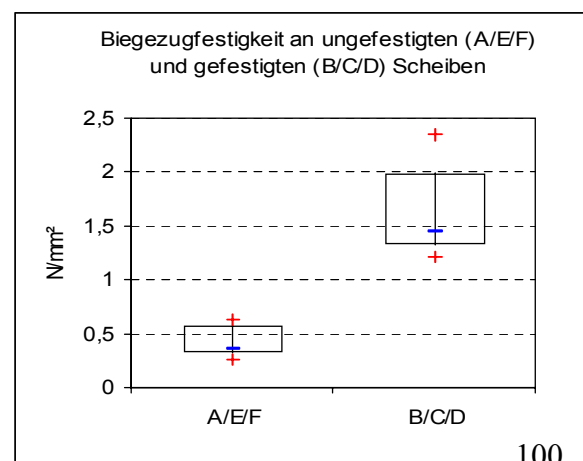
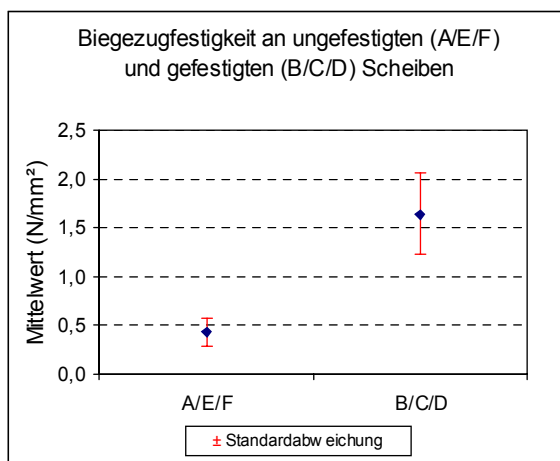


Image 63 deformation curves from the measurements of the biaxial bending strength at the treated and untreated samples. The affiliation of series is marked in the vertex of the curve. At this point the tensile strength F_{max} is also read off for the calculation of the bending strength. The E module is calculated from the lower linear increase of the curve



Stabilisation of loess clay surfaces at the example of the Terracotta army in Lintong

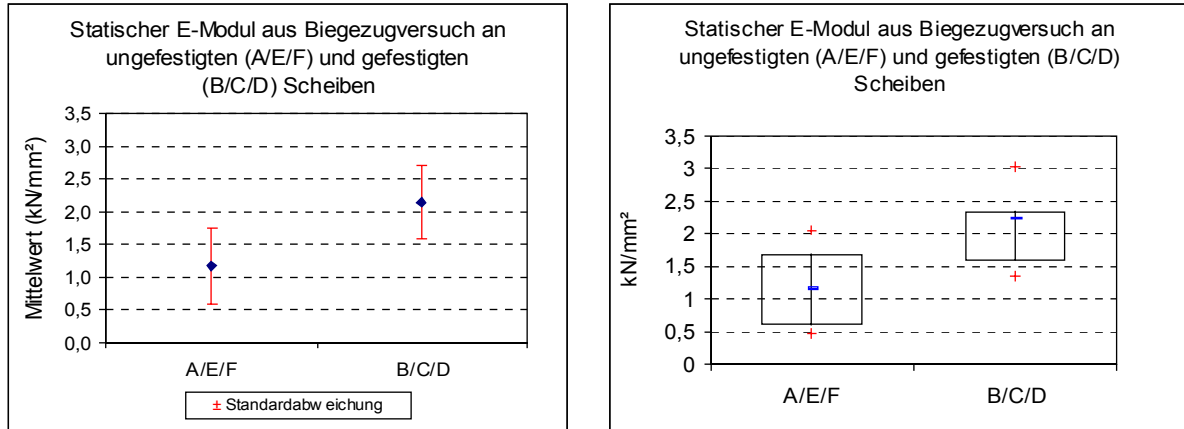


Image 64 above: Statistical evaluation of the biaxial bending strength. (Left: average value with standard deviations; Right: Gauss's allocation curve in the Box&Whisker diagram)

Below: statistical deviations of the statistical E module (Left: average value with standard deviations; Right: Gauss's allocation curve in the Box&Whisker diagram)

The initial value of the middle biaxial bending strength of the untreated samples is with 0.43 N/mm² very low (image 64) However it is very close to the values, that Micoulitsch (1996) has determined with the uniaxial bending strength test on the stamped soil prisms from Lintong (see image 70). There are not a lot of values for the bending strength of adobe to compare out of the literature; because the dry bending strength has no important specific value for building clays, for these the comprehensive strength is important. The few comparable measurements of silty and clayey adobe mortars have also bending strengths between 0.4 and 0.8 N/mm² (Böttger, 1999); (Minke, 1995). The dry bending strength of clays depends strongly on the amount of clay minerals. HOFMANN (1967) proved, for the dry bending strength of clays, a direct correlation between the strength and the cation exchange capacity of the clay minerals. The consolidation with SE leads to an increase of the average dry bending strength up to the factor of 3.8 up to 1.64 N/mm². In consideration of keeping the mechanical compatibility between the unconsolidated and consolidated material, SASSE & SNETHLAGE (1996) and SNETHLAGE (2002) recommend for stone consolidation, with the increase of the pressure, tensile strength and the bending strength from the non consolidated to the consolidated material in relation to consolidated material does not exceed the factor 1.5. Therefore, in principal the rule applies:

$$(\beta_{(\text{treated})} - \beta_{(\text{untreated})}) / \beta_{(\text{untreated})} < 0.5$$

Respectively, the increase of the strength the treatment of the soil with F300E is significant over consolidated. However, in the case of the soil it has to be considered, that the differences in the strength due to moisture, are in the untreated

material, has the same amount. The increase of the strength in the hygroscopic area (0-6 mass % water content) in image 70 shows an increase for the comprehensive strength of a factor of 0.75 up to 1.2. The bending strength is changing in this area by a factor of 2.3 up to 3.3. In contrary to this, on schilfsandstone the bi axial bending strength changes in the sorption humidity only to a factor of 0.4. (Sattler, 1992). The question arises, if it is possible to transfer these requirements from the stone conservation. The static E module of the untreated sample is at the values of 1.2 kN/mm². Reference values for the static E module on dry clay samples are between 1 and 6 kN/mm² (Böttger, 1999). The static E module from the bending strength measuring increases by the SE consolidation from 1.2 to 2.2 kN/mm² (image 64). That is a increase of the factor 1.8. The mentioned requirements for the natural stone conservation are $E_{(treated)} \leq 1,5 E_{(un\ treated)}$. The increase of the elasticity index is therefore less than the increase of the breaking strength. According to the day mechanism, the change of the elasticity is the more important factor for the mechanical compatibility to the untreated material.

The relation from changes of the breaking strength and the changes of the elasticity is also postulated as important evaluation criteria for the durability of natural stone consolidations. In SASSE & SNETHLAGE (1996), the following evaluation criteria is postulated:

$$E_{(treated)} / E_{(untreated)} \leq \beta_{(treated)} / \beta_{(untreated)}$$

For the results, above, there is a relation of $1.8 \leq 3.8$. Therefore, the relation between stability and elasticity is improved.

The specific expansion ε ($\Delta x/x$) is calculated, due to the Hooks law, from the proportion of the breaking strength and E Module of the disc samples: $\varepsilon = \beta_{bz} / E_{bz}$

They represent the upper limit of the elastic, reversible expansion. By exceeding the specific expansion, this leads to a long term to irreversible deformation, that can be seen in general as the start and reason for material detachments and decay (Snethlage, 2002). The correlation between breaking stress and breaking expansion, E- module and the specific expansion is shown in image 65.

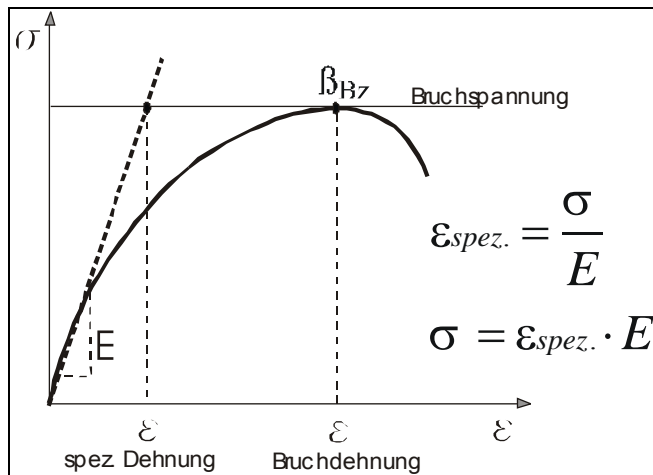


Image 65 relation between the breaking expansion, specific expansion, breaking stress and E module at the example of a tension –expansion curve.

The correlation between the breaking strength and the elasticity of the disc samples is shown in image 66 and image 67. The average specific expansion is for the treated samples increased from, 0.33% to 9.77%. In average, the consolidated samples can buffer elastically more than the double amount of the expansion. That this correlation is also valuable for the breaking expansion this can be seen in the values in image 67. Thereby, it is to regard, that the breaking expansion is in percentage. It exceeds the elastic specific expansion more than one cubing.

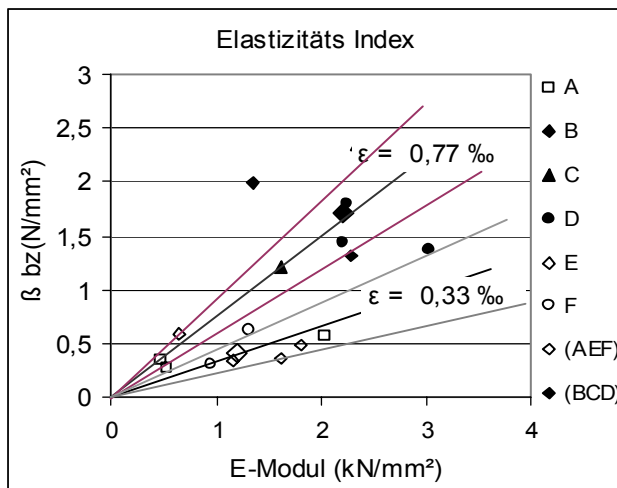


Image 66 Relation between the static elasticity module and the bending strength in the consolidated (B, C, D) and unconsolidated (A, E, F) samples. The average specific bending strength expansion ϵ – the upper limit of the elastic expansion – increases from 0,33 ‰ +/- 0,1‰ to 0,77 ‰ +/- 0,1‰.

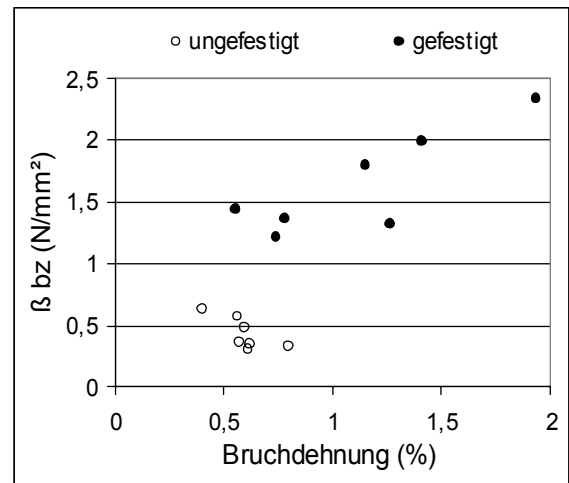
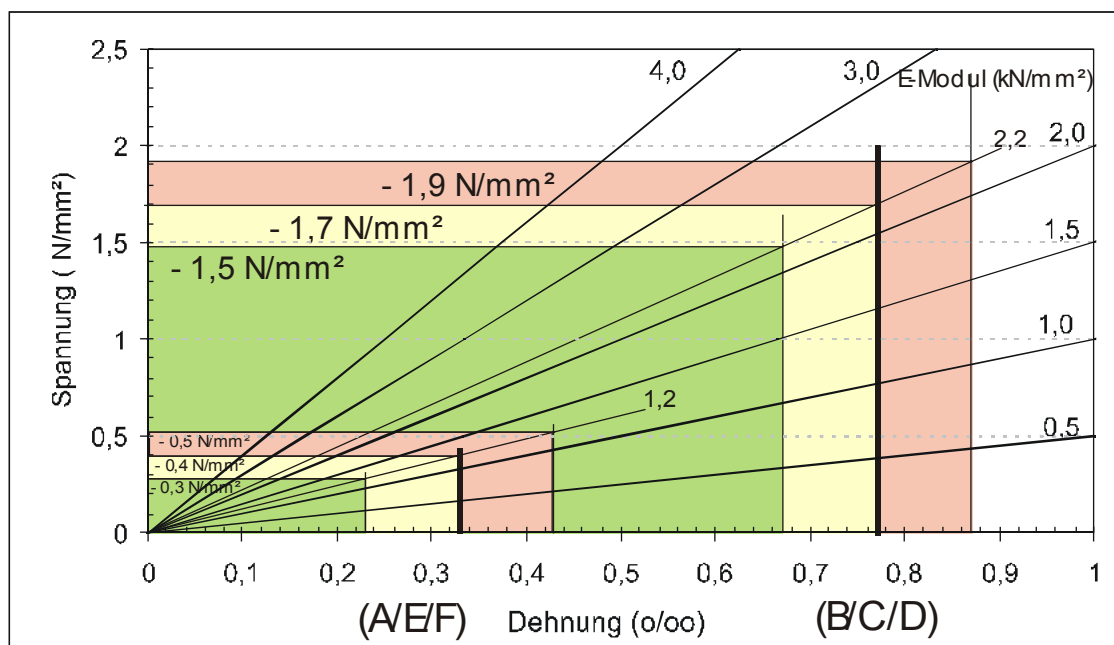


Image 67 Relation between the bending strength (β and/or expansion at the break of the bending strength samples. The consolidated samples can resist despite the increased E module, on average approximately the double deformation.

For the **liability to decay** of the soil of the excavations of the terracotta army, the material tensions are especially important, that occurs during the **hygric expansion** deviations of the atmospheric humidity. If these hygric material expansions regularly exceed the specified expansion, this can lead to destabilization of the mineral structure. Image 68 shows the tension-expansion diagram of the specific swelling of the consolidated and the non-consolidated series including their variation limit (Layout of the graphic after SNETHLAGE, 2002). Regarding the marked out E-modules (A/E/F: 1.2kN/mm²; B/C/D: 2.2kN/mm²) at the y- axis there is for the untreated series a specific tension area up to 0.5N/mm² marked and for the treated series a specific tension area up to 1.9N/mm². Inside these areas, due to the theory of the specific expansion- there is no danger of destabilization of the mineral structure (Sneathlage, 2002). In the corresponding table, there are, for every series, material expansions listed, that occurs at the hygric expansion during different relevant atmospheric humidity (image 68). The specific material tensions are calculated from the product of hygric expansion (‰) (see table 14) and the E-module values. Values, that exceed over this area of the specific material tension and that can therefore lead to the destabilization of the structure, are marked in red.



Stabilisation of loess clay surfaces at the example of the Terracotta army in Lintong

Change of relative humidity (%)		Tension (N/mm ²) within the humidity changes					
		A	B	C	D	E	F
possible	26 - 98	2,304	7,436	3,784	3,652	1,368	1,524
often	30 - 85	1,44	4,84	2,53	2,31	0,84	0,9
normal	40 - 70	0,72	1,76	1,1	0,99	0,3	0,3
aim	45 - 65	0,3	0,88	0,55	0,55	0,12	0,12

Image 68. The absolute values and variation limits of the specific expansion, results in the treated and untreated samples in separate areas of stress in the graphic. In the table are calculated the maximal stress, out of the formula: $\sigma = \varepsilon_{\text{hygric}} \cdot E$, that occurs inside material in the reset areas during the fluctuation of the humidity. The marking corresponds to the colours of the graphic. Stress that leads to the damage of the structure, which is calculated out of expansion values, higher than the fluctuations of the specific expansion, are marked in red.

In the table in image 68, the stability properties and the hygroscopic swelling values of the series, with the climate stress in the excavations of Lintong are correlated. At first it is obvious, that the non consolidated soil keeps the allowable tension stress only in the aimed climate fluctuation area between 45 and 65% relative humidity. Due to this calculation base, the climatic stress in the museum halls of Lintong leads to a destabilisation of the surface. However, because the observations in situ leads to another result (see chapter 1.2), it shows how low the allowed stress is determined for the calculation of the specific expansion.

For a differentiated evaluation of the specific stress, due to the treatment in table 15, the quotient out of the calculated stress of the changes of the atmospheric humidity and the allowed specific expansion is inscribed.

All treatments improve the tension situation in the atmospheric humidity between 40% and 70% relative humidity, nearly every day exceeded in the museum halls (see appendix 7.4).

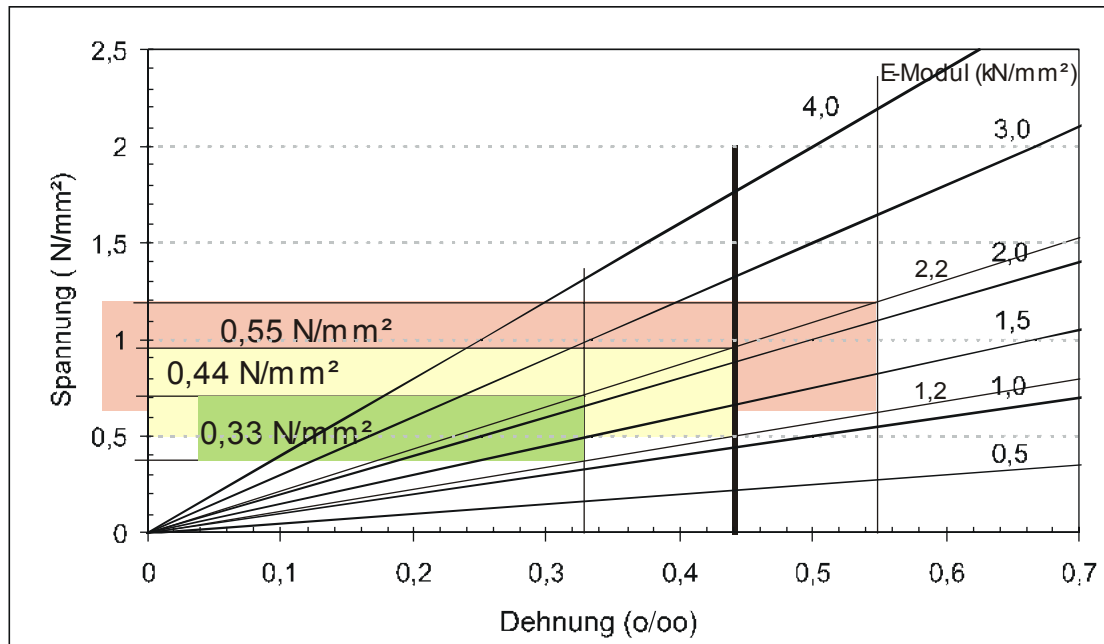
Dramatic changes in the atmospheric humidity, how they are “often and possible” in the museum halls, result in all series to an excess of the specific tension. While the tension in the single consolidated material of the series B stays at the level of the untreated sample, for the combination treatment, the inner hygroscopic tension is cut in half. In addition, the single treatment with tenside shows similar reductions of the inner tension. Compared with the untreated soil, with the combination treatment and the tenside treatment it is possible to cut in half the risk of destabilisation by hygroscopic swelling in the climate change. At the single consolidation (B), the calculated risk complies approximately with the untreated condition (A). However, one should not forget, that the level of tension in the single consolidated series B has trebled in relation to series A (see image 68-table).

Stabilisation of loess clay surfaces at the example of the Terracotta army in Lintong

change of atmospheric humidity possible	rel.humidity (%)	A	B	C	D	E	F
often	26 – 98	4,3	3,9	1,9	1,9	2,5	2,8
normal	30 – 85	2,7	2,5	1,3	1,2	1,6	1,7
aim	40 – 70	1,4	0,9	0,6	0,5	0,6	0,6
	45 – 65	0,6	0,5	0,3	0,3	0,2	0,2

Table 15: Quotient out of the calculated hygroscopic expansion stress (see image 68) and the allowed specific tension (0.53 N/mm² - non-consolidated; 1.9N/mm² - consolidated).

Along with the hygric stress within the treated surfaces of the hygric tensions, that occurs during the change of the climate between the treated surface and the untreated subsurface, are an important criteria for the evaluation of the resistance against decay of surface treatments. The tensions between the treated and the untreated zone results out of the differences in the amount of the hygric expansion and the difference of the E-module of the materials next to each other, after the formula $\sigma = \Delta\varepsilon_{\text{hygr.}} * \Delta E$. If the tensions in the transition zone succeed a preset value, that is calculated after the formula $\Delta\sigma = \Delta\varepsilon_{\text{spez.}} * \Delta E$, the formation of scales cannot be excluded (Snethlage, 2002). The allowed tensions between consolidated and non-consolidated zones are inscribed in the zero of the tension-expansion diagram. The tension differences, calculated out of the expansion differences of the series, for the different atmospheric humidity are shown in the associated table.



Change of humidity (%)	Tension (N/mm ²) within the humidity change					
	A - B	A - C	A - D	C - E	C - B	
possible 26 - 98	1,46	0,2	0,26	0,58	1,66	
often 30 - 85	1	0,05	0,15	0,45	1,05	
normal 40 - 70	0,2	0,1	0,15	0,25	0,3	
aim 45 - 65	0,15	0	0	0,15	0,15	

Image 69

The stress areas, that are allowed at the inter connection from the non-consolidated (AEF E-module = 1.2) to the consolidated (BCD E-module = 2.2) material, result out of the difference of the specific expansion and the difference of the E-module. In the difference of the specific expansion there are included in the variation limits of +/-0.1‰. Additional to the average expansion difference with $\Delta\varepsilon = 0.44\text{‰}$, (yellow) there are also the expansion widths for $\Delta\varepsilon = 0.33\text{‰}$ (green) und $\Delta\varepsilon = 0.55\text{‰}$ (Rosa). Out of the table, the tensions are obvious, which result from the expansion differences in the transition zones.

The strong hygric swelling of the single consolidated soil (series B) leads to the excess of the allowed tension difference at the boundary layer between the non-consolidated and consolidated zone (see table in image 69). With the application of a single consolidation, there is therefore the danger of the formation of scales.

In contrary, the combination treatments are very similar to the untreated soil in the hygric expansion properties (see table 14). Therefore at the transition of the treatment type A and C or A and D no dangerous tensions are expected.

The columns both marked; in the table in image 69, show by the example of the combination treatment C the possible tensions on the additional transitions, in the case of an irregular penetration of the swelling reducers and the consolidant. If the swelling reducer penetrates deeper as the silica acid consolidation in the surface treatment, then at the interaction zone occurs, as the case C-E. In this case, the

difference in tension of the hygric swelling is innocuous. However, if the consolidant penetrates deeper than the swelling reducing tenside then at interaction zone the tensions of column C-B is possible.

In this instance, there is the danger of the formation of scales. During the application of a combination treatment, it is necessary to take care, that the penetration of the swelling reducer penetrates as deep, or deeper than the consolidation. Looking at the curve progression of the hygric expansion in the hygroscopic area (see image 57) then it becomes clear, that at the transition zones the biggest tensions occur during the drying out under 50% relative humidity, because in the dry area, there are the biggest differences in the swelling values of the treatment types. The problem of the formation of scales has to be owed more to the dry area than the humid area.

In contrast, within the single treatments, the strongest swelling amounts and therefore the biggest inner tensions has to be expected in humidity between 65% and 98%.

Comparable calculations of the development of the tension in combination material have been done for the risk of shrinking cracks in plaster on natural stone (Knöfel, 1992). They are used for the calculation of the risk, but cannot show the real situation at the object. The real situation of the tension at the object should be much lower than the calculated stress limits based on the E-modules, that have been measured at stress rates, that would not occur at this rate at the hygroscopic change of climate. The E- modules and the tensions resulting from them are very highly set. Furthermore, the creeping ability (Relaxation) of the material has not considered.

The **influence of the water content** on the mechanical properties of adobe building materials is very high. The load ability of the material to tensile strength is reduced in the hygroscopic area between 30% and 98% relative humidity at marginal 70% from about 0.8 to 0.25N/mm² (see image 70).

The longitudinal wave speed at the column samples, allows further differentiation of the differences of the stability due to the treatment and also the observation of the effect of the hygroscopic water inclusion on the stability of treated and untreated test items (see image 71 and image 72).

Stabilisation of loess clay surfaces at the example of the Terracotta army in Lintong

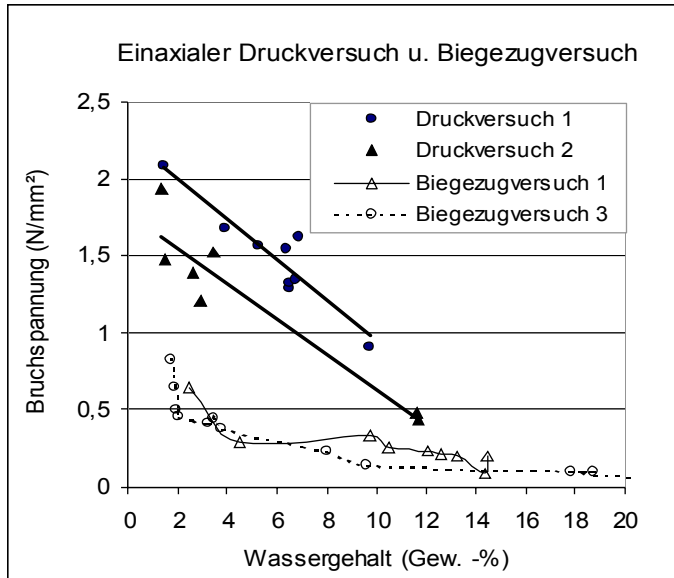


Image 70 Relation of the stability from the water content of the soil.

The tests have been carried out on the undisturbed prism of the stamped soil of Lintong. Diagram: After the results in MICOULITSCH, 1996.

Notable, is the strong decline tensile strength in the area of the hygroscopic humidity, up to 6 weight percentage water content. The tensile loading of the phase contacts is widely dissolved by the water inclusion from the capillary condensation of over 60% relative humidity (≈ 3 weight -% water content).

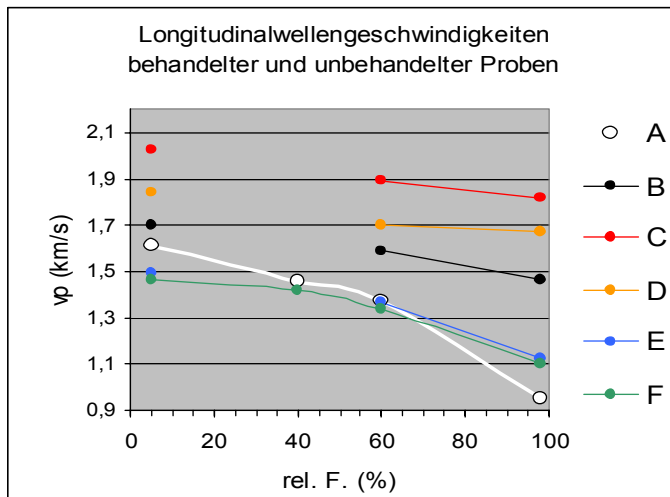


Image 71: Average values of the longitudinal wave speed in the treated and untreated column samples.

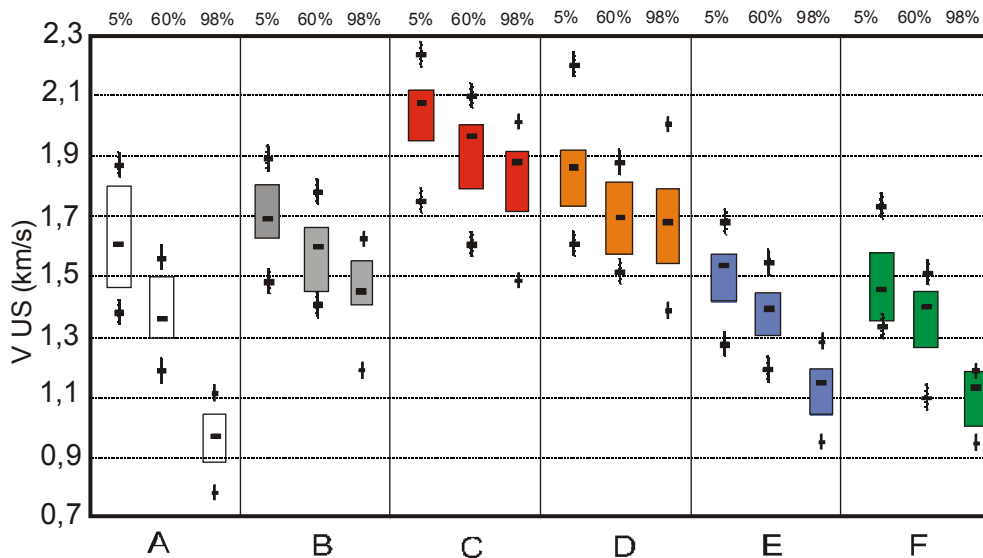


Image 72: Gaussian distribution curve of the longitudinal speed in the Box&Whisker diagram for the humidity areas of 5%, 60% and 98% atmospheric humidity.

The consolidated series (B, C, D) reach, at 5% humidity, longitudinal wave speeds between 1.7 and 2.0 km/s, while the speeds of the non consolidated series (A,E F) reach only 1.5-1.6 km/s. That corresponds to an increase of the factor of 1.06 -1.33. In contrary to the bending strength measurement, the single series can be differentiated with the differences in the US (ultra sonic) speed accurately. While the single consolidation, (series B), at a constant weight in 5% relative humidity, has little influence on the sonic speed, it significantly increases at the combination treatment (C and D). The longitudinal wave speed of the dry soil column samples correlate therefore, very well with the dry raw density of the samples (see image73).

The water incorporation in the hygroscopic range leads, in all series, to a reduction of the transmission speed.

In accordance with the measurements of MICOULITSCH, 1996 (see image 70) this effect is very significant in the range between 60 and 98% relative humidity (see image 71 and 72).

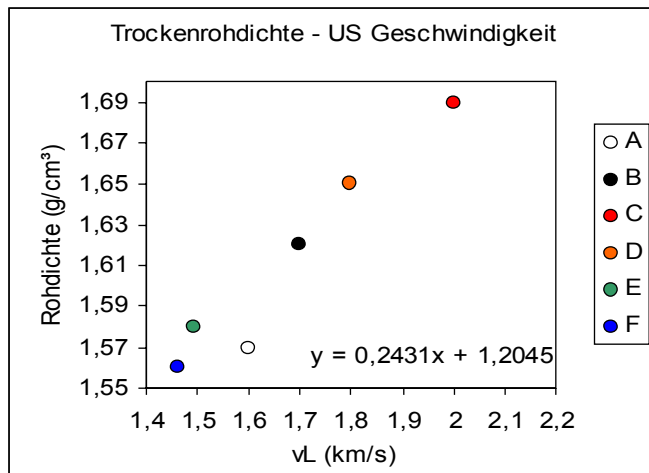


Image 73: The correlation between the average dry raw density and the average longitudinal speed (v_L) of the dry series (5% relative humidity) are approximately linear.

In marble, limestone and most of the sandstones, the ultra sonic transmission speed rises with increasing water content, up to 35% (Esbert, 1989). The bridging of the pores, with water, increases the integral impulse speed, because the sonic speed (v_L) is in water (1.48 km/s), four and a half times higher than in the air (0.33 km/s).

For clayey sandstones, declining sonic speed at increasing humidity content, are known (Simon, 2001). In the clay bound sandstones, similar to the stamped soil of Lintong, water inclusion in the clayey grain bridges and contact areas leads, in the hygroscopic humidity range, to the softening of the structure. The starting "plastification" of the grain contact, directly reduces the E-module of the complete grain structure. With the E module, the ultrasonic speed is reduced according to the

previously explained correlation between v_L and $\sqrt{\frac{E}{\rho}}$ (see chapter 4.3.6. Examination methods). The decline of the longitudinal wave speed between 55 and 98% relative humidity, is in the series A 41% (see table 16). All treated series register a smaller decrease of the sonic speed. Particularly balanced are the consolidated samples of the series B, C and D. In addition, the single treatment with swelling reducers decreases the humidity-conditioned reduction of the longitudinal wave speed to 25%. Both treatments affect balancing the humidity-conditioned fluctuations of the sound impulse speed. The small fluctuations in the combination-treated series C and D refers to a phase addition of the effects.

Stabilisation of loess clay surfaces at the example of the Terracotta army in Lintong

A	B	C	D	E	F
41 %	14 %	10 %	9 %	25 %	25 %

Table 16: Reduction of the longitudinal wave speed between 5% and 98% relative humidity in % of the speed with 5 % relative humidity.

Because the water content, at 5 % and 98% relative humidity in all series, are very similar (see image 46), it is possible to trace back the effects of the treatments on the humidity-conditioned impulse speed decrease. This probably derives directly from improvement of the "water resistance" on the grain contacts.

The values for the dynamic elastic module from the elongation wave measurement are shown in image.74. The range of the measured values falls between 0.75 and 5 kN/mm². However, it is to be noted that all results for sample C1 falls entirely out of the range of the other values, and all other measurements do not exceed 3 kN/mm². Therefore, the results of the dynamic E- module measurement falls in the same range as those of the static E-modules from the bending measurement, namely between 0.5 - 3 kN/mm² (see imgae.64). The results of the measurement, with comparable sample conditioning (40% relative atmospheric humidity), are in accordance with the bending measurement of between 1 and 2.5 kN/mm² (sample C1 excluded).

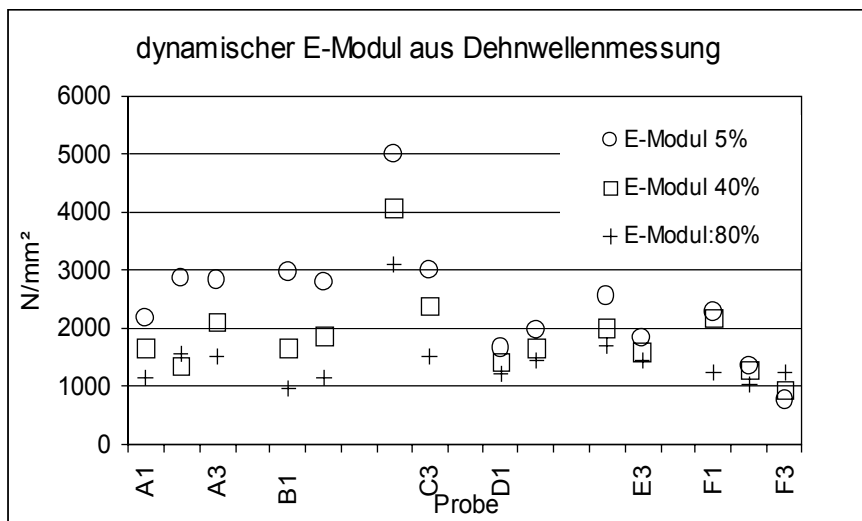


Image.74
Measurement values to the dynamic E-module at the individual column samples of all series. The measurements have been carried out in order with weight constant in 5, 40 and 80% relative humidity.

Independently of the amount, heights of the individual e-modules, which seem to depend much on the individual condition of the single sample, and due to the limited sample numbers, it does not show a clear trend in comparison of the treatments (results in image.74). The average decreasing in the E- module, derived from it, in

Stabilisation of loess clay surfaces at the example of the Terracotta army in Lintong

Table 17 clearly point out the strong influence of the humidity on the elastic module in the series A, B and C. For the series D, E and F however the E- module is far less affected by the hygroscopic water content. The series D, E and F have smaller E-modules in the "dry measurement" (5% relative humidity, image.74). This indicates a fundamental improved flexibility of the grain contacts flexibility by the tenside coupling. The special development of this flexibility effect for the series D and F, which have distinctively longer alkyl chains than C and E, seems to confirm this observation.

A	B	C	D	E	F
49 %	62 %	43 %	26%	27 %	20 %

Table 17: Average decreasing of the dynamic E-modules from the dilatation wave measurement between 5% and 80% relative humidity in % of the E-modules at 5 % relative humidity.

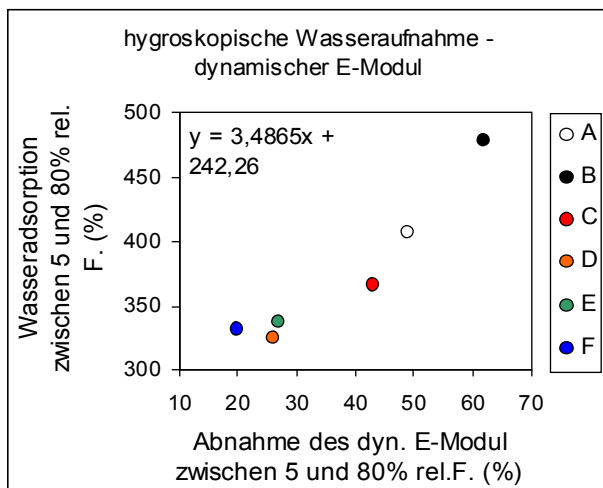


Image 75 The proportional increase of the water vapour adsorption, of the water content at 5% relative humidity measured is linear for the decrease in percentage of the dynamic E module between 5% and 80 % relative atmospheric humidity.

The tenside treatment stabilizes the elasticity of the grain bondages within the hygroscopic range. That applies also to the combination treatment in series of D. Comparing the changes for the dynamic E- module within the range between 5% and 80%, relative humidity with the adsorptive water inclusion in volume percentage, it results a linear dependence between the adsorbed quantity of water and the reduction of the dynamic E-module (image 75). The dynamic E-module of the soil reacts much stronger to the water adsorption in the micropores of the grain contacts than the longitudinal wave speed, which depends, like the pressure strength, on the elasticity and above all on the gross density of the material. Consolidation with silica acid silicate ester does not seem to cause qualitative stabilization of the grain bonds in the hygroscopic range against the softening of adsorbed water. For the E-module

of the single consolidated series, due to the increased water adsorption of this sample series (see chapter 4.3.3), even higher fluctuations in the elastic module occurs than at the untreated samples.

The **scratching resistance measurement** did not give a clear differentiation for the humidity steps (see image 76). In comparison of the treatments however, very clear differences resulted in the scratching resistance. While the spike penetrates at the untreated samples, (A), deeply into the surface and causes a deep scratch, in the consolidated series (B, C, D) only light superficial scratches can be seen. Also at the samples, which are treated only with the swelling reducers (E, F) the penetration of the spike is clearly reduced. Independent from the water content, the tenside treatment seems to cause a small improvement of the mechanical stability of the treated surfaces.

Stabilisation of loess clay surfaces at the example of the Terracotta army in Lintong

The scratching resistance test shows the low abrasion resistance of the untreated soil. It shows also that silicate ester consolidation (B, C, D) can offer by far sufficient protection against the mentioned mechanical surface stress in the museum of the Terracotta army (see chapter 1.2). Additionally the scratching tests proved, that also the tenside treatment could improve the resistance of the soil surfaces against tensile stress, shear stress and compression strength. Perhaps the tenside treatment actually causes a molecular coupling of the mineral surfaces in the range of the grain contacts. The coupling over the alkyl chains would cause a "rubber band effect"; on the one hand the softening in the "dry condition" (see: image 74), described above, on the other hand in addition, an increased tensile strength at the grain contacts (see: image 77). A small decrease of the E module and a small increase of the tensile strength at the grain contacts, could be conceived as the catalyst for the increased abrasion resistance of the tenside treated samples

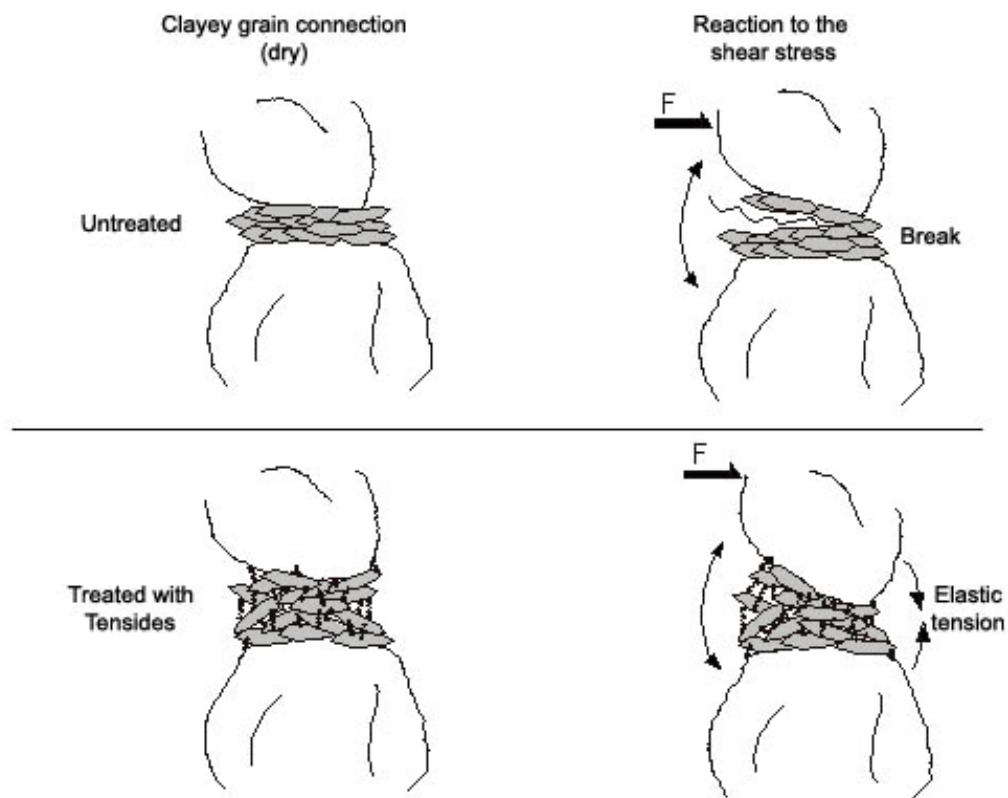


Image 77: "elastic band effect": The bi functional tensides create a flexible connection between the mineral surfaces. The expansion and the linkage of the clay mineral structure with flexible tensides soften the "dry" grain contacts. The E- module sinks. Low shear stress does not lead to the breakage so easily with treated soil. The longer the alkyl chains, the more the "elastic band effect" is. The dynamic E- module in

series C and E (only short ethyl chains) is higher than in the series D and F, which contain also longer Butyl and Hexyl chains.

Summary of the results of the mechanical stability

The results of the biaxial bending measurement, the ultrasonic measurement and the scratch hardness test show, that the consolidation with silicate ester clearly increases the breaking stress and the elasticity of the soil. The correlation of stability and elasticity is thereby improved. With a single treatment with bifunctional tensides, the changing of the bending strength of the material cannot be proved. The ultrasonic results point out, however, that the tenside treatment makes the grain connections more flexible and consequently improves the mechanical stress capacity. The specific expansion, as a limit for the elastic ductility of the material, increases for the consolidated samples from 0.33 to 0.77‰. This means an improvement of the structural stability on internal tensions, as they occur in the case of the excavations of Lintong at hygric expansions in the atmospheric humidity change. The climatic fluctuations in the museum halls, causes continuous excess of the specific expansion on the untreated material. Thereby internal stress develops, which are outside of the secured flexible range. The destabilization risk, which exists, is halved by the combination treatment and by the single treatment with tenside. A single consolidation (series B) improves the resistance of the soil. However, the values of the hygroscopic expansion and thus the internal stress increases with this type of treatment so strong, that the destabilization risk in the atmospheric humidity change, corresponds to that of the untreated soil.

Additionally, for this treatment type, exists the danger of the climatically caused destabilization at the transition zone between the consolidated surface and the non-consolidated subsoil, due to the high hygroscopic expansion difference to A. Such destabilization phenomena can lead scale formations on the surface. The hygroscopic expansion of the combination treatments is so similar to the untreated soil, that this type of treatment will not tend to form scales. However, the swelling reducer must penetrate deeper than the consolidant, in the case of a surface application. In the opposite case, the material transition "combination treatment > single consolidation" and "single consolidation > untreated earth" would occur, which would lead to the formation of scales, due to their mechanical properties in the humidity change.

In contrast to the bending measurement, it is better possible to differentiate the small differences in stability of the individual series with the ultrasonic transmission measurement. The longitudinal wave speed at 5% relative humidity correlates very well with the dry gross density of the samples. With the ultrasonic measurements it could be also proven that the water storage already softens the mineral structure in the hygroscopic humidity range and that it reduces the E-module of the entire grain structure in all series. With the comparison of the change in the dynamic E- module within the range between 5% and 80% relative humidity, a linear correlation between the adsorbed quantity of water and the reduction of the E-module can be determined.

Thus derives the following differentiations:

The tenside treatment can reduce distinctly the range of the E- module within the hygroscopic humidity range. That applies also to the combination treatments with the following consolidation (series of C and D). In contrast to the single consolidation with silicate ester, within the hygroscopic range, it does not cause qualitative stabilisation of the grain connections against the softening by adsorbed water. For the E-module of the single consolidated series B result even stronger fluctuations, than at the untreated samples, due to the increased water adsorption of this sample series. In the case of the tenside treatment, lower e-modules in the "dry measurement" at 5% relative humidity and the increased scratching resistance, indicate a basic increase of the ductility of the grain contacts by the tenside coupling.

4.4 Modelling of the heat and moisture transport for building elements made out of stamped soil, with and without surface treatment.

The influence of the treated surfaces on the moisture equilibrium with the untreated soil underneath, was examined with help of the computer program WUFI-2D for modelling of inter stationary heat and moisture transport functions. The calculation functions of this computer simulation, are based on fundamental material properties data, as they were compiled in chapter 4.3. The simulation allows a very differentiated estimation of possible moisture stress in the depth profile for the soil, depending to the given climatic benchmark data. The PC program WUFI 2D was developed to simulate two-dimensional heat and moisture transport functions in building elements, such as roof constructions, walls or foundations. The theoretical bases of the program are explained in KUENZEL (1995A). The program is based on the Finite elements method. For the modelling of the inter stationary heat and moisture transport processes, fundamental material parameters are combined with

"climatic transition coefficients" and climate data. For the display of the result parameters, temperature, relative humidity and water content in the building element, the program offers various forms of illustrations (Künzel, 2000). Thereto belong profiles for temperature, water content, relative humidity and also the behaviour curves of the result parameters at monitor positions, which can be set freely at particularly interesting places.

4.4.1 Input parameters for the modelling, with Wufi-2D- building element layout, material data and climate data

To ease the comparison of the results in the display format and also exclude accidentally deviations in the input masks, the simulation for three surface treatment types and an untreated surface was calculated simultaneous in one building element (see: image78). This combination consists of four stamped clay cuboids laying on top of each other, each of 10cm height and 38cm width. The cuboids are marked according to the type of their surface treatment with A - untreated, B - consolidated, C/D - combination treatment and E/F – swelling reduction treatment. They are shielded from each other with heat- and humidity-insulating interfaces. The building elements are divided from right to left, in treatment zones (3cm), close range behind the treatment (5cm) and deep range (30cm). These three elements of each building part can be allocated independently with variable material properties. The allocation for the simulation of the surface treatments is marked with coloured grids in image:78. The division of the finite computing elements can be designed for each layer of the building element individually (sum of the elements in a vertical or horizontal element level). It opens from the external surface of the building element (right) to the deep range (left). This reduction of the space dissolution from the surface into the depth of the building element reduces the effort of the computation.

It is justified, because short term and small-scale climatic fluctuations affect the surface near parts of the building elements. The width of the finite elements is within the treatment area between 2.5 and 4.5 mm, at close range between 2.5 mm and 12mm and in the deep range between 2.5mm and 10cm. For the display of the climatic fluctuation during this time, four monitors were positioned in each of the four building elements.

This combination building element is surrounded by three sides with a "modulation system border" in each construction unit. At this border the actual values (temperature and humidity) of the adjacent elements "are reflected" computationally.

Stabilisation of loess clay surfaces at the example of the Terracotta army in Lintong

The program simulates here the unlimited expansion of the material with the condition of the border element, so therefore, from these boundary surfaces, no influence on the climatic situation in the building element proceeds. At the right side of the building element, the soil surface with the treatments is simulated. Since there does not exist a continuous climate file with hourly values for the situation in the museum halls, and the climatic stress should be assumed as high as possible, for the basic file for the simulation of an external climate, the outside climate data from "Holzkirchen" South Bavaria was used. From this climatic file, with the help of the PC software "Wufi Climate generator", the precipitation data was eliminated and the radiant heat of the sun for a laying surface with 0° inclination was computed. In the simulation the hourly values of the outside temperature, the relative outside humidity and the radiant heat of the sun are added. For the transition coefficients, the defaults for the interior were selected. The climate, creating the base of the simulation, is, apart from the base values, adapted to the situation in museum-hall 1; Roofing, no wind, no rain, but also no climatic insulation and direct sun exposure over the window. The general monthly average values of the climate in Xi'an and Holzkirchen are added in appendix 7.7. The material data for the Wufi 2D modelling are determined from the investigations in chapter 4.3. Due to the correlation of the characteristic values at the swelling reducing treatments (series E and series F) and of the combination treatments (series C and series D), for the building elements C/D and E/F, the average values of the series types were used. The modelling with Wufi-2D, is based on the following material specific values: Gross density, porosity, thermal capacity dry, thermal conductivity dry, diffusion resistance number, thermal conductivity addition, moisture storage capacity (adsorption isotherm). The data for the thermal conductivity and the thermal capacity are taken from the data, from comparable clay materials in MINKE (1995). The factor for the increase of the thermal conductivity, due to moisture, is adapted to the results of the conductivity tests in (Hiraiwa, 2000). The used materials data are listed in appendix 7.7.

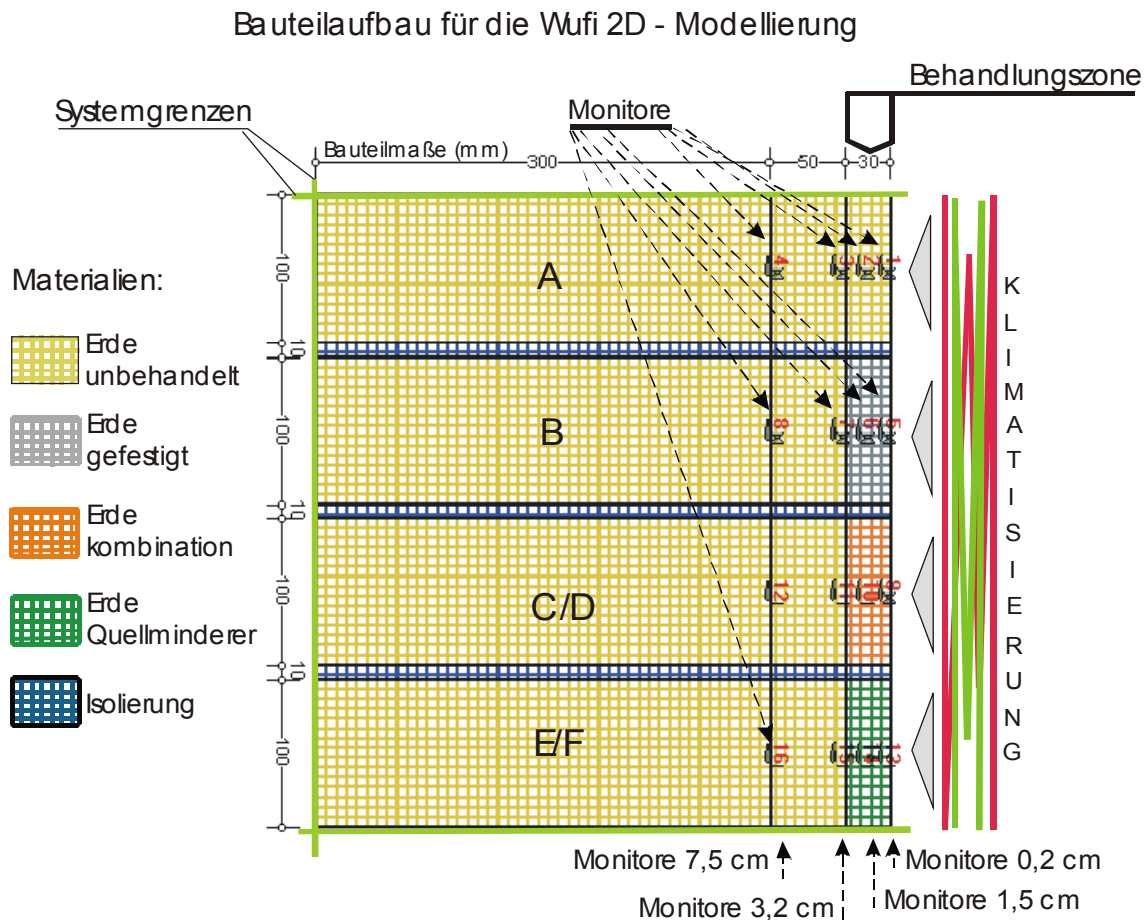


Image 78: Configuration of the building element, for the calculation of the moisture transport in Wufi 2D; Four building elements with and without surface treatment (A, B, C/D, E/F) are separate over insulation layers and are modelled at the same time. Twenty computing elements, horizontal from right to the left: Treatment zone (3cm) - 9 elements, close range behind the treatment zone (5cm) 7 - elements, deep range (30cm) - 4 elements. Computing elements vertically: Three computing elements per building element > altogether 21 computing elements.

4.4.2 Modelling results in the behaviour of the untreated soil in atmospheric humidity change.

The three-year modelling of the humidity fluctuations on the monitor positions, results in an even development without long-term humidification or dehumidifying tendencies (image:79) for the untreated soil (A) (The years in the model calculation are fictitious and have a no significance). The humidity in the soil rises rapidly, starting from September, and drops continuously from the end of January to the end of the summer. The fluctuations of the relative humidity are recorded in Image: 79. for four monitor positions. The ranges of outside air (32 - 100% relative humidity) are strongly buffered in the depth profile. They values are: in 2 millimetres of depth between 43 and 98 % relative humidity.; in 1.5 centimetres depth between 66 and 92 % relative humidity; in 3.2 centimetres depth between 72 and 86 % relative humidity and in 7.5

cm depth only between 76 and 85 % relative humidity. With the example of the 14.06.1992, the design principles of the humidity profile in addition to the depth dispersion in short, middle and long-term climatic developments, should be examined. In addition, one compares several snapshots of the moisture distributions (image: 81) during one day. For the interpretation of these humidity profiles from the 14.06.1992, the development of the relative humidity at the monitor positions from the beginning of June until the middle of June (image:80), has to be considered. Turning points in the external climate, "are stored" as turning points in the humidity profile. At the time, which has passed since a climatic change, and at the position, in which the associated turning points in the humidity profile appear, it is possible to read off one depth effect in short, middle and long-term climatic developments. At the beginning of June, the soil is in the middle of the summer drying off period (see: image: 79). In the preceding first days of June, the external climate was particularly dry for a period of ten days; subsequently the earth on the 14th June, despite the long-term summer drying, is in a medium-term phase of moistening. On the 14th June, between 9:00 and 18:00, the humidity of the outside air decreased (see: image: 81). This drying reacts, up to 1cm depth, as an actual drying out (> scope 9 h).

At the same time, the relative humidity in the range of between 1 and 3 centimetre of depth increases. It follows thereby a trend, that has already started the evening before (monitor A - 0.2 cm in image.80) and spread during the night to a 1.5 cm depth (monitor A - 1.5 cm image.80) (> scope 24 h). At the 14.06 in the range of between 3 - 5 cm depth, the humidity is still decreasing. This trend, again comes from the 10th June (> scope 4 days), in which a four to five day long phase, of the increasing humidity, which in the meantime penetrated to a 7 cm depth (> scope 10 days), was replaced by dry outside air. The linear decline of the humidity between 16 cm and 7 cm is part of the long-term summer drying out, that already dries the soil in the depth profile from the beginning of April, in the long term, under the annual average value of 80% relative humidity. (See: image.79: Monitor A - 3.2 cm and monitor A - 7.5 cm) (> scope 2 month).The summer drying spreads further to the centre of the soil until September and the beginning of November. Image 82 is shows the situation at the end of the dry period. The drying front is penetrated in the model calculation, up to 28cm under the surface. The difference between outside air and the soil moisture in the depth is in this moment at 24 % relative humidity. (56% outside - 80% inside). However, 98% of the drying gradients are, in the first 16 centimetres, under the surface.

Stabilisation of loess clay surfaces at the example of the Terracotta army in Lintong

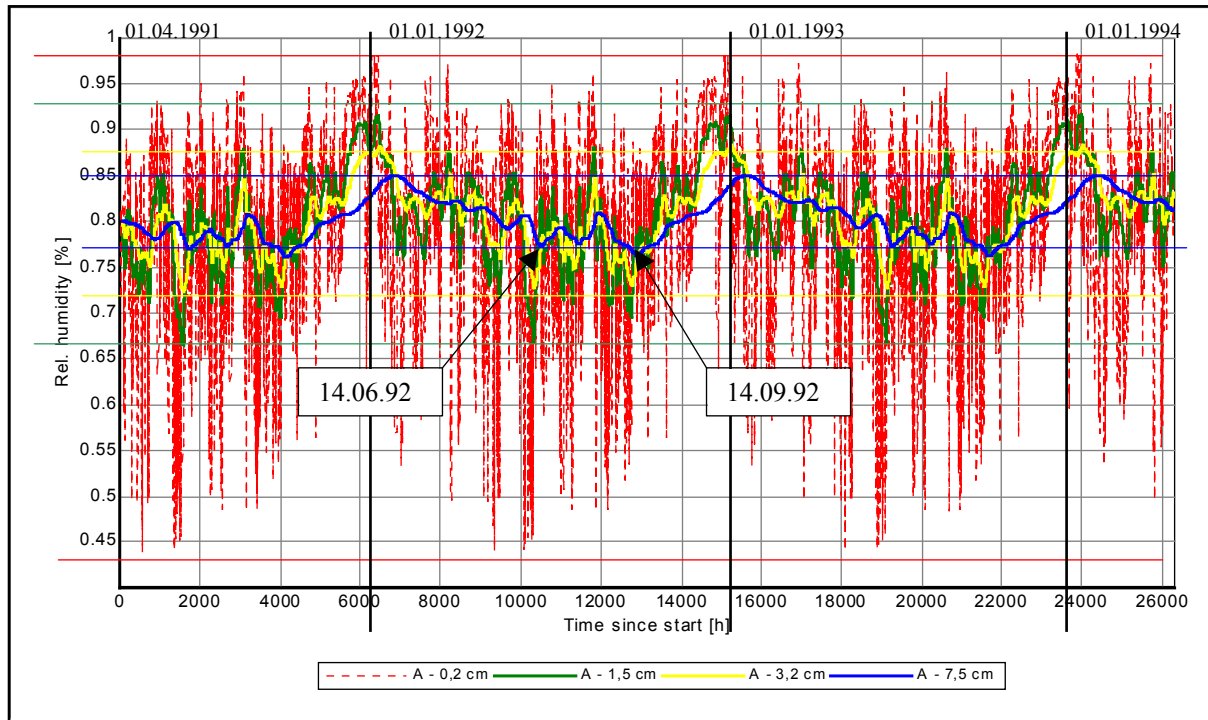


Image79 Behaviour curves of the relative humidity for the untreated soil (A) at monitor positions 1 – 4, over three years, with identical air conditioning. The model calculation starts from the 01.04.1991 at midnight. The monitor positions are in the profile of the soil within the distances of 0.2 cm, 1.5 cm, 3.2 cm, and 7.5 cm to the air-conditioned surface. The initial moisture of the soil is with 80% relative humidity adapted to the average annual external climate. The process curves are, therefore, balanced and do not follow any long-term drying or humidification trend.

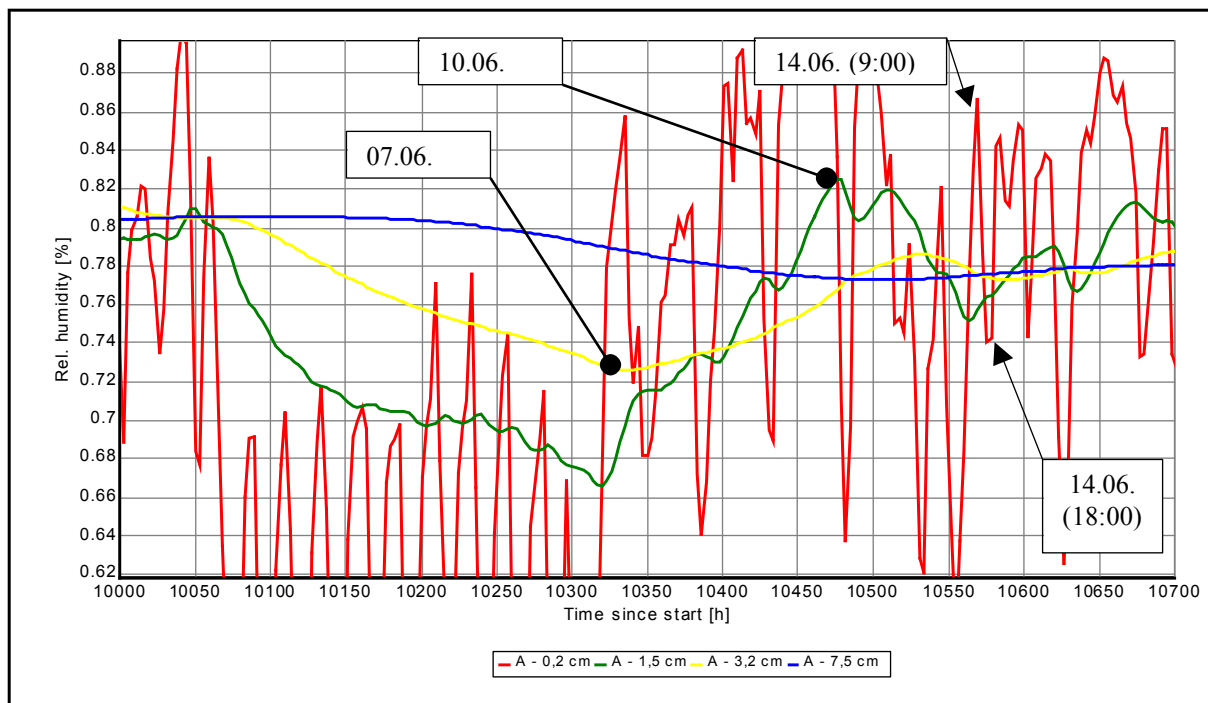


Image.80 Cut out from image.79 from June 1992. The soil is still in the summer drying phase. After eleven days of a strong drying process with external humidity under 45 %, the internal air humidity rises again. According to their deep positioning the process curves of the monitors, react to short -, middle and long-term trends of the internal climate development

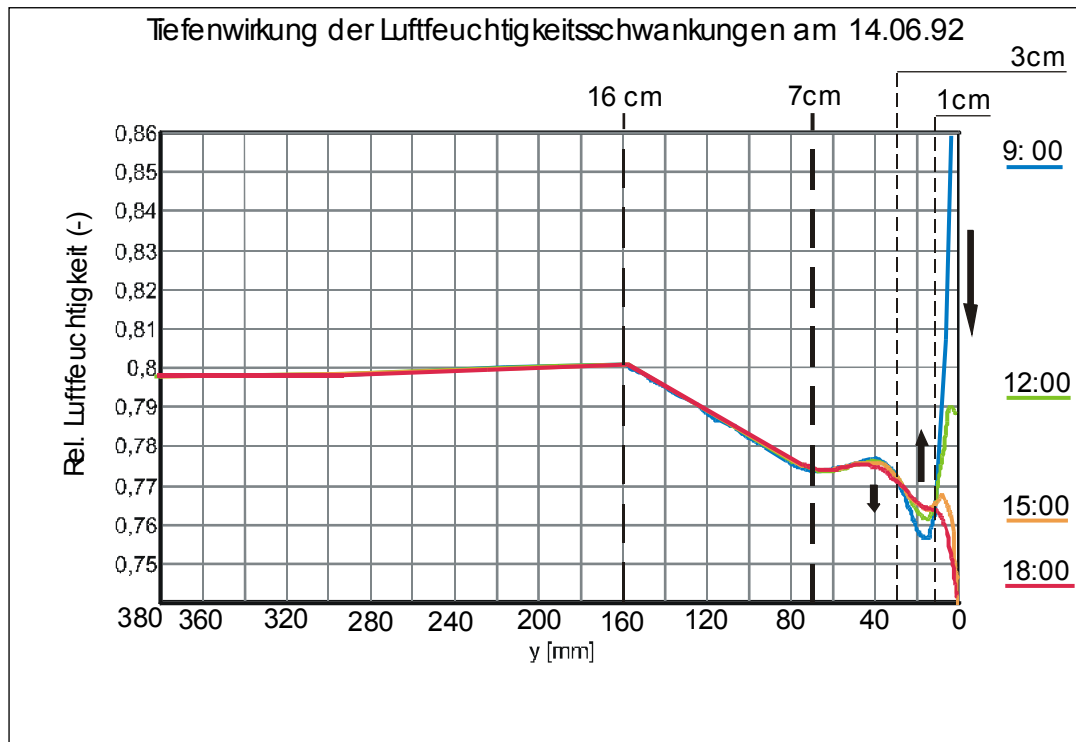


Image 81 The distribution of the relative humidity in the profile of the soil, for four times a day on the 14.06.1992. The air-conditioned surface is on the right. The entire depth of profile is 38 cm. For some turning points of the curves, the distance to the surface is indicated above. The black arrows refer to drying or humidification tendencies in different layers of depth. Between 9:00 and 18:00 hours, the surface dries off. However, the climatic development under the surface follows; depending on the depth, medium-term or long-term climatic developments. The direct influence of the drying between 9:00 and 18:00 reaches 10mm under the surface. Altogether, in this period, solving changes of humidity take place at a 4 cm depth, whose process is also affected by the daily fluctuation.

Stabilisation of loess clay surfaces at the example of the Terracotta army in Lintong

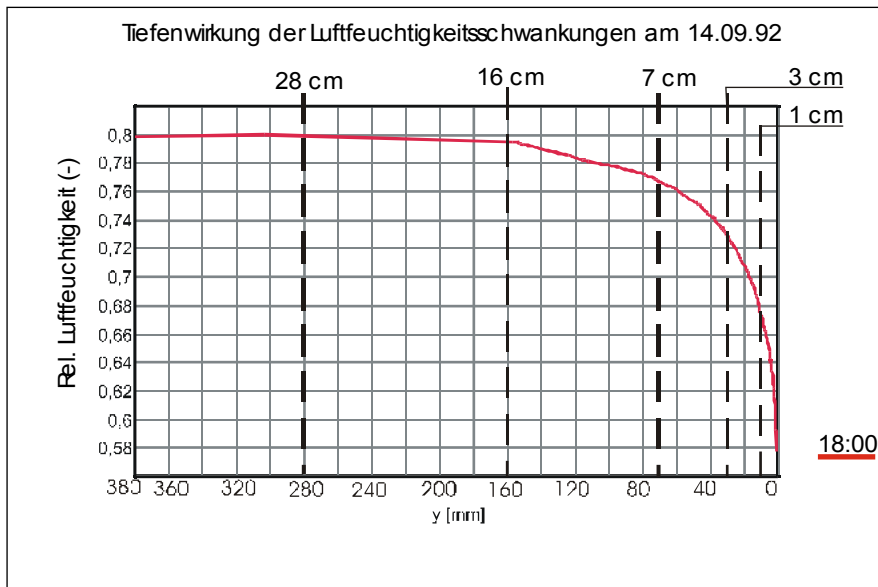


Image.82 Profile curve for the moisture distribution in the untreated soil on the 14.09.1992 approximately 18:00. At the beginning of September the summer drying off, is replaced by a continuous increase of the atmospheric humidity (see: Image.79). Mid September, the long summer drying period, reaches, with the falling below of the annual average value of 80% relative humidity, 28cm under the surface, their maximum effective depth.

The speed of the depth propagation of climatic fluctuations on the surface, depends naturally also on the balance between the material moisture and the external humidity values. In this modelling, it was calculated with the climatic data of a freestanding measuring point. Even when the climatic situation in the museum halls of Lintong are far away from the museum standard, smaller fluctuations of the weeks and daily averages can be expected in the interior. The actual depth effect of the climatic fluctuations into the museum will be therefore slightly weaker, than it was modelled here. The penetration speeds in tab. 18: can be therefore be regarded as the upper limit. Nevertheless, modelling with real climate data is always closer to the real conditions, than simple computations of stationary drying or moistening situations. Since short-term climate change; such as the daily cycles or brief drying and moistening situations; substantially affect the propagation conditions of long-term changes (Kuenzel, 1995).

Penetration depth	28cm	16cm	7cm	5cm	3cm	1cm
Time after the start of the trend	5 month	2 month	10 days	4 days	24 hours	9 hours

Table. 18: Depth effect of natural climate fluctuations on the stamped soil of Lintong. Results from the modelling on untreated soil with Wufi 2D.

Stabilisation of loess clay surfaces at the example of the Terracotta army in Lintong

Compared with other building materials, the climatic fluctuations penetrate quickly into the material. That applies to all periodic groups of different duration (yearly, monthly, daily fluctuations). For clarification in an additional model, calculation at one of the four building element positions (see: image.78), a solid brick with the material data of the IBP data base was used (Kuenzel, 2002). The profile in the brick shows, that the summer drying on the 14.06.1992 penetrated only up to 8 cm under the surface (image.83). In the depth of the building element can still be seen the rest of the humidity infiltration from the last winter (moisture contents over 80% relative humidity). The high adsorption capacity of the soil and the fast distribution of adsorbed moisture, into deep areas under the surface, are the physical cause for the good breathability of the building material clay, as described in MINKE (1994). Clay building elements are considered as a excellent buffer against humidity fluctuations

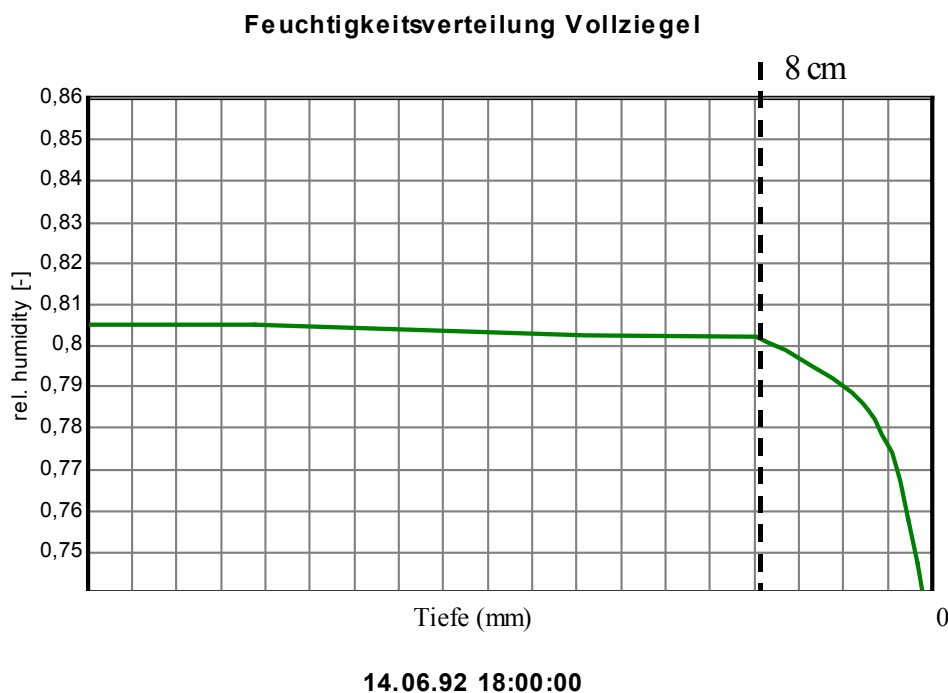


Image.83 Profile curve for the moisture distribution in a solid brick on the 14.06.1992 at 18:00. Apart from of the material characteristic data, all modelling parameters correspond to the computation in image 82.

The results of the modelling at the non-consolidated stamped soil of Lintong, leads to following conclusions:

- Zones, with more than 3 cm distance to the surface are exposed to only small humidity changes. The amounts of the moisture fluctuations are, in the whole year cycle below 15% relative humidity. The penetration of a drying front into this depth takes at least 24h. The most serious climatic changes within this range, remain under an amount of 10% relative humidity over a period of at least 10 days (see: image.79 and image.80). Therefore, the maximum stress amounts from the hygroscopic dilatation are in this depth so small that according to the computations in chapter 4.3.6, including the untreated and treated soil, together with the transition areas between the treated and untreated zone structure, damaging tensions can be excluded.
- In the zones with more than 1.5 cm distance to the surface, the annual humidity fluctuations are at a maximum of 25% relative humidity. During the year, there are repeatedly short term drying and moistening events with changing amounts of up to 20% relative humidity, that can build-up in five to ten days (see: image 79 and image.80). In addition, here there are still no structure-damaging tensions to be expected for the single materials and for the material transitions.
- The first 1.5 cm, under the surface are exposed - from the outside to the weaker inside - to the daily fluctuations of the air humidity changes. Humidity change of 50% relative humidity within 24 hours are possible, fluctuations with amounts of over 30% happen approximately every days. According to the calculations in chapter 4.3.6 structural damages are expected, at least for the untreated soil (series A) and the single consolidated soil (series B), for these climate fluctuations. Even at sufficient penetration of the consolidant, the material transition border exceeds at least at the outcrop line of the treatment, the required depth.
- The treatments with the shown methods should penetrate at least 2 to 3cm. For treatments with less than 1.5 cm penetration, depth scale formations cannot be excluded with climatic fluctuations, as they were set in the model calculation.

4.4.3 Effect of the treatment methods on the moisture transport in the surface-treated soil

The influence on the surface treatment, on the climatically influenced development of the humidity resources in the soil, precipitates in the model calculation are very small. In image 84 and image 85, there are shown, the humidity profiles for the untreated building elements and the three treated building elements, in the evening of the

above mentioned, 14th June 1992. The profiles of the relative humidity in the building elements, with consolidation and swelling reduction treatment, at this time does not differ from the profile of the untreated soil. The drying in summer, is in the profile with the combination treatment on the surface, is practically unchanged, even when the relative humidity in the depth profile compares to the other construction units is computationally over 2% relative humidity higher (Abb.84). The profiles of the water contents, in the soil behind the treatment zones, are almost identical (image 85). Analogue to the respective run of the adsorption isotherm, the water contents in the treatment zones are different.

The gradient curves of the relative humidity in the treatment zone (see: image.86) and behind the treatment zone (see: image.87) confirm the observations from the profiles. The annual fluctuation of the relative humidity in treated building elements with 3cm depth of treatment and in the untreated soil deviates only slightly from each other. In addition, with the surface-treated soil, no long-term moistening or dehumidifying trend develops. There are no humidity maxima behind the treatment zone. The depth effect of short-term climatic vertex is fastest in the untreated building element. According to the changed vapour diffusion resistances (see: chapter 4.3.4) the desorption of the summer humidity is at the combination treatment slightly halted (see: image 87). With the treatment of the swelling reducers, the summer drying is, even slightly faster than in the untreated soil. Through the swelling reducer treatment, with high moisture contents of around 88%, the moisture transport into the depth of profile is slightly held back (image 86). Compared with the normal daily and monthly fluctuations in the profile depths of 1.5 and 3.2 cm, the shown moisture differences in image 86 and image 87, due to the treatment, are insignificant. Although the μ -value in the humid range lays more than 60% with all treatment types over the untreated soil (in the case of the combination treatments even up to 400%), (in SASSE & SNETHLAGE (1996) it is recommended that this value should not rise any more than 20%) the permeability of the soil is still too high, that a single climatic change, without rain entry, rain nodes can appear behind the treatment zones. These small affects of the treatments on the adsorption and transmission of the humidity are certainly intensified in the case of larger treatment depths. If the treatments penetration depth is less, the effects are probably weaker. Altogether, none of the presented treatments has a noticeably negative reaction, in the modelling on the transport of material humidity in the hygroscopic range.

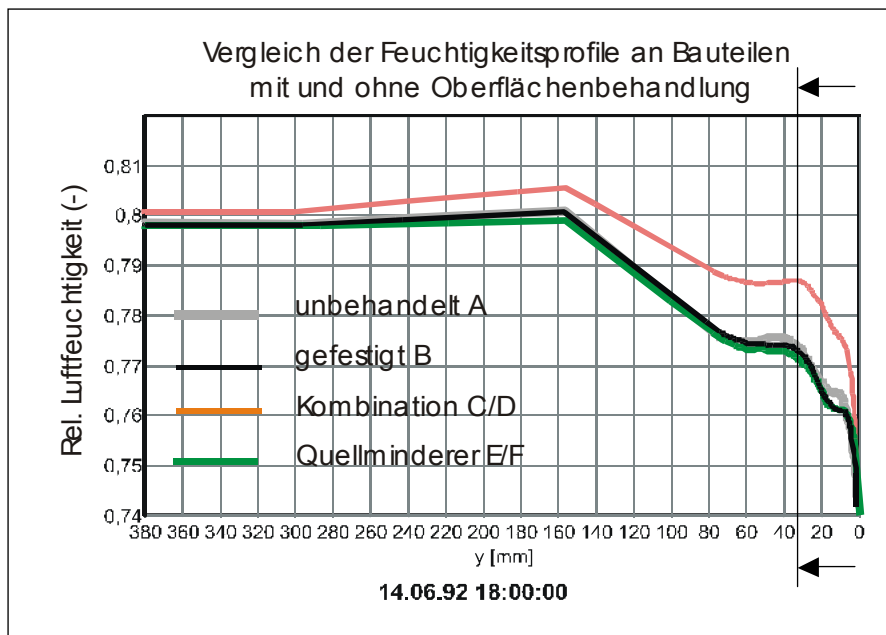


Image.84 Humidity profiles (**relative humidity**) in building elements with and without surface treatment. The treatment depth is 3cm, it is marked with arrows (see also: Structure of the building elements of the modelling in image.78). The changes of the moisture distribution in the profile are even one year of climatization very small.

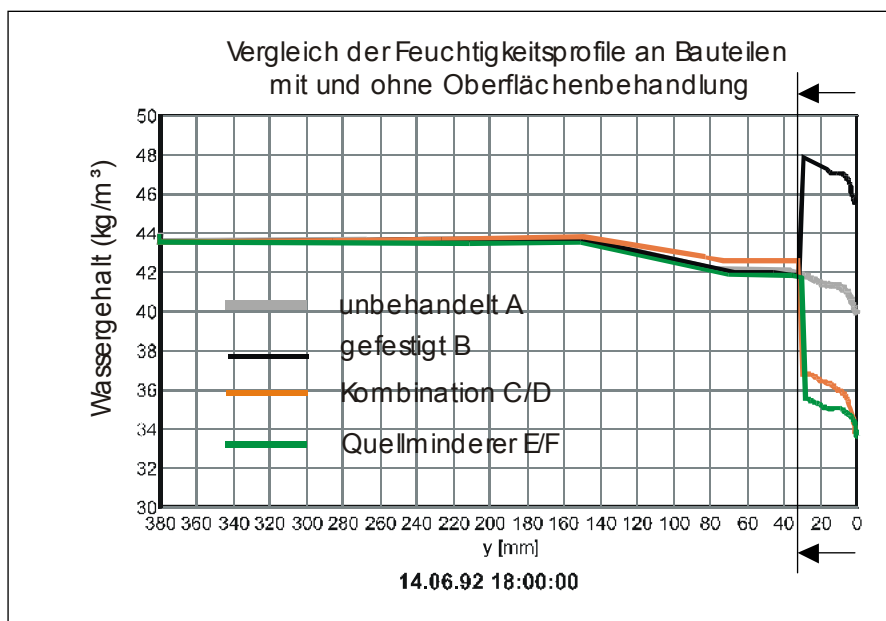


Image 85 Feuchtigkeitsprofile (**water content**) in construction units with and without surface treatment. The treatment depth amounts to 3cm, it is marked with arrows (see also: Structure of construction unit of the modelling in Abb.78). The treatment-conditioned changes of the water contents in the depth profile behind the treated zone are marginal. The water contents within the treated zone result from the differences in the dampness memory function, with more or less same water vapour partial pressure

Stabilisation of loess clay surfaces at the example of the Terracotta army in Lintong

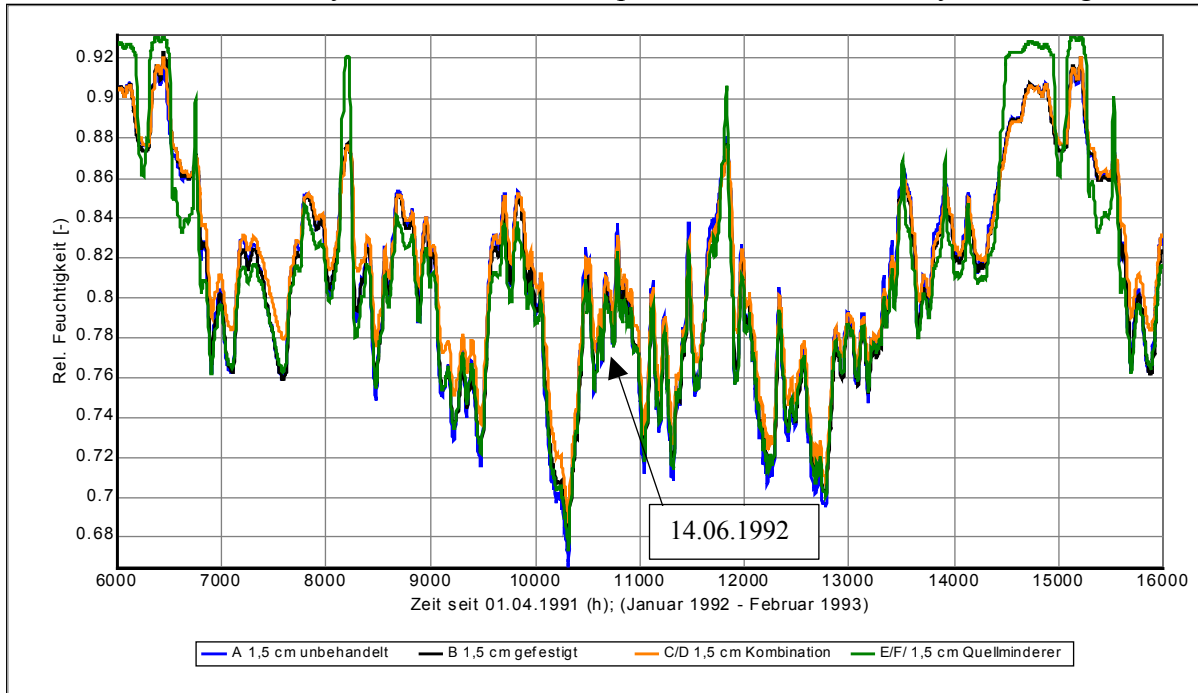


Image 86 Profile curve of the relative humidity in the treatment zone (1,5cm distance to the surface), in model year 1992. The humidity differences of the treated and untreated building elements remain under 3% relative humidity. In relation to the annual range in this depth (25% relative humidity), the changes caused by the treatment are small.

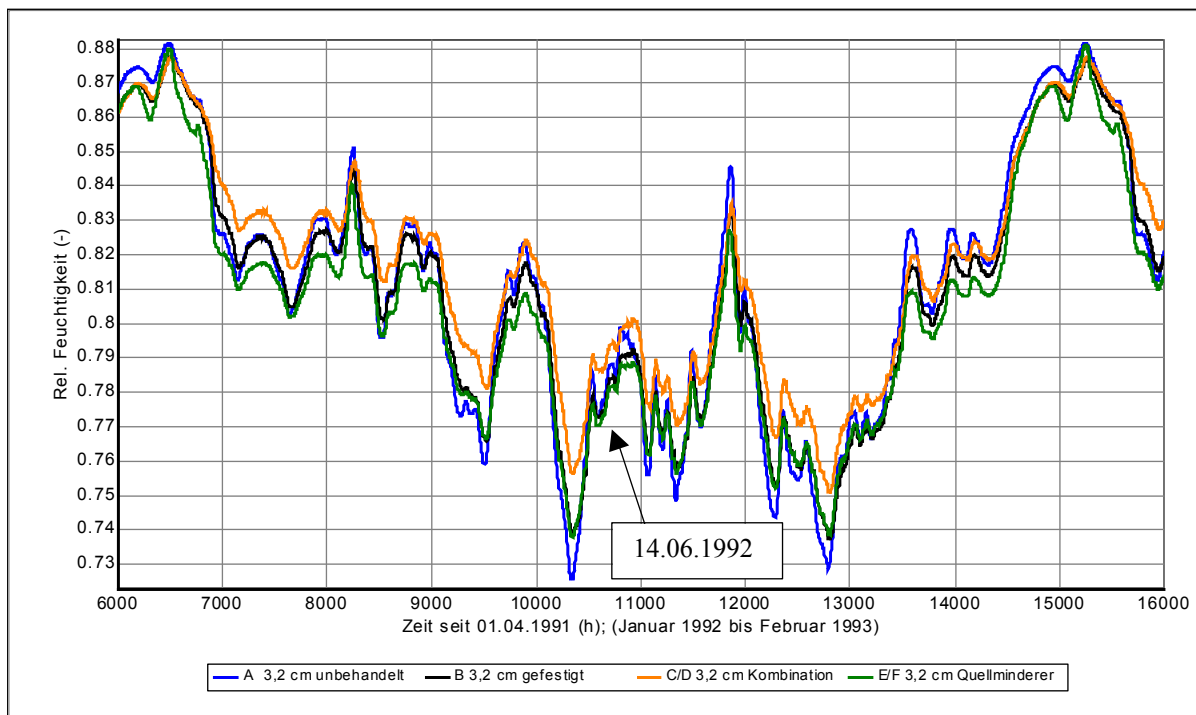


Image 87: Profile curve of the relative humidity directly behind the treatment zone (3.2cm distance to the surface), in the model year 1992.

5. Summary and fundamental evaluation of the results on treatment methods – referring to the situation in the pits of the Terracotta army

The investigation in chapter 4.3 shows that it is possible, also with soil, to work with small formatted undisturbed original samples. Additionally it becomes clear, that for the stamped soil of Lintong, or comparable soils, the method catalogue, apart from methods with direct water contact and the pore space model from the field of stone conservation of stone, can be applied in principle.

The following results and conclusions apply primarily to the application of the presented treatment methods on the stamped soil of Lintong. In principle, they should be also transferable to other soils with comparable mineral composition, gross density and pore space structure.

5.1 Swelling reduction treatment

The treatment of the stamped soil of Lintong, with the modified swelling reducers DE and DEBH, have no influence on the visual appearance of the soil. In contrary to the results of the preliminary tests with Antihydro and overdosed, modified swelling reducers, the treatment with DE and DEBH decreases, if it is adapted to the cation exchange capacity of the substrate, the hygroscopicity of the soil. This treatment has no verifiable influence on the dry gross density, the complete porosity and the internal surface of the soil, attainable with nitrogen. With the water vapour adsorption isotherm up to 60% relative humidity, for the treated soil a reduction of water infiltration in pore radii under $0.002\mu\text{m}$ could be proved. Also with this effect, there is no measurable difference between the formulations DEBH and DE.

On untreated soil samples the water vapour diffusion is in the humid range (50 - 100% relative humidity), because of the high amount of surface diffusion, three times as higher as in the dry range (0 - 50% relative humidity). The swelling reducer treatment does not affect the vapour diffusion in the dry range. By disturbing the surface diffusion, it reduces however, the diffusion flow in the humid range by around 50%. This leads in the modelling of the moisture transport to slight congestions, if the moisture stress in the profile exceeds 88% relative humidity. The fast capillary absorbency of the soil of Lintong ($w\text{-value} 10 - 16 \text{ kg/m}^2\text{h}^{0.5}$) promotes a good penetration property of the treatment material. On clay materials with a higher proportion of clay and a smaller amount of capillary pores, treatment

depths of at least 2-3 cm are, as it has to be recommended due to the results of the Wufi-2D modelling, not always to be realized. The swelling reducer treatment has no influence on the w-value of the soil. Because with this treatment the water adsorption coefficient remains high, the vapour diffusion in the humid area is halved, the drying characteristics in the case of capillary water absorption worsens. The Künzel number of this treatment type is with, 121 – 144, twice as high as at the untreated or consolidated soil. The treatment reduces the swelling within the hygroscopic humidity range by 35 to 60%. By this, the internal tensions reduced clearly with the changes of climate. For the two-tenside mixtures (DE and DEBH), there are significant differences at this point.

Through the exchange of the hydrateable cations and bridging of the loaded clay mineral surfaces the bifunctional Tenside limits the accessibility of the mineral contacts for water, so that no "unlimited" osmotic pressure can develop there. In water storage, the grain contacts are not being "blown up" anymore. The samples remain stable underwater. However, they are so softened by the water saturation, that in the case of external mechanical stress or at large sized samples, they collapse under their own weight. In the bending test, no increase of the stability could be proven for the treatment with swelling reducers. Due to the smaller amounts of extension in the change of climate, the risk of destabilization, caused by the hygric expansion, halves for surfaces treated with swelling reducers.

Variances, due to the moisture, of the mechanical properties within the hygroscopic humidity range are clearly reduced by the treatment. Thus, the reduction of the ultrasonic speed in the hygroscopic range between 5 and 98% relative humidity is reduced from 40% to 25%. The range of the dynamic elastic module is also substantially reduced. It can be expected, that additionally, the climatically initiated tensions in the treated material become weaker; an effect, which again increases the climatic stress load. In the scratching resistance test, a clear improvement of the abrasion resistance could be observed. It can probably be traced back on the reduction of the elastic module, due to the treatment, which can be explained with the "rubber band effect" of the tenside coupling. The treatment with swelling reducers is also able to reduce the mechanical abrasion of the surfaces in the excavation of Lintong.

In contrary to the treatments with consolidant, by the treatment with swelling reducers, the soil is not changed irreversibly. The characteristics of the material

change, in particular in the way that the soil has a by far smaller risk of destabilization in the change of climate after the treatment, the abrasion resistance increases slightly and the destruction potential of water contact is limited. By external exposition, without rain protection, no improvement of the stability is to be expected. In this case, the treatment could even cause damages, because it affects the drying behaviour (Künzel factor) of the soil negatively.

5.2 Consolidation Treatment

The visual appearance of the samples is not changed by the treatment with F300E. Because of the gel reposition into the pore system of the soil, the dry gross density increases clearly, and the true porosity of the soil is reduced by 5 - 10%. Compared with the range of variation of the dry gross density on clay building materials, these treatment-conditioned differences are small. From the view of conservation, the constriction of the porosity is a clear change of the material properties. The effect of the constriction of the pore space due to the gel reposition during the consolidation with silicate ester is an inherent part of this method. However, this effect can differ quantitatively and qualitatively with every consolidation. Apart from the formulation of the silicate ester, also the existing pore structure, the mineral composition of the substrate and the application conditions have a large influence on the intensification or weakening of this effect. As in stone conservation, it is recommended for the consolidation of soil, to carry out an investigation of the pore space reduction, due to the consolidation, before the application on the object.

In the test series on the original soil of Lintong, the silica gel inclusion took place in the pores with pore radii over 0.1 micrometers. The mercury porosimetry resulted, that the gel closes many pores in the lower capillary pore space with pore radii between 0.1 and 1 μ m. Larger pore spaces are only lined with gel at the walls. Due to self-porosity and the shrinkage cracks in the gel film, the inflow of water into the micro porosity is not shielded. The silica gel reduces the capillary pores, but brings along with its self-porosity an additional portion of micro porosity. The proportion between micro porosity and capillary porosity shifts toward micro porosity. Therefore, the consolidation with silicate ester causes, on one side, an increase of the water vapour adsorption and, on the other side, a reduction of the capillary water transport. In comparison to the untreated soil, the capillary water absorption coefficient is halved.

Stabilisation of loess clay surfaces at the example of the Terracotta army in Lintong

The consolidation reduces the water vapour diffusion in the humid area, only slightly. At the Wufi-2D modelling (that takes place predominantly within the humid range) the humidity fluctuations in the depth profile correlate well with the untreated soil. From the view of conservation, the consolidation has an effect that questions the sustainability of this treatment. Due to the consolidation, the swelling within the hygroscopic humidity range increases by 30 to 80%. Additional to the increased water adsorption, here the effect of the "reduced swelling space" is of importance. From the rigid sealing of the pore membranes at a constant or increasing water adsorption, an additional swelling pressure forms behind the gel film and therefore an additional swelling. This effect will occur at all consolidations with SE systems, or other systems, which line the pore space with an "inflexible" gel film.

Regarding the consolidation effect, the SE- film is very successful. Despite the additional swelling pressure, the structural stabilization of the pore space is strong enough, to ensure fully the inherent stability of small sized column samples, also in water storage of several days. The silicate ester consolidation offers sufficient protection against the mechanical surface stress in the museum halls of Lintong. The consolidation increases the average bending strength from 0.4 to 1.6 N/mm² by the factor 3.8. The average E module increases through the consolidation from 1.2 to 2.2 kN/mm². With the consolidation, the correlation of stability and elasticity improves. The specific extension increases from 0.33‰ in the non consolidated material to 0.77‰ after the treatment with silicate ester.

Because of the increased hygric expansion, the internal tensions increase up to the quadruple value, depending on the change of climate. The improvement of the specific expansion can adsorb the increase in tension, due to the treatment. The destabilization risk caused by the hygric expansion corresponds thereby computationally to that of the untreated soil. Due to the higher extension rates of the consolidation, the danger of scaling formation occurs at the boundary to the untreated soil. This damage progress has to be expected to at least on the outcrop edges of the treatment, where the outside climate can attack unhindered. The modelling shows, that the humidity fluctuations are sufficiently levelled at a consolidation depth of 2 cm that from this depth of the profile for the treatment border no more irreversible tensions arise.

While the resistance of the samples within the hygroscopic range stabilized (for this speaks for itself, the humidity-conditioned reduction of the ultrasonic speed, which

reduces itself at the consolidated samples, in the humidity between 5 and 98% relative humidity, from 40% to approximately 14%), the variance in the E-module, due to the humidity, seems to increase (the relative reduction of the elastic module between 5 and 80% relative humidity rises from 49% to 62%). This intensified variance in the elastic module will additionally strengthen the climatically initiated tensions in the treated material.

In total, the treatment of the soil with SE consolidant produces a new material with clearly increased mechanical stability. In addition, at the same time, the internal tension potential rises so strong in the humidity, that the long-term climatic stress capacity of the consolidated soil is probably lower than at the untreated soil. The ageing process of the gel was, at the time of the investigation, not yet completed. It would be important to examine the material parameters, worked on in chapter 4.3, after further condensation of the silica gel. In addition, the observation of the affects of an artificial ageing in the hygroscopic climate change, or in moistening drying cycles, would be necessary, to verify the long-term damage potential of this treatment as it derives from the material data.

1.3 Combination treatment

During the combination treatments, the influences of the swelling reducers and the influences of the consolidation treatment have an effect. In the resulting effect of the combination treatment, both additions are possible, but also the coverage and the balancing of these influences. For the complete evaluation, it is necessary to consider all characteristic data. The treatment with DE or DEBH and the following consolidation with F300E do not create any visual changes at the stamped soil of Lintong. The abrasion resistance is clearly improved, as with the single consolidation. It fulfils the requirements very well for the museum hall of Lintong.

Due to the consolidation treatment, the dry gross density rises strongly, while the porosity is reduced by up to 10%. The preliminary treatment with swelling reducers decreases the swelling of the soil before and during the silica gel consolidation. The soil is consolidated in a "more compact condition". Therefore, the increase of the dry gross density and the reduction of porosity are higher by the combination treatments than by the single consolidation.

Pore radius distribution and isotherm:

Concerning the pore radii distribution, in the capillary pore space, dominates the constriction due to the consolidation with silicate ester. The shielding of the micropores because of the treatment with swelling reducers affects the isotherm more, than the increase of micro porosity due to the self-porosity of the gel. The adsorption in the hygroscopic range is reduced by the combination treatment. The isotherm curves lay between the untreated soil and the treatment with swelling reducers.

At the diffusion transport both effects are effective, the reduction of open porosity through the consolidation and the reduction of the surface diffusion by the swelling reduction treatment. Consequently, the water vapour diffusion within the entire hygroscopic range is strongly reduced. Therefore, the soil with the combination treatment reacts in the modelling slowest to the change of climate on the surface. Without additional infiltration of running water, there is no significant difference in the depth profile (> 3cm) to the untreated soil. There is no danger of the formation of moist nodes behind the treatment layer

Similar to the single consolidation, the water absorption coefficient is halved, according to the elimination of large parts of the capillary pore volume. During the hygroscopic swelling, the effects of the increased extension rates, from the consolidation treatment and the reduced swelling, due to the tenside treatment are balanced. The resulting swelling in the hygroscopic range corresponds to the swelling of the untreated soil or lays slightly below. In the case of the combination treatment with the DEBH tenside mixture, the effect of the swelling reducers is stronger.

The samples with the combination treatment remain just as stable under water as the single consolidated. However, the reduced swelling pressure one can expect smaller internal tensions and increased stability in the moistening- drying cycle. Similar to the single consolidation, the average bending strength increases from 0.4 to 1.6 N/mm² by the factor 3.8. The average E- module increases during the consolidation, by 40% relative humidity, from 1.2 to 2.2 kN/mm², the relationship from stability to elasticity improves. As a result of the reduced amount of extension in the hygroscopic climate change and the rise of the ultimate elongation, the destabilization risk, halves at the combination treatment by the hygroscopic elongation.

Stabilisation of loess clay surfaces at the example of the Terracotta army in Lintong

The hygric expansion is so similar to the untreated material, that at the material transitions, theoretically, no shear stress arises. However, it must be guaranteed with unequal depth of penetration during the treatment steps, that the swelling reducer penetrates deeper than the consolidant. Even more than at the single consolidation, the strength of the samples within the hygroscopic range stabilises (the reduction of the ultrasonic speed, due to humidity between 5 and 98% relative humidity decreases to 10%). Differently, as with the single consolidation, due to the reduced water absorption, the reaction of the E- module is reduced in humidity changes. Similar to the swelling reduction treatment, due to this effect, less material stress is built-up in the climate change.

For the combination treatment D (DEBH-F300E), the influence of the swelling reducer is always stronger than at the combination treatment C (DE-F300E), and the influence of the consolidation is less. Whether this has to do with a larger potential of the tenside mixture DEBH (the stronger affect of DEBH does not show up clearly, in the direct comparison of the series E and F, but rudimentary) or with differences in the compatibility of consolidant and swelling reducer, is not visible. This should however be the subject of further investigations.

In general, the combination treatment creates a new material with clearly increased mechanical stability. The soil is stable under water and has the highest long-term life expectation in the change of climate, due to a low-tension potential, in comparison to the untreated soil and the other treatments. This type of treatment seems to be suitable for the requirements in the pits of the Terracotta army.

6. Literature

- Agnew, N., 1990. The Getty adobe research project at Fort Selden I: Experimental design for a test wall project, 6th international conference on the conservation of earthen architecture, Las Cruces, New Mexico, pp. 243-249.
- Agnew, N., 2002. Persönliche Mitteilung, Los Angeles, USA.
- Alfes, C., 1989. Korrelation zwischen Gefüge und Strukturparametern sowie mechanischen Eigenschaften beispielhafter Gesteinsvarietäten. Bautenschutz und Bausanierung, Sonderausgabe: 51-55.
- Alvarez de Buergo, M., et al., 2000. Efficiency of stone conservation treatments by means of scanning electron microscopy, 8th euroseminar on microscopy applied to buildings materials, Athen, pp. 503-510.
- Arbeitsbericht, 2000. Archäologischer Arbeitsbericht des Mausoleums des Qin Shihuang 1999 - vom Institut der Archäologie der Provinz Shaanxi und dem Museum der Terrakottaarmee des Qin Shihuang. Science Press, Beijing.
- Atterberg, A., 1911. Die Plastizität der Tone. Int. Mitt. Bodenkde., 1: 10-43.
- Bailey, S.W., 1954. X-ray diffraction criteria for the characterization of chloritic material in sediments. Clays & Clay Minerals, 2: 324-334.
- Bailey, S.W., 1988. Chlorites: Structures And Crystal Chemistry. Reviews in Mineralogy, 19 Hydrous Phyllosilicates (exclusive of micas): 347-403.
- Bartsch, C. et al., 1989. Abhängigkeit der Schallgeschwindigkeit von anderen petrographischen Parametern bei Sandsteinen. Z. angew. Geol., 35(5): 149-152.
- Biscaye, P.E., 1964. Distinction between kaolinite and chlorite in recent sediments by x-ray diffraction. Am. Mineral., 49: 1281-1289.
- Bökemeier, R., 2001. Das Puzzle des Jahrhunderts. Geo(7): 68-84.
- Boos, M., et al., 1999. Möglichkeiten und Grenzen der Steinfestigung im Kieselsäuresilicate ester-System. Einsatzmöglichkeiten elastifizierter Kieselsäuresilicate estertypen, 5. Internationales Kolloquium Werkstoffwissenschaften und Bauinstandsetzen-"MSR '99". AEDIFICATIO Publishers, D-79104 Freiburg, Esslingen, pp. 1305-1314.
- Böttger, K.G., et al., 1999. Kunststoffmodifizierter Lehm, 5. Internationales Kolloquium Werkstoffwissenschaften und Bauinstandsetzen- "MSR '99". AEDIFICATIO Publishes, D-79104 Freiburg, Esslingen, pp. 207-218.
- Bourges, A., Simon, S., 2003. Physical-mechanical properties on artificial adobe, Getty conservation institute, Los Angeles.

Stabilisation of loess clay surfaces at the example of the Terracotta army in Lintong

- Brinker, H., 1980. Monumentale Grabplastik im Auftrag des "Ersten Kaisers von China". In: Ausstellungskatalog (Editor), Kunstschatze aus China; 5000 v. Chr. bis 900 n. Chr. - Neue archäologische Funde aus der Volksrepublik China. Kunsthaus Zürich, Zürich.
- Brunauer, S., et al., 1938. Adsorption of Gases in Multimolecular Layers. *Journ. Amer.Chem. Soc.*, 60(2): 309-319.
- Casagrande, A., 1934. Die Aärometer-Methode zur Bestimmung der Kornverteilung von Böden und anderen Materialien. Springer, Berlin, 56 pp.
- Chiari, G., 1990. Chemical surface treatments and capping techniques of earthen structures: a long term evaluation., 6th international conference on the conservation of earthen architecture. Adobe 90 preprints, Las Cruces, New Mexico, pp. 267-273.
- Chiari, G., 2000a. Materials and craftsmanship, Terra 2000: 8th international conference on the study and conservation of earthen architecture, Torquay, United Kingdom, pp. 107-114.
- Chiari, G., 2003. Persönliche Mitteilung, Villfontaine, France.
- Chiari, G., et al., 2000b. Treatment of an adobe painted frieze in Cardal, Peru and its evaluation after 12 years, Terra 2000: 8th international conference on the study and conservation of earthen architecture, pp. 216-217.
- Coffman, R., et al., 1990. The Getty adobe research project at Fort Selden II: A study of the Interaction of Chemical Consolidants with Adobe and Adobe Constituents, 6th international conference on the conservation of earthen architecture, Las Cruces, New Mexico, pp. 250-254.
- Corti, G., et al. , 1999. A modified Kjeldahl procedure for determining strongly fixed NH₄⁺ -N. *European Journal of Soil Science*, 50: 523-534.
- Cousin, I., et al., 1999. Gas Diffusion in a silty-clay soil: experimental study on an undisturbed soil core and simulation in its three-dimensional reconstruction. *European Journal of Soil Science*, 50(2): 249-259.
- Derbyshire, E., 1982a. On the morphology, sediments, and origin of the loess plateau of central China, Large scale landforms. Scouging H., Gardener R.,.
- Derbyshire, E., 1982b. Origin and characteristics of some Chinese loess at two locations in China. *Developments in Sedimentology*, 38 Eolian sediments and processes(69-89).
- DIN4022T1, 1987. Benennen und beschreiben von Boden und Fels; Schichtenverzeichnis für Bohrungen ohne durchgehende Gewinnung von gekernten Proben im Boden und Fels.

Stabilisation of loess clay surfaces at the example of the Terracotta army in Lintong

- DIN18122T1, 1976. Zustandsgrenzen (Konsistenzgrenzen); Bestimmung der Fließ- und Ausrollgrenze.
- DIN18122T2, 1987. Zustandsgrenzen (Konsistenzgrenzen); Bestimmung der Schrumpfgrenze.
- DIN18123, 1983. Bestimmung der Korngrößenverteilung.
- DIN18124, 1989. Bestimmung der Korndichte, Kapillarpyknometer - Weithalspyknometer.
- DIN18129, 1990. Kalkgehaltsbestimmung.
- DIN18196, 1988. Erd- und Grundbau; Bodenklassifikation für bautechnische Zwecke.
- DIN18952, 1956. Vornorm DIN 18952 Blatt 2: Lehm, Prüfung von Baulehm (10/56).
- DIN19684, 1977. Bestimmung der Austauschkapazität des Bodens und der austauschbaren Kationen.
- DIN52615, November 1987. Bestimmung der Wasserdampfdurchlässigkeit von Bau- und Dämmstoffen, DIN 52615.
- Echeverria, J.C., et al., 1999. Characterization of the porous structure of soils: adsorption of nitrogen (77K) and carbon dioxide (273K), and mercury porosimetry. *European Journal of Soil Science*, 50: 497-503.
- Einstein, H.H., 1993. Swelling Rock. *Int. Soc. Rock Mech. - News Journal*, 1(3): 57-60.
- Erfurt, W., Krompholz, R., 1996. Anwendung der Dehnwellenmessungen für Baustoffuntersuchungen. *Beiträge zur Baustoffforschung-Wissenschaftliche Zeitschrift*, 4/5: 95-101.
- Esbert, R.M., et al., 1989. Ultrasonic Velocity and Humidity in Monumental Stone, *Proceedings of the European Symp. on Science, Technology and Cultural Heritage*. N. S. Baer, C. Sabbioni, A.I. Sors, Bologna, pp. 597-600.
- Fitzner, B., 1988. Untersuchung der Zusammenhänge zwischen dem Hohlraumgefüge von Naturstein und physikalischen Verwitterungsvorgängen. *Mitteilung Ing.- u. Hydrogeologie Aachen*, 29: 217.
- Fitzner, B., Basten, D., 1994. Gesteinsporosität-Klassifizierung, meßtechnische Erfassung und Bewertung ihrer Verwitterungsrelevanz., *Jahresberichte Steinerfall - Steinkonservierung 5*. Verlag Ernst u. Sohn, Berlin, pp. 19-32.
- Goodman, M., 2002. Site preservation at Gordian, an Iron Age city in Anatolia. *Conservation and management of archaeological sites*, 5(4).
- Grasegger, G., 1992a. Charakterisierung der Gel-Strukturen von Kieselsäuresilicate ester-Steinfestigern unter verschiedenen Erhärtungsbedingungen mittels

Stabilisation of loess clay surfaces at the example of the Terracotta army in Lintong

- thermoanalytischer Methoden (DTA/TG)., Jahresbericht Steinzerfall Steinkonservierung. Verlag Ernst & Sohn, Berlin 1992, Berlin, pp. 179 - 185.
- Grasegger, G., 1992b. Untersuchungen zur Entwicklung der mikroskopischen Gefüge von Kieselsäuresilicate ester-Gelen in Porenräumen mit und ohne Salz-, Feuchtestöreffekte, Jahresbericht Steinzerfall Steinkonservierung 4. Verlag Ernst & Sohn, Berlin, pp. 127 - 133.
- Gregg, S.J., et al., 1982. Adsorption, Surface Area and Porosity. Academ. Press, London.
- Hakimi, A., et al., 1996. Resultats d' essais de resistance mecanique sur echantillon de terre comprimée. Material and Structures/Materiaux et Constructions, 29: 600-608.
- Heim, D., 1990. Tone und Tonminerale: Grundlagen der Sedimentologie und Mineralogie. Enke, Stuttgart, 157 pp.
- Hilbert, G., Wendler, E., 1995. Zielgerichtete Natursteinkonservierung: Zur Reduzierung des hygrischen Quellens. Bautenschutz und Bausanierung, 3.
- Hiraiwa, Y., Kasubuchi, T., 2000. Temperature dependence of thermal conductivity of soil over a wide range of temperature 5-75°C. European Journal of Soil Science, 51(2): 211-218.
- Hofmann, U., et al., 1967. Die Trockenbiegefestigkeit von Kaolinen und Tonen. Berichte der Deutschen Keramischen Gesellschaft, 44(4): 131-140.
- Höltling, B., 1996. Hydrogeologie: Einführung in die Allgemeine und Angewandte Hydrogeologie, 5. Auflage. Ferdinand Enke Verlag, Stuttgart.
- Houben, H., Guillaud, H., 1994. Earth Construction: A Comprehensive Guide. Intermediate Technology Publications, London.
- Huang, K., et al., 1990. The weathering characteristics of the rocks of the Kezier Grottoes and research into their conservation, 6th international conference on the conservation of earthen structures, Las Cruces, New Mexico.
- ISRM, 1994. Comments and recommendations on design and analysis procedures for structures in agrillaceous swelling rock. Int. J. Rock Mech. Min. Sci. & Geomech. Abstr., 31(5): 535 - 546.
- Keßler, T., 2000. Untersuchungen des Einflusses von Quellminderenden Stoffen in Kombination mit Hydrophobierung auf das Quellverhalten des Lettenkohlsandsteines. Diplomarbeit, Göttingen.
- Kießl, K., 1983. Kapillarer und dampfförmiger Feuchtetransport in mehrschichtigen Bauteilen. Dissertation Thesis, Universität Gesamthochschule Essen, Essen.

Stabilisation of loess clay surfaces at the example of the Terracotta army in Lintong

- Kießl, K., Gertis, K., 1980. Feuchtetransport in Baustoffen. Eine Literaturlauswertung zur rechnerischen Erfassung hygrischer Transportphänomene. Forschungsberichte aus dem Fachbereich Bauwesen, 13.
- Klockmann, F., 1978. Klockmanns Lehrbuch der Mineralogie/überarb. u. erw. von Paul Ramdohr und Hugo Strunz. Enke Verlag, Stuttgart.
- Klopfer, H., 1974. Wassertransport durch Diffusion in Feststoffen. Bauverlag GmbH, Wiesbaden, 235 pp.
- Klopfer, H., 1979. Das Kapillarverhalten poröser Baustoffe, Techn. Akade. Esslingen, Lehrgang Nr. 4280/79.88.
- Klopfer, H., 1985. Lehrbuch der Bauphysik. Teubner, Stuttgart.
- Knöfel, D., Schubert, P., 1992. Zur Beurteilung von Putzmörtel für historische Bauwerke, Jahresbericht Steinzerfall - Steinkonservierung. Ernst und Sohn, Berlin.
- Kocher, M., 2003. Quelldruck von Sandsteinen (in Arbeit), Dissertation, Ludwig Maximilians Universität, München.
- Köhler, W., 1991. Untersuchungen zu Verwitterungsvorgängen an Carrara-Marmor in Potsdam Sanssouci, Berichte zu Forschung und Praxis der Denkmalpflege in Deutschland, Steinschäden-Steinkonservierung 2, Hannover, pp. 50-53.
- Köhler, W., 1996. Investigations on the Increase in the Rate of Weathering of Carrara Marble in Central Europe, 8th International Congress on Deterioration and Conservation of Stone, Berlin, Germany, pp. 167-173.
- Koob, S.P., et al., 1990. Preserving the eighth century BC. Mud brick architecture at Gordion, Turkey: approaches to conservation., 6th international conference on the conservation of earthen architecture, Las Cruces, New Mexico.
- Kretschmar, R., 1984. Ausführung der Bestimmung, Arbeitsvorschrift nach Mehlich, Kulturtechnisch-Bodenkundliches Praktikum, Ausgewählte Labormethoden - eine Anleitung zum selbstständigen Arbeiten, Kiel, pp. 271-276.
- Krus, M., 1995. Feuchtetransport- und Speicherkoeffizienten poröser mineralischer Baustoffe. Theoretische Grundlagen und neue Meßtechniken, Universität Stuttgart, Stuttgart, 107 pp.
- Künzel, H.M., 1969. Anforderungen an Außenanstriche und Beschichtungen aus Kunstharzdispersionen. Kunststoffe im Bau, 12: 6-32.
- Künzel, H.M., 1994. Verfahren zur ein- und zweidimensionalen Berechnung des gekoppelten Wärme- und Feuchtetransports in Bauteilen mit einfachen Kennwerten. Dr. -Ing. Thesis, Universität Stuttgart, Stuttgart.

- Künzel, H.M., et al., 2000. Wufi-2D: Program Description. A PC-Program for Analyzing the Two-Dimensional Heat and Moisture Transport in Building Components, Fraunhofer - Institut for Building PHysics, Holzkirchen, pp. 156.
- Künzel, H.M., et al., 1995. Feuchtemigration und langfristige Feuchteverteilung in exponierten Natursteinmauern. *Bauinstandsetzen*, 1(4): 267-280.
- Künzel, H.M., et al., 2002. Wufi-Pro Version 3.3. Fraunhofer Institut für Bauphysik, Holzkirchen.
- Lagaly, G., Weiss, A., 1969. Determination of layer charge in mica-type silicates, International Clay Conference (1969) Tokyo. Israel University Press, Jerusalem, pp. 61-80.
- Laurenzi-Tabasso, M., et al., 1988. Consolidation of Stone: Comparison between a Treatment with a Methacrylic Monomer and the Corresponding Polymer. In: *Marinos&Koukis (Editor), Engineering Geology of Ancient Works, Monuments and Historical Sites*, Balkema, Rotterdam, pp. 933-942.
- Ledderose, L., 1998. *Ten thousand things: module and mass production in Chinese art*. Princeton University Press, New Jersey.
- Li, Z., 1990. Consolidation of a neolithic site with potassium silicate, 6th international conference on the conservation of earthen architecture, Las Cruces, New Mexico, pp. 295-301.
- Lissenko, V., et al., 1998. The Conservation of Calcareous Stone -Evaluation of Protective Treatments- Pilot Object: Odessa Gigantic Stairway, Restoration, Reconstruction, Urboecology, ICOMOS Tagung 4.-6. September 1998, Odessa (Ukraine), pp. 195-213.
- Liu, D.S., Chang, T. H., 1962. The Loess of China. *Acta Geologica Sinica*, 42: 1-14.
- Liu, D.S., et al., 1966. *Composition and Texture of the Loess*. Science Press, Beijing, 132 pp.
- Mac Ewan, D.M.C., Wilson M. J., 1984. Interlayer and intercalation complexes of clay minerals. In: B. Brown (Editor), *Crystal structures of Clay Minerals and their X-Ray Identification*. Mineral. Society, London, pp. 197-248.
- Madsen, F.T., Müller-Vonmoos, M., 1988. Das Quellverhalten der Tone. In: Lang (Editor), *Tonmineralogie und Bodenmechanik*. Mitt. des Inst. f. Grundbau u. Bodenmechanik ETH Zürich, Zürich, pp. 39-50.
- Mamillan, M., 1958. Methode de classification des pierres calcaires, *Annales de l'Institut Technique du Batiment et des Travaux Publics*, pp. 270-526.
- Meinhardt-Degen, J., Sneathlage, R., 2002. Alte Pinakothek in Munich and Schillingsfürst Castle Investigation of the effects of retreatment on consolidated as well as hydrophobed sandstone facades, 13th Workshop -

Stabilisation of loess clay surfaces at the example of the Terracotta army in Lintong

- EU 496 Euromarble. Bavarian State Department of Historical Monuments, Munich.
- Metzger, K., 2003. Grundlegendes über Lößgesteine und die aus ihnen hervorgegangenen Böden; Löß, das Gestein aus Luft und Staub geboren. www.macumee.de.
- Miculitsch, V., Gudehus, G., 1996. Messungen der physikalischen Eigenschaften von Boden- und Steinproben aus dem Terracottamuseum, Lintong (VR China), Institut für Bodenmechanik und Felsmechanik d Universität Fridericana Karlsruhe, Im Auftrag d. Bayer. Landesamtes f. Denkmalpflege, München (interner Bericht, unveröffentlicht).
- Minke, G., 1994. Lehm-Handbuch. Der Baustoff Lehm und seine Anwendung. Ökobuch, Staufen, 321 pp.
- Minke, G., 1995. Materialkennwerte von Lehmbaustoffen. Bauphysik, 17(4): 124-130.
- Müller, U., 2002. Earth as a Building Material, Getty Conservation Institute, Los Angeles.
- Murawski, H., 1992. Geologisches Wörterbuch/Hans Murawski.-9., völlig überarb. und erw. Aufl. Enke Verlag, Stuttgart.
- Neumüller, O.-A., 1979. Römpps Chemie-Lexikon. Franckh., Stuttgart.
- Nienhauser, W.H., 1994. The Grand Scribe's Records. Vol. 1: The Basic Annals of Pre-Han China. Bloomington & Indianapolis University Press, Indiana.
- Obruchev, V.A., 1911. The question of the origin of loess - in defense of the aeolian hypothesis. Izvestiya Tomskogo Teknologicheskogo Instituta, Russia.
- Pimentel, E., 1996. Quellverhalten von diagenetisch verfestigtem Tonstein. Dissertation Thesis, Universität Fridericana Karlsruhe (TH), Karlsruhe, 184 pp.
- Poschod, K., 1990. Das Wasser im Porenraum kristalliner Naturwerksteine und sein Einfluss auf die Verwitterung. Münchner geowissenschaftliche Abhandlungen: Reihe B, Allgemeine und angewandte Geologie, 7.
- Prinz, H., 1991. Abriß der Ingenieurgeologie: mit Grundlagen der Boden- und Felsmechanik, des Erd- Grund- und Tunnelbaus sowie der Abfalldeponien, 2. neubearb. und erw. Auflage. Enke Verlag, Stuttgart, 466 pp.
- Reineck, H.E., Singh, I.B., 1980. Depositional Sedimentary Environments With Reference to Terrigenous Clastics (Second Revised and Updated Edition, Corrected Second Printing). Springer-Verlag, Berlin, Heidelberg, New York, 551 pp.

Stabilisation of loess clay surfaces at the example of the Terracotta army in Lintong

- Rentsch, W., Krompholz, G., 1961. Zur Bestimmung elastischer Konstanten durch Schallgeschwindigkeitsmessungen. *Fachzeitschrift der Bergakademie Freiberg*, 13: 492-504.
- Richard, G., et al., 2001. Effect of the compaction on the porosity of a silty soil: influence on unsaturated hydraulic properties. *European Journal of Soil Science*, 52: 49-58.
- Riederer, J., 1973. Bibliographie der deutschsprachigen Literatur über die Verwitterung und Konservierung von Naturstein. *DKD*, 1(2): 106-118.
- Rogner, I., 2000. Festigung und Erhaltung der polychromen Qi-Lackschichten der Terrakottakrieger des Qin Shihuangdi durch Behandlung mit Methacryl-Monomeren und Elektronenbestrahlung, LMU-München, München.
- Ruhe, R.V., 1982. Clay minerals in thin loess, Ohio river basin, U.S.A. *Developments in Sedimentology*, 38 Eolian sediments and processes: 91-102.
- Sasse, H.R., Snethlage, R., 1996. Methods for the Evaluation of Stone Conservation Treatments. In: N.S. Baer, Snethlage, R. (Editor), *Dahlem Workshop on Saving our architectural heritage: The conservation of historic stone structures*. John Wiley & Sons, Berlin, pp. 223-243.
- Sattler, L., 1992. Untersuchungen zu Wirkung und Dauerhaftigkeit von Sandsteinfestigung mit Kieselsäuresilicate ester. *Forschungsbericht 1992/9 Bayerisches Landesamt für Denkmalpflege - Zentrallabor*, 9. Bayerisches Landesamt für Denkmalpflege.
- Scheffer, F., Schachtschabel, 1998. *Lehrbuch der Bodenkunde*. Enke, Stuttgart.
- Schmidt, H.H., 1993. Die große Mauer. In: L. Ledderose, Schlombs, A. (Editor), *Jenseits der großen Mauer; Der erste Kaiser von China und seine Terrakotta-Armee*. Bertelsmann Lexikon Verlag, Dortmund, pp. 76-79.
- Schuh, H., 1987. Physikalische Eigenschaften von Sandsteinen und ihren verwitterten Oberflächen. *Münchener geowissenschaftliche Abhandlungen: Reihe B, Allgemeine und angewandte Geologie*, 6: 17-43.
- Schwarz, B., 1972. Die kapillare Wasseraufnahme von Baustoffen. *Gesundheits-Ingenieur*, 93(7): 206-211.
- Schwertmann, U., 1984. Tonminerale. In: Scheffer/Schachtschabel (Editor), *Lehrbuch der Bodenkunde*. Enke, Stuttgart, pp. 23-28.
- Selwitz, C., 1995. Saving the Fort Shelden Ruins: The use of a composite blend of chemicals to stabilize fragile historic adobe. *Conservation and Management of Archaeological Sites*, 1: 109-116.
- Selwitz, C., et al., 1990. The Getty adobe research project at Fort Selden III: An evaluation of the application of chemical consolidants to test walls, 6th

- international conference on the conservation of earthen architecture. Adobe 90 preprints, Las Cruces, New Mexico, pp. 255-260.
- Shekede, L., 2000. Wall paintings on earthen supports Evaluating analytical methods for conservation, Terra 2000: 8th international conference on the study and conservation of earthen architecture, Torquay, United Kingdom.
- Simon, S., 2001. Zur Verwitterung und Konservierung Kristallinen Marmors, München.
- Sing, K.S.W., et al., 1985. Reporting physisorption data for gas/solid systems with special reference to the determination of surface-area and porosity. Pure and Applied Chemistry, 57: 603-619.
- Smalley I. J., et al., 1973. Observations on the Kaiserstuhl loess. Geol. Mag., 110: 29-36.
- Smalley I. J., et al., 1968. The formation of fine particles in sandy deserts and the nature of "desert" loess. J. Sediment. Petrol., 38: 766-774.
- Smalley, I.J., 1966. The properties of glacial loess and the formation of loess deposits. Journal of Sediment Petrology, 36: 669-676.
- Smalley, I.J., Smalley, V., 1982. Loess Material And Loess Deposits: Formation, Distribution And Consequences. Developments in Sedimentology, 38 Eolian Sediments and Processes: 51-68.
- Snethlage, R., 1984. Steinkonservierung 1979 - 1983, Arbeitshefte des Bayerischen Landesamtes für Denkmalpflege. Verlag Karl M. Lipp, München, pp. 203.
- Snethlage, R., 1991a. Geologische und mineralogische Eigenschaften als Festigkeitsparameter von Gesteinen, Denkmalpflege und Naturwissenschaften im Gespräch, Workshop in Fulda 1990, pp. 18-23.
- Snethlage, R., 1997a. Leitfaden Steinkonservierung. Planung von Untersuchungen und Maßnahmen zur Erhaltung von Denkmälern aus Naturstein. Fraunhofer IRB Verlag, Stuttgart.
- Snethlage, R., Meinhardt-Degen, J., 2002. Requirements for Re-treating Natural Stone Facades; An Overview over the Assessment Parameters, 13th Workshop - EU 496 Euromarble. Bavarian State Department of Historical Monuments, Munich, pp. 60-67.
- Snethlage, R., et al., 1991b. Tenside im Gesteinsschutz- bisherige Resultate mit einem neuen Konzept zur Erhaltung von Denkmälern aus Naturstein. In: R. Snethlage (Editor), Natursteinkonservierung in der Denkmalpflege - Arbeitshefte d. Bayerischen Landesamtes für Denkmalpflege. Ernst u. Sohn, Berlin.

Stabilisation of loess clay surfaces at the example of the Terracotta army in Lintong

- Snethlage, R., Wendler, E., 1997b. Methoden der Steinkonservierung. Anforderungen und Bewertungskriterien. In: R. Snethlage (Editor), Denkmalpflege und Naturwissenschaft, Natursteinkonservierung I. Ernst & Sohn, Berlin, pp. 3-40.
- Snethlage, R., Wendler, E., 2000. Chemical Compounds for Conservation of Natural Stone, Ludwig Maximilian Universität München, Fakultät Geowissenschaften, Munich.
- Soergel, W., 1919. Löss, Eiszeiten und paläolithische Kulturen. Eine Gliederung und Altersbestimmung der Löss. Gustav Fischer, Jena, 177 pp.
- Soos, P.v., 1980. Eigenschaften von Boden und Fels; ihre Ermittlung im Labor, Grundbultaschenbuch, Teil 1, 3. Aufl. Ernst & Sohn, Berlin, pp. 59-116.
- Steiger, M., Dannecker, W., 1995. Hygroskopische Eigenschaften und Kristallisationsverhalten von Salzgemischen, Jahresberichte Steinerfall - Steinkonservierung. Ernst u. Sohn, Berlin.
- Tariq, A., Durnford, D., 1993a. An analytical equation for swelling clay soils. Soil Science Society of America, 57: 1183-1187.
- Tariq, A., Durnford, D., 1993b. Soil volume shrinkage measurements: a simple method. Soil Science, 155: 325-330.
- Taylor, M.R., 2000. Conservation, maintenance and repair of earthen architecture. Which way do we hold the map?, Terra 2000: 8th international conference on the study and conservation of earthen architecture, Torquay, United Kingdom, pp. 189-194.
- Teutonico, J., M., 2001. Protective shelters for archaeological sites in the southwest USA. Conservation and management of archaeological sites, 5(2).
- Thieme, C., 1993. Zur Farbfassung der Terrakottaarmee des ersten Kaiser Qin Shihuangdi, In -Arbeitsbericht der Arbeiten im China Projekt am bayerischen Landesamt für Denkmalpflege, München.
- Torraca, G., 1979. Physico-chemical deterioration of porous rigid building materials. Notes for a general model. In: L.p.I.S.d.D.d.G.m.d.C.U.d. Venezia (Editor), Il Mattone di venezia,. Atti del Convegno presso Fondazione Cini, Venezia, 22-23.10.1979, pp. 95-144.
- Tributh, H., 1979. Vorschläge für eine sinnvolle Unterteilung der Tonfraktion und Abgrenzung von Begriffen. Mitt. Deut. Bodenk. Ges., 19: 1049-1058.
- Troll, C., 1942. Neue Gletscherforschungen in den Subtropen der Alten und Neuen Welt (Karakorum und argentinische Anden). Zeitschrift der Gesellschaft für Erdkunde Berlin: 54-65.

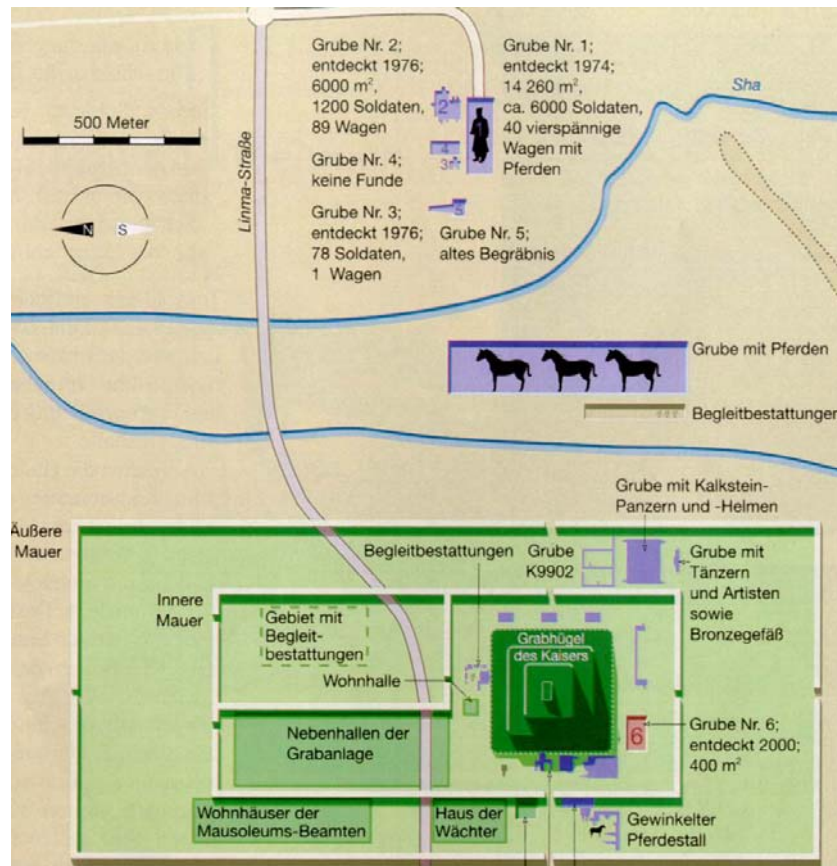
Stabilisation of loess clay surfaces at the example of the Terracotta army in Lintong

- Utz, R., 2001a. Investigation on the texture and on the mechanical properties of terracotta fragments from the Museum of the Terracotta Warriors and Horses in Lintong, In: Work Report of the Years 1999 and 2000 for the Project: "Testing and optimising of Conservation Technologies for the Preservation of Cultural Heritage of the Shaanxi Province, PR China. -Bayerisches Landesamt für Denkmalpflege -, Munich.
- Utz, R., 2001b. Klimamessungen in der Grube II, In: Work Report of the Years 1999 and 2000 for the Project: "Testing and optimising of Conservation Technologies for the Preservation of Cultural Heritage of the Shaanxi Province, PR China". -Bayerisches Landesamt für Denkmalpflege -, Munich.
- Utz, R., 2001c. Survey and investigations on the distribution of the soil moisture in the earthen construction of pit one and two, In: Work Report of the Years 1999 and 2000 for the Project: "Testing and optimising of Conservation Technologies for the Preservation of Cultural Heritage of the Shaanxi Province, PR China". -Bayerisches Landesamt für Denkmalpflege -, Munich.
- Utz, R., 2003a. The hygric and mechanic properties of Qin terracotta 2002 - Complementary investigations to the results presented in the annual report 1999/2000, In: Work Report of the Years 2001 and 2002 for the Project: "Testing and optimising of Conservation Technologies for the Preservation of Cultural Heritage of the Shaanxi Province, PR China -Bayerisches Landesamt für Denkmalpflege -, Munich.
- Utz, R., 2003b. Work Campaign of Rupert Utz in Lintong, September 9 to 23, 2001, In: Work Report of the Years 2001 and 2002 for the Project: "Testing and optimising of Conservation Technologies for the Preservation of Cultural Heritage of the Shaanxi Province, PR China" -Bayerisches Landesamt für Denkmalpflege -, Munich.
- Van Olpen, H., 1963. Compaction of clay sediments in the range of molecular particle distances. *Clays Clay Miner.*, 11: 178-187.
- Visher, G.S., 1969. Grain size distributions and depositional processes. *J. Sediment. Petrol.*, 39: 1077-1106.
- Volhard, F., Röhlen, U., 1998. *Lehmbau Regeln; Begriffe, Baustoffe, Bauteile.* Vieweg&Sohn Verlagsgesellschaft mbH, Braunschweig/Wiesbaden.
- Walker, P., 2000. Review and experimental comparison of erosion tests for earth blocks, *Terra 2000: 8th international conference on the study and conservation of earthen architecture*, Torquay, United Kingdom, pp. 176-188.

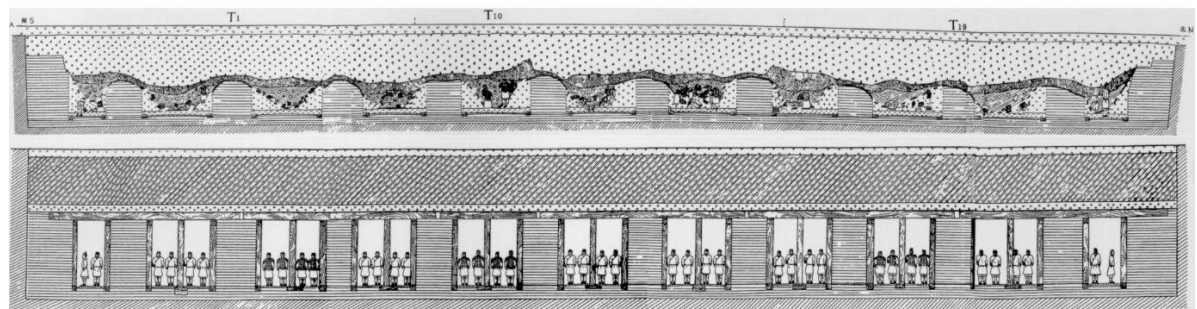
- Wang, Y.-y., et al., 1980. On the stratigraphic problems of the loess on the plateau north of Weihe river, Shaanxi Province in accordance with the paleomagnetic data. *Geological Review*, 26: 141-147.
- Warscheid, T., 2001. Preliminary summary on the actual results of the microbiological investigations on object and soil samples from the excavation of the Terracotta Army, In: Work Report of the Years 1999 and 2000 for the Project: "Testing and optimising of Conservation Technologies for the Preservation of Cultural Heritage of the Shaanxi Province, PR China". - Bayerisches Landesamt für Denkmalpflege -, Munich.
- Wendler, E., 1996a. New Materials and Approaches for the Conservation of Stone. In: N.S. Baer, Snethlage, R., (Editor), Dahlem Workshop on Saving our architectural heritage: The conservation of historic stone structures. John Wiley & Sons, Berlin, pp. 181-198.
- Wendler, E., et al., 1991. Contour Scaling on Building Facades - Dependence on Stone Type and Environmental Conditions, *Materials Research Society Symp. Proc. Vol. 185: Materials Issues in Art and Archaeology II*, Pittsburgh, pp. 265-272.
- Wendler, E., et al., B., 1996b. Quell-und Schwindverhalten als Wirksamkeitskriterium zur Beurteilung von Steinschutzstoffen, *Jahresberichte Steinerfall-Steinkonservierung 1994-1996*.
- Wendler, E., Snethlage, R., 1988. Die Veränderung der Kationenaustauschkapazitäten von Sandsteinen im Zuge der Verwitterung an Gebäuden. In: T.A. Esslingen (Editor), *Umwelteinflüsse auf Oberflächen, Ostfildern*.
- Xia, Y., Li, P-Y., 1980. Four stages in the development of Quaternary sedimentation around Xi'an. *Geographical Journal (PHysical)*, 10: 52-70 (Chinesisch).
- Yuen, et al., 1988. Die Gruben der Terrakottakrieger und -pferde aus der Grabanlage des Qin Shihuang. Bericht über die Ausgrabung der Grube 1, 1974-1984. (Hrsg.) Archäologisches Institut der Provinz Shaanxi / Archäologisches Team für die Ausgrabung der Gruben der Terrakottaarmee am Mausoleum des Qin Shihuang, Peking.
- Zhang, Z., 1980. Loess in China. *GeoJournal*, 4(6): 525-540.
- Zhou, S., 2000. Conservation of soil materials in museum of terracotta army, Beijing University, Beijing.
- ZTVE-StB76, 1976. Zusätzliche Technische Vorschriften und Richtlinien für Erdarbeiten im Straßenbau.

7. Appendix

7.1 Plans



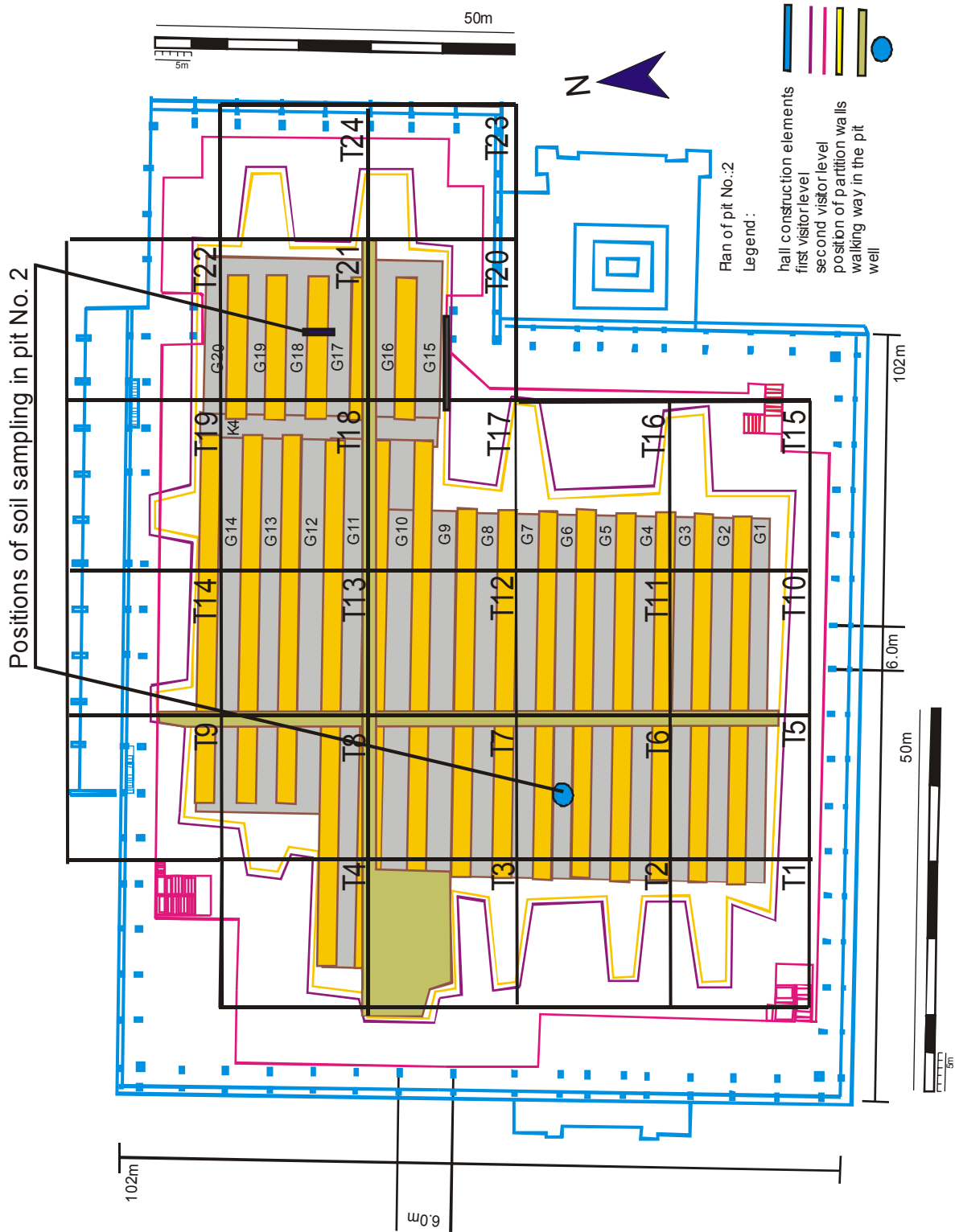
burial area of the emperor grave (Bökemeier, 2001)

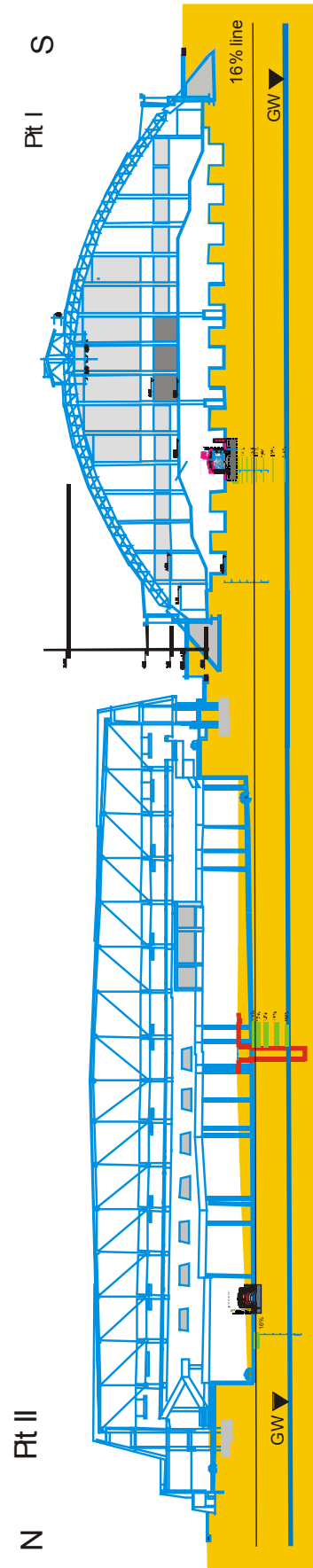


Cross section of pit 1 with the excavation (above) and reconstruction of the original condition (below); Illustration out of (Ledderose, 1998)

Stabilisation of loess clay surfaces at the example of the Terracotta army in Lintong

Plan true to scale of pit 1 with the position of the drilling soundings in the well and at a soil partition wall in T21





Maßstabgetreuer Aufriss der Gruben 1 und 2, mit Lage der Bodenfeuchtesondierungen

7.2 History of the excavation

Compilation of the excavation history of the Terracotta army (after Catharina Blänsdorf)

Pit 1 (12 600 m² or 14 260 m²)

March 1974	Discovery of the Terracotta army at the digging of a well by farmers
July 1974- March 1975	excavation in the open air; uncovering of the eastern side of the pit with over 500 terracotta soldiers, 24 horses and some bronze weapons
October. 1975-Jan. 1976	Restoration of the excavated figures; determination of the ground plan by soundings; filling of the test excavation.
Sept. 1976-1978-791	Building of the shelter halls
May 1978-April 1979	remove of the filling
April 1979-Sept. 1981	Excavation of the eastern sectors T 1, 2, 10, 19 and 20 (each 20x20m)
1986	Excavations in the middle and rear range (today again filled)
1989-90	Strong cracks in the soil bridges; First stabilisation tests eastern
1998	twelve easterly sectors completely excavated soil bridges between them teared off. In T 1, 2, 10, 19, 20 the figures had been restored and re situated. The soil had been removed up to height of the ceiling beams (except of T 8, 9, 17, 18, 27). In the middle sectors the corridors are covered with plastic foils

Pit 2 (6,000 m²)

May 1976	Discovery of the pit
May -August 1976	Probes ; Determination of the ground plan; 17 test excavations in the size of 3x5 up to 15x20m, filling of the test diggings
1989-1992 (1994)	building of the shelter hall
Since 1994	remove of the fillings, expansion of the test diggings (out of this the fragments 1991, 1992, 1995, 1998, 1999)
Since October 1994	open for the public
Until end of 1997	complete uncovering of the beam layer
Since February 1998	excavation of the sectors T18 and 21 (fragments 2001)

Stabilisation of loess clay surfaces at the example of the Terracotta army in Lintong

July –August 1999 excavation of the sectors T21 G18 and K4, conservation of 6 polychrome kneeling soldiers in the pit

Since 2000 stop of the excavations

Since 2001 again excavations in T21 G18,19 and 20, three kneeling bow men conserved

Pit 3 (520 m²)

June 1976 Discovery

March-December 1977 First part of the excavation

September 1978-79 building of the shelter hall

Since October 1988 open for the public

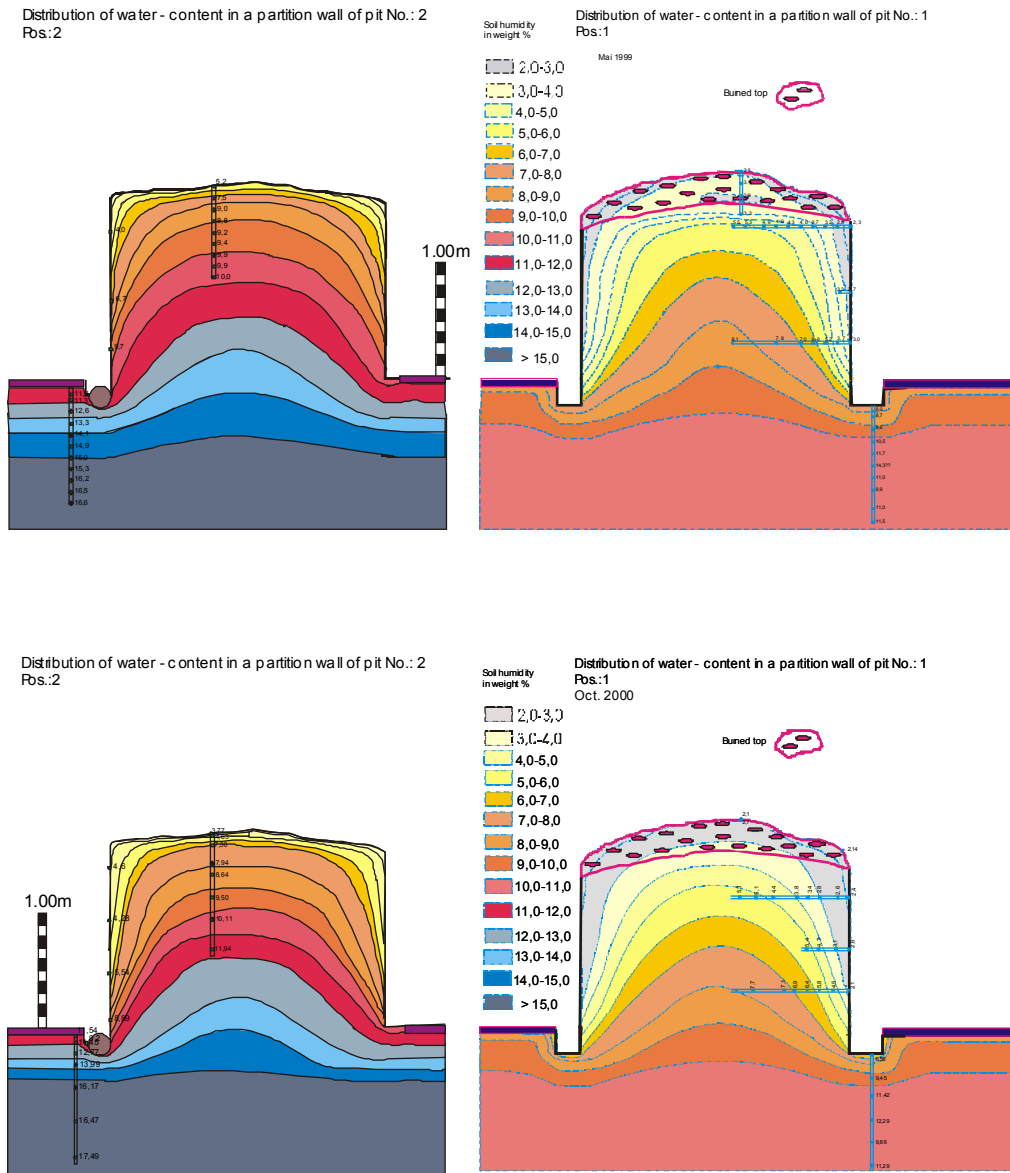
December uncovering of the north corridor (figures are left in situ of the excavation)

Pit no.	type of troop formation	size of the pit		number of		
				warriors	chariots	horses
1	infantry and chariots (mixed)	62 x 230 m	12600 m ²	6 000	50	200
2	archers (unit 1)	26,6 x 38 m	5988 m ²	800 to 1000	80	470
	war chariots (unit 2)	52 x 48 m				
	infantry, war chariots, cavalry (u. 3)	68 x 16 m				
	cavalry (unit 4)	50 x 20 m				
3	guard of honour or head quarter		520 m ²	66 or 68	1	4

Overview of the sizes of the pits and the number and kind of the Terracotta figures

Stabilisation of loess clay surfaces at the example of the Terracotta army in Lintong

7.3 Soil-moisture profiles



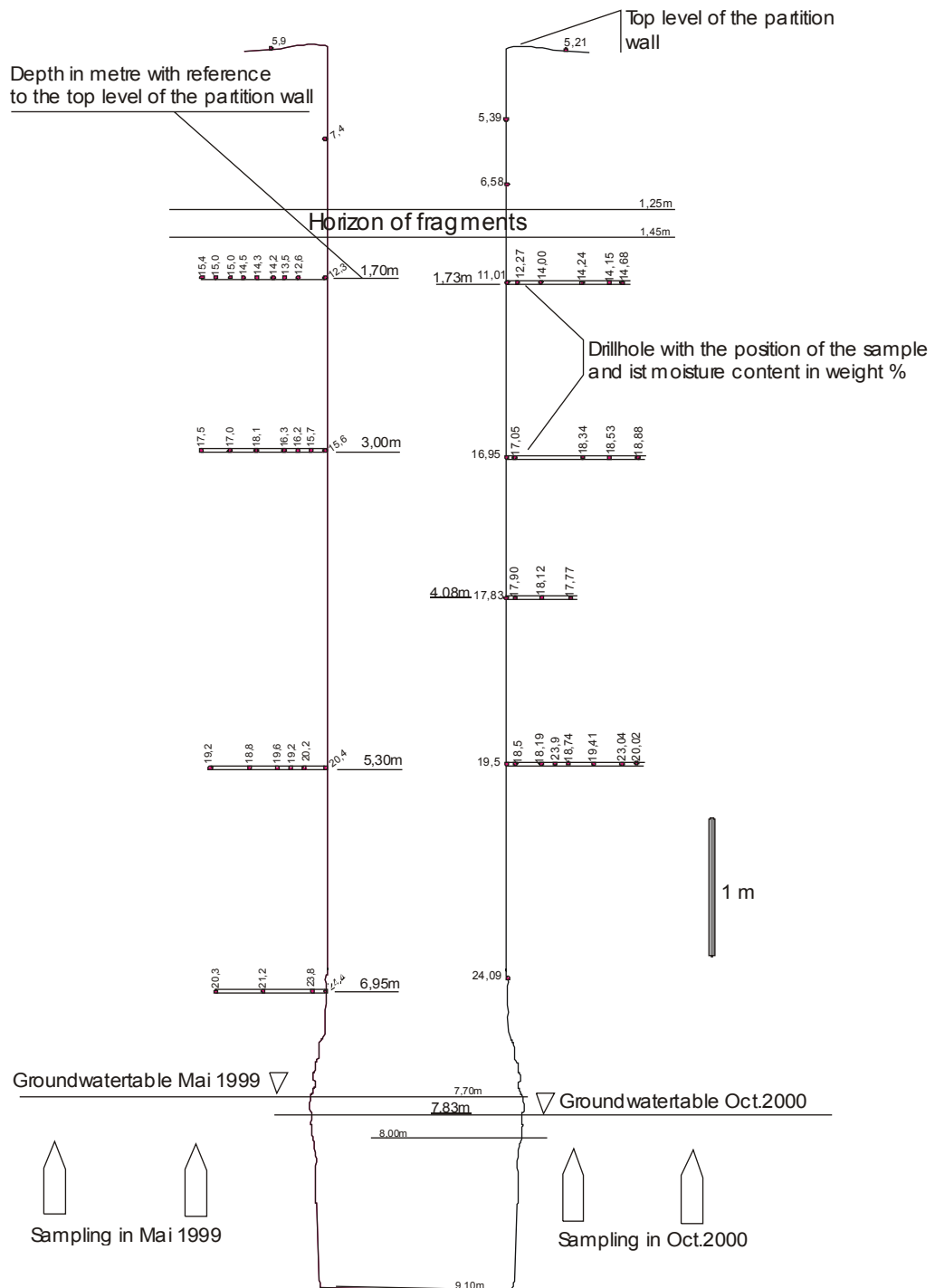
Interpolated moisture distribution in a soil bridge of pit 2 (left) and a soil bridge of pit 1 (right). The drilling soundings were accomplished in May 1999 (above) and in October 2000 (down). The water content of the taken samples is gravimetrically determined.

Sampling position in pit 2: T21, bridge between G17 and G18; Excavation: February. 1998,

Sampling position in pit 1: T20, bridge between G9 and; Excavation: 1979 - 1982

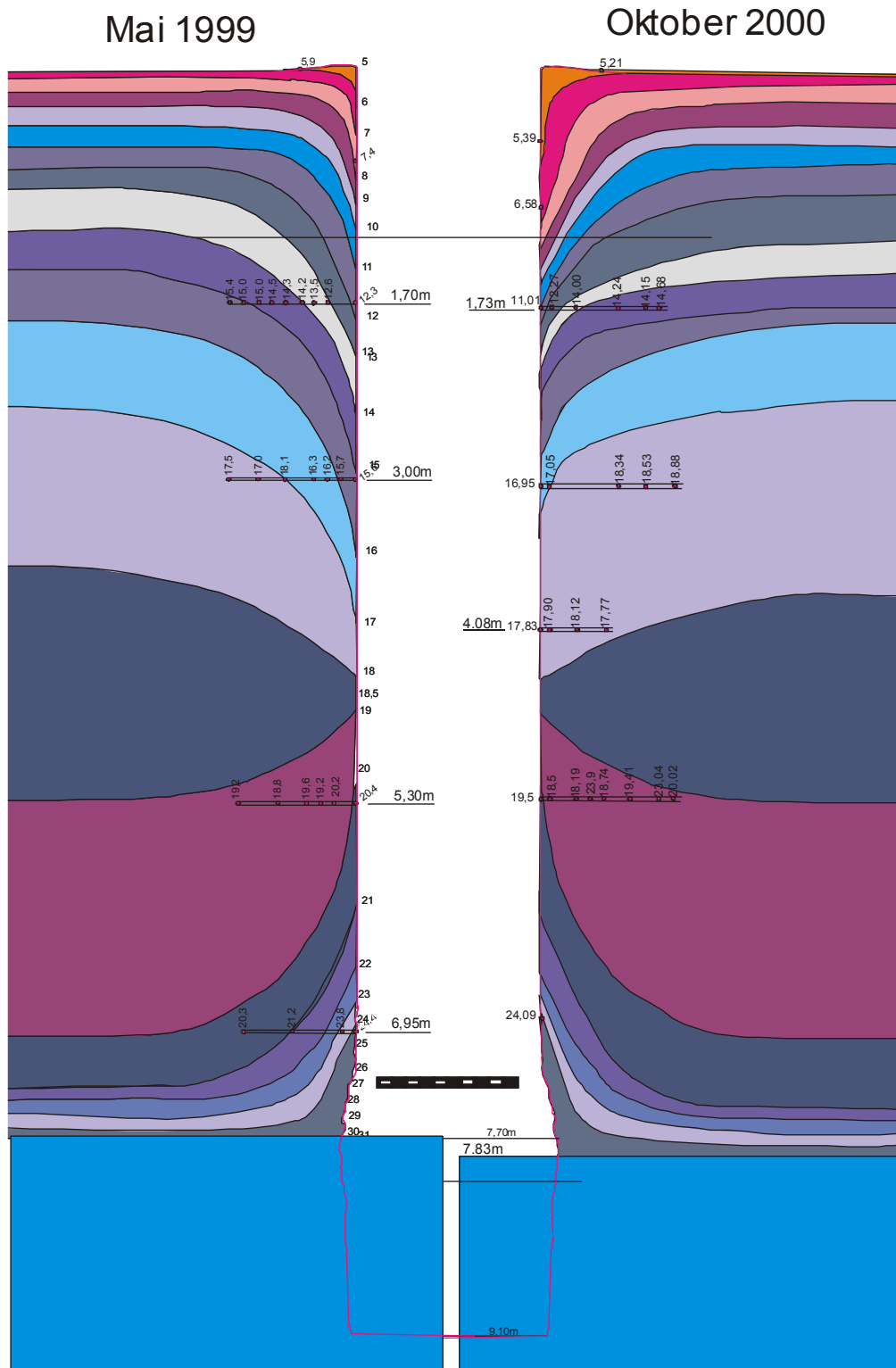
Stabilisation of loess clay surfaces at the example of the Terracotta army in Lintong

Positioning plan for the soil sampling in the well of pit No 2 in the years 1999 and 2000



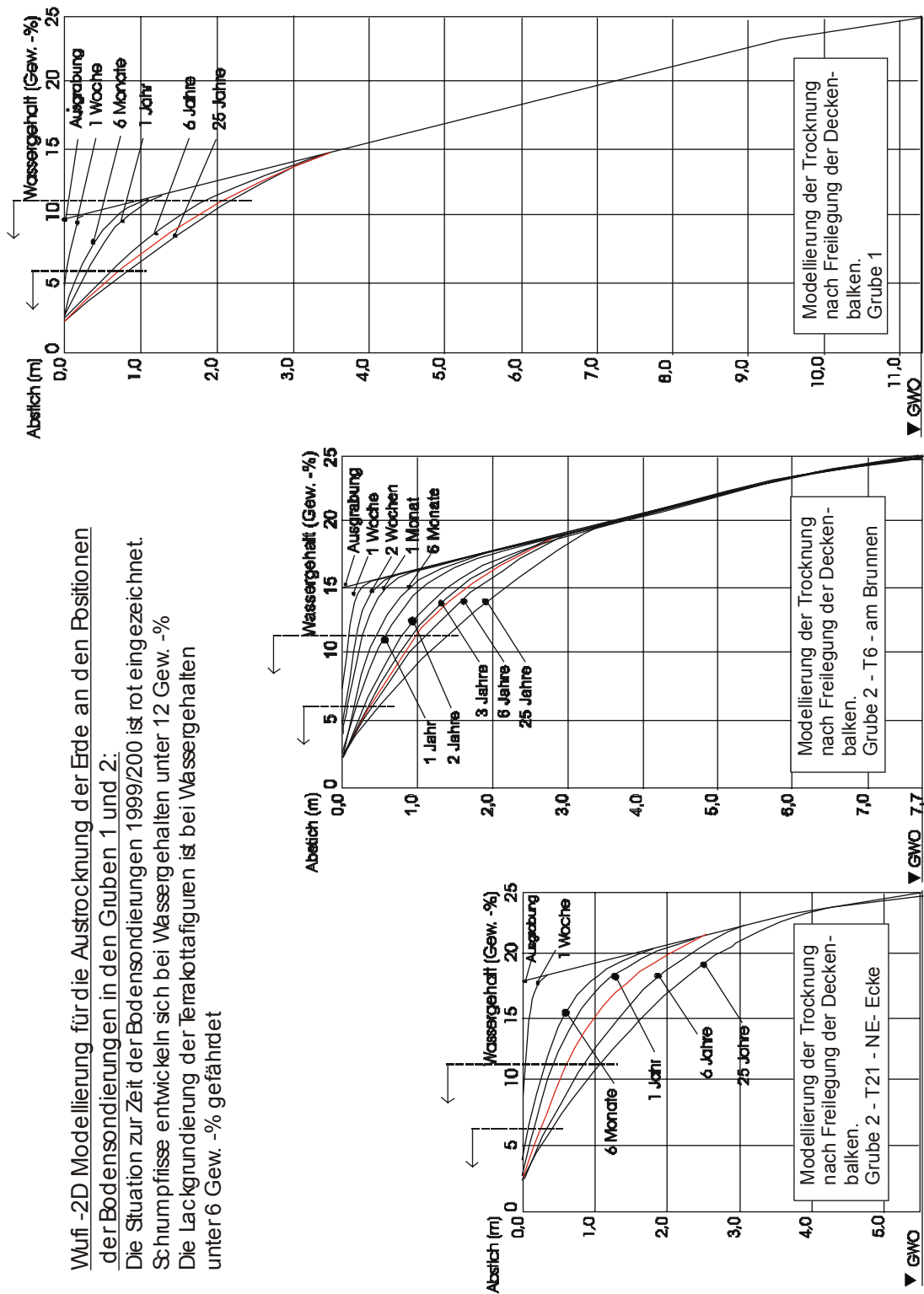
Sampling plan, true to scale, of the drilling soundings in the well of pit 2. Position in pit 2: T6; G6. Excavation up to the position of the ceiling beams: 1994 - 1997.

Stabilisation of loess clay surfaces at the example of the Terracotta army in Lintong



Interpolation of the moisture distribution in the soil of pit 2, based on the data of the drilling soundings in May 1999 and October 2000

Wufi 2D modelling for the drying of the soil, in the positions of the soil soundings in pit 1 and 2



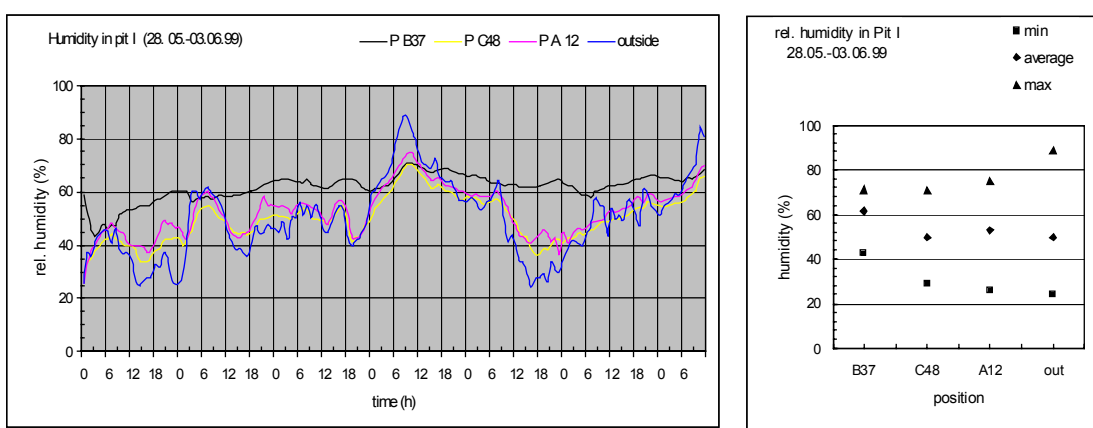
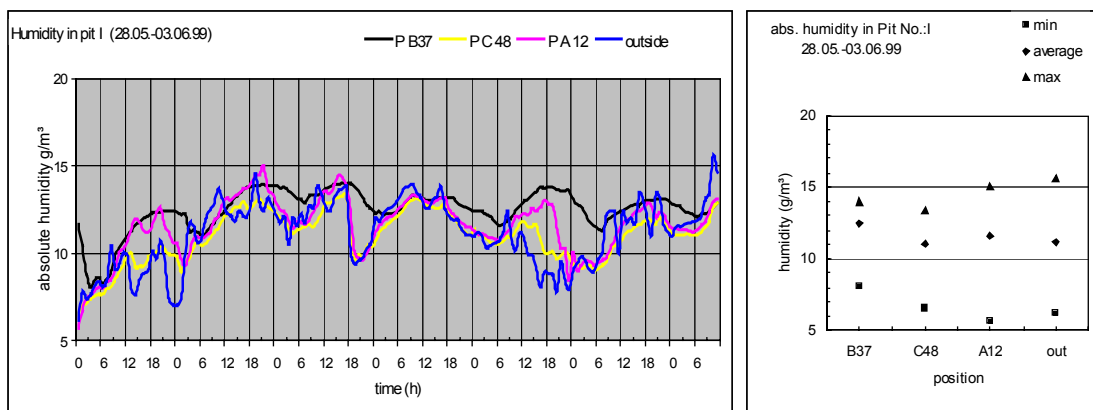
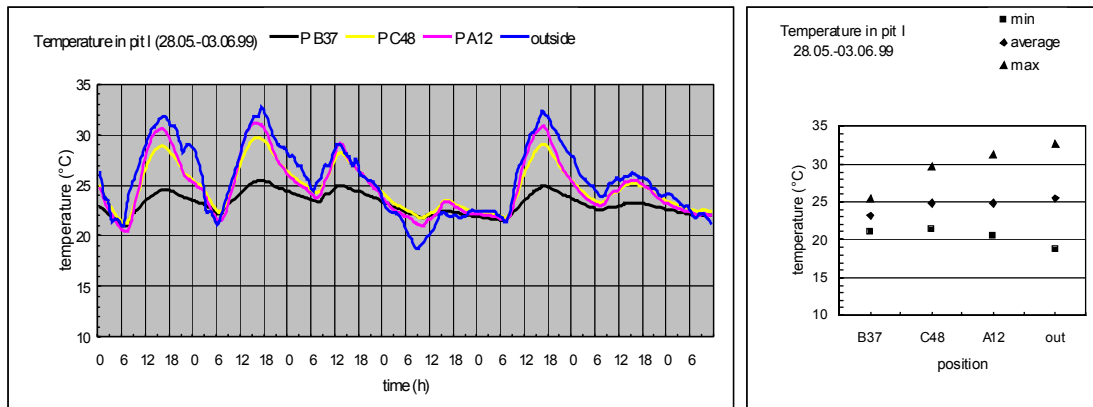
Wufi -2D Modellierung für die Austrocknung der Erde an den Positionen der Bodensondierungen in den Gruben 1 und 2:
 Die Situation zur Zeit der Bodensondierungen 1999/2000 ist rot eingezeichnet.
 Schumpfrisse entwickeln sich bei Wassergehalten unter 12 Gew.-%
 Die Lackgrundierung der Terrakottfiguren ist bei Wassergehalten unter 6 Gew.-% gefährdet

Stabilisation of loess clay surfaces at the example of the Terracotta army in Lintong

7.4 Climate Data

Weekly measurements in pit 1

Wochenmessungen in Grube 1:

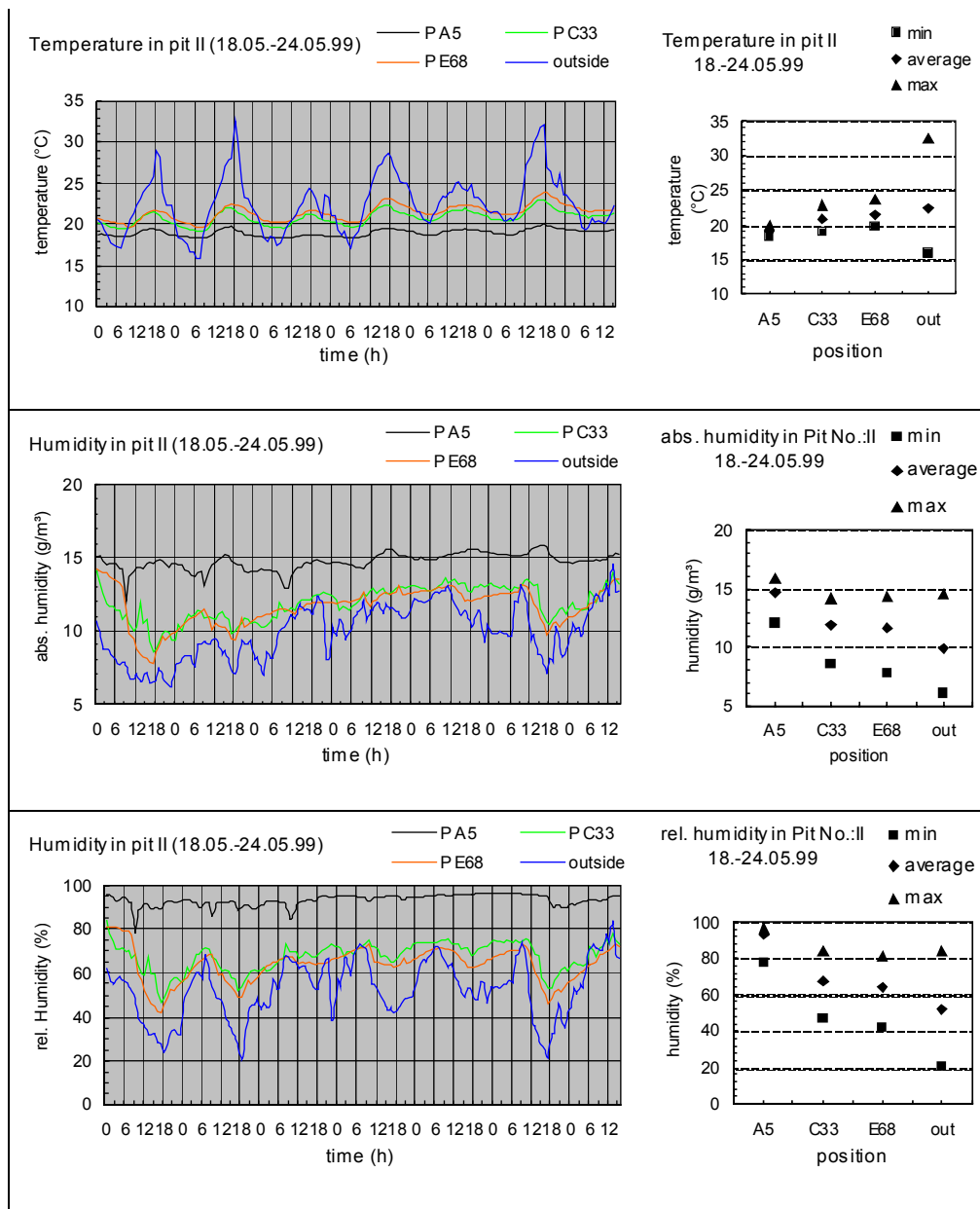


Measurement points: B37- on the floor of the corridors; C48- height of the beam layer; A12- Visitor level; out- outside climate

Stabilisation of loess clay surfaces at the example of the Terracotta army in Lintong

Weekly measurements in pit 2

Wochenmessung in Grube 2

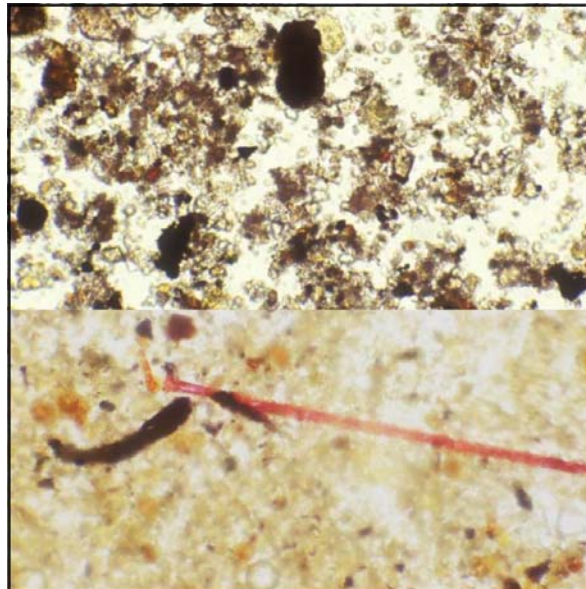


Measurement points: A5- on the floor of the corridors; C33- height of the beam layer;
E68- Visitor level; out- outside climate

Stabilisation of loess clay surfaces at the example of the Terracotta army in Lintong

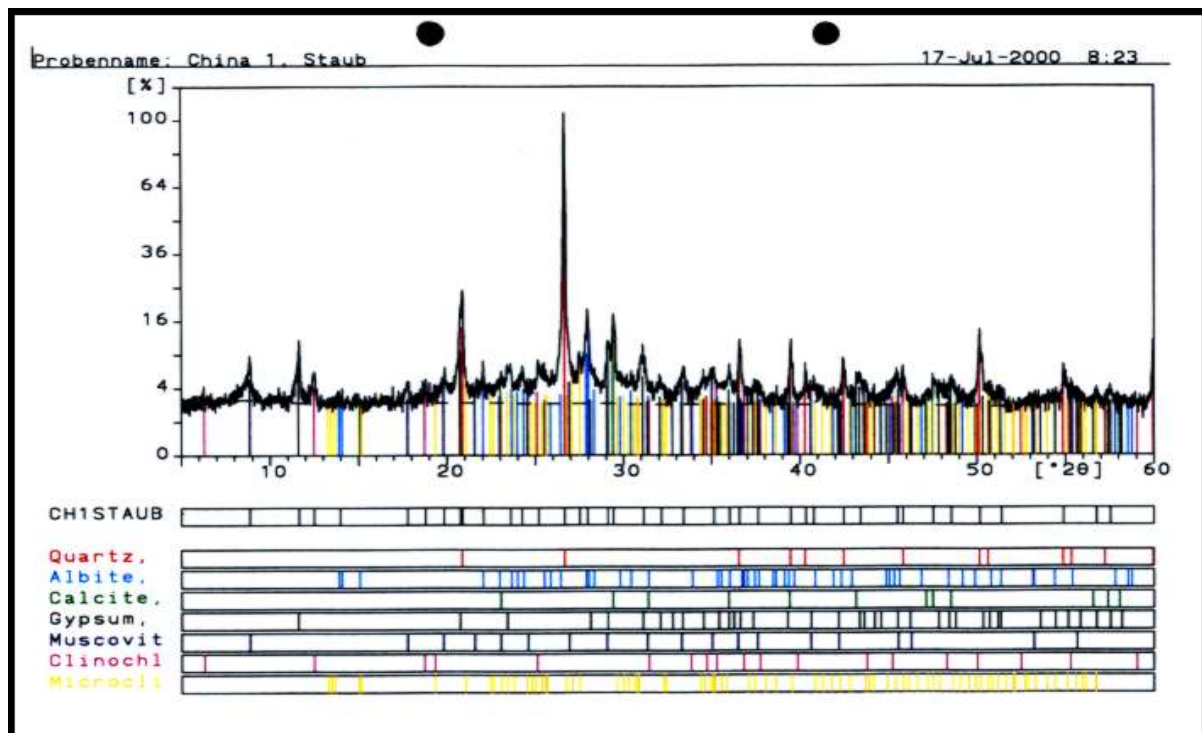
7.5 Dust analyses

Microscopic images of the meteoric dust in the pit (above) and of a dust sample of the stamped soil (below). Soot particles stain the dust grey.



Baseline: approx. 0.5mm

SEM- image of the meteoric dust on the Terracotta soldiers. The amount of gypsum lays between 5 and 10%



7.6 Selected measurement values of the laboratory tests

Dilatation and water adsorption of the single samples (preliminary tests with modified swelling reducers):

	90% rel.F.	90% rel.F.	100% rel. F.	100% rel. F.	
	Dilatation	Wasseraufnahme	Dilatation	Wasseraufnahme	
Probe	(%)	(%)	(Gew.-%)	(Gew.-%)	
SH2O 1	0,12	3,50	0,17	6,16	
SH2O 1	0,11	3,48	0,13	6,73	
SH2O 2	0,07	5,28	0,08	8,67	
SH2O 2	0,15	3,28	0,17	5,53	
SE_1	0,06	4,54	0,10	6,89	
SE_2	0,01	4,56	0,01	6,60	
SE_2	0,04	4,50	0,09	10,54	
SB_1	0,04	5,09	0,09	9,64	
SB_2	0,06	6,64	0,24	11,32	
SB_2	0,03	5,81	0,04	11,79	
SH_1	0,21	8,42	1,14	13,88	
SH_2	0,14	7,41	0,73	13,39	
SH_1	0,07	6,93	0,45	13,73	
SEBH_1	0,02	8,14	0,12	12,72	
SEBH_2	0,04	6,35	0,08	10,97	
SEBH_1	0,03	6,79	0,24	13,90	
P1	0,24	4,36	0,32	6,45	
Probe		m(g)(trocken)	d(90%)-d1(mm)	d90(mm/m)	Dilatation %

Stabilisation of loess clay surfaces at the example of the Terracotta army in Lintong

Measurement to the Sorption isotherm:

Adsorption:

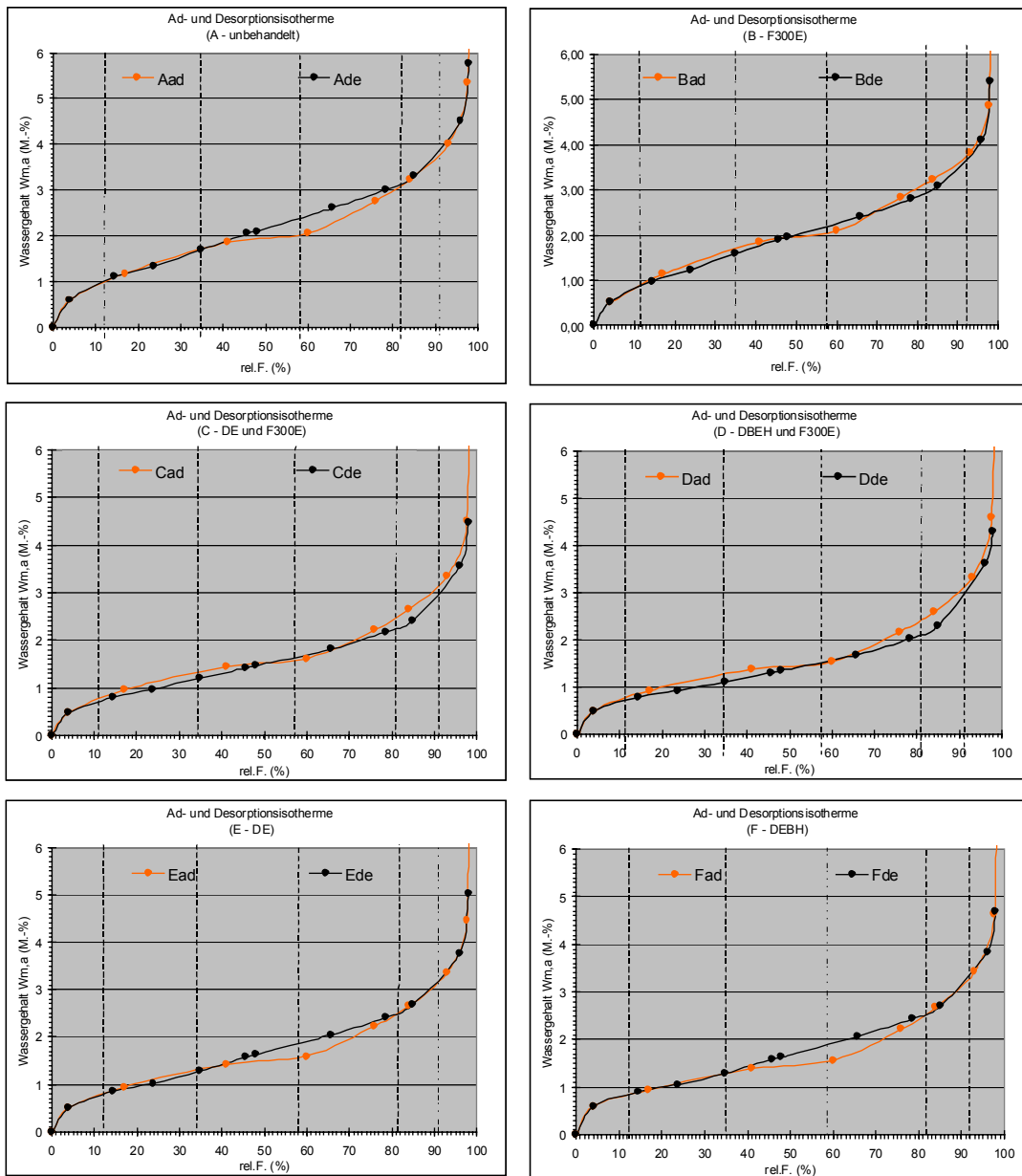
		träger	prbe u. träger		ADSORPTION											
A		m (g)	m (g)	m (g)	28.07.13:00	29.07.13:00	30.07.14:00	31.07.02	01.08.02	06.08.02	07.08.02	09.08.02	10.08.02	19.08.02	02.09.02	
unbehandelt			dry	17% r.F. 25°C	17% r.F. 25°C	41% r.F. 25°C	41% r.F. 25°C	60% r.F. 23°C	74.3% r.F. 24.76% 25°C	84% 25°C	93% 25°C	97.7% 26°C				
Sa	1	3,454	18,276	18,449	18,454	18,535	18,556	18,585	18,675	18,688	18,758	18,872	19,077			
	2	3,441	25,354	25,602	25,604	25,718	25,753	25,797	25,932	25,954	26,056	26,223	26,52			
B																
F300E																
Sa	1	3,392	25,556	25,8	25,803	25,92	25,956	26,001	26,128	26,151	26,234	26,358	26,566			
	2	3,452	35,008	35,369	35,374	35,539	35,612	35,693	35,926	35,96	36,092	36,283	36,633			
C																
DE/F300E																
Sa	1	3,47	33,161	33,443	33,447	33,557	33,6	33,651	33,824	33,852	33,996	34,228	34,59			
	2	3,536	14,092	14,191	14,193	14,231	14,242	14,259	14,309	14,315	14,355	14,419	14,536			
D																
DEBH/F300E																
Sa	1	3,398	30,034	30,284	30,288	30,383	30,42	30,47	30,628	30,655	30,772	30,969	31,284			
	2	3,401	14,525	14,623	14,626	14,66	14,67	14,686	14,739	14,75	14,793	14,877	15,024			
E																
DE																
Sa	1	3,511	24,599	24,801	24,804	24,889	24,912	24,951	25,079	25,1	25,199	25,36	25,603			
	2	3,791	22,605	22,778	22,778	22,846	22,861	22,892	22,985	22,998	23,071	23,193	23,387			
F																
DEBH																
Sa	1	3,558	33,988	34,282	34,284	34,4	34,435	34,493	34,677	34,71	34,861	35,098	35,471			
	2	3,527	16,606	16,724	16,726	16,77	16,778	16,798	16,865	16,876	16,933	17,027	17,185			

Desorption:

		Desorption										
A		12.12.02	20.12.02	23.12.02	10.01.03	13.01.02	15.01.03	20.01.	22.01.	30.01.		
unbehandelt		96% 26°C	85,30%	77%	65,80% 48% /25°C	45,70%	34,90%	23,80%	14,4% 52°C	4%		
Sa	1	18,95	18,77	18,724	18,665	18,589	18,581	18,528	18,478	18,44	18,366	
	2	26,336	26,071	26,009	25,919	25,809	25,798	25,721	25,643	25,591	25,478	
B												
F300E												
Sa	1	26,414	26,207	26,145	26,068	25,977	25,969	25,904	25,827	25,774	25,671	
	2	36,377	36,032	35,942	35,794	35,643	35,624	35,515	35,401	35,319	35,168	
C												
DE/F300E												
Sa	1	34,311	33,92	33,838	33,716	33,607	33,596	33,523	33,452	33,401	33,303	
	2	14,434	14,332	14,31	14,277	14,243	14,237	14,216	14,194	14,175	14,141	
D												
DEBH/F300E												
Sa	1	31,042	30,707	30,635	30,524	30,427	30,415	30,351	30,292	30,52	30,168	
	2	14,909	14,757	14,728	14,695	14,662	14,656	14,642	14,625	14,609	14,581	
E												
DE												
Sa	1	25,457	25,21	25,147	25,064	24,964	24,953	24,885	24,827	24,789	24,71	
	2	23,258	23,07	23,021	22,963	22,89	22,881	22,832	22,787	22,755	22,695	
F												
DEBH												
Sa	1	35,255	34,893	34,808	34,681	34,534	34,519	34,419	34,336	34,282	34,176	
	2	17,067	16,925	16,891	16,85	16,798	16,793	16,758	16,735	16,715	16,681	

Stabilisation of loess clay surfaces at the example of the Terracotta army in Lintong

Adsorption and Desorption isotherms of all treatment types:



Stabilisation of loess clay surfaces at the example of the Terracotta army in Lintong

Calculation of the vapour diffusion resistance (μ -value)

Zur Anwendung im Labor wird folgende Formel benutzt:

$$m = dL \cdot p_s \cdot Da \cdot A \cdot t / s \cdot D_m$$

dL (kg / Pa m s) = Wasserdampf-Diffusionsleitkoeffizient
 p_s (Pa) = Partialdruck der gesättigten Luft
 Da (-) = Differenz der relativen Luftfeuchte
 s (m) = Schichtdicke der Probe
 A (m²) = Fläche der Probe
 t (s) = Zeit
 D_m (kg) = Gewichtsänderung

Bei einer Temperatur von 21°C haben dL und p_s folgenden Wert:

dL = 1,96 · 10⁻¹⁰ kg / Pa m s
 p_s = 2,49 · 10³ Pa

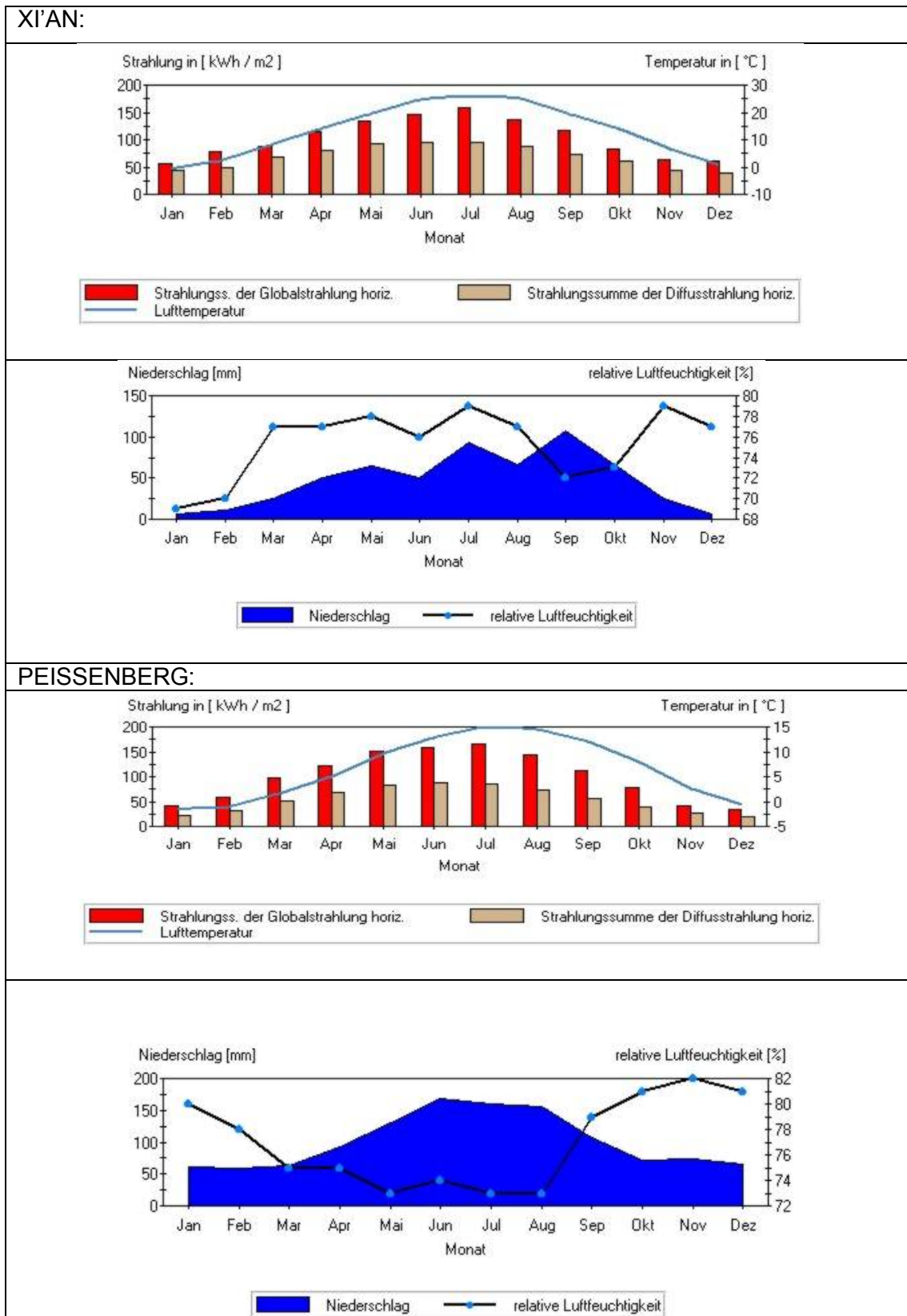
Probe	Probenscheibe		Luftfeuchte		Zeit t [h]	Anfangs-End-		Wasserdampf-		
	Dicke s [cm]	Durchmesser d [cm]	außen [%]	im Glas aGlas [%]		m vor [g]	m nach [g]	Diffusions- widerstandszahl	m(dry) / m(wet)	
B1	0,612	4,4	50	0	48	71,441	71,866	μ (dry) =	24,7	1,8 :1
B1	0,612	4,4	50	100	138,5	76,377	74,199	μ (wet) =	13,9	
F2	0,65	4,43	50	0	48	73,080	73,535	μ (dry) =	22,0	1,6 :1
F2	0,65	4,43	50	100	118	78,295	76,489	μ (wet) =	13,6	
D1	0,64	4,42	50	0	48	74,604	75,002	μ (dry) =	25,4	1,7 :1
D1	0,64	4,42	50	100	161,5	74,696	72,421	μ (wet) =	15,0	
C1	0,61	4,4	50	0	48	74,407	74,728	μ (dry) =	32,7	1,7 :1
C1	0,61	4,43	50	100	118	75,506	74,107	μ (wet) =	18,7	
D3	0,897	4,44	50	0	118	81,452	82,375	μ (dry) =	19,4	1,5 :1
D3	0,897	4,44	50	100	116	81,433	80,103	μ (wet) =	13,2	
F3	0,82	4,36	50	0	118	75,737	76,929	μ (dry) =	15,8	1,6 :1
F3	0,82	4,36	50	100	116	76,162	74,317	μ (wet) =	10,1	
B4	0,71	4,35	50	0	161,5	75,689	77,169	μ (dry) =	20,1	1,9 :1
B4	0,71	4,35	50	100	170	76,543	73,561	μ (wet) =	10,5	
B2	0,78	4,4	50	0	118	79,987	81,153	μ (dry) =	17,3	1,2 :1
B1	0,612	4,42	50	100	161,5	76,682	74,199	μ (wet) =	14,3	
A3	0,8	4,4	50	0	161,5	78,042	79,723	μ (dry) =	16,0	2,0 :1
A3	0,8	4,4	50	100	170	79,507	76,036	μ (wet) =	8,2	
E4	0,67	4,49	50	0	161,5	76,034	77,737	μ (dry) =	19,7	2,1 :1
E4	0,67	4,49	50	100	170	76,535	72,734	μ (wet) =	9,3	
A4	0,71	4,34	50	0	48	76,757	77,138	μ (dry) =	23,1	2,8 :1
A4	0,71	4,34	50	100	118	76,480	73,882	μ (wet) =	8,3	
F1	0,65	4,5	50	0	118	66,773	68,148	μ (dry) =	18,4	1,6 :1
E3	0,62	4,5	50	100	118	76,804	74,531	μ (wet) =	11,7	
E1	0,69	4,5	50	0	118	75,499	76,847	μ (dry) =	17,7	1,4 :1
C4	0,72	4,36	50	100	118	73,388	71,654	μ (wet) =	12,4	
E2	0,96	4,4	50	0	118	81,625	82,764	μ (dry) =	14,4	1,2 :1
B3	0,75	4,4	50	100	118	77,165	75,377	μ (wet) =	11,8	
C3	0,94	4,46	50	0	118	75,212	76,156	μ (dry) =	18,3	1,5 :1
D4	0,76	4,36	50	100	118	78,159	76,500	μ (wet) =	12,3	

Measurement values and calculation of the w-value: (deleted!)

7.7 Input parameter for the Wufi-2D-modellings (deleted!)

Monthly average values for the atmospheric humidity and temperature in Xi'an und Peissenberg

(source: Database METEONORM VERSION 4.0)



Stabilisation of loess clay surfaces at the example of the Terracotta army in Lintong

7.8 Technical Data sheet (deleted!)